DISSERTATION

COMBINED FENTON'S OXIDATION AND BIODEGRADATION FOR THE TREATMENT OF PENTACHLOROPHENOL-CONTAMINATED WATER

Submitted by

Julio Arturo Zimbrón-Nieto

Department of Chemical and Bioresource Engineering

In partial fulfillment of the requirements

For the Degree of Doctor of Philosophy

Colorado State University

Fort Collins, CO 80523

Fall 2000

COLORADO STATE UNIVERSITY

October 27, 2000

WE HEREBY RECOMMEND THAT THE DISSERTATION PREPARED UNDER OUR SUPERVISION BY JULIO ARTURO ZIMBRÓN-NIETO ENTITLED

COMBINED FENTON'S OXIDATION AND BIODEGRADATION FOR THE TREATMENT OF PENTACHLOROPHENOL-CONTAMINATED WATER

BE ACCEPTED AS FULFILLING IN PART THE REQUIREMENTS FOR THE DEGREE OF DOCTOR OF PHILOSOPHY

Committee on Graduate Work

Advisor

Department Head

ABSTRACT OF DISSERTATION

COMBINED FENTON'S OXIDATION AND BIODEGRADATION FOR THE TREATMENT OF PENTACHLOROPHENOL-CONTAMINATED WATER

Combinations of chemical and biological degradation processes can be more effective for the treatment of recalcitrant pollutants than either chemical or biological treatment alone. Many chemical oxidation technologies rely on the generation of hydroxyl free radicals (•OH), and can partially oxidize recalcitrant compounds and generate more biodegradable intermediates. In a laboratory-scale project, pentachlorophenol (PCP) was studied as a model recalcitrant compound for a sequential combined system of chemical oxidation and biodegradation. For this combination, Fenton's reagent was selected as the oxidation method. The combined treatment was achieved in a continuous-flow stirred-tank Fenton's reactor and a packed-bed bioreactor.

The goal of this research was to rationally optimize the combined system. Kinetic and stoichiometric data for chemical oxidation and biodegradation were measured in separate studies for both the chemical and the biological processes, and then integrated into a combined reactor model. The mathematical model was used to provide an understanding of the combined system and to test two project hypotheses: (i) the combined system can achieve higher mineralization than a single step process, and (ii)

recycle of the effluent from the bioreactor back to the chemical reactor can improve the efficiency of the mineralization.

To characterize the •OH-mediated degradation of PCP, the second-order rate constant for PCP was measured by the method of competitive kinetics. The value obtained for PCP ($4.4x10^{09}$ L/mol·s), together with experimental and previously reported values for other chlorophenols (which were all higher than the value for PCP) were correlated by means of a group contribution method (Hammett's equation), the number of chlorine atoms in the aromatic ring, and also with estimated diffusion coefficients. Since correlation of kinetic data might be indicative of common reaction mechanisms, this analysis provided insight in generalizations about the mechanism of the reaction between •OH and chlorophenols. It was found that all of these correlations were equally valid, which indicates that the very fast rate of reaction between •OH and chlorophenols might be diffusion-limited, instead of limited by the reaction mechanism. Thus, generalizations on the reaction mechanism of these reactions based exclusively on correlations are limited.

Data from batch experiments revealed strong dependence of PCP degradation on the hydrogen peroxide dose, and chloride production concomitant to the PCP degradation. Hydrogen peroxide doses of $2.5x10^{-04}$ mol/L achieved almost complete degradation of PCP, and lower hydrogen peroxide doses achieved partial degradation of the contaminant. However, the total carbon concentration (TOC) of the solution was not decreased at any of the hydrogen peroxide concentrations tested; i.e. mineralization did not occur. Different PCP intermediates were observed, but only tetrachlorohydroquinone could be identified. A kinetic model for the degradation of PCP under Fenton's reaction

was developed, based on previously reported reactions and rates among all the relevant chemical species (ferrous and ferric iron, hydrogen peroxide, and different free radicals) as well as the reaction rate of the reaction of PCP and hydroxyl free radicals, accounting for scavenging effects of the PCP by-products on the degradation of PCP. The model was validated and applied to predict the experimental time-course concentrations of hydrogen peroxide and ferrous iron, in the absence and the presence of PCP as a hydroxyl free radical scavenger, and also the experimental time-course and equilibrium concentrations of PCP oxidized with hydrogen peroxide and ferrous iron in batch reactors. The model was in good agreement with data obtained during time-course reactions (which in most cases reached completion in the first few minutes) and also with equilibrium concentrations of PCP.

Treatment of PCP-contaminated solution in a continuous Fenton's reactor (operating at a retention time of 1.5 h) showed similar behavior to the batch experiments: PCP degradation and dechlorination were strongly dependent on the hydrogen peroxide dose, although reaction extents were lower than in batch experiments. No reduction of TOC was observed. Previously observed intermediates during batch experiments were produced in the continuous Fenton's reactor. Further treatment of the effluent from Fenton's with a continuous bioreactor that included a packed bed column (operating at a retention time of 5.5 h) showed that TOC was biodegraded, although no further reduction of PCP or dechlorination in this reactor were achieved. These biodegradation extents were consistent with the measured production of biomass by this reactor. A small part of the biodegradation observed in the bioreactor was attributable to the biodegradation of the observed intermediates. Experiments in which the retention time in the bioreactor

was doubled did not yield significantly different biodegradation results. Recycle of the effluent from the bioreactor to the chemical reactor improved the TOC degradation, but not the extent of the PCP degradation or dechlorination.

The Fenton's kinetic model for the degradation of PCP was applied to the continuous Fenton's reactor. Additionally, kinetic information about the biodegradation process was obtained from the continuous operation of the bioreactor and incorporated into a biodegradation model. The two models were integrated into a combined model, which also accounted for recycle effects. The model over-predicted the degradation of PCP and TOC in the combined system, but adequately predicted the sensitivity of PCP and TOC degradation achieved by the combined system at different hydrogen peroxide doses and recycle rates. Given these considerations, the model provided information supporting the two project hypotheses.

A suggested reactor operating strategy to improve the system performance was to increase the recycle rate to improve the mineralization of the waste. The model also indicated that the effect of recycle rates was highly dependent on the microbial degradation kinetic parameters.

As opposed to many of the previous empirical or semiempirical studies on combinations of chemical oxidation and biodegradation, the approach followed in this work provides basic understanding of the combined system, and provides an alternative tool for process design and optimization.

Julio Arturo Zimbrón-Nieto
Department of Chemical
and Bioresource Engineering
Colorado State University
Fort Collins, CO 80523
Fall 2000

ACKNOWLEDGMENTS

This work would not have been possible without contributions from many people.

I thank my committee members, Dr. Jim Linden, Dr. Vince Murphy, Dr. Bob Siegrist and Dr. Ken Reardon for their suggestions and insight into my work. I thank my advisor Ken Reardon for advice, support and for teaching me the path of research. I am sure this experience will positively influence the rest of my life in many ways.

I acknowledge financial support from Consejo Nacional de Ciencia y Tecnología-México, the Superfund Basic Research Program, the Colorado Institute for Research in Biotechnology, and the American Water Resources Association.

Many people provided assistance on the different chemical analysis used along this research. Dr. Rajiv Bhadra, Brian Cranmer, and Don Dick provided invaluable guidance on the analysis of intermediates. I thank Dr. Jim Linden and Dr. Pat Gilcrease for the HPLC analysis, Dr. Ken Carlson and Dean Gregory for the TOC analysis, and Brian Cranmer for the GC/MS analysis. To all of them I am grateful.

I thank all my lab co-workers for bringing insight and humor into my research. Thank you especially to Jessie Deal, Jim Lasnick, and Kristin Carpenter for their help in the lab, and to Julie Rogers for being such a good colleague and friend.

Most of all, I thank my wife Claudia León for help with statistical analysis, for endless personal support and for understanding the path that I have chosen to become a better person.

LIST OF SYMBOLS AND ABBREVIATIONS

α	recycle rate, equal to the ratio of the flow rate of the effluent from the bioreactor that is recycled back to the chemical reactor with respect to the inlet flow rate to the combined system
τ_{BR}	residence time (time units) in the bioreactor
τ_{ChRx}	residence time (time units) in the chemical reactor
μ_i	microbial growth rate (1/h)
$\mu_{i,max}$	maximum microbial growth rate (1/h)
$\bullet O_2^-$	superoxide free radical; this is the deionized form of the perhydroxyl free radical
$\bullet O_2H$	perhydroxyl free radical
$\bullet OH$	hydroxyl free radical
AOP	Advanced Oxidation Process
CG/MS	Gas Chromatography/Mass Spectrometry
Fe^{+2}	ferrous iron
Fe^{+3}	ferric iron
H_2O_2	hydrogen peroxide
HO_2^-	perhydroxyl ion; this is the deionized form of hydrogen peroxide
HPLC	High Pressure Liquid Chromatography
k_i	half saturation constant for microbial degradation (mol/L)
k_{ii}	second order kinetic constant for the initiation reaction i (L/mol•s)
$k_{OH,C}$	second order kinetic constant for the reaction between the competitive substrate C and the hydroxyl free radical (L/mol•s)
$k_{OH,M}$	second order kinetic constant for the reaction between the substrate M and the hydroxyl free radical (L/mol•s)
k_{pi}	second order kinetic constant for the propagation reaction i (L/mol•s)
k_{ti}	second order kinetic constant for the termination reaction i (L/mol•s)
k_{tPCP}	second order kinetic constant for the reaction between PCP and the hydroxyl free radical (L/mol•s)
k_{tscav}	second order kinetic constant for the reaction between PCP-by products and the hydroxyl free radical (L/mol•s)
PCP	pentachlorophenol
$rate_{i,Bio}$	rate of reaction of chemical species *i* under biodegradation treatment
$rate_{i,Ch}$	rate of reaction of chemical species i under oxidation due to Fenton's reaction; equal to the summation of all the rates of reactions in which the chemical species *i* is involved
$S_{i,BioRx}$	concentration (mol/L) of the chemical species *i* in the bioreactor
$S_{i,ChRx}$	concentration (mol/L) of the chemical species *i* in the chemical reactor

$S_{i,FbioRx}$	concentration (mol/L) of the chemical species *i* in the feed to the bioreactor (which in the combined model was equal to the concentration of this species *i* n the chemical reactor)
$S_{i,FChRx}$	concentration (mol/L) of the chemical species *i* in the feed to the chemical reactor
TCHQ	tetrachlorohydroquinone, a PCP by-product of Fenton's oxidation
TOC	total organic carbon
X_T	packed bed biomass content (mg)
$Y_{X/Si}$	yield of biomass to carbon substrate consumption (as TOC) in mg of biomass/mol of total organic carbon

TABLE OF CONTENTS

LIST OF FIGURES

LIST OF TABLES

CHAPTER I

INTRODUCTION AND PROJECT GOALS

1.1. Pentachlorophenol

Pentachlorophenol (PCP; Figure 1.1) has been used as a biocide in wood treatment and other applications. It is also generated from bleaching operations from the pulp and paper industry. PCP contamination is often found at wood treating sites, usually combined with polycyclic aromatic compounds (PAHs) and lower chlorophenols. PCP is one of the most recalcitrant chlorophenols. At contaminated sites, PCP is slow to biodegrade because it is inhibitory or toxic to microorganisms at the high concentrations normally found (Litchfield and Rao, 1998). PCP is also present in water due to leaching into groundwater from contaminated soil, generation during bleaching operations from the pulp and paper industry, and generation of wastewater from wood treating facilities (Hale, et al., 1994). Due to the nature of these PCP sources, it is often present in mixtures with other contaminants, constituting the most recalcitrant fraction of such mixtures (Graves and T. Joyce, 1994; Leuenberger, et al., 1985). Even though its human toxicity has not been demonstrated, public concern about its contamination exists, and it has been designated a priority pollutant by the US EPA. Many PCP contaminated sites have been selected for cleanup in Europe and the US (by means of the Superfund Program) (Puhakka, et al., 1996).

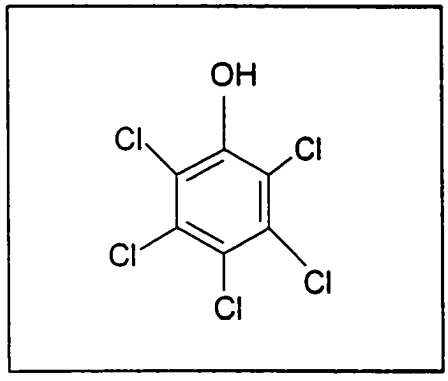

Figure 1.1. Chemical structure of pentachlorophenol (PCP).

1.2. PCP Biodegradation

Biodegradation systems have provided cost-effective alternatives for the degradation of many contaminants. Thus, bioremediation usually is the treatment technology of choice when a contaminant is biodegradable. However, bioremediation is limited when the pollutant is either recalcitrant to biodegradation or toxic to the microbial culture.

Aerobic biodegradation of PCP requires the enzyme pentachlorophenol monooxygenase, which catalyzes the transformation of PCP to 2,3,5,6-tetrachlorohydroquinone. Further catalysis by reductive dehalogenases yields 2,3,6-trichlorohydroquinone and 2,6-dichlorohydroquinone, sequentially. The enzyme 2,6-dichlorohydroquinone can induce ring cleavage on the latter compound, to dichloro-hydroxy muconic semialdehydes (Hale, et al., 1994; Zeng, 2000). Mixed culture experiments done in several studies achieved only partial degradation of PCP, ranging only from 24% to 50% after intervals of 12 to 30 days, although fixed film bioreactors amended with PCP-degrading microorganisms achieved higher than 96% degradation at residence time from 1.8 to 9 h (Puhakka, et al., 1996).

Anaerobic degradation of PCP involves reductive dechlorination to lower chlorinated tetra-, tri-, di- and mono-chlorinated phenol mixtures. In freshwater sediments, PCP was completely transformed to these lower chlorophenols after 8 months (Hale, et al., 1994).

1.3. Advanced Oxidation Processes as Alternatives to Biodegradation

Because of these low PCP biodegradation rates, alternative treatment technologies such as advanced oxidation processes (AOPs) have received increased interest. The term AOPs includes all technologies that generate hydroxyl free radicals (OH•). Examples include the combination of hydrogen peroxide and ultraviolet light, ozonation, Fenton's reaction (the combination of hydrogen peroxide and transition metal catalysts), photocatalysis with semiconductors (such as titanium dioxide), and combinations of these (such as the photo-Fenton's reaction) (Venkatadri, et al., 1993).

The hydroxyl free radicals generated by AOPs are powerful, relatively non-selective oxidants. The oxidation potential of the hydroxyl free radical is second only to fluorine, twice that of chlorine, and 25% higher than ozone (Van Kemenade, et al., 1996). Other chemical oxidation methods such as oxidation with permanganate, chlorine dioxide, or UV light have been tested but in general are less efficient (Venkatadri, et al., 1993).

1.4. Combination of AOPs and Biodegradation for the Treatment of Recalcitrant Compounds

Given sufficient residence time and oxidant, most AOPs are able to completely mineralize recalcitrant substances, including polyclyclic aromatic hydrocarbons (PAHs), chlorinated aromatic compounds, and azo dyes (Stockinger, et al., 1995; Scott, et al., 1995; Heinzle, et al., 1992; Tang, et al., 1997).

However, mineralization by chemical oxidation is not a one-step process. Intermediates are produced by breaking bonds in the parent compound or by oxidizing aldehyde and ketone groups of these smaller molecules. Intermediates typically exhibit lower oxidant reactivity but higher biodegradability than the original compound. Since biological processes are known to be 5 to 20 times less expensive than chemical processes (Marco, et al., 1997), addition of a biodegradation stage can improve the economy of the overall process.

Combinations of advanced oxidation and biological processes have potential applications for different waste streams. Most intermediates generated in the chemical process are both chemically degradable and biodegradable, and total mineralization of these intermediates could be achieved in either a biological or a chemical reactor. However, some intermediates have low affinity for hydroxyl free radicals, and a long residence time in a chemical reactor is required for complete mineralization. Despite their low rate constants for oxidation by •OH, intermediates can adversely affect the oxidation of the parent compound by competing for •OH (Marco, et al., 1997). This situation suggests that the optimal combination of an AOP and biological degradation is

one in which most of the parent compound is chemically oxidized and most of the intermediates are biodegraded.

Thus, the objectives of chemical treatment in a combined system are to maximize both the destruction of parent compounds and the production of biodegradable intermediates (which directly affects the maximum effectiveness of the biological reactor). Many reports exist for the combination of chemical oxidation and biodegradation processes (Scott, et al., 1995). Most of them provide results which indicate that the combined system is advantageous over a single step process (either chemical oxidation or biodegradation alone). However, most of these results are semi-empirical and provide little information to extrapolate results to other applications. Given this situation, it is clearly necessary to provide a process design tool, an alternative to costly pilot treatment studies, to determine the suitability of different design decisions for different wastes.

1.5. Research Approach and Project Goals

Chemical engineering reactor design has traditionally relied on the use of reaction rates and by-product yield data for reactor design and optimization, with positive results in many industries (e.g., pharmaceutical, petroleum). Despite the fact that several experimental studies on the combination of chemical oxidation and biodegradation have been carried out, complete mechanistic information is not available for such processes (Scott, et al., 1995; Scott, et al., 1996). The complex chemistry of AOPs has helped broaden this gap between basic chemistry and applicability studies.

Abundant mechanistic information exists about the degradation of many aromatic compounds treated by different AOPs:

- The reaction mechanism and rate of hydroxyl free radical initiation, propagation and termination by means of a variety of AOPs operating under different conditions (Walling, 1975; Glaze, et al., 1989; Stockinger, 1995);
- the production of some intermediates, such as formate and oxalate, which are common to many chlorinated aromatic AOP-treated wastes (Wang, 1992; Nakamura, et al., 1997; Stockinger, et al., 1995);
- the second-order reaction rate constants of hydroxyl free radical attack on these reported intermediates (Buxton, et al., 1988; Bielski, et al., 1985; Fartahazis and Ross, 1977); and
- the second-order reaction rate constants of common aqueous chemicals that react with hydroxyl free radicals (and therefore can interfere with AOPs), such as carbonates, phosphates, and nitrates (Buxton, et al., 1988; Bielski, et al., 1985; Fartahazis and Ross, 1977; Staehelin, et al., 1985).

Because of this lack of a mechanistic approach for the combination of AOPs and biodegradation, it has been stated that integration of processes must be experimentally evaluated on a case-by-case basis (Vogelpohl, et al., 1996). In contrast, the objective of this work is to use a more mechanistic approach that emphasizes rate laws for parent compounds and intermediates in both the chemical and biological processes, and thus allows extrapolation of results to other wastes.

In this project, a combined Fenton's and immobilized cell bioreactor system were used for the treatment of water contaminated with recalcitrant compounds. The goal of

this research is to determine the optimal combination of chemical oxidation and biodegradation for recalcitrant wastes, utilizing mechanistic information about Fenton's oxidation and biodegradation. A rational chemical reactor design and optimization strategy was used to study the combination of processes.

The efficiency of this type of process can be defined as the achievement of one or more treatment goals for the contaminated stream under study upon a given use of the resources used for treatment (defined as specific reactor operating conditions). Some options for treatment goals are degradation of the parent compound, reduction of waste toxicity, dechlorination (conversion of the organic chloride into free chloride) or mineralization (conversion of the organic carbon into carbon dioxide). The resources used to achieve one or more of these treatment goals are residence time (which relates to the capital cost of the reactor(s)) or cost (either capital or operating costs).

From these options for treatment goals, reduction of toxicity is probably the most desirable one for a waste contaminated with a recalcitrant compound; however, it is difficult to measure. In contrast, mineralization is readily measurable and guarantees reduction of toxicity as well as destruction of the parent compound. Thus, it might be a more stringent treatment goal than the other ones proposed.

On the other hand, it has been stated that most of the costs of a combined chemical oxidation and biodegradation system are related to the operation of the chemical oxidation processes (Marco, et al., 1997). Since it does not require specialized equipment, Fenton's treatment involves low capital costs (with respect to other AOPs), and most of the operating costs are related to the consumption of hydrogen peroxide (Bigda, 1995). Thus, it is expected that most of the costs involved with the operation of a

combined chemical oxidation and biodegradation system will be related with the hydrogen peroxide use.

For these reasons, efficiency in this work was defined as the ratio of PCP mineralization with respect to the hydrogen peroxide dose. Optimization was then defined as maximizing the efficiency. Potentially, different operating conditions will lead to (relative or absolute) maximum efficiencies, and thus, multiple relative or absolute optimal operating conditions might exist for a combined system.

Pentachlorophenol (PCP) in aqueous solution was the model waste stream. The rates of reactions of PCP and by-products were obtained for both chemical oxidation and biodegradation processes, and incorporated into a mathematical model. This model was then used to propose optimization strategies for the combined system. This research plan allowed testing of two hypotheses:

Hypothesis 1: A combined chemical and biological process can achieve higher PCP mineralization than either process alone, given a fixed hydrogen peroxide consumption.

Hypothesis 2: Multicycle chemical-biological treatment can achieve higher PCP mineralization than one chemical-biological cycle, given a fixed hydrogen peroxide consumption.

Work on five specific objectives was used for hypothesis testing and achievement of the project goals:

1. Experimentally determine reaction rates at which PCP is degraded in a Fenton's treatment.

2. Experimentally determine the nature of the Fenton's degradation of PCP: mineralization, production of intermediates, and factors that might reduce the efficiency of this reaction.
3. Perform experiments using a Fenton's reactor plus a packed bed bioreactor system for the treatment of the model waste stream.
4. Determine biodegradation rates for PCP and major intermediates.
5. Develop a mathematical model for the combined process and use the mathematical model for reactor design and optimization of the combined system.

These specific objectives were developed in separate studies, presented in this work in different chapters (and integrated as indicated in Figure 1.2.). Each one of these chapters has been written to be self-standing, and as a result each typically includes background information, methods, results and discussion sections. Chapter II includes a literature review about combined systems of chemical oxidation and biodegradation applied to contaminated media of different characteristics. Chapter III provides a comprehensive compilation of the materials and methods used throughout this work. Chapter IV provides a study in which the rates of PCP degradation upon free radical degradation were estimated and validated by comparison with the rates of hydroxyl free radical oxidation of lower chlorophenols (Specific Objective 1). Chapter V provides a mechanistic study for the PCP degradation in aqueous solutions due to Fenton's reaction (achieved in batch reactors) which includes a mechanistic kinetic model for these complex systems (Specific Objective 2). Chapter VI describes a study for a continuous combined system for Fenton's reactor and biodegradation for the treatment of PCP-

contaminated water, together with the development and application of a model for the combined system (Specific Objectives 3, 4 and 5). Finally, Chapter VII provides conclusions from these different studies that are relevant to this project as a whole, as well as recommendations for future work.

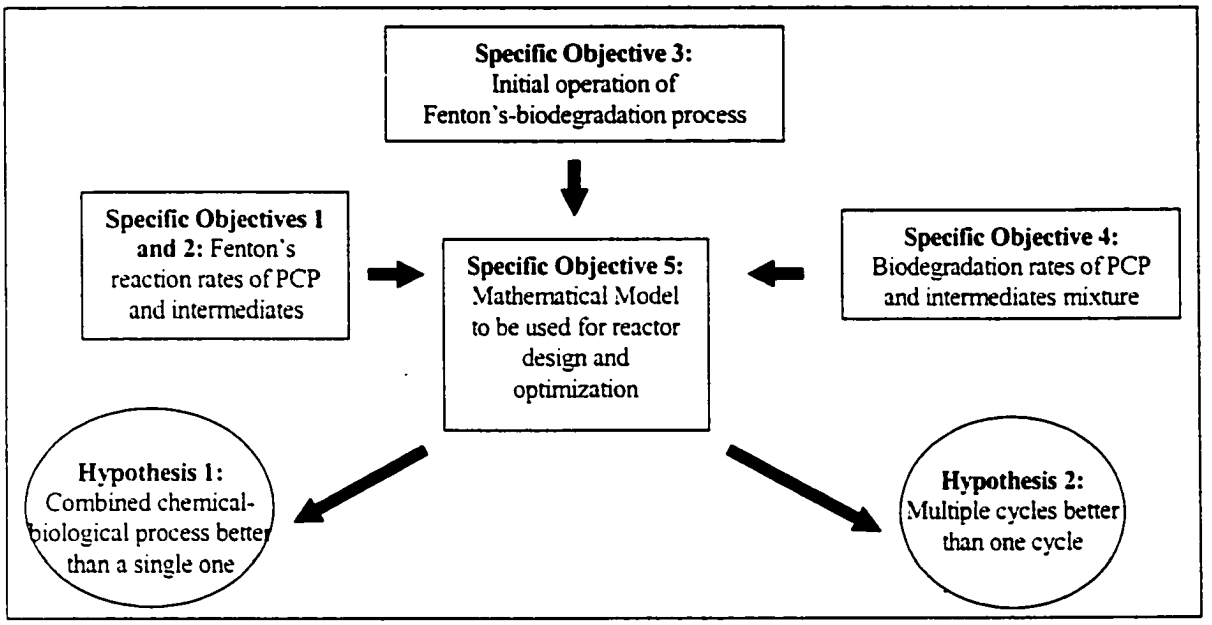

Figure 1.2. Relationships of specific project objectives and intended use of data.

1.6. References

1. Bielski, B. H. J., D.E. Cabelli, R.L. Arudi, and A. Ross. 1985. Reactivity of HO_2/O_2- Radicals in Aqueous Solution. J. Phys. Chem. Ref. Data.

2. Bigda, R. 1995. Consider Fenton's Chemistry for Wastewater Treatment. Chemical Engineering Progress. 62-66.

3. Buxton, B. V., C. L. Greenstock, W. P. Helman, and A. B. Ross. 1988. Critical Review of Rate Constants for Reactions of Hydrated Electrons, Hydrogen Atoms and Hydroxyl Radicals in Aqueous Solution. J. Phys. Chem. Ref. Data. 17:513-886.

4. Fartahazis, P. and Ross, B. 1977. Selected Specific Rates of Reactions of Transients from Water in Aqueous Solution. Washington: NBS.

5. Glaze, W. and J. Kang. 1989. Advanced Oxidation Process. Description of a Kinetic Model for the Oxidation of Hazardous Materials in Aqueous Media with Ozone and Hydrogen Peroxide in a Semibatch Reactor. Ind. Eng. Chem . Res. 28,1573-1580.

6. Graves, J. W. and T. Joyce. 1994. A critical review of the ability of biological treatment systems to remove chlorinated organics discharged by the paper industry. Wat. S.A. 20(2):155-159.

7. Hale, D.; W. Reineke, and J. Wiegel. 1994. Biological Degradation and Bioremediation of Toxic Chemicals. Chaudry, R., ed. Portland: Dioscorides Press; pp. 74-91.

8. Heinzle, E., F. Geiger, M. Fahmy, and O. Kut. 1992. Integrated Ozonation-Biotreatment of Pulp-Bleaching Effluents Containing Chlorinated Phenolics. Biotech. Prog. 8:67-77.

9. Leuenberger, C., W. Giger, R. Coney, J.W. Graydon , and E. Molnar-bica. 1985. Peristent Chemicals in Pulp Mill Effuents. Wat. Res. 19(7):885-894.

10. Litchfield and Rao. 1998. Pentachlorophenol Degradation: Laboratory and Field Scales, in Biological Treatment of Hazardous Wastes. Lewandowski, G. and L. De Filippi, eds. New York: John Wiley and Sons; pp. 271-298.

11. Marco, A., S. Esplugas, and G. Saum. 1997. How and Why combine Chemical and Biological Processes for Wastewater Treatment. Wat. Sci. Tech. 35(4):321-327.

12. Nakamura, Y., T. Sawada, F. Kobayahshi , and M. Godliving. 1997. Microbial Treatment of Kraft Pulp Wastewater Pretreated with Ozone. Wat. Sci. Tech. 35(2-3):277-282.

13. Puhakka, J. and E. Melin. 1996. In: Crawford, R. and D. Crawford, eds. Bioremediation: Principles and Applications. Cambridge University Press; pp. 254-299.

14. Scott, J. and D. Ollis. 1995. Integration of Chemical and Biological Oxidation Processes for Water Treatment: Review and Recommendations. Env. Prog. 14:88-103.

15. Scott, J. and D. Ollis. 1996. Engineering Models of Combined Chemical and Biological Processes. J. Env. Eng. 122(12):1110-1114.

16. Staehelin, J. and J. Hoigne. 1985. Decomposition of Ozone in Water in the Presence of Organic Solutes Acting as Promoters and Inhibitors of Radicsl Chain Reactions. Environ. Sci. Technol.. 19:1206-1213.

17. Stockinger, H. Removal of Biorefractory Pollutants in Wastewater by Combined Ozonation-Biotreatment. Zurich: Swiss Federal Institute of Technology; 1995.

18. Stockinger, H., E. Heinzle, and O. Kut. 1995. Removal of Chloro and Nitro Aromatic Wastewater Pollutants by Ozonation and Biotreatment. Environ. Sci. Technol.. 29:2016-2022.

19. Tang, W. Z. and C. Huang. 1997. Stoichiometry of Fenton's Reagent in the Oxidation of Chlorinated Aliphatic Organic Pollutants. Env. Technol. 18:13-23.

20. Van Kemenade, W. A. Anderson I., J.M. Scharer , and M. Moo-Young. 1996. Chemical Pre-oxidation for Enhancing Bioremediation of Contaminated Soils. Trans. I. Chem. E. 74:125-131.

21. Venkatadri, R. and R. Peters. 1993. Chemical Oxidation Technologies: Ultraviolet Light/Hydrogen Peroxide, Fenton's Reagent, and Titanium Dioxide-Assisted Photocatalysis. Haz. Waste Haz. Mat. 10:107-149.

22. Vogelpohl, A. and S. Geissen. 1996. Conference Review: International Conference of Oxidation Technologies for Water and Wastewater Treatment.

23. Walling, C. 1975. Fenton's Reagent Revisited. Acc. Chem. Res. 8:125-131.

24. Wang, Y. 1992. Effect of Chemical Oxidation on Anaerobic Biodegradation of Model Phenolic Compounds. Wat. Environ. Res. 64:268-273.

25. Zeng, Y, Page Author. Pentachlorophenol Family Pathway Map [Web Page]. 2000 Aug 24; Accessed 2000 Oct 9. Available at: http://www.labmed.umn.edu/umbbd/pcp/pcp_map.html.

CHAPTER II:

BACKGROUND INFORMATION

COMBINED CHEMICAL OXIDATION AND BIODEGRADATION FOR THE TREATMENT OF RECALCITRANT COMPOUNDS

2.1. Introduction

Many technologies have been evaluated for the treatment of different compounds in water and soil. Ideal treatment technologies involve the actual destruction of the contaminant, rather than the mere transfer of the contaminant to another phase. Bioremediation provides a cost-effective alternative when the contaminant or contaminants are biodegradable, but it is limited when these are recalcitrant. Because of their ability to degrade many contaminants (despite their biodegradability) chemical oxidation technologies have gained wide acceptance for the treatment of recalcitrant compounds and their mixtures.

Once the recalcitrant compounds have been transformed by means of the chemical treatment, their properties, including biodegradability are also modified. Often the intermediates have reduced recalcitrance with respect to the parent compound. Since biological processes are known to be 5 to 20 times less expensive than chemical processes (Marco, et al., 1997), addition of a biodegradation stage can improve the economy of the overall process.

Combinations of chemical oxidation and biological processes have potential applications to different wastes. The sequence of the combined system and the optimal configuration depend on the type of waste and contaminants, and require knowledge of their physical, chemical and biological properties, as well as the properties of the major reaction intermediates.

The purpose of this literature review is to collect reports about combinations of chemical oxidation and biodegradation, and to discuss design parameters that are relevant to the combined process. A previous extensive review for combined processes for water treatment (Scott and D. Ollis, 1995) included fifty studies published in the twenty years prior to its publication; another review included few additional reports of combined chemical oxidation and biodegradation for the treatment of contaminated soils (Van Kemenade, et al., 1996). This compilation includes twenty-four more reports of combined processes for water treatment, and eleven more for soil treatment, most of them published in the last few years that have elapsed since the above mentioned reviews.

2.2. Literature Review

Table 2.1summarizes the information on combined chemical oxidation and biodegradation studies for water contaminated with recalcitrant compounds, either alone or mixed with other contaminants. Table 2.2. is similar to Table 2.1., except that it lists reports on soil treatment, most of them *ex situ*. Some of these reports did not include biodegradation treatment. Although many other studies have been done for *in situ* soil treatment scenarios (in which water flows through porous media in the absence of active mixing) (Urynowicz and R. Siegrist, 2000; Li and F. Schwartz, 2000), or even *in situ*

field applications (Oberle and D. Schroder., 2000), these reports did not consider combination with biodegradation. For this reason, these *in situ* soil treatments were not included in this literature review. For the combined treatment scheme, "Ch" indicates the chemical process, and "Bio" the biodegradation processes. These tables contain information relevant to the type of chemical oxidation and biodegradation process used in each specific case, as well as parameters used to evaluate the efficiency of the combined process and/or the efficiencies of the individual processes. The order of the combined sequential process, as well as the reactor configuration (batch vs. continuous or fed batch, corresponding to the superscripts B, C and FB, respectively) are included. Finally, a qualitative evaluation of the results is included, together with special remarks about each specific combination of processes. The reports in these tables are discussed in the following sections.

Table 2.1. Combined chemical oxidation and biodegradation processes for the treatment of contaminated water.

Reference	Chemical (conc.) and Medium	Chemical Process	Biodegradation Process	Measure of Biodegradability	Combined Treatment Scheme	Results/Remarks
(Adams, et al., 1997)	Chloro-, nitro-, and aminophenols, as single solutions (<200 ppm as COD) in water	Ozone (variable RT, to achieve 99% deg. of substituted phenols)	Aerobic activated sludge RT <300 h	COD, EC_{50}, Cl^-, and N release, degradation of substituted phenols.	$Ch^B \rightarrow Bio^B$	Beneficial effects of ozonation on biodegradability of chloro- and nitrophenols, but detrimental for aminophenols.
(Balcioglu and F. Cecen., 1999)	Pulp beaching waste (Up to 1866 ppm as COD) in water	Photocatalysis (TiO_2) combined with H_2O_2 (RT<300h)	Aerobic activated sludge, using a fed batch reactor. (48h<RT<150h)	BOD_5/COD, Cl^- formation, Absorbance at 4 wavelenghts	$Bio^B \rightarrow Ch^B$	Combined process reduced COD and BOD_5/COD, but did not achieve dechlorination. Absorbance was not modified by Bio, but it was by Ch.
(Beltran, 1999b)	Debittering olive wastewater (from 5.5 to 8.8 g/L as TOC)	Ozonation, combined with H_2O_2 or UV (RT <2h)	Activated sludge (RT = 10 d)	COD, BOD_{10}, TOC, color	$Ch^C \rightarrow Bio^B$ when used, H_2O_2 addition was at the beginning	Biodegradation process was BOD analysis itself. Ozonation neutralized the strongly alkaline waste.
(Beltran, et al., 1999) and (Beltran, 1999a)	Wine distillery waste, mixed with domestic sewage (up to 8000 ppm as TOC) in water	Ozonation (RT from 1 to 5h)	Aerobic mixed culture, using a fed batch reactor, acclimated to non-ozonated and ozonated waste (RT < 30 h)	COD, BOD, TOC, UV_{254} absorbance, and Contois inhibitory microbial kinetics	$Ch^C \rightarrow$ Bio	Ch improved combined system. Improvement was higher for mixed distillery and sewage waste than for distillery waste alone. Mathematical models provided for both processes, but were not integrated into combined model.
(Jochimsen and M. Jekel, 1997)	Tannery wastewater previously treated anaerobically/aerobically (60-185 ppm as TOC)	Ozonation	Aerobic activated sludge (RT <14 d)	COD, TOC, COD/TOC, UV, EC_{20}, molecular weight distribution from TOC and UV analysis	Bio(previous) $\rightarrow$Ch$\rightarrow$ Bio	Effective combined system. Ch reduced toxicity

(Kamiya and H. Hirotsuje, 1998)	Synthetic, biodegradable sewage (200 ppm as TOC) in water	Ozonation (intermitent and continuos)	Aerobic Activated Sludge (RT = 12h)	TOC	Bio^C, recirculation to Ch	Ch improved the settling characteristics of biomass and reduced biomass accumulation, without reducing system efficiency
(Karrer, et al., 1997)	m-chloronitrobenzene (2 mM=306 ppm, 250 ppm as COD) Landfill leachate (350 ppm as COD)	Ozonation (RT <180 min)	Aerobic Activated Sludge (RT = 5 d)	COD, TOC, BOD_5, Ozone consumption rate	$Ch^B \rightarrow Bio^B$ Several cycles were repeated	BOD_5 test itself was the biodegradation stage. Filtration of biomass was done before subsequent Ch
(Kornmuller and U. Wiesmann, 1999)	Benzo(e)pyrene (6.2 μM) and benzo(k)fluoranthene (2.3 ppm) in dodecane-water emulsions	Two stage ozonation (RT = 10 min.)	Aerobic suspended cells (culture not specified). RT = 30h	Two benzo(e)pyrene by-products (accounting for most of the C balance) and dodecane were biodegraded. Toxicity by Ames Test	$Ch^C \rightarrow Bio^C$	Improved combined process. Effluent from oxidation was conditioned (reaction to completion) before biodegradation stage. No effects on toxicity were detected
(Larking, et al., 1999)	Polyvinyl Alcohol (0.5% w/v) in water	Fenton's Reagent (RT = 24h)	Pure culture of white rot fungus (RT = 30 d)	Polyvinyl alcohol degradation, enzymatic activity	$Ch^B \rightarrow Bio^B$	Increased combined process efficiency with respect to Bio alone.
(Marco, et al., 1997)	Synthetic waste: 2,4-dichlorophenol (300 ppm) acetic acid (1200 ppm) formic acid (1200 ppm) in water	Ozonation (RT<100min)	Aerobic activated sludge (RT = 5 d)	BOD_5, COD, TOC, BOD_5/COD, DOC/TOC, ozone consumption	$Ch^B \rightarrow Bio^B$	BOD_5 test was used as biodegradation stage. Formate and acetate degraded very slow under chemical oxidation but reduced the oxidation rate of the dichlorophenol.
(McKinzi, et al., 1999)	Pentachlorophenol (6.5μM) in water	Fenton's-type driven by microbial system	Aerobic with monoculture (*Shewanella putrefaciens*) grown under aerobic-anaerobic cyclic conditions RT <30 h	Degradation of PCP and production of two major intermediates	Coupled Ch^B -Bio^B	The microorganism reduced Fe(III) and produced H_2O_2 under aerobic conditions, and allowed the degradation of PCP, which otherwise was inhibitory at concentrations < 1ppm

(Mobius, et al., 1997)	Pulp bleaching waste (500 mg/L as COD)	Ozone (RT=1 h)	Two stage packed-bed bioreactor (RT not specified)	COD, BOD_5, BOD_5/COD, AOX, Cl-	$Ch^C \rightarrow Bio^C$	Settling tank used after ozonation for conditioning waste before biodegradation.
(Monteverdi, et al., 1992)	Wool scouring waste (triglycerides, long chain alcohols and steroids) (14 g/L as COD)	Ozone/H_2O_2 (RT = 5 min)	Anaerobic fixed bed mixed culture (RT = 2-5 d)	TOC, COD, gas production	$Bio^C \rightarrow Ch^B$	Ozonation effluent was bubbled with N_2 for 10 min. Combined system achieved reduction of a TOC fraction that could not be degraded in biodegradation stage. H_2O_2 did not improve ozonation.
(Nakamura, et al., 1997)	Pulp bleaching waste (40 g/L lignin) in water	Ozonation (RT<20h)	Aerobic activated sludge immobilized in polyurethane foam (RT<100h)	UV absorbance, Muconic, maleic and oxalic acids as by-products of ozonation. Biodegradation of by-products vs. dilution rate was characterized.	$Ch^B \rightarrow Bio^B$	Effective combined process for the degradation of lignin.
(Oeller, et al., 1997)	Pulp mill waste previously biodegraded by means of different processes (up to 1300 ppm as DOC, 350 ppm as TOC)	Ozone and ozone/UV (RT = 1 h)	First biodegradation stage not specified. Second biodegradation stage was BOD_5 assay	COD, TOC, BOD_5, BOD_5/COD, AOX, color	Bio(previous) $\rightarrow$Ch $\rightarrow$Bio	Combined system effective to degrade COD. Ineffective to degrade AOX. UV/ozonation did not improve COD with respect ozonation alone. BOD_5 measured, but otherwise biodegradation after ozonation did not exist.
(Stern, et al., 1997)	3-Methylpiridine (2 mM) 5-ethyl-2-methylpyridine (2 mM) in water	Ozonation (RT< 8 h)	Fluidized bed bioreactor (RT = 7h)	By-products (formate, oxalate, and acetate), TOC, NO_3^- production	Mixing tank, with recirculation to Ch^C and Bio^C. Also, Ch^B alone	Combined system removed high concentration of COD

(Stockinger, et al., 1995)	Synthetic waste: Chloronitroaromatics, nitroaromatics (from 0.1 to 0.8 mM; mixture was about 100 ppm as TOC) in water	Ozonation (RT = 7-12 h)	Aerobic Fluidized Bed Bioreactor (RT = 12 h approx.)	TOC, Oxygen uptake, production of Cl^- and NO_3^-; biodegradation of oxidation by-products such as acetate, formate, oxalate and glyoxylate	Ch^B and $Ch^C \rightarrow Bio^C$ Both processes connected by mixing tank with recirculation to Ch and Bio	Recycle improved dechlorination and TOC degradation. High recycle rate to bioreactor used.
(Trapido, et al., 1997)	two monochlorophenols, chlororesorcinol, chlorocresol and dichlorophenol	Ozonation (RT from 0 to 50 min.)	None	Degradation of parent compounds, formation of quinones, chloride. EC_{50} to *Daphnia magna*	Ch^{FB}	Ozonation reduced toxicity.
(Yeber, et al., 1999)	Pulp bleaching waste (up to 1240 ppm as TOC)	Photocatalysis (TiO_2 and ZnO) (RT = 1 min to 2 h)	Aerobic activated sludge, including bacteria and protozoa (RT = 3 d)	TOC, color, AOX, BOD_5, COD, EC_{50}	$Ch^B \rightarrow Bio^B$	Effluent from photooxidation was conditioned before biodegradation. BOD_5/COD ratio increased from 0.3 to 0.5; TOC, COD, AOX and color were reduced
(Yu, et al., 1994)	5 chlorophenols as single solutions (500 mg/L each)	Ozonation (RT = 5 min)	Aerobic activated sludge (acclimated and not acclimated to chlorophenolic waste). Fed batch (RT = 24h)	TOC, COD, BOD, chlorophenol concentrations measured during biodegradation.	$Ch^B \rightarrow Bio^B$	Ozonation improved biodegradability using chlorophenol-unacclimated culture, but retarded biodegradability by acclimated culture.
(Zeng, et al., 2000a)	Pyrene (crystallized on glass beads)	Ozone (CSTR combined with packed plug flow reactor filled with glass beads). (RT <120 min)	Batch, aerobic suspended culture. Commercial mixed culture used for BOD_5. RT <20 d	COD, BOD_5, toxicity to *E. coli*, Biodegradation of pyrene intermediates, characterized by first order constant (as BOD_5).	$Ch^B \rightarrow Bio^B$ and $Ch^C \rightarrow Bio^C$	Multiple simultaneous processes were likely to occur during ozonation: mass transfer, oxidation in liquid phase, oxidation at solid-liquid interface. Intermediates reached higher concentration than the expected from the solubility of the parent compound.

(Zeng, et al., 2000b)	Benzo(a)pyrene (crystallized on glass beads)	Same as above (RT <50 min)	Same as above	Same as above	Same as above	Same as above
(Zhu, et al., 1999)	Five naphthalene derivatives (up to 540 ppm as TOC) in water	Ozonation (RT<2 h)	Aerobic Suspended (RT = 8 h)	TOC, oxygen uptake, COD	$Ch^B \rightarrow Bio^B$	Ch did not reduce TOC, but affected COD and oxygen uptakes.

Table 2.2. Chemical oxidation of contaminated soil. Combination with biodegradation is indicated in the fourth column.

Reference	Chemical (conc.) and Medium	Chemical Process	Biodegradation Process	Measure of Biodegradability	Combined Treatment Scheme	Results/Remarks
(Li, et al., 1997)	Soil slurries (150-210 mg/L) from ^{14}TNT-contaminated soil (500 to 4500 mg/kg)	Fenton's (RT = 8-24 h)	None	TNT concentrations. Soil-washed toxicity as germination capacity of plant seeds (*Festuca arundinacea*). Mineralization through $^{14}CO_2$ production	Ch^B	Soil slurry was pH adjusted to 3.0 before Fenton's. Phytoremediation was used for the washed soil (no results reported).
(Martens, et al., 1995)	Nine polycyclic aromatic hydrocarbons (PAHs) in soil (400 mg/kg soil of each)	Fenton's (RT = 7 d)	Aerobic, using indigenous microbial population (RT = 56d)	Degradation of PAHs, mineralization through CO_2 production.	$Ch^B \rightarrow Bio^B$	Fenton's increased the mineralization due to biodegradation of PAHs an average of 87% with respect untreated controls.
(Stokley, et al.,)	PAHs and total petroleum hydrocarbons (TPH). Concentrations not specified.	Fenton's (RT = 1 d)	Aerobic, using indigenous microbial population (RT = 8 week)	Degradation of PAHs	$Ch^B \rightarrow Bio^B$	No beneficial effects of Fenton's pretreatment were observed, compared to a biodegradation-only experiment.
(Tyre, et al., 1991)	Pentachlorophenol, trifuralin, hexadecane and dieldrin (200 mg/kg soil of each)	Fenton's-like (using geotite and hematite native to soil) and Fenton's (RT = 5 h-2 d)	None	Contaminant degradation	Ch^B only	Organic matter in soil reduced the degradation rates of PCP and trifuralin, but not the ones of hexadecane and dieldrin. Native iron minerals proved more efficient than ferrous iron
(Watts, et al.,)	Pentachlorophenol, 250 mg/kg in sand	Fenton's-like, using iron minerals added to the sand (RT = 24 h)	None	Contaminant degradation	Ch^B only	Fenton's-like based on iron minerals was more effective than Fenton's based on soluble iron. PCP degradation was accompanied by TOC degradation and increase in Cl^-, suggesting mineralization

(Watts, et al., 1997)	Trichlorobenzene, tetrachlorobenzene, pentachlorobenzene and hexachlorobenzene in soil (0.1 mM each/kg soil)	Fenton's-like, using iron minerals native to soil	None	Contaminant degradation	Ch^B only	Evidence that oxidation occurred in the sorbed state. Use of a probe compound (nitrobenzene) to estimate oxidation strength
(Miller, et al., 1996)	Pendimethalin (100 mg/kg soil)	Fenton's (RT not specified, but a value of a few min. was implied in the text)	Leachate from Fenton's treated soil was inoculated with soil microbes (RT = 200 h), since native population was non-culturable after Fenton's	Contaminant degradation, inhibitory effects by $^{14}CO_2$ production from ^{14}C-glucose uptake rate, BOD (long term), COD, TOC, nitrate, EC_{50}	$Ch^B \rightarrow Bio^B$	Soil was pH adjusted to pH 2-3 before Fenton's. After Fenton's treatment, *Pseudomonas* became the predominant species in the microbial community. Some of the increases in BOD, COD and TOC after Fenton's were attributed to release of organics from NOM
(Gates, et al., 1995)	Trichlorethylene (1.9 to 34 mg/kg of soil) as slurry and in soil columns	Fenton's (RT = 2-24h for soil slurries and 1-2h for columns)	None	Contaminant degradation and generation of by-products (formate, ammonia, nitrate and CO_2)	Ch^B	TCE degradation independent of TCE concentration. Iron in soil was up to 3.5%. Supplementary iron was not used. TOC increased, probably due to release of soil organics.
(Ho, et al., 1995)	Nitrobenzene (1mg/L) in sand, under a simulated aquifer situation	Fenton's-like with iron minerals of sand (RT=15 d)	None	Contaminant degradation and hydrogen peroxide consumption	Ch^B	An *in situ* injection system for H_2O_2 was developed. The rate of production of hydroxyl free radicals was estimated by means of the probe contaminant.
(Bier, et al., 1999)	RDX (35 mg/kg soil)	Fenton's	None	Contaminant degradation	Ch^B	Optimal pH for Fenton's was around 3.0. Stepwise addition of Fenton's reagent was more effective that a single dose.
(EPA, 1997a) and (EPA, 1997b)	PAHs in soil slurry (6200 mg/kg)	Fenton's (RT = 1-2 d)	Aerobic, mixed culture indigenous to soil (1^{st} stage RT = 10-20 d, 2^{nd} stage RT=7.5-20 d).	PAHs concentration	$Bio^C \rightarrow Ch^C \rightarrow Bio^C$	High efficiency of combined process. Foaming was operating problem in Fenton's. First stage supplied with additional biodegradable C sources

2.2.1. Types of Contamination Amenable to Combined Treatment

A useful classification of types of contamination amenable to combined chemical and biodegradation treatment has been proposed previously (Scott, et al., 1995). Wastes with similar characteristics often required similar combined system configurations and/or operating strategies. In general, contaminated wastes that can benefit from a combined chemical oxidation and biodegradation system can be biologically recalcitrant (due to low biodegradability or inhibitory effects), largely biodegradable with small amounts of recalcitrant contaminants, or might contain a biodegradation by-product that interferes with the biodegradation stage by itself.

2.2.1.1. Recalcitrant Compounds

Many organic compounds are very slow to biodegrade due to low bioavaliability and low solubility. Chemical oxidation often creates more soluble, biodegradable intermediates. For example, ozonation of sorbed pyrene and benzo(a)pyrene sorbed to glass beads generated a complex chemical mixture in which the total concentration of organics was much higher than the solubility of the parent compounds (Zeng, et al., 2000a), resulting in higher biodegradation rates.

A study of biodegradation of Fenton's-treated polyvinyl alcohol by the white rot fungus *Pycnoporus cinnabarinus* showed higher biodegradation rates for the treated polymer with respect to the untreated one (Larking, et al., 1999). The observed increased polymer biodegradability was independent of the extent of the chemical oxidation, and further increases of the biodegradability were observed with the addition of glucose after

chemical oxidation. Biodegradation of the polyvinyl alcohol was linked to the enzymatic ligninolytic activity of the fungi. These results suggested that the chemical oxidation produced biodegradable compounds that stimulated enzyme production for the degradation of the recalcitrant parent compound. The increase in biodegradation rate that was observed after glucose addition is in accordance with this proposed mechanism.

It is likely that a chemically treated mixture of recalcitrant parent compound and biodegradable intermediates could offer the possibility of cometabolism: the enzymes used to biodegrade the intermediates as the primary energy source could fortuitously degrade the parent compound, which could not be degraded by itself (Cookson, 1995).

Highly chlorinated aliphatic compounds (normally recalcitrant to biodegradation) provide a good example of this potential. It has been observed that AOP treatment of chlorinated recalcitrant compounds (such as tetrachlorethylene and trichloroethylene) induces dechlorination and oxidation to chlorinated acetic acids (Hirvonen, et al., 1996). Although many of these highly chlorinated compounds are non-biodegradable, they can be cometabolized in the presence of a primary substrate (Cookson, 1995). Thus, AOP treatment of these compounds might have a two-fold effect: dechlorination of a portion of the parent compound to more biodegradable intermediates yields a mixture in which the biodegradable intermediates can serve as the primary carbon source, enabling the fortuitous biodegradation of the chlorinated parent compound.

A novel approach for combinations or AOP and biodegradation has also been developed for this type of waste. A study found that Fe(III)-supplemented bacteria (*Shewanella putrefaciens*) produced hydrogen peroxide by reduction of molecular oxygen and reduced Fe(III) to Fe(II), effectively creating the necessary conditions for

Fenton's reaction. When the system was operated under conditions leading to Fenton's reaction, PCP that otherwise inhibited microbial growth was instead degraded (McKinzi, et al., 1999).

2.2.1.2. Inhibitory Compounds

Some compounds are toxic or inhibitory to microbial cultures; often these effects are concentration-dependent. Chemical oxidation of the parent compound can enhance a subsequent biodegradation step by reducing the concentration of the inhibitory compounds to levels that allow the parent compound to be biodegraded rapidly. Additionally, production of chemical oxidation intermediates with lower toxicity might provide additional carbon sources.

The toxicity of wastes has been characterized by its quantitative effects on microbial degradation kinetics. Additionally, it has been measured by using specific tests: the Microtox test, based on the bacterium *Photobacterium phosphoreum* (Yeber, et al., 1999; Jochimsen, et al., 1997), the protozoan *Daphnia* (Trapido, et al., 1997) and the Ames assay, based on *Salmonella typhimurium* (Kommuller, et al., 1999). These tests measure the concentrations of different wastes required to generate a change in a given percentage of a live population: mutations, physiological activity, or cell viability. The organisms are specific for each test. Although results from some of these tests are correlated (Bulich, 1995), they have not been related to inhibitory effects on the microbial population used for the degradation stage.

A study on the ozonation of different chlorophenols reported dechlorination of the parent compounds after only a few minutes of treatment, and a subsequent reduction of toxicity to *Daphnia*, compared to the original untreated waste (Trapido, et al., 1997).

However, inhibitory by-products can become more toxic and detrimental to the biodegradation stage than the parent compound. An ozonation study of different substituted phenols found that the toxicity of chloro- and nitrophenols increased as a result of the chemical oxidation, but the opposite was found for aminophenols (Adams, et al., 1997). This toxicity was tested using *Photobacterium phosphoreum*, but the toxic effects to the microbial population used for the biodegradation stage were not evaluated.

One study measured inhibitory effects in the presence of the contaminant pendimethalin (after previous treatment with Fenton's reagent) based on the uptake of a readily available substrate (^{14}C-labeled glucose) by the same mixed culture inoculum used to perform the biodegradation step (Miller, et al., 1996). Although this study also measured the EC_{50} and BOD values of leachates from treated soil, values of ^{14}C-labeled glucose were not measured in the same samples, and thus a correlation between inhibitory effects (on the degradation of glucose) and toxicity effects (given by the EC_{50} values) was not established.

2.2.1.3. Mixed Biodegradable and Recalcitrant Compounds

Many wastes generated due to agricultural industries belong to this type, including effluents from olive debittering, tannery, wool scouring, wine making, and pulp and paper bleaching operations. The organic carbon load of these wastes is extremely high, sometimes in the order of several g/L (Nakamura, et al., 1997; Monteverdi, et al.,

1992). These wastes are complex mixtures, and include organic polymers (such as lignin or proteins) as well as aromatic and aliphatic compounds. Although a fraction of these might be biodegradable (typically the smaller monomers), the higher molecular weight compounds are generally non-biodegradable.

Most of these industrial wastes were taken directly from the process. Presumably, biodegradation of these wastes had been previously attempted, without satisfactory results (Oeller, et al., 1997; Jochimsen, et al., 1997; Monteverdi, et al., 1992). An exception was the ozonation of synthetic waste composed of the recalcitrant 2-4-dichlorophenol and the biodegradable acetic and formic acids (Marco, et al., 1997), in which the hydroxyl free radical scavenging effects of the biodegradable organic acids on the chemical degradation of dichlorophenol were demonstrated.

Characterization of these generally complex wastes (especially the non-synthetic ones) is a difficult task, and lumped parameters such as total organic carbon (TOC), biochemical oxygen demand (BOD), chemical oxygen demand (COD) and adsorbable organic halogenated compounds (AOX) are often used for this purpose. One of these parameters by itself provides limited information, and two or more are generally required. Ratios of these parameters (such as BOD/COD or COD/TOC) have been used to provide a rough measurement of a property of the mixture, such as biodegradability or oxidation state. The degree of chlorination of the waste (a measurement implied in the AOX analysis) is not always reported, but can be important for biodegradation. The estimate of the average oxidation state of the waste (given by the formula 4(TOC-COD)/TOC) proposed to characterize mixed chemical waste (Scott, et al., 1995) has not been used to characterize these wastes.

2.2.1.4. Dead-end Products from Biodegradation Processes

A previous report (Scott, et al., 1995) included three different studies in which intermediates that accumulated during biodegradation processes (and in some cases lead to inhibitory effects) were degraded by means of a chemical oxidation processes. Table 2.1. includes only one additional application since previous reviews (Scott, et al., 1995) in which a chemical oxidation process was used to improve such a biodegradation process (Kamiya, et al., 1998). In that study, biomass itself was a by-product that reduced the effectiveness of the activated sludge reactor. Intermittent ozonation was beneficial for the activated sludge processes, breaking excess filaments and improving the settling characteristics of the biomass.

2.2.2. Types of Contaminated Media Amenable to Combined Treatment

In addition to the contaminant, the type of contaminated medium is very important in the selection and design of a combined process. Although the same basic chemical oxidation principles can be applied to contaminated water and soil, soil presents a far more complex *situ*ation. Compared to water, additional mechanisms that can affect the fate of contaminants during a combined process are contaminant sorption, mass transfer, the presence of natural organic matter (NOM), and the possibility of heterogeneous reactions.

2.2.2.1. Water

Most of the combined chemical oxidation and biodegradation processes reported in literature were applied to water. This is probably the result of a more extensive experience for the application of chemical oxidation and biodegradation processes for water and wastewater treatment.

Water provides a simpler system for the study of the combined systems. Most of the relevant reaction mechanisms for AOPs have been studied in water (Buxton, et al., 1988; Walling, 1975; Glaze, et al., 1989). In addition, water systems are usually considered well mixed. Thus, adjustment of conditions important for the reaction (such as pH or concentration of oxidizing agents) is easily accomplished in aqueous media.

2.2.2.2. Soil

It has been postulated that natural organic matter (NOM) can sorb contaminants, reducing their effective availability in the free aqueous solution and modifying the reaction mechanism (Lindsey, et al., 2000). The reaction rates of ozone and hydroxyl free radicals in water with NOM of different origin are strongly dependent on the chemical structure, mainly on the degree of unsaturation and the aromatic content (Westerhoff, et al., 1999). Although NOM usually has a net effect of reducing the efficiency of the chemical oxidation, mechanisms than enhance the rates of hydroxyl free radical production due to NOM have also been proposed. A study demonstrated that fulvic acid (a type of NOM) formed pH-dependent complexes with iron(II) that reacted at higher rates with hydrogen peroxide than pure iron(II) in water (Voelker, et al., 1996).

Once an organic is attacked by free radicals in the presence of NOM, the possibility of organic radicals to bind to NOM exists. A study for the degradation of aniline by hydroxyl free radicals in the presence of NOM found that after oxidation, a significant portion of the original contaminant was incorporated into the polymeric structure of the NOM through covalent bonds (Fukushima, et al., 2000).

Due to the •OH scavenging effects of NOM in soils, the oxidant dose must be in excess in order to degrade both the contaminant and to account for the unavoidable degradation of organic matter (Gates, et al., 1995). The efficiencies used to evaluate the oxidation processes, often measured as molecules of oxidizing agent per molecule of contaminant destroyed, are often several times higher for soils than for contaminated water. For example, a study for the degradation of PCP in water and sand with Fenton's reagent used molar ratios of H_2O_2: PCP up to 10 in aqueous media, but up to 2,000 when sand was present to achieve almost total degradation of the contaminant (Tyre, et al., 1991). A previous study on the degradation of PCP in water that used an equimolar hydrogen peroxide dose with respect to PCP achieved only marginal PCP degradation (Lee, et al., 1992).

Contaminants in soil tend to sorb to particles, in some cases irreversibly. Non-aqueous phase liquids (NAPLs) can get entrapped inside soil pores. Due to this reduced availability of soil contaminants, the use of surfactants combined with chemical oxidation has shown potential to improve the efficiency of the process (Martens, et al., 1995), even though many surfactants react with hydroxyl free radicals (Pelizzetti, et al., 1989) and therefore can scavenge them and reduce the degradation efficiency of the contaminant of

interest. Thus, the use of surfactants requires careful weighing of mass transfer enhancement and interference with the chemical oxidation of the contaminant.

Soil typically includes iron minerals (such as hematite, α-Fe_2O_3 and geotite, α-FeOOH) that can enhance the oxidation efficiency of hydrogen peroxide due to reaction mechanisms of heterogeneous nature (Watts, et al., 1997; Tyre, et al., 1991). Although some of these mechanisms might be similar to Fenton's reaction (and generate hydroxyl free radicals), side reactions might catalyze the decomposition of hydrogen peroxide, thus reducing the effective yield of hydroxyl free radicals. Heterogeneous mechanisms might even occur in cases in which the contaminant is sorbed to inert surfaces, such as glass. Studies of ozonation of glass beads covered with pyrene and benzo(a)pyrene suggested that oxidation of the parent compounds and production of intermediates might have occurred at higher rates than the dissolution of the parent compounds (Zeng, et al., 2000a). In these studies, the resulting mixture of parent compound and oxidation intermediates reached concentrations several times higher than the solubility of the parent compound.

A study of ozonation of the contaminants benzo(e)pyrene and benzo(k)fluoranthene in dodecane-water emulsions (Kommuller, et al., 1999) indicated that complex processes of heterogeneous nature might occur not only at the soil-water interface, but also at the interface of the nonaqueous contaminant and water.

Most chemical oxidations in soil have been performed for extended times. This probably has been done with the intention of complete usage of the oxidizing reagents, which increases the extent of the degradation of the parent compound, and also eliminates or reduces the need to condition the medium prior to further biodegradation. Fenton's

treatment of soil often has been carried out for up to several days (Tyre, et al., 1991; Ho, et al., 1995).

When used in combination with AOP treatment in soil, biodegradation stages are also performed for much longer times than in AOP-treated water. For example, two studies used bioremediation stages of 8 weeks (Martens, et al., 1995; Stokley, et al.,) after Fenton's treatment of the contaminated soil.

Continuous soil slurry reactors for the combined Fenton's oxidation and biodegradation of PAH (EPA, 1997a) also used residence times much higher than continuous combined AOP-biodegradation systems for the treatment of PAH in water (Zeng, et al., 2000b).

2.3. Considerations for Combined Treatment Processes

2.3.1. Choice of Processes

Several chemical oxidation technologies exist, many of them based on free radical oxidation. Many options also exist for biodegradation systems that offer potential for their combination with chemical oxidation. These two types of treatment can be combined by means of different reactor configurations. These options will be discussed in this section, as well as the potential mutual effects of one type of treatment over the other. Finally, considerations for their integration into a combined process will be discussed, including potential synergistic effects, combined system constrains and evaluation of the combined system.

2.3.1.1. Factors Influencing the Choice of Chemical Oxidation Processes

The performance of a remediation treatment must be evaluated based on treatment goals. Many treatment goals, such as reduction of toxicity are difficult to evaluate. On the other hand, mineralization as a treatment goal also warranties reduction of toxicity. The remediation goal might be the complete mineralization of the organic compounds, which consists in the stoichiometric generation of carbon dioxide, a harmless compound, in which form carbon exists at its highest oxidation state. Since oxidation processes have demonstrated mineralization capabilities, they provide an alternative to biodegradation processes. Other chemical treatments exist that are reductive in nature (such as zero valent iron). Although these reductive technologies have been extensively used alone, and probably offer some potential in combination with biodegradation processes, due to the lack of practical combined applications with biodegradation they will not be discussed in this work.

Other oxidation and reduction technologies that do not rely on hydroxyl free radicals are oxidation with permanganate, chlorine dioxide, UV light (Venkatadri and Peters, 1993), electrochemical oxidation (Li, et al., 2000), wet air oxidation (Haag, et al., 1992; Scott, et al., 1995) and the reductive dechlorination of chlorinated compounds by means of zero-valent metals (Sfeir, et al., 2000). These technologies are thought to be more selective and slower than AOPs (Venkatadri and Peters, 1993), and even though most of them can achieve complete mineralization, they have not been extensively used in conjunction with biodegradation processes. There is no doubt that they offer potential for combination with biodegradation (specially to *in situ* treatment, due to the high reduction of efficiency related to self-decomposition and high scavenging rates of AOPs

under these circumstances) but due to the lack of published studies on this regard they will not be discussed in this work.

Because of this high reactivity of the hydroxyl free radicals, most AOPs are able to completely mineralize recalcitrant substances, including polyclyclic aromatic hydrocarbons (PAHs), chlorinated aromatic compounds, and azo-dyes (Stockinger, et al., 1995; Scott, et al., 1995; Tang, et al., 1997), given sufficient residence time and oxidant dose. Due to the production of oxidized intermediates that have low affinity for hydroxyl free radicals, a long treatment time and high oxidant doses in a chemical reactor is required for complete mineralization. Despite their low rate constants for oxidation by •OH, intermediates can adversely affect the oxidation of the parent compound by competing for •OH (Marco, et al., 1997). These scavenging effects are enhanced due to the stoichiometry of the degradation of larger compounds (such as PAHs), in which a single molecule can generate multiple molecules of smaller hydroxyl free radical scavengers.

Besides the common feature of AOPs of relying on the generation of hydroxyl free radicals, many side reactions lead to alternative reaction mechanisms. For example, ozone is a strong electrophile that can directly react with unsaturated molecules, but it also generates hydroxyl free radicals, which can react with organics by different reaction mechanisms than ozone. High pH values enhance the production of hydroxyl free radicals, while low pH values favor the direct reaction of ozone with the organic substrates (Hoigne, et al., 1976). These different reaction mechanisms can affect the kinetics of the degradation of the parent compound and the nature of the by-products generated from the degradation of different contaminants (Boncz, et al., 1997). As a

result, the biodegradability of ozone-treated wastes is also pH-dependent. A study in which a chlorophenolic waste stream was ozone-treated at different pH values showed that ozonation under alkaline conditions resulted in higher biodegradability of the waste than ozonation at acidic pH (Yu, et al., 1994).

Another example of side reactions during AOPs is the use of photocatalysts, in which different reaction rates and mechanisms have been observed for the UV-photoactivated forms of PAHs. Furthermore, singlet oxygen, a photoactivated form of molecular oxygen, leads to different effects on the by-products formed under oxygen saturated conditions, than those observed in oxygen-free solutions (Zepp, et al., 1979).

Some strong oxidizers that do not rely on free radicals (such as potassium permanganate) have been used for *in situ* soil treatment. Increased interest exists for these technologies, since they are less prone to self decomposition during mass transport in porous media than free radical technologies (Urynowicz, et al., 2000). However, these *in situ* treatments have not been studied in combination with biodegradation, and therefore they will not be discussed in this work.

For *ex situ* soil treatment, Fenton's reactant (and Fenton's-type oxidations using iron minerals and hydrogen peroxide) is the only AOP applied to contaminated soil, due to the availability of the oxidizing agents in the aqueous phase. A strong limitation of free radical applications is the very fast reaction rate (diffusion-limited), which implies that a significant amount of the active species is lost on side reactions (such as the oxidation of natural organic matter present in soil) before these oxidants can react with the contaminant of interest. Other AOPs present strong limitations when applied to soil. For example, technologies that rely on ultraviolet light (such as H_2O_2/UV or photocatalysis)

are limited by soil turbidity. Ozone treatment is limited by mass transfer from the gas in which ozone is generated due to the lack of efficient mixing in soil and/or the high viscosity of soil slurries.

2.3.1.2. Biodegradation

Different options exist for the biodegradation step to be combined with chemical oxidation treatment. Some of the considerations used to select the biodegradation steps involve oxygen requirements (aerobic vs. anaerobic), suspended cell cultures vs. biofilms, acclimation of the culture, and pure vs. mixed cultures. This selection depends not only on the waste to be treated, but also on the chemical oxidation process to be combined with the biodegradation stage. It has been pointed out that the optimal requirements for a culture degrading the parent compound might be entirely different than the ones for a culture degrading the chemically oxidized parent compounds (Yu, et al., 1994; Scott, et al., 1995).

A few studies included BOD analysis as a biodegradation stage itself. BOD might offer an easy-to-use tool to measure microbial activity in the presence of the carbon source being tested, but is an empirical parameter that strongly depends on the conditions used to run the test (APHA, et al., 1980). Although the BOD analysis does involve microbial degradation, it lacks engineering variables that are important in other biodegradation treatments, such as variable residence time, the possibility of continuous operation, and the option of using reactor configurations (e.g., packed-bed bioreactors) other than batch, shake flask aerobic cultures.

2.3.1.2.1. Oxygen Requirements

Few studies have used anaerobic cultures. Most of these anaerobic cultures were used to degrade waste with a high organic load and only small amounts of recalcitrant compounds, and were used before chemical oxidation (Jochimsen, et al., 1997; Oeller, et al., 1997). An additional benefit of anaerobic cultures is the low production of biomass (Cookson, 1995), although the degradation of contaminants is in general slower than the achieved by an aerobic culture.

All the biodegradation stages in soil were aerobic, probably due to the previous usage of Fenton's reagent (which generates excess oxygen) or due to the soil mixing during treatment.

Because many AOPs (such as ozonation or Fenton's reagent) generate oxygen, media treated by AOP are often saturated with oxygen. Other AOPs (such as photocatalysis and ozonation) directly generate oxygen or hydrogen peroxide, an oxygen precursor (Alnaizy, 1999; Stockinger, 1995; Trapido, et al., 1997). Thus, an anaerobic biodegradation stage immediately after such an AOP is unlikely to be used. The few reports that used anaerobic cultures for biodegradation processes after AOP oxidation of wastes required oxygen removal by purging with N_2 and sometimes providing sulfites to achieve a reducing environment (Wang, 1992; Koyama, et al., 1994). This kind of conditioning is unlikely to be practical for pilot and industrial scale applications. An alternative is the use of an aerobic stage that could deplete the oxygen of the media. If the biodegradable organic load of the waste is high, the rate of oxygen consumption might be faster than the oxygen transfer from the surrounding medium (air), enabling anaerobic conditions. Combinations of aerobic-anaerobic bioreactors have not been used

with chemical oxidation, although they might be beneficial for certain high organic load wastes. For example, an anaerobic fluidized bed reactor combined with an aerobic trickling filter proved useful to degrade pulp bleaching effluents. For this waste, the anaerobic stage achieved dechlorination, while the aerobic stage achieved COD and BOD reductions (Haggblom, et al., 1991).

In evaluating the biodegradability under anaerobic conditions, the biochemical methane potential (BMP) has been used to provide a rough measure of biodegradability equivalent to the BOD used for aerobic cultures (Wang, 1992).

2.3.1.2.2. Culture Acclimation

Many of the studies included in Tables 2.1 and 2.2 used a non-acclimated microbial population to conduct the biodegradation stage. One of these investigations found that the use of a chlorophenol-acclimated microbial population was less effective than a non-acclimated mixed culture at degrading the ozone-treated chlorophenolic waste (Yu, et al., 1994). Direct comparisons like this one are not common, but highlight the importance of the selection of the microbial culture.

Acclimation might be important not only with respect to the chemical intermediates and residual parent compound mixture, but also to other secondary conditions generated by the chemical oxidation step (such as residual oxidants). Acclimation of a single suspended culture of *Xanthobacter flavus* to hydrogen peroxide (achieved by previous exposure to sublethal concentrations) yielded higher tolerance to Fenton's reactions (including hydrogen peroxide and hydroxyl free radicals), attributed mainly to the enzymes catalase and superoxide dismutase (Buyuksonmez, et al., 1998).

The implications of this study on the feasibility of combining Fenton's reaction with biodegradation in the same reactor were discussed by the researchers. Another study of the combined ozonation and biodegradation of pyridines in water indicated that adaptation of biomass to residual ozone for about 60 days increased the efficiency of the combined system (Stern, et al., 1997).

For soil treatment, biodegradation in most cases was done using the native microbial community, which might have been acclimated to the contaminants of interest for a long time. Although previous chemical oxidation might initially decrease the microbial population of the soil, these microorganisms recovered after a period of 5 to 10 days. For this reason, a lag in microbial mineralization was observed after Fenton's chemical oxidation of PAH contaminated soil (Martens, et al., 1995). A study about the sequential biodegradation-Fenton's treatment for soil slurry indicated that despite the severe conditions during Fenton's, the microbial culturable count ranged up to 10^4 CFU/mL (EPA, 1997a).

There have been few reports of bioaugmentation (inoculation of the treated soil) with a mixed, non-acclimated culture (activated sludge) for bioremediation purposes. One study inoculated with non-acclimated activated sludge after oxidation of phenanthrene in soil using a peroxymonosulphate compound (Van Kemenade, et al., 1996). This study found that the combined treatment doubled the degradation of phenanthrene with respect to chemical oxidation alone. Another study found that culturable microorganisms were non-detectable in leachate from Fenton's-treated soil previously contaminated with pendimethaline (Miller, et al., 1996). For this reason, these researchers used a mixed non-acclimated inoculate before proceeding to the biodegradation stage. Despite the fact

that the inoculum used was a mixed culture, it was observed that *Pseudomonas sp.* (detected by means of microbial tests in selective media, compared to plating in non-selective media) dominated this microbial community after oxidation of soil with Fenton's reagent, presumably due to their ability to grow at higher rates under conditions of high nutrient availability (Miller, et al., 1996).

2.3.1.2.3. Single and Mixed Cultures

Most of the reports included in this compilation used mixed cultures to perform the biodegradation stage. From these, activated sludge was the most commonly used inoculum, followed by commercial inoculum used for different bioassays (mostly BOD). Although specialized (often pure) cultures may be required to degrade the highly recalcitrant compounds, once these compounds are transformed into the more biodegradable intermediates, a non-specialized culture is usually able to perform the biodegradation step. Additional benefits of non-specialized cultures include higher stability to disturbances in the environment, interactions among different species that lead to more complete degradation pathways, and higher degradation rates.

All of the studies in which biodegradation was applied to contaminated soil used mixed cultures, either the native microbial population or mixed culture inoculum.

In cases in which pure cultures were used to degrade a recalcitrant waste, comparison of the single biodegradation stage with a two-stage combined chemical oxidation-biodegradation system was done using the same specialized culture (Larking, et al., 1999; Scott, et al., 1995). A more realistic approach would had been comparison with biodegradation with a non specialized culture after the chemical oxidation.

2.3.1.2.4. Suspended Cells and Biofilms

As opposed to suspended cells, biofilms are cells entrapped within a matrix of water and extracellular polymers secreted by the cells themselves (Bryers, 1991). In some studies researchers provided a support material for biomass to grow as a biofilm (Stockinger, et al., 1995); (Nakamura, et al., 1997; Stern, et al., 1997; Monteverdi, et al., 1992). Compared to suspended cultures, biofilm reactors can achieve higher culture densities and higher extracellular enzymatic activities, and are more stable to disturbances of the medium (Friday, et al., 1991). Because the cells are retained in the reactor, the dilution rate can be optimized without considering cell growth. Additionally, the net growth of biofilms is minimal, which reduces the trace nutrient requirements and the ability to survive at low substrate concentrations. A potential disadvantage of biofilms with respect to suspended cells are mass transfer limitations from the surrounding media to the cells inside the biofilm.

Biofilms also have shown increased tolerance to hydrogen peroxide and other biocides. One of the mechanisms of microbial tolerance to hydrogen peroxide is the enzyme catalase, which generates oxygen from hydrogen peroxide (Stewart, et al., 2000). It has been found that biofilms have increased resistance to hydrogen peroxide compared to suspended cell cultures, tolerating up to 0.3% hydrogen peroxide in solution. This hydrogen peroxide resistance was observed even in the presence of catalase inhibitors, which implied an alternative protective mechanism against hydrogen peroxide (Liu, et al., 1998). Increased tolerance has also been observed for other antimicrobial agents such as antibiotics, chlorine, monochloramine, and iodinated compounds (Liu, et al., 1998).

Higher tolerance of biofilms to other toxic chemicals present during AOPs (such as ozone) can thus be expected.

2.3.2. Combined System Configuration

A successful combination of chemical oxidation and biodegradation will depend on the composition of the waste. Generalizations in this regard have been noted in an earlier work (Scott, et al., 1995).

Most of the combined chemical oxidation and biodegradation systems presented in Tables 2.1 and 2.2. consisted of a first step of chemical oxidation, followed by biodegradation. This is probably the result of using the combined systems as an alternative to bioremediation in cases in which the latter alone has demonstrated a lack of feasibility. Most of these chemical oxidation treatments followed by biodegradation were done for either recalcitrant or inhibitory wastes, for both water and soil contamination. The few exceptions in which biodegradation was performed prior to chemical oxidation corresponded to mixed high organic load and small amount of recalcitrant compound wastes (Nakamura, et al., 1997; Monteverdi, et al., 1992; Beltran, et al., 1999; Beltran, et al., 1999). For the case in which chemical oxidation was used to remove dead-end intermediates of biodegradation processes, a continuous or pulsed oxidation was used with a fed-batch bioreactor (Kamiya, et al., 1998).

2.3.2.1. Effects of Chemical Oxidation on Biodegradation

In general terms, the effects of a chemical oxidation stage previous to biodegradation can be on the nature of the organic compounds or on the medium. While

changes in the nature on the contaminants (to be used as carbon sources during the biodegradation stage) are the main goal of the chemical oxidation treatment, changes to the medium are secondary side effects that are sometimes unavoidable.

As can be observed in Table 2.1., by-products from AOP oxidation typically showed increased biodegradability, measured as BOD (Beltran, 1999a) or BOD/COD ratios (Marco, et al., 1997). Dechlorination of highly chlorinated compounds such as pentachlorophenol has been observed (Watts, et al., 1990). The degree of chlorination in aromatic compounds has been related to biodegradability. In some cases, dechlorination due to AOP treatment was not observed, although there was an increase in biodegradability, measured as COD (Balcioglu, et al., 1999).

Some secondary effects can induce changes in the medium, which should be taken into consideration before a biodegradation step might take place. For example, due to the production of oxygen or oxygen precursors, AOP-treated medium is oxygen saturated (see Section 2.3.1.2.1). Residual oxidizing agents might also be present, depending on their initial dose and the reaction time. If the medium was pH adjusted to optimize the chemical treatment, further conditioning might be necessary. Neutralization after Fenton's reaction also has the additional effects of precipitating iron oxides and depleting hydrogen peroxide. In some cases, passive conditioning (e.g. a holding tank for ozonation waste without any further treatment) might be enough to deplete the highly reactive ozone (Kornmuller, et al., 1999; Mobius, et al., 1997), although in other cases neutralization or destruction of residual oxidizers (such as hydrogen peroxide) to non-toxic concentrations might be necessary (Monteverdi, et al., 1992; Yeber, et al., 1999).

For Fenton's, Fe(II)-organic complexes (such as the ferrous-nitriloacetic acid complex) can be toxic to microbial populations even in the absence of hydrogen peroxide (Buyuksonmez, et al., 1998). Iron hydroxide precipitates might require filtration before biotreatment, although the toxicity of this Fenton's by-product has not been reported, and a microbial culture used after Fenton's treatment did not show these toxic effects (Scott, et al., 1995)

2.3.2.2. Effects of Biodegradation on Chemical Oxidation

During an aerobic biodegradation stage, the biodegradable carbon sources are converted to biomass and to carbon dioxide (through respiration). Thus, residual biomass is expected in the effluent from a biodegradation stream, and its presence should be taken into consideration if the waste stream will then be chemically oxidized. Hydroxyl free radicals have shown reactivity towards polymeric materials (including cellular polymers). For example, the reaction rate constants of DNA and different proteins with hydroxyl free radicals are $5x10^8$ and on the order of 10^9 L/mol• s, respectively (Buxton, et al., 1988). Thus, presence of this biomass during a chemical oxidation stage can effectively scavenge hydroxyl free radicals.

Besides biomass, nutrients (such as phosphates, nitrogen and trace minerals) are often added to the influent waste stream to promote microbial growth. As is the case with biomass, residual nutrients can potentially interfere with AOP treatment of the waste. For example, phosphate, hydrogen phosphate and dihydrogen phosphate (required nutrients for microbial growth) have reported second order rate constants of $1x10^7$, $1.5x10^5$, and $2x10^4$ L/mol•s, respectively (Buxton, et al., 1988).

If part of the carbon in a waste is transformed to CO_2 through a biological mineralization process, some of this dissolved gas is expected in the effluent from the biodegradation stage. Although at acidic conditions this carbon is rapidly eliminated from the aqueous medium, the high concentrations prevalent at neutral pH (the most natural for biodegradation) can scavenge hydroxyl free radicals.

2.3.2.3. Combination of Processes

The vast majority of the studies included in this review used batch reactors. The advantage of such a choice is the ability to run multiple reactors (usually in the form of shake flasks) simultaneously, which increases considerably the amount of data that can be generated. Traditionally, batch reactors have provided valuable information before continuous systems are studied. Operation of continuous systems (usually until steady state is reached) imposes a time constraint. On the other hand, continuous systems are more representative of reactor configurations used at larger (industrial) scale.

For the biodegradation stage, continuously operating systems have the advantage of maintaining a consistent biomass concentration, while batch reactors require inoculum at startup of every cycle. Steady state operation of the continuos system might not be very sensitive to the size of the inoculum, but the operation of batch reactors might be. As is the case of continuous systems, fed-batch reactors utilize previously generated biomass for further operation.

Continuous systems were used in a few cases. Continuous reactors allowed testing of reactor configurations that are not possible in batch reactors. For example, different recycle configurations have been done for the continuous ozonation and

biodegradation treatment of chlorinated aromatics (Heinzle, et al., 1992), chloro- and nitro- aromatic compounds (Stockinger, et al., 1995), and pyridines (Stern, et al., 1997). These recycle configurations offer the potential of closely coupling both chemical oxidation and biodegradation. Ideally this configuration would achieve chemical oxidation of the parent compound, minimizing the usage of oxidants for the degradation of intermediates, and allowing the biodegradation of these intermediates as soon as they are produced.

The simplest recycle configuration consists of diverting part of the effluent from the second treatment back to the first reactor (Heinzle, et al., 1992). More complicated reactor configurations include a conditioning tank to which recycle streams to both chemical oxidation and biodegradation stages are connected (Stockinger, et al., 1995; Stern, et al., 1997). Some of these different recycle configurations were found to increase the overall process efficiency.

There was only one continuous system for the combined Fenton's and biodegradation treatment of soil slurry contaminated with PAHs (EPA, 1997a). This study also tested the effect of a third step: Fenton's degradation after the second biodegradation step. Except a few cases, most of the PAH degradation occurred in the first two stages.

Performing more than one chemical oxidation-biodegradation sequence has also been studied in batch mode, for treatability purposes (Karrer, et al., 1997). These researchers performed ozonation of m-chloronitrobenzene with alternate BOD measurements on the waste. These BOD measurements also constituted the biological treatment. At the end of the BOD measurement, the biomass was filtered and the

ozonation-biodegradation treatment cycle repeated up to two additional times. In this study, the ratio of COD degradation to ozone consumption during ozonation alone (a measurement of the efficiency of the ozone usage) was considerable lower than multiple (up to three) ozonation-biodegradation cycles.

Sequential two-step treatments can be in the form of chemical oxidation-biodegradation and biodegradation-chemical oxidation. The option of recycle configurations further expands the opportunities for a more integrated treatment. A higher level of process integration is the performance of the two types of treatment simultaneously in the same reactor. This type of approach is already possible for other integrated technologies, such as aerobic-anaerobic biodegradation treatment.

This type of two-treatment, one-reactor integrated approach would require compromising the operating conditions for both types of treatments: tolerance of the microbial population to conditions resulting from chemical oxidation, and scavenging of oxidizing species (e.g., hydroxyl free radicals) from biodegradation by-products (such as biomass) or reactants necessary for biodegradation. Different degrees of tolerance of each part of the process to the other (see Sections on Oxygen Requirements, Culture Acclimation, as well as Effects of Chemical Oxidation on Biodegradation and Effects of Biodegradation on Chemical Oxidation) indicate that overlapping conditions in which both chemical oxidation and biodegradation might coexist, enabling the occurrence of both processes in the same reactor. The very fast reaction kinetics of AOPs (near the diffusion-limited range) and the possibility of biomass to form biofilms might enable different microenvironments in which either chemical oxidation of biodegradation are prevalent.

2.3.2.4. Synergistic Effects

Synergistic effects are defined as the positive effects due to the interaction of the two treatment steps, rather than the effects of the separate treatment steps. For instance, considering mineralization as the treatment goal for a hypothetical example in which a recalcitrant compound is chemically oxidized (but not mineralized) to form biodegradable intermediates that are mineralized during a biodegradation stage, the majority of the observed efficiency would correspond to the interaction of both treatment steps. For this same case, since mineralization only would proceed during biodegradation of the chemically-oxidized waste, the efficiency of each treatment step in the absence of the other would be null but the efficiency due to combined (synergistic) effects might account for most of the overall system efficiency.

Another example of a synergistic effect would be the one of combined AOP treatment and biodegradation/cometabolism for aliphatic aromatics (see section on Recalcitrant Compounds), if the treatment goal is degradation of the parent compound. As in the previous hypothetical example, the interaction of both treatment steps would provide a higher efficiency than the mere summation of the efficiencies achieved in each process in the absence of the other treatment step.

Synergistic effects might also be observed in the form of improved system stability. For example, ozonation of waste contaminated with 5 different chlorophenols enabled the biodegradation of the waste by an unacclimated culture. A study on the ozonation of chlorophenols found that in the absence of ozonation, biodegradation could only be performed by a chlorophenol-acclimated culture (Yu, et al., 1994). In this case,

the benefit of a combined system would be the usage of a non-specialized culture, which might have less stringent requirements than a specialized one (Scott, et al., 1995).

2.3.2.5. System Constraints

The practice of constraining some of the operating conditions of a combined system has been proposed, under the reasoning that systems (either chemical or biological ones) at industrial or pilot scale operate under limited allocation of resources (Scott, et al., 1995). Such resources are often present in the form of residence time for reactor design purposes (Scott, et al., 1996). Thus, the constrained residence time of the combined system (a typical design limitation) would be the summation of the residence time in the chemical oxidation and biodegradation stage.

However, for the combination of chemical oxidation and biodegradation processes, a direct comparison of residence time in a chemical reactor and a bioreactor (or the implicit summation of both to calculate the residence time on the overall system) is difficult. Tables 2.1 and 2.2 clearly show that the residence time used for biodegradation stages are always longer than for chemical oxidation processes. In some cases, a residence time of a few minutes in a first stage of chemical oxidation was used, compared to the residence of several days in the biodegradation stage used in other cases. Thus, given these considerations, the residence time of the combined system approaches the value of the residence time in the biodegradation stage.

On the other hand, the cost of the chemical oxidation treatment might be several times higher than the cost of the biodegradation stage. Therefore, the cost of the

combined system (another typical design limitation) might be heavily influenced by the chemical oxidation stage.

2.3.2.6. Study and Evaluation of the Combined System

Treatment goals for combined systems might vary. Table 2.1 and Table 2.1 indicate that mineralization, detoxification, degradation of the parent compound, or reduction of specific parameters such as BOD or COD are some options. Often, several parameters used to characterize the original waste were monitored during a combined treatment, without a treatment goal explicitly stated, despite the fact that this should be an essential step.

For soil contamination it has been common practice to set the process treatment goal in terms of the degradation of a recalcitrant compound, rather than on complete mineralization (stoichiometric production of CO_2). Other soil parameters, such as TOC or COD, are not monitored often as in contaminated water, probably due to the high background levels naturally occurring in this medium. For example, mineralization might originate from the contaminant as well as the oxidation (chemical or biological) of natural organic matter (NOM) or NOM-by products formed due to chemical oxidation. Radiolabeled contaminant studies have proved useful to differentiate between different sources of mineralization (Miller, et al., 1996) or other NOM-contaminant interactions (Fukushima, et al., 2000).

Many areas of chemical reactor engineering (including environmental applications) have traditionally been based on rate laws for the different existing

chemical species. There are some issues related to a rigorous approach applied to the combination of AOPs and biodegradation for the treatment of contaminants:

a) The approach of accounting for all chemical species and their interactions during AOP and biodegradation, although rigorous, might not be practical due to the very fast and complex nature of AOPs. Many AOP-based treatments on single compounds generate numerous (up to dozens) intermediates. A significant amount of work has been done only to characterize such chemical mixtures. Much more work would be required to estimate the kinetics of such a system, and to apply a rigorous approach (including different biodegradabilities of all compounds and possible interactions among different compounds) to study the biodegradation kinetics of such a mixture.

b) The treatment goal is often the reduction of a lumped parameter that provides a rough measurement of a property of the waste (such as TOC, BOD, COD, EC_{50}, and so on). For some of these parameters, contributions from individual compounds might be direct (such as TOC or even COD), but for other lumped parameters related to biodegradability or toxicity these contributions might be complex. The way in which a traditional reactor design approach (based on degradation of particular compounds through rate laws) relates to some of these parameters might be a major challenge for reactor design of combined chemical oxidation and biodegradation systems. Correlations among specific chemical species and lumped parameters might be a useful tool in achieving this goal.

The efficiency of the system can be defined based on achievements toward the treatment goal. Scott and Ollis (Scott, et al., 1995) have proposed evaluation of the global treatment efficiency as the summation of the efficiencies of the individual chemical and biodegradation steps. A second method estimates synergistic (interaction) effects, which can be considered by calculating the ratios of the efficiencies of each treatment steps while operating as a combined system with respect the efficiencies of each treatment operating alone. Part of this analysis is frequently reported in Table 2.1. and Table 2.2., by comparing the performance of the combined system with respect the performance of one of the steps by itself. However, a more complete analysis (for example comparison of the performance of the combined system with respect the performance of each of the separate steps) is rarely done.

2.4. Conclusions

Combinations of chemical oxidation and biodegradation have potential for the treatment of different wastes. The type of reactor configuration will depend on the type of waste. Most of the studies to date have been done on inhibitory or recalcitrant compounds, for which chemical oxidation followed by biodegradation has proven to be a successful combined treatment configuration. A few more studies have been done on mostly biodegradable waste mixed with small amounts of recalcitrant compound. For this type of waste, a previous biodegradation stage (which in practice is sometimes anaerobic) can enhance the performance of a further chemical oxidation stage due to the removal of oxidant scavengers. Only one study was found in which a dead-end

biodegradation by-product was chemically oxidized to enhance the performance of the biodegradation process.

Selection of both chemical oxidation and biodegradation options should be done considering the combined system, due to the large number of potential effects of one stage of the process over the other. For example, a specialized cell culture might be required to degrade an inhibitory compound during a single biodegradation process, but a non-specialized mixed culture can provide more efficient to degrade the same waste if it is previously chemically oxidized.

Although most of the basic processes inherent to oxidation of contaminants in water are thought to be applicable to contaminated soil, additional processes that exist in soil are sorption, mass transfer, the presence of natural organic matter, and probably chemical reactions of heterogeneous nature. Another consideration for the treatment of soils is that native microbial populations seem to survive the chemical oxidation process, eliminating the need of inoculum. Due to the nature of soils, Fenton's is almost exclusively the only AOP used. Scavenging effects impose the requirement of using higher oxidation strengths for the treatment of contaminated soil than water. For soils, chemical oxidation using Fenton's as well as biodegradation (if used in combination) are performed for considerably longer treatment times than in water.

The rigorous chemical engineering approach for reactor design, which accounts for all possible reactions and their rates, can provide a useful tool for the study of combined systems. However, the fast and complex nature of AOPs makes this approach difficult. AOP-treated waste often results in complex mixtures, even in the simplest case in which the waste is a single compound. A further complication is the fact that often the

treatment goal for such a combined system is based on an empirical (lumped) parameter (such as BOD) that might be related to the composition of the mixture in complex ways.

Direct comparisons of both chemical oxidation and biodegradation stages under typical reactor design constrains are difficult. For example, chemical oxidation is usually a very fast, expensive treatment. On the other hand, biodegradation is usually a slower, economically favorable treatment. It is likely that imposing design constraints on the combined system in any of these variables (e.g., treatment cost or residence time) will result in uneven allocation of the resources. For example, if the objective is a short treatment time, the combined system analysis will favor the chemical oxidation process. On the other hand, if treatment cost is the major system design constraint, it is likely that evaluation of the treatment steps will favor biodegradation. Since many systems work under more than one system constraint, probably a weighing system for allocation of resources (for example, cost weighted for treatment time) might prove useful in making direct comparisons for both parts of the combined system.

2.5. References

1. Adams, C., R. Cozzens, and B. Kim. 1997. Effects of Ozonation on the Biodegradability of Substituted Phenols. Wat. Res. 31(10):2655-2663.

2. Alnaizy, R. Mechanism and Kinetic Study for the Hydroxyl Free Radical Mediated Photoxidation of Organic Contaminated Aqueous Solutions. Fort Worth: Texas A&M University; 1999.

3. APHA, AWWA, and WPCF. Standard Methods for the Examination of Water and Wastewater. 15th ed. Washington; 1980.

4. Balcioglu, I. A. and F. Cecen. 1999. Treatability of Kraft Pulp Bleaching Wastewater by Biochemical and Photocatalytic Oxidation. Wat. Sci. Tech. 40(1):281-288.

5. Beltran, F. J. Garcia-Araya and P. Alvarez. 1999a. Wine Distillery Wastewater Degradation. 2. Improvement of Aerobic Biodegradation by Means of an Integrated Chemical (Ozone)-Biological Treatment. J. Agric. FoodChem. 47:3919-3924.

6. Beltran, F. J. Garcia-Araya J. Fradex P. Alvarez and O. Gimeno. 1999b. Effects of Single and Combined Ozonation with Hydrogen Peroxide or UV Radiation on the Chemical Degradation and Biodegradability of Debittering Table Olive Industrial Wastewaters. Wat. Res. 33(3):723-732.

7. Beltran, F., J. Garcia-Araya, and P. Alvarez. 1999. Wine Distillery Wastewater Degradation. 1. Oxidative Treatment Using Ozone and Its Effect on the Wastewater Biodegradability. J. Agric. FoodChem. 47:3911-3918.

8. Bier, E., J. Singh, Z. Li, S. Comfort, and P. Shea. 1999. Remediating Hexahydro-1,3,5-Trinitro-1,2,5-Triazine- Contaminated Water and Soil by Fenton Oxidation. Env. Toxicol. and Chem. 18(7):1078-1084.

9. Boncz, M., H. Bruning, W. Rulkens, E. Sudholter, G. Harmsen , and J. Bijsterbosch. 1997. Kinetic and Mechanistic Aspects of the Oxidation of Chlorophenols by Ozone. Wat.Sci. Tech. 35(4):65-72.

10. Bulich, A. 1995. Bioluminiscence Assays. in: Bitton, G. and B. Dutka, eds. Toxicity Testing Using Microorganisms.

11. Buxton, B. V., C. L. Greenstock, W. P. Helman, and A. B. Ross. 1988. Critical Review of Rate Constants for Reactions of Hydrated Electrons, Hydrogen Atoms and Hydroxyl Radicals in Aqueous Solution. J. Phys. Chem. Ref. Data. 17:513-886.

12. Buyuksonmez, F., T. Hess, R. Crawford, and R. Watts. 1998. Toxic Effects of Modified Fenton Reactions on Xanthobacter flavus FB71. Appl. Env. Microbiol. 64(10):3759-3764.

13. Cookson, J. 1995. Bioremediation Engineering. Design and Application. New York: McGraw-Hill.

14. EPA. 1997a. Emerging Technology Bulletin: Innovative Methods for Bioslurry Treatment. EPA/540/F-96/505. EPA.

15. EPA. 1997b. Emerging Technology Summary: Innovative Methods for Bioslurry Treatment. EPA/540/SR-96/505. EPA.

16. Friday, D. and R. J. Portier. 1991. Development of an Immobilized Microbe Bioreactor for VOC Applications. Env. Prog. 10(1):30-39.

17. Fukushima, M., K. Tatsumi, and K. Morimoto. 2000. The Fate of Aniline after a Photo-Fenton Reaction in an Aqueous System Containing Iron(III), Humic Acid, and Hydrogen Peroxide. Environ. Sci. Technol. 34:2006-2013.

18. Gates, D. and R. Siegrist. 1995. In-Situ Chemical Oxidation of Trichloroethylene Using Hydrogen Peroxide. J. Environ. Eng. (9):639-644.

19. Glaze, W. and J. Kang. 1989. Advanced Oxidation Process. Description of a Kinetic Model for the Oxidation of Hazardous Materials in Aqueous Media with Ozone and Hydrogen Peroxide in a Semibatch Reactor. Ind. Eng. Chem . Res. 28,1573-1580.

20. Haag, W. and C. D. Yao. 1992. Rate Constants for Reaction of Hydroxyl Radicals with Several Drinking Water Contaminants. Environ. Sci. Technol. 26: 1005-1013.

21. Haggblom, M. and M. Salkinoja-Salonen. 1991. Biodegradability of Chlorinated Organic Compounds in Pulp and Paper Bleaching Effluents. Wat. Sci. Tech. 24(3/4):161-170.

22. Heinzle, E., F. Geiger, M. Fahmy, and O. Kut. 1992. Integrated Ozonation-Biotreatment of Pulp-Bleaching Effluents Containing Chlorinated Phenolics. Biotech. Prog. 8:67-77.

23. Hirvonen, A., R. Ruhkannen , and P. Kallioskoski. 1996. Removal of Chlorinated Ethylenes in Contaminated Ground Water by Hydrogen Peroxide Mediated Oxidation Process. Env. Toxicol. 17:263-272.

24. Ho, C., M. Shebl , and R. Watts. 1995. Develpmento of an Injection System for In Situ Catalyzed Peroxide Remediation of Contaminated Soil. Haz. W. and Haz. Mat. 12(1):15-25.

25. Hoigne, J. and H. Bader. 1976. The Role of Hydroxyl Radical Reactions in Ozonation Processes in Aqueous Solutions. Wat. Res. 10:377-386.

26. Jochimsen, J. and M. Jekel. 1997. Partial Oxidation Effects During the Combined Oxidative and Biological Treatment of Separated Streams of Tannery Wastewater. Wat. Sci. Tech. 35(4).

27. Kamiya, T. and H. Hirotsuje. 1998. New Combined System of Biological Porcess and Intermittent Ozonation for Advanced Wasteater Treatment. Wat. Sci. Tech. 38(8-9):145-153.

28. Karrer, N. J., G. Ryhiner, and E. Heinzle. 1997. Applicability Test for Combined Biological-Chemical Treatment of Wastewaters Containing Biorefractory Compounds. Wat. Res. 31(5):1013-1020.

29. Kornmuller, A. and U. Wiesmann. 1999. Continuous Ozonation of Polycyclic Aromatic Hydrocarbons in Oil/Water Emulsions and Biodegradation of Oxidation Products. Wat. Sci. Tech. 40(4-5):107-114.

30. Koyama, O., Y. Kamagata, and K. Nakamura. 1994. Degradation of Chlorinated

Aromatics by Fenton Oxidation and Methanogenic Digester Sludge. Wat. Res. 28 (4):895-899.

31. Larking, D., R. Crawford, F. Christie, and F. Lonergan. 1999. Enhanced Degradation of Polyvinyl Alcohol by *Pycnoporus cinnabarinus* after Pretreatment with Fenton's Reagent. Appl. and Env. Microbiol. 65(4):1798-1800.

32. Lee, S. and J. Carberry. 1992. Biodegradation of PCP enhanced by chemical Oxidation Pretreatment. Wat. Environ. Res. 64(5):682-690.

33. Li, D. and F. Schwartz. Efficiency Problems related to Permanganated Oxidation Schemes. In: G. Wickramanayake; A. Gavaskar, and A. Chen., eds. Remediation of Chlorinated and Recalcitrant Compounds; 2000; Monterey. Batelle Press; 2000.

34. Li, T. and J. Farrell. Kinetic and Mechanistic Investigation of Halocarbon Reduction at Iron Cathodes. In: G. Wickramanayake; A. Gavaskar, and A. Chen., eds. Remediation of Chlorinated and Recalcitrant Compounds; 2000; Monterey. Batelle Press; 2000.

35. Li, Z. M., M.M.Peterson, S.D. Comfort, P.J. Shea, and B.T. Oh. 1997. Remediating TNT-Contaminated Soil by Soil Washing and Fenton Oxidation. Sci. Tot. Environ. 204:107-115.

36. Lindsey, M. and M. Tarr. 2000. Inhibition of Hydroxyl Radical Reaction with Aromatics by Dissolved Natural Organic Matter. Environ. Sci. Technol. 34:444-449.

37. Liu, X., F. Roe, A. Jesaitis, and and Z. Lewandowski. 1998. Resistance of Biofilms to the Catalase Inhibitor 3-Amino-1,2,2-triazole. Biotech. and Bioeng. 59(2):156-162.

38. Marco, A., S. Esplugas, and G. Saum. 1997. How and Why combine Chemical and Biological Processes for Wastewater Treatment. Wat. Sci. Tech. 35(4):321-327.

39. Martens, D. and W. Frankenberger. 1995. Enhanced Degradation of Polycyclic Aromatic Hydrocarbons in Soil Treated with an Advanced Oxidative Process-Fenton's Reagent. J. Soil Contam. 4(2):1-16.

40. McKinzi, A. and T. Dichristina. 1999. Microbially Driven Fenton Reaction for Transformation of Pentachlorophenol. Environ. Sci. Technol. 33:1886-1891.

41. Miller, C., Ri. Valentine, M. Roehl, and P. J. J. Alvarez. 1996. Chemical and Microbiological Assesment of Pendimethalin-Contaminated Soil after Treatment with Fenton's Reagent. Wat. Res. 30(11):2579-2586.

42. Mobius, C. and M. Cordes-Tolle. 1997. Enhanced Biodegradability by Oxidative and Radiative Wastewater Treatment. Wat. Sci. Tech. 32(2-3):245-250.

43. Monteverdi, A., B. Rindone, V. Andreoni, A. Rozzi , and C. Sorlini. 1992. Analysis, Anaerobic Treatment and Ozonation of Wool Scouring Wastewater. J. Environ. Sci. Healh. A(4):1157-1172.

44. Nakamura, Y., T. Sawada, F. Kobayahshi , and M. Godliving. 1997. Microbial Treatment of Kraft Pulp Wastewater Pretreated with Ozone. Wat. Sci. Tech. 35(2-3):277-282.

45. Oberle, D. and D. Schroder. Design Considerations Fo In-Situ Chemical Oxidation. In: G. Wickramanayake; A. Gavaskar, and A. Chen., eds. Remediation of Chlorinated and Recalcitrant Compounds; 2000; Monterey. Batelle Press; 2000.

46. Oeller, H. J., I. Demel , and G. Weinberger. 1997. Reduction in Residual COD in Biologically Trated Paper Mill Effluents by Means of a Combined Ozone and Ozone/UV Reactor Stages. Wat. Sci. Tech. 35(2-3):269-276.

47. Pelizzetti, E., D. Minero, V. Maurino, A. Sciafani, H. Hidaka , and N. Serpone. 1989. Photocatalytic Degradation of Nonylphenol Ethoxylated Surfactants. Environ. Sci. Technol. 23:1380-1385.

48. Scott, J. and D. Ollis. 1995. Integration of Chemical and Biological Oxidation Processes for Water Treatment: Review and Recommendations. Env. Prog. 14:88-103.

49. Scott, J. and D. Ollis. 1996. Engineering Models of Combined Chemical and Biological Processes. J. Env. Eng. 122(12):1110-1114.

50. Sfeir, H.; A. Randall; D. Reinhart; M. Chopra; C. Clusen, and D. Geiger. Biotic Attenuation and Zero-Valent Iron Permeable Barrier Technology. In: G. Wickramanayake; A. Gavaskar, and A. Chen., eds. Remediation of Chlorinated and Recalcitrant Compounds; 2000; Monterey. Batelle Press; 2000.

51. Stern, M., E. Heinzle, O. Kut , and K. Hungerbuhler. 1997. Removal of Substituted Pyridines by Combined Ozonation/Fluidized Bed Biofilm Treatment. 35. 4:329-335.

52. Stewart, P., F. Roe, J. Rayinier, J. Elkins, Z. Lwandowski, U. Ochsner, and D. Hassett. 2000. Effect of Catalase on Hydrogen Peroxide Penetration into Pseudomonas aeruginosa Biofilms. Appl. Environ. Microbiol. 66(2):836-838.

53. Stockinger, H. Removal of Biorefractory Pollutants in Wastewater by Combined Ozonation-Biotreatment. Zurich: Swiss Federal Institute of Technology; 1995.

54. Stockinger, H., E. Heinzle, and O. Kut. 1995. Removal of Chloro and Nitro Aromatic Wastewater Pollutants by Ozonation and Biotreatment. Environ. Sci. Technol.. 29:2016-2022.

55. Stokley, K.; E. Drake, and R. Prince. The role of Fenton's reagent in Soil

Bioremediation. Foruth International In Situ and On Site Bioremediation Symposium. pp. 484-492.

56. Tang, W. Z. and C. Huang. 1997. Stoichiometry of Fenton's Reagent in the Oxidation of Chlorinated Aliphatic Organic Pollutants. Env. Technol. 18:13-23.

57. Trapido, M., Y. Veressinina, J. Hentunen, and A. Hirvonen. 1997. Ozonation of Chlorophenols: Kinetics, By-products and Toxicity. Environ. Technol. 18:325-332.

58. Tyre, B., R. Watts, and G. Miller. 1991. Treatment of Four Biorefractory Contaminants in Soils Using Catalyzed Hydrogen Peroxide. J. Environ. Qual. 20:832-838.

59. Urynowicz, M. and R. Siegrist. Chemical Degradation of TCE DNAPL by Permanganate. In: G. Wickramanayake; A. Gavaskar, and A. Chen., eds. Remediation of Chlorinated and Recalcitrant Compounds; 2000; Monterey. Batelle Press; 2000.

60. Van Kemenade, W. A. Anderson I., J.M. Scharer , and M. Moo-Young. 1996. Chemical Pre-oxidation for Enhancing Bioremediation of Contaminated Soils. Trans. I. Chem. E. 74:125-131.

61. Voelker, B. and B. Sulzberger. 1996. Effects of Fulvic Acid on Fe(II) Oxidation by Hydrogen Peroxide. Environ. Sci. Technol. 30(4):1106-1114.

62. Walling, C. 1975. Fenton's Reagent Revisited. Acc. Chem. Res. 8:125-131.

63. Wang, Y. 1992. Effect of Chemical Oxidation on Anaerobic Biodegradation of Model Phenolic Compounds. Wat. Environ. Res. 64:268-273.

64. Watts, R. M. Udell and R. Monsen. Use of Iron Minerals in Optimizing the Peroxide Treatment of Contaminated Soils. Wat. Environ. Res. 65(7):839-844.

65. Watts, R., A. Jones, P.Cheng, and A. Kelly. 1997. Mineral-catalyzed Fenton-like Oxidation of Sorbed Chlorobenzenes. Wat. Env. Res. 69(3):269-275.

66. Watts, R., M. Udell, P. Rauch, and S. Leung. 1990. Treatment of Pentachlorophenol-Contaminated Soils Using Fenton's Reagent. Haz. W. Haz. Mat. 7(4):335-345.

67. Westerhoff, P., F. Aiken, G. Amy , and J. Debroux. 1999. Relationships between the Structure of Natural Organic Matter and Its Reacivity towards Molecular Ozone and Hydroxyl Radicals. Wat. Res. 33(10):2265-2276.

68. Yeber, C., J. Rodriguez, J. Baeza, J . Freer, C. Zaror, N. Duran, and H. Mansilla. 1999. Toxicity Abatement and Biodegradability Enhancement of Pulp Mill Bleaching Effluent by Advanced Chemical Oxidation. Wat. Sci. Tech. 40(11-12):337-342.

69. Yu, Y. and S. Hu. 1994. Preoxidation of Chlorophenolic Wastewaters for their Subsequent Biological Treatment. Wat. Sci. Tech. 29(9):313-320.

70. Zeng, Y., P. K. A. Hong, and D. Wavrek. 2000a. Chemical-Biological Treatment of Pyrene. Wat. Res. 34(4):1157-1172.

71. Zeng, Y., P. K. A. Hong, and D. Wavrek. 2000b. Integrated Chemical-Biological Treatment of Beno(a)pyrene. Environ. Sci. Technol. 34:854-862.

72. Zepp, R. and P. Schlotzhauer. 1979. Photoreactivity of Selected Aromatic Hydrocarbons in Water. In: P.W. Jones and P. Leber, eds. Polynuclear Aromatic Hydrocarbons. Ann Arbor: Ann Arbor Science Publishers; pp. 141-156.

73. Zhu, S., Q. Zhang, L. Wang, J. Chen, and H. Lian. 1999. Effect of Ozonation of Naphthalene Derivatives on Their Elimination, TOC and Biodegradability. Bull. Environ. Contam. Toxicol. 63:101-108.

CHAPTER III

MATERIALS AND METHODS

3.1. Chemicals

All chlorophenols were purchased from Sigma, as were nitrobenzene (used for competitive kinetics experiments) and the surrogate and internal standards used for extraction and analysis. The purity of these chemicals was 98% or higher (except for dibromophenol, which was 95% pure). $FeCl_2 \cdot 4H_2O$ (99%+) was purchased from Baxter.

Hydrogen peroxide (non-stabilized, 31.4%), sodium chloride (99.9%) and perchloric acid (conc., 67%) were all purchased from Fisher. Dilute perchloric acid (0.1 N) was prepared from concentrated acid for safe handling and storage before use. pH adjustment was achieved by either diluted sodium hydroxide, sulfuric acid or perchloric acid. Perchloric acid was used for pH adjustment during the competitive kinetics experiments. Sulfuric acid was used for pH adjustment during continuous operation of the Fenton's-biodegradation system and batch experiments of Fenton's oxidation of PCP to avoid any toxic effects of perchlorates on the microbial population. Sodium hydroxide was used to adjust the pH of the continuous system, and to prepare PCP saturated solutions.

Pesticide-grade solvents used for organic analysis (chloroform and ethyl acetate) were purchased from Fisher.

Standards for organic acid previously reported as by-products of phenol and chlorophenol under different AOP treatments were compared to the observed by-products analyzed by different techniques. These organic acid standards were: maleic (Aldrich, 99%), muconic (Aldrich, 99%), glyoxylic (Aldrich, 50% solution in water), formic (Sigma, reagent grade), succinic (Sigma, reagent grade), fumaric (Sigma, reagent grade), and oxalic (Sigma, reagent grade).

3.2. Analytical Methods

3.2.1. Organic Substrates

The concentration of the different substrates (chlorophenols) was determined with an HP 5890 Series II gas chromatograph with a mass spectral detector and a 50-m HP-5 crosslinked 5% PH ME silicone capillary column of 0.2 mm I.D. and 0.33 μm film thickness. The GC temperature program was: 50 °C initial temperature held for 2.0 min followed by increases of 20 °C/min to 160 °C and then at 6 °C/min to 250 °C (total run time = 22.5 min). One mL of each aqueous sample was spiked with 0.2 mM dibromophenol (as surrogate) in acetone solution, adjusted to pH less than 1.0, extracted with 0.5 mL of chloroform, and then dosed with dibromobenzene as internal standard before injection (the final concentration of the internal standard in the extracted solution was 0.05 mM). Acidification and dosage of the surrogate solution was done immediately after sampling. Quenching of the PCP degradation was achieved by acidification of the sample and an excess of acetone dosed from the surrogate solution. The effectiveness of this quenching procedure was verified by the quantitative recovery of the surrogate. Quantification of each analyte was performed on the basis of the

respective main ion in the mass spectrum (e.g., 266 for PCP, 252 for the surrogate and 236 for the internal standard) normalized with respect the internal standard. The extraction efficiency was evaluated by means of the surrogate, which typically was higher than 90%. Data from samples with surrogate concentrations out of the interval of ±15% around the mean were analyzed a second time. Two different sets of standard solutions were used for the cases in which retention times and quantitating ions in the spectra lead to interferences of different analytes (e.g., the two trichlorophenol isomers). Detection limits for the analytes ranged close to 0.25 ppm. Solvent (chloroform) blanks were run before the samples containing the analytes to ensure that there were no interferences with the quantitating ions.

3.2.2. Oxidizing Reagents

3.2.2.1. Hydrogen Peroxide

Concentration of the stock hydrogen peroxide solution was determined before use with standard 0.3 N potassium permanganate to confirm its lack of degradation during storage. The end point was identified by a slight pink color due to an excess of potassium permanganate. Hydrogen peroxide solutions were diluted to 250.0 mL with water for analysis to a final concentration between 0.1 and 0.5%. Aliquots (25.0 mL) of this dilute solution were diluted with about 250 mL in an Erlenmeyer flask, then acidified with 10.0 mL concentrated sulfuric acid before titration.

Lower concentrations of hydrogen peroxide (< 30 ppm) were analyzed by means of the titanium sulfate method (APHA, et al., 1980). The detection limit of this method is about 1.0 mg/L ($3x10^{-05}$ mol/L). One mL samples were added to 100 μL of 6.7 g/L

$TiSO_4 \cdot 8H_2O$ in 17% sulfuric acid aqueous solution. The color of the yellow peroxo-complex was allowed to develop, and then the absorbance was read at 405 nm and compared to a series of six calibration standards (made by diluting the potassium permanganate-titrated hydrogen peroxide solution). Hydrogen peroxide analysis was done immediately after sampling (by adding the sample to a 1.5 mL cuvet containing the titanium reactant) to avoid the need for quenching with sulfites since an excess of these was shown to interfere with this assay. Lack of interference of ferrous and ferric iron (at the concentrations used in this work) with this analysis was tested and confirmed. A more sensitive 2,9 dimethyl, 1,10-phenanthroline method (Kosaka, et al., 1998) could not be used due to interference of ferrous iron.

3.2.2.2. Ferrous Iron

Ferrous iron was measured by the 1,10 phenanthroline method. One mL samples were treated with 200 μL of ammonium acetate buffer solution (pH = 3.2, 250 g/L in water), and 150 μL of 1,10 phenanthroline solution (1.0 g/L in water). Absorbance was measured at 508 nm and compared to ferrous iron calibration standards with a concentration range from 0 to 10 ppm (APHA, et al., 1980). Ferrous iron calibration standards were prepared from stock iron solution at 100 ppm (containing 0.7022 g $Fe(NH_4)_2(SO_4)_2 \cdot 6H2O$ dissolved into 29% H_2SO_4 in water and then the volume adjusted to 1.0 L). One hundred μL of hydroxylamine solution (10 g $NH_2OH \cdot HCl$ in 100 mL ddH_2O), 100μL of sodium acetate buffer (100 g $NaC_2H_3O_2 \cdot 3H_2O$ in 400 mL glacial acetic acid) and 150 μL of 1,10 phenanthroline solution (1.0 g/L in water) were added to 1.0 mL of the calibration standard solutions. Ferrous iron analysis was done immediately

after sampling (by adding the sample to a 1.5 mL cuvet containing the rest of the reactants) to avoid the need for quenching with sulfites since an excess of these was shown to interfere with this assay. Lack of interference of hydrogen peroxide with this assay at concentrations lower than 1 mM was confirmed by spiking treated samples with hydrogen peroxide (up to 1%) without change in absorbance after the color had been formed. The detection limit of this assay is close to $5.0x10^{-07}$ mol/L (approximately 0.3 ppm).

3.2.3. Chemical Oxidation By-products

3.2.3.1. Chloride Analysis

Chloride ion was measured by means of the mercuric thiocyanate method. One mL of sample was added to 80 μL of mercuric thiocyanate solution (Hach # 22121) and 40 μL of ferric ion solution (Hach # 22122-42). The color was allowed to develop, absorbance was read at 455 nm and compared to calibration standards (from 0 to 10 ppm). Chloride analysis was done immediately after sampling (by adding the sample to a 1.5 mL cuvet containing the rest of the reactants) to avoid the need for quenching with sulfites since an excess of these was shown to interfere with this assay. Lack of interference of residual hydrogen peroxide with this analysis was confirmed by spiking treated samples with hydrogen peroxide (up to 1%) without change in absorbance after the color had been formed. Quenching achieved by this procedure was probably due to the excess of methanol in which the ferric iron solution was prepared.

3.2.3.2. Organic PCP By-products

3.2.3.2.1. Concentration by Solid Phase Extraction

Ionizable by-products were concentrated by means of 100 mg ion-exchange Supelclean C-SAX solid phase extraction (SPE) tubes (Supelco). The tubes were conditioned with 2 mL of 1 M NaCl, and washed with 10 mL of deionized water. The neutralized sample was drawn through the tube at 1 mL/min by means of a peristaltic pump, and then washed with 2 mL of deionized water. Finally, the concentrated ionizable compounds were eluted with 500 μL of HCl 0.1 M in water before HPLC analysis.

3.2.3.2.2. High Pressure Liquid Chromatography

After concentration with SPE, ionizable by-products were analyzed by means of a method optimized for organic acids, using a Waters HPLC with a Bio-Rad Aminex HPX-87H column (Bio-Rad 125-0140) and a UV detector at 210 nm. The mobile phase was 0.008 N sulfuric acid, prepared in Nanopure water with a conductivity of 18 mΩ and degassed by boiling for 20 min under vacuum. A flow rate of 0.6 mL/min was used at a temperature of 35 °C. The retention time of different standards of previously reported by-products observed during different Advanced Oxidation Process treatment of phenol and chlorophenol is given in Table 3.1.

Table 3.1. Previously reported phenol and chlorophenols by-products and their retention time using the HPLC method described.

Standard	**Retention time (min)**	**References**
Catechol	6.5	(Alnaizy, 1999; Gould, et al., 1976)
Oxalic Acid	6.85	(Alnaizy, 1999; Gould, et al., 1976; Wang, 1992)
Maleic Acid	8.77	(Alnaizy, 1999; Gould, et al., 1976)
Glyoxylic Acid	9.84	(Alnaizy, 1999; Gould, et al., 1976; Wang, 1992)
Formic Acid	14.24	(Alnaizy, 1999; Wang, 1992)
Fumaric Acid	16.52	(Alnaizy, 1999; Gould, et al., 1976)
Muconic Acid	31.05	(Alnaizy, 1999; Gould, et al., 1976)

3.2.3.2.3. Derivatization

A derivatization procedure developed to analyze organic acids in urine (H. Liebich , et al., 1999) was applied to the SPE-concentrated samples for identification purposes, combined with gas chromatography and mass spectrometry. This method is suitable for derivatization of organic acids in aqueous solution, using trimethyl oxonium tetrafluoroborate (TMO, obtained from Aldrich).

The derivatization with trimethyl oxonium tetrafluoroborate (TMO) consists of:

a) Add approximately 20 mg of Na_2CO_3 to 2.0 mL of sample, to alkalize.

b) Add approximately 30 mg of TMO in five equal portions, during 4 minutes. Wait one minute and neutralize with approximately 15 mg $NaHCO_3$.

c) Repeat previous step two more times (three times total).

d) Repeat step b) one more time, omitting neutralization. Instead, alkalize to pH 8 with approximately 20 mg Na_2CO_3.

e) Repeat step b) one more time, but neutralize with 20 mg $NaHCO_3$ (instead of 15 mg).

f) Stopper vial and incubate for 2 min at 100 °C.

g) Cool to room temperature.

h) Extract with 0.5 mL of chloroform before GC analysis.

Derivatized samples were run on the same GC/MS equipment used for the analysis of chlorophenols. The derivatization method was validated with formate, oxalate, maleate, succinate and muconate standards in water at a concentration of 10 ppm each. The GC temperature program was optimized for separation of the derivatized organic acid standards presented in Table 3.2. as follows: 30 °C initial temperature held for 2.0 min followed by increases of 10 °C/min to 260 °C (total run time = 25 min). The mass spectrometer was initially on, then turned off from 5.5 to 7.5 min to avoid the solvent peak. The derivatized (methylated) organic acids were identified by their mass spectra, with their respective retention time indicated in Table 3.2. Derivatization of the PCP ionizable by-products observed by SPE-HPLC (See Sections 3.13.2.3.2.1 and 3.2.3.2.2) was not successful.

Table 3.2. GC/MS analysis of derivatized organic acid standards.

Analyte	Retention time (min)
Methyl Formate	From 3 to 4.2 min (before solvent front)
Dimethyl Oxalate	7.52
Dimethyl Maleate	12.55
Dimethyl Succinate	12.65
Dimethyl Muconate	16.95

3.2.3.2.4. Liquid-Liquid Extraction

PCP reaction by-products were analyzed by means of extraction with ethyl acetate after acidification with phosphoric acid. Fifty μL of concentrated phosphoric acid and 2.0 mL of ethyl acetate were added to 2.0 mL of sample. The mixture was shaken for 20 min. and the organic phase was then concentrated to 100 μL under a gentle N_2 stream. Dibromobenzene was used as internal standard before analysis: a concentrated dibromobenzene solution in acetone was added to achieve a final concentration of 0.025 mM. These solutions were analyzed using the same GC/MS method used to analyze PCP (see Section 3.2.1), except that a modified temperature profile was used to achieve better separation of the different observed peaks: 50 °C initial temperature held for 2.0 min followed by increases of 20 °C/min to 150 °C and then 3 °C/min to 250 °C (total run time = 37 min).

3.2.4. Total Organic Carbon

Purgeable total organic carbon (TOC) was analyzed with a Dohrmann DC-80 TOC Analyzer after acidifying the sample with phosphoric acid (2 drops per 25 mL) and purging with oxygen for 7 min to eliminate interferences from CO_2. One mL of sample was injected into the analyzer. Calibration for this analysis was done using a potassium phthalate solution equivalent to 10.0 ppm of TOC (this solution was prepared by diluting a 2000 ppm standard solution, which contained 0.425 g/L of reagent-grade potassium hydrogen phthalate). This assay is based on oxidation of the organic carbon in the sample by means of oxidation with potassium persulfate (2% solution) in the presence of ultraviolet light, generating stoichiometric amounts of CO_2, which is detected with a non-dispersive infra-red (NDIR) detector. The integrated area of the NDIR signal is directly related to the carbon concentration in the sample.

Samples that contained biomass were first centrifuged at 13,200xg using acid-washed teflon bottles. The supernatant was used for TOC analysis, after being transferred to an acid-washed glass vial. The solids from centrifugation were used for protein analysis (see Section 3.2.5.1).

3.2.5. Biomass Analysis

Two quantitative assays were used to measure biomass indirectly: protein and DNA. In addition, plating tests were used to determine the ability of the biomass to grow on two different carbon sources: PCP and TSB media (non-selective).

3.2.5.1. Protein

Biomass was estimated indirectly by means of a protein assay since iron oxide and hydroxide precipitates could interfere with direct dry mass determination or the measurement of optical density (600 nm) that is commonly used to estimate biomass concentration. Samples were collected and frozen until analysis. Samples were centrifuged in 250 mL Teflon bottles for 25 min. at 13200xg. The biomass pellet was washed (resuspended) with potassium phosphate pH 7 buffer (0.04 M KH_2PO_4 and 0.061 M K_2HPO_4) and centrifuged again. The resuspension-centrifugation cycle was repeated twice, and the biomass was concentrated to a final volume of 3.0-10.0 mL. The biomass concentrate was lysed with a sonicator (Ultrasonic Processor XL, Heath Systems) for 20 min (in 50% on-off mode during 4-s cycles) and analyzed for protein using the micro-BCA assay (Pierce Catalog No. 23235ZZ). An aliquot of 500 µL of freshly prepared BCA reactant were added to 500 µL of the cell lysate and incubated at 60 °C for 1 h. The absorbance was read at 562 nm and compared to bovine serum albumine standards. Protein concentrations were estimated by means of the dilution factor achieved during the biomass concentration stage.

3.2.5.2. DNA

Large size DNA was extracted from effluent from the bioreactor, after shaking the packed column. The sample was centrifuged and transferred to a 40-mL polycarbonate centrifuge tube. An aliquot of 75 mg of lysozyme and 7.5 mL 200 mM phosphate buffer (pH 8.0) were added to the tube. The tube was then vortexed for 30 s and heated for 90 min at 37 °C. After heating, 450 µL of 20% sodium dodecyl-sulfate (SDS) were added to

the tube and the tube was vortexed for 30 s. The centifuge tubes were frozen at –80 °C for 30 min to begin a freeze-thaw lysis cycle. After 30 min, the tube was placed in a 65 °C water bath for 20 min to thaw. The freeze-thaw cycle was repeated twice more and then the tube centrifuged at 10,000xg for 15 min. The supernatant (containing the cell lysate) was separated and saved. This last step was repeated again, after resuspending the pellet and heating the suspension for 10 min at 65 °C. The supernatant from this step was combined with the one obtained from the previous step. An aliquot of 15 mL of Tris-buffered liquid phenol (pH 8.0) were added to the tubes with the supernatant to remove contaminating compounds and protect the DNA from nucleases. The tube was centrifuged at 10 °C and 5500xg for 5 min. The upper aqueous phase was recovered again into another 40 mL centrifuge tube. Potassium acetate (2.8 mL, 8M) was added to the tube, and the tube placed in an ice bath for 10 min. Then the tube was centrifuged again for 15 min at 10000xg. The supernatant was recovered again into a 40 mL tube containing 30 mL of 95% ethanol. The suspension was kept at –20 °C overnight to precipitate the DNA. Then the tube was centrifuged for 25 min at 10000 g. The supernatant was discarded and the pellet dried for 8-16 h at room temperature over a tared weigh boat, before final gravimetric determination of the DNA.

3.2.5.3. Microbial Plating

The ability of the biomass present in the packed bed to degrade PCP was tested by means of plating tests on an agar medium that contained PCP as the only carbon source at a concentration of 0.5 mg/L. This low concentration of PCP was chosen to avoid potential inhibitory effects. This medium was made by mixing 7.5 g of Bacto-Agar with

38.5 mL PAS concentrate (which includes phosphates and nitrogen) and 5 mL of PAS 100x salts solution (which includes trace minerals required for microbial growth), and then diluted to 500 mL (Bedard, et al., 1986). The composition of the solutions used to make this medium is given in Table 3.3. Plates were poured after autoclaving the medium.

Table 3.3. Composition of the two solutions used to make PAS Medium.

PAS Concentrate (added to 500 mL water)	**PAS 100x Salts (added to 500 mL water)**
NH_4Cl 13.8 g	$CaCl_2 \cdot 2H_2O$ 0.15g
KH_2PHO_4 10.97g	$FeSO_4 \cdot 7H_2O$ 0.5g
K_2HPO_4 28.39 g	$MnSO_4 \cdot H_2O$ 2.5g
	$MgSO_4$ 9.75g
	H_2SO_4 2 drops

The ability of the biomass present in the packed bed to grow on a readily available carbon source was tested by plating on ¼-strenght Tripticase Soy Broth (TSB; Difco), which is a non-selective medium. The less concentrated medium was chosen to simulate an oligotrophic (low nutrient) environment, representative of the Fenton's-treated PCP wastewater. The plates were prepared by dissolving 3.75 g TSB and 7.5 g Bacto-Agar in 500 mL water. Plates were poured after autoclaving the medium for 30 min at 121 °C.

3.2.6. pH

pH was measured using an Orion Research digital ionalyzer/501, previously calibrated with phosphate buffer solutions at pH 7.0 and 4.0.

3.2.7. Dissolved Oxygen

Dissolved oxygen was measured with a Cole Parmer Model 01971-00 analyzer, equipped with a 16-mm steam-sterilizable polarographic oxygen electrode (Phoenix Electrode Co.). The electrode was calibrated at 0% oxygen saturation with N_2-purged water for 20 min, and at 100% with water bubbled with air for 20 min. Measurements were temperature-compensated.

3.3. Experimental Setup

3.3.1. Batch Experiments

Two types of batch experiments were performed during this work. In the first type of experiment, reaction rates of chlorophenols with unknown reaction rates with hydroxyl free radicals were estimated by means of the competitive kinetics method. In this method, a compound with a known reaction rate with hydroxyl free radicals was degraded in the presence of one or more substrates with unknown rates of reaction. These solutions were treated with different doses of hydrogen peroxide, and the dimensionless extent of degradation of the compounds were used to estimate the unknown rate constants of the compounds of interest.

In the second type of batch experiment, aliquots of PCP solutions were treated with combinations of hydrogen peroxide and ferrous iron to achieve degradation of the contaminant. The effect of combinations of different reactants on the degradation of PCP was tested in these experiments.

3.3.1.1. Competitive Kinetics Experiments

The following chlorophenols were tested in two-substrate (the chlorinated phenol and nitrobenzene) experiments: 2,4,6-trichlorophenol (246TCP), 2,3,4,6-tetrachlorophenol (2346TeCP), and pentachlorophenol (PCP). Solutions of one of these selected chlorophenols and nitrobenzene (initial concentrations about 0.01 mM) were prepared in Reagent Type I Grade water and stirred for 24 hr. The pH of these solutions was adjusted to 3.5 with 0.1 M $HClO_4$. Sodium chloride was added to adjust the ionic strength to 0.05 M (accounting for the previous pH adjustment and further additions of ferrous salts). Oxygen was eliminated from the solution by bubbling it with N_2 for 30 min to avoid possible interference due to singlet oxygen. The solution was then stoppered and transferred to an anoxic chamber to avoid redissolution of atmospheric O_2. Aliquots of this solution (35 mL) were dosed into 40-mL amber glass vials and ferrous chloride was added to a final ferrous ion concentration of 0.2 mM. The resulting solutions were spiked with variable amounts of H_2O_2 (zero for the control), shaken for a few seconds and left stationary to react overnight. Each treatment was conducted in duplicate. Chemical analyses were performed the following day to minimize sample degradation.

3.3.1.2. Batch Experiments for the Degradation of PCP

Experiments with pure PCP solutions were conducted to study the degradation of PCP in aqueous media due to Fenton's reaction. These data were used to validate a kinetic model for Fenton's systems in the presence and absence of the contaminant of interest (PCP). The effects of some additional treatments on the degradation of PCP were also tested in batch experiments. These reactants were hydrogen peroxide (in the absence of ferrous iron), the presence of high initial concentrations of chloride, the use of ferric sulfate instead of ferrous sulfate, the presence of biomass, and the presence of microbial nutrients.

Fenton's batch degradation experiments of PCP were performed in two different ways:

a) the reactants were mixed and allowed to react for extended periods (12 h) before analysis (steady state experiments), and
b) the reactants were mixed and then aliquots taken at different reaction time were analyzed (time course experiments).

3.3.2. Continuous System

3.3.2.1. Continuous System Setup and Operation

A bench-scale continuous system was used to study the combination of Fenton's degradation of PCP and the biodegradation of the Fenton's-treated waste. The system consists of two continuously stirred tank reactors (CSTR) in series (2.0 L Bioflo C-30 reactors, from New Brunswick Scientific). The volume of each of these reactors (250 mL for the chemical reactor and 750 mL for the bioreactor) was controlled by means of an

exit tubing line attached to a peristaltic pump and set at a the desired height. In the first reactor, Fenton's treatment of the PCP was achieved at pH 3.5, which is the reported optimum (Glaze, et al., 1989; Bigda, 1995). pH control for this reactor was achieved by means of a Markson pH/ORP controller Model 630 equipped with an Ingold combination pH electrode. The solution used for pH control was 0.5 N NaOH. Ferrous iron and hydrogen peroxide were dosed at the levels at which experiments were run (ferrous iron at $2.0x10^{-04}$ mol/L and hydrogen peroxide at concentrations below $5.0x10^{-04}$mol/L). This reactor was protected from light to avoid direct production of hydroxyl free radicals due to photocatalyzed degradation of hydrogen peroxide.

The effluent from the Fenton's reactor was fed to a bioreactor, in which the low-pH exit stream from the Fenton's reactor was neutralized with 0.2 N NaOH solution. pH control was achieved by means of an Omega pH/ORP controller Model PHCN-36 630 equipped with an Ingold combination pH electrode. The solution used for pH control was 0.2 N NaOH. This bioreactor was originally inoculated with activated sludge from the Fort Collins wastewater treatment plant. Supplementary nutrients (phosphates, trace minerals and nitrogen) were fed to this reactor.

Since the concentration of carbon in the feed stream was limited by the low solubility of PCP (14 ppm, or $5.5x10^{-05}$ mol/L), there was the concern that a microbial culture of suspended cells might not grow at high enough rates. Thus, a packed-bed column was provided in this reactor. High recirculation flow rates to the packed bed ensured a well-mixed bioreactor. The rate of recirculation to the packed bed was 20 times higher than the feed rate to the stirred tank.

Additional benefits of this packed bed bioreactor configuration with respect to a suspended-cell bioreactor using are improved resistance of the biofilm to inhibitory chemicals from the chemical reactor (such as hydrogen peroxide) and reduced growth rates.

In addition to the basic reactor configuration of sequential chemical and biodegradation treatment, the effect of recycling part of the bioreactor effluent back to the chemical reactor was tested. Two recycle rates (20% and 40%) were used for this purpose. This recycle rate is defined as the ratio of the flow rate of the bioreactor effluent that is send back to the chemical reactor (represented by a dotted line in Figure 3. 1) with respect the total inlet flow to the system.

After a new operating condition was established, 48 h were allowed to pass to achieve steady before sampling. This period of 48 h represents 32 residence times for the chemical reactor and 8.7 residence times for the bioreactor (operating at a residence time of 5.5 h). A set of samples at a hydrogen peroxide dose of $2.2x10^{-04}$ mol/L was also taken at 36 hours. The 36-h samples from the chemical reactor were analyzed for PCP and the ones from the bioreactor were analyzed for TOC, yielding similar results than the samples taken at 48 h, supporting the idea that 48 h was enough time for the system to achieve steady state.

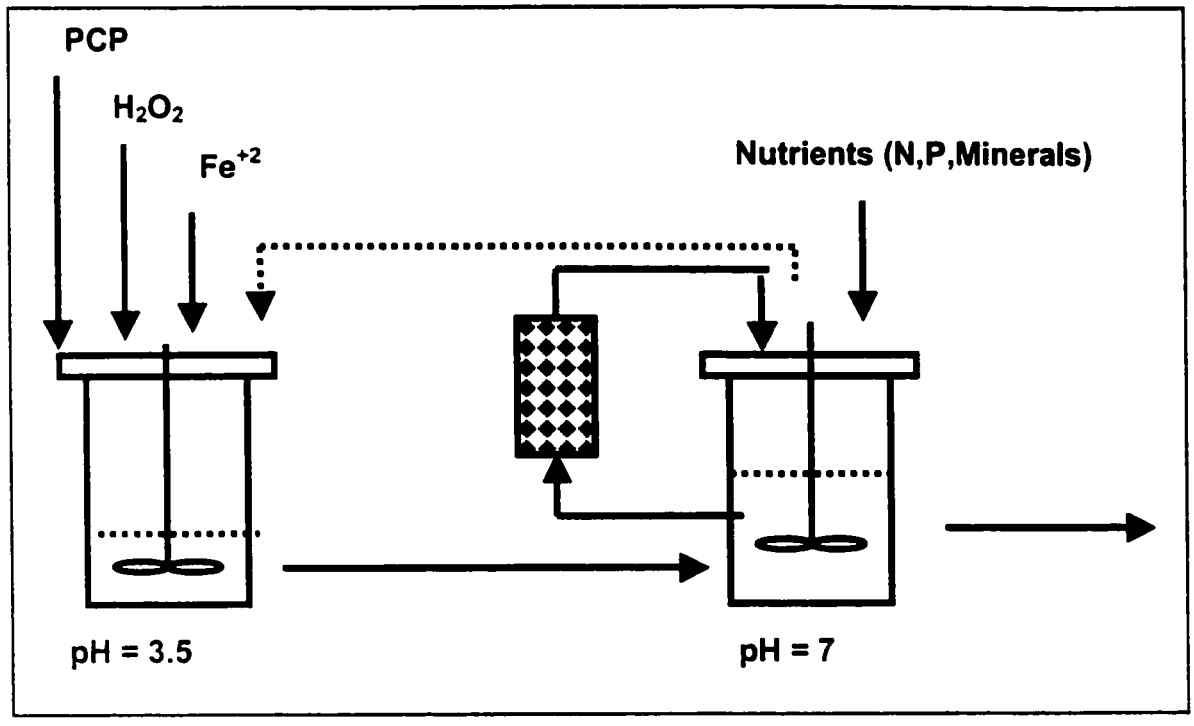

Figure 3. 1. Continuous combined system for Fenton's oxidation and biodegradation of PCP contaminated water.

3.3.2.2. Continuous System Reactants

3.3.2.2.1. PCP solution

The PCP solution was prepared with deionized and dechlorinated water. Residual chlorine concentrations were of concern to both the Fenton's oxidation stage and to the biodegradation stage since chlorine rapidly degrades H_2O_2 and is also a microbial inhibitor.

Dechlorination of the water used to prepare the PCP solution was achieved by bubbling compressed air through the deionized water for at least 24 h and then autoclaved (121°C for 20 min) and allowed to cool to room temperature. Then, 0.8 mL of 0.1 M NaOH per L of solution were added to facilitate the dissolution of PCP. Finally, PCP

was weighed to achieve the reported solubility at neutral pH (14 ppm) and added to the previously prepared water. The final pH of solutions prepared in this way was close to 10.0. PCP dissolution under these conditions was achieved in less than 48 h. If the pH adjustment were omitted, PCP would take about one week to dissolve. In some cases, without pH adjustment, PCP dissolution was not complete. The flow rate of this solution to the combined chemical oxidation and biodegradation system was 3.5 L/day. Actual dosage of this solution was verified by volume measurements on a volumetric scale in the 26-L glass carboys used to prepare and hold the solution.

3.3.2.2.2. Hydrogen Peroxide

Hydrogen peroxide solutions were prepared with Reagent Type I Grade water (Nanopure Barnstead water with a conductivity of 18 mΩ) by dissolving concentrated (31.5%) hydrogen peroxide to achieve a final concentration of 0.3 and 0.6 g/L ($8.8x10^{-03}$ and $1.8x10^{-02}$ mol/L, respectively). After preparation, this solution was protected from light using aluminum foil. Flow rate of this reactant to the system was kept at low levels to avoid dilution effects of the main PCP feed. Actual dosage to the system was measured by weighing the flask holding the solution. This solution was fed to the chemical reactor at a flow rate of 85 mL/day, which represented about 2.5% of the total flow rate to the combined system. Accounting for dilution rate, the 8.8e-03 and 1.8 e-02 mol/L solutions yielded actual dosages of $2.2x10^{-04}$ mol/L and $4.4x10^{-04}$ in the chemical reactor, respectively.

3.3.2.2.3. Ferrous Iron

The solution used to dose ferrous iron to the continuous system was prepared with Reagent Type I Grade water (Nanopure Barnstead water with a conductivity of 18 mΩ). Ferrous salts, as $FeSO_4 \cdot 7H_2O$ (2.3 g, Baker) were dissolved in about 700 mL of water. Concentrated H_2SO_4 (6.4 mL) was added to avoid spontaneous oxidation of ferrous iron before the solution reached the Fenton's reactor and the volume was adjusted to 1.0 L. A solution prepared in this way contained $8.3x10^{-03}$ mol/L of ferrous iron. After preparation, this solution was protected from light using aluminum foil. Flow rate of this reactant to the system was kept at low levels, to avoid dilution effects of the main PCP feed. The actual dosage of this reactant to the system was measured by weighing the holding flask. This solution was fed to the chemical reactor at a flow rate of 85 mL/day, which represents about 2.5% of the total flow rate to the combined system. This dilution rate yielded an effective dosage of $2.0x10^{-04}$ mol/L in the chemical reactor.

3.3.2.2.4. Supplementary Nutrient Medium

The supplementary nutrient medium was based in the composition of the mineral salts based agar (PAS) used for plating tests. This medium was modified in order to eliminate chloride that could interfere with the chloride ion analysis (according to Table 3.4).

The effect of recycling the effluent from the biodegradation stage back to the Fenton's reactor was tested in this project. Thus, a certain residual amount of nutrients in this recycle stream was expected. For this reason, nitrogen in the supplementary nutrient medium was in the form of nitrates instead of the ammonium chloride originally included

in the formulation. The reported reactivity of nitrate towards hydroxyl free radical is about two orders of magnitude smaller than the one of ammonia, and about five orders of magnitude smaller than the one of nitrite (Buxton, et al., 1988; Fartahazis and Ross, 1977).

Since the process of assimilatory nitrate reduction (which allows the utilization of nitrates as the nitrogen source and involves intracellular enzymatic reduction of nitrates to nitrite and then to ammonia) is widespread among bacteria (Prescott and others, 1999), the bioavailability of this substitute nitrogen source was not an issue.

Nitrogen supplementation was stoichiometric to the carbon concentration in the PCP feed, based on an estimated optimal nitrogen-to-carbon molar ratio of 0.2:1 (Shuler and Kargi, 1992). The ratio of phosphates and trace nutrients to nitrogen was the same as the ones in the PAS medium (see Section 3.2.5.3).

Table 3.4. Composition of the two solutions used to make chloride-free PAS supplementary nutrients.

Cl^--free PAS Concentrate (added to 500 mL water)	**Cl^--free PAS 100x Salts (added to 500 mL water)**
$NaNO_3$ 22.1g	$CaSO_4 \cdot 2H_2O$ 0.18g
KH_2PHO_4 10.97g	$FeSO_4 \cdot 7H_2O$ 0.5g
K_2HPO_4 28.39 g	$MnSO_4 \cdot H_2O$ 2.5g
	$MgSO_4$ 9.75g
	H_2SO_4 2 drops

3.4. References

1. Alnaizy, R. Mechanism and Kinetic Study for the Hydroxyl Free Radical Mediated Photoxidation of Organic Contaminated Aqueous Solutions. Fort Worth: Texas A&M University; 1999.

2. APHA, AWWA, and WPCF. Standard Methods for the Examination of Water and Wastewater. 15th ed. Washington; 1980.

3. Bedard, D., R. Unterman, L. Bopp, M. Brenna, M . Haberl , and C. Johnson. 1986. Rapid Assay for Screening and Characterizing Microorganisms for the Ability to Degrade Polychlorinated Biphenyls. Appl. Environ. Microbiol. 51(4):761-768.

4. Bigda, R. 1995. Consider Fenton's Chemistry for Wastewater Treatment. Chemical Engineering Progress. 62-66.

5. Buxton, B. V., C. L. Greenstock, W. P. Helman, and A. B. Ross. 1988. Critical Review of Rate Constants for Reactions of Hydrated Electrons, Hydrogen Atoms and Hydroxyl Radicals in Aqueous Solution. J. Phys. Chem. Ref. Data. 17:513-886.

6. Fartahazis, P. and Ross, B. 1977. Selected Specific Rates of Reactions of Transients from Water in Aqueous Solution. Washington: NBS.

7. Glaze, W. and J. Kang. 1989. Advanced Oxidation Process. Test of a Kinetic Model for the Oxidation of Organic Compounds with Ozone and Hydrogen Peroxide in a Semibatch Reactor. Ind. Eng. Chem . Res. 28,1580-1587.

8. Gould, J. and W. Weber. 1976. Oxidation of Phenols by Ozone. Journal WPCF. 48(1):47-60.

9. H. Liebich and E. Gesele. 1999. Profiling of organic acids by capillary gas chromatography-mass spectrometry after direct methylation in urine using trimethyloxonium tetrafluoroborate. J. of Chromatography A . 843:237-245.

10. Kosaka, K., H. Yamada, S. Matsui, S. Echigo, and K. Shishida. 1998. Comparison among the Methods for Hydrogen Peroxide Measurements to Evaluate Advanced Oxidation Processes: Appliation of a Spectrophotometric Method Using Copper(II) Ion and 2,9-Dimethyl-1,10-phenanthroline. Environ. Sci. Technol. 32:3821-3824.

11. Prescott, L.; J. Harley , and D. Klein. 1999. Microbiology. Boston: McGraw-Hill.

12. Shuler, M. and Kargi. 1992. Principles of Biochemical Engineering.

13. Wang, Y. 1992. Effect of Chemical Oxidation on Anaerobic Biodegradation of Model Phenolic Compounds. Wat. Environ. Res. 64:268-273.

CHAPTER IV

HYDROXYL FREE RADICAL REACTIVITY TOWARDS CHLORINATED PHENOLS

4.1. Introduction

Chlorinated phenols are a broad group of contaminants generated during wood treating and pulp and paper bleaching operations. The annual world-wide production of chlorophenols is estimated at about 200,000 tons (Hale, et al., 1994). Major environmental releases of these contaminants result from direct application to soil as biocides, leaching from wood products, synthesis during pulp and paper bleaching operations and emissions from operating facilities (Hale, et al., 1994). Chlorophenols are often mixed with other, more toxic compounds, such as polychlorinated phenoxyphenols, dibenzodioxins and dibenzofurans (Puhakka, et al., 1996). Many chlorophenols are toxic to humans. In addition, they have bacteriocidal properties and are very persistent in the environment (Haggblom, et al., 1995). Some chlorophenols have been designated as priority pollutants by the US EPA, and many chlorophenol contaminated sites have been targeted for cleanup in Europe and the US (Puhakka, et al., 1996).

Because most of these compounds (singly or in mixtures) are recalcitrant to biodegradation, alternative treatment technologies such as advanced oxidation processes (AOPs) have received increased interest. The term AOP includes all technologies that

generate hydroxyl free radicals. Examples include the combination of hydrogen peroxide and ultraviolet light, ozonation, Fenton's reaction, photocatalysis with semiconductors (such as titanium dioxide), and combinations of these (such as the photo-Fenton's reaction) (Glaze, et al., 1989b). The oxidation potential of the hydroxyl free radical is second only to fluorine, twice that of chlorine, and 25% higher than ozone (Buxton, et al., 1988). Because of the high reactivity of the hydroxyl free radicals, they rapidly attack most organic molecules and generate more oxidized intermediates, which are generally characterized by lower toxicity and higher biodegradability (Scott, et al., 1995). Extensive oxidation of organic wastes can achieve complete mineralization and stoichiometric production of CO_2 (Stockinger, et al., 1995; W.Z. Tang, 1992).

Many researchers have reported the treatment of chlorophenols using different AOPs operating under a variety of conditions (Scott, et al., 1995). Most of these reports dealt with pseudo first-order rate constants, the identification of end products, or the effect of certain operating parameters. However, the reaction rate constants of hydroxyl free radicals with the chlorophenols are seldom reported, despite the need for these data for reactor design and optimization. Some of this mechanistic information relevant to the degradation of chlorinated aromatic compounds treated by different AOPs is available:

- The reaction mechanism and rate of hydroxyl free radical initiation, propagation and termination by means of a variety of AOPs operating under different conditions (Glaze, et al., 1989a; Walling, 1975; Staehelin, et al., 1985);
- the production of intermediates, such as formate and oxalate, which are common to many chlorinated aromatics treated by AOPs (Stockinger, et al., 1995; Staehelin, et al., 1985; Wang, 1992; Trapido, et al., 1997; Koyama, et al., 1994);

- the second-order reaction rate constants of hydroxyl free radical attack on these reported intermediates (Buxton, et al., 1988; Hoigne, et al., 1976); and
- the second-order reaction rate constants of common aqueous chemicals that react with hydroxyl free radicals (and therefore can interfere with AOPs), such as carbonates, phosphates, and nitrates (Buxton, et al., 1988; Sedlak, 1991; Staehelin, et al., 1985)

However, none this information can be used for a fundamental approach to reactor design unless the second-order kinetic constants for the hydroxyl free radical reaction with the original contaminants are known.

Second-order kinetic constants have only been reported for five chlorophenols: the three monochlorophenol isomers, 2,4-dichlorophenol and 2,4, 6 trichlorophenol (Buxton, et al., 1988; W.Z. Tang, 1992; Fartahazis and Ross, 1977). No data are available for the higher chlorinated phenols. Thus, the information required to extrapolate results from one AOP to another and to design and optimize AOP treatments for different chlorophenols and their mixtures is not available.

Although it is widely accepted that the main reactive species of Fenton's reaction is the hydroxyl free radical, alternative reaction mechanisms involving iron in higher oxidation states, such as Fe(IV) or its oxygen complexes (the peroxo $(Fe(OOH)^{+})$ and ferryl (FeO_2^{+}) radicals) have been postulated (Walling, 1975; McKinzi, et al., 1999). However, there is no evidence that confirms the role of any of these species in alternative reaction mechanism, and if these Fe (IV) complexes exist in homogeneous solution, their properties are indistinguishable from those of •OH (Sutton, et al., 1989). The lack of dependence of Fenton's reaction on ionic strength supports the role of an uncharged reactive species (such as the hydroxyl free radical), and provides evidence that oxygen

complexes such as the ferryl ion (which would be charged if it exists at all) are not involved. Moreover, the existence of these Fe(IV)-oxygen complexes has not been independently demonstrated (Walling, 1975; Sutton, et al., 1989). Thus, the hydroxyl free radical still remains as the most accepted reactive species involved in the Fenton's system.

The two objectives of this study were (a) to determine the second-order kinetic constants for nine chlorophenols: 2- chlorophenol (2CP), 2,4-dichlorophenol (24DCP), 2,5-dichlorophenol (25DCP), 2,4,6-trichlorophenol (246TCP), 2,4,5-trichlorophenol (245TCP), 2,3,5-trichlorophenol (235TCP), 2,3,4,6-tetrachlorophenol (2346TeCP), 2,3,5,6-tetrachlorophenol (2356TeCP), and pentachlorophenol (PCP), and (b) to evaluate correlations for the reaction rate constants. Identification of a reliable correlation would allow the estimation of rate constants for other chlorophenols for which no experimental rate constants have been reported, and would facilitate the evaluation of common reaction mechanisms.

4.2. Experimental Section

4.1.1. Chemicals

All chlorophenols were purchased from Sigma, as were nitrobenzene and the surrogate and internal standards used for extraction and analysis. The purity of these chemicals was 98% or higher (except for dibromophenol, which was 95% pure). $FeCl_2 \cdot 4H_2O$ (99%+) was purchased from Baxter. Hydrogen peroxide (non-stabilized, 31.4%), sodium chloride (99.9%) and perchloric acid (conc.) were all purchased from Fisher.

Dilute perchloric acid (0.1 N) was prepared from concentrated acid for safe handling and storage.

4.1.2. Competitive Kinetics Method

The competitive kinetics method is based on the degradation of two compounds in the same solution. The velocity of the degradation of each of these compounds follows the relationship $d[M]/dt = k_{OH,M}[\bullet OH][M]$, in which $k_{OH,M}$ is the second-order kinetic constant, $[\bullet OH]$ is the concentration of the hydroxyl free radical and $[M]$ is the concentration of the substrate (Buxton, et al., 1988; Hoigne, et al., 1976; Haag, et al., 1992). One of these two compounds has a known second-order kinetic constant and is used as a reference. The concentrations of both compounds are measured before and after exposure to hydroxyl free radicals. The competitive reaction obeys the relationship

$$k_{OH,M} = k_{OH,C} \frac{\ln\left[\frac{[M_f]}{[M_o]}\right]}{\ln\left[\frac{[C_f]}{[C_o]}\right]} \qquad (1)$$

in which the subscripts o and f denote the initial and final concentrations of the reference compound C and the measured substrate M (e.g., a chlorophenol). Thus, $k_{OH,M}$ can be determined using Equation 1.

The reaction rates for substrates C and M must be similar (within a factor of 3) to obtain accurate $k_{OH,M}$ values. However, the relative solute concentration before reaction (M_o/C_o) can be varied through the range of 1:5 to 5:1 without influencing the accuracy of the results (Hoigne, et al., 1976). In contrast to direct methods, the competitive kinetics method is not sensitive to free radical scavengers, since these affect the reaction rates of

both substrates proportionally. For the same reason, multiple substrates can be tested in the same solution without affecting the outcome of the experiment (although stronger oxidation treatments are required in the presence of other substrates or hydroxyl free radical scavengers).

Since the competitive kinetics method determines relative reaction constants, the selection of the reference substrate is very important. In particular, the uncertainty of the second-order kinetic constant for a reference substrate must be low. A list of suitable reference substrates has been suggested by Buxton and coworkers (Buxton, et al., 1988). From this list, nitrobenzene (NB) was selected for this work. The suggested value of the second-order rate constant (an average of values obtained by different methods) for NB ($k_{OH,NB}$) is 3.9×10^{09} $M^{-1}s^{-1}$ (Buxton, et al., 1988). A second experiment was performed for PCP, using 2,4-dichlorophenol (24DCP) as the reference substrate, to obtain an alternative measurement. The value used for this second-order kinetic constant ($k_{OH,24DCP}$) was 5.5×10^{09} $M^{-1}s^{-1}$, as determined in this work.

A different form of the competitive kinetics method, in which ferrous iron is the competitive substrate, has been used extensively to determine the second order rate constants for alkanes, alcohols, and aromatic compounds (Walling, 1975; Haag, et al., 1992). This method included reactions 1 and 2, and chain reactions of various organic free radicals generated from different reactive sites on the substrate (reactions 3 to 5). These organic free radicals formed stable compounds by dimerization, reduction of ferric iron, or oxidation of ferrous iron (reactions 2a to 2c). Since this scheme accounted for significant production of oxidized substrate by-products (for both the organic and the ferrous iron), simplification to Equation 1 was not possible.

$$H_2O_2 + Fe^{2+} \xrightarrow{k_1} Fe^{3+} + OH^- + \bullet OH \quad (2)$$

$$OH\bullet + Fe^{+2} \xrightarrow{k2} Fe^{+3} + OH^- \quad (3)$$

$$OH\bullet + R_iH \xrightarrow{k_{4i}} H_2O + R_i\bullet \quad (4i)$$

$$OH\bullet + R_jH \xrightarrow{k_{4j}} H_2O + R_j\bullet \quad (4j)$$

$$OH\bullet + R_kH \xrightarrow{k_{4k}} H_2O + R_k\bullet \quad (4k)$$

$$Fe^{+3} + R_i\bullet \xrightarrow{k5} Fe^{+2} + intermediates \quad (5)$$

$$2R_k\bullet \xrightarrow{k6} dimer \quad (6)$$

$$Fe^{+2} + R_k\bullet + H^+ \xrightarrow{k7} Fe^{+3} + R_kH \quad (7)$$

The rate expressions for ferrous iron and hydrogen peroxide can be put in terms of the concentrations of the original compound, the ferrous iron concentration, the hydrogen peroxide concentration, and the concentrations of the free radicals. Expressions for the concentrations of the free radicals can be found using the pseudo-steady state approximation, valid for short-lived species. Then, the ratio of the reaction rate of Fe^{2+} to H_2O_2 is given by:

$$\frac{d[Fe^{+2}]}{2d[H_2O_2]} = \frac{2k_3[Fe^{+2}] + k_{4i}[R_jH] + 2k_{4k}[R_kH]}{2k_3[Fe^{+2}] + 2k_{4i}[R_jH] + 2k_{4j}[R_jH] + 2k_{4k}[R_kH]} \quad (8)$$

This expression can be linearized in the form

$$R = 2ar(1 - R) + b \quad (9)$$

in which $R = d[Fe^{+2}]/d[H_2O_2] \approx \Delta[Fe^{+2}]/\Delta[H_2O_2]$ (9a)

$$r = [Fe^{+2}]/2\,[RH] \qquad (9b)$$

$$a = k_2/(k_{3i} + k_{3j} + k_{3k}) \qquad (9c)$$

$$b = (k_{3j}+2\,k_{3k})/(2(k_{3i} + k_{3j} + k_{3k})) \qquad (9d)$$

A plot of 2r(1-R) vs. R is linear. Since k_2 is known, the overall second order kinetic rate constant of the organic compound with hydroxyl free radicals, $k_{40}=(k_{4i} + k_{4j} + k_{4k})$, can be determined. R and r depend only on the initial and final values of $[Fe^{+2}]$ and the initial concentration of the substrate and H_2O_2 (assuming complete depletion of this reactant). R and r depend only on the initial and final values of $[Fe^{+2}]$ and the initial concentration of the substrate and H_2O_2 (assuming complete depletion of this reactant). This is done by reacting different amounts of H_2O_2, Fe^{+2}, and the substrate, and measuring the consumed ferrous iron after the reaction proceeded to completion. The total consumption of hydrogen peroxide is ensured by an initial low dose of this reactant and concentrations of substrate and ferrous iron in excess.

Application of this simplified reaction mechanism to more general situations (e.g. high degradation rates, or higher pH than 2) was not possible, since many secondary reactions that take place after initial reaction conditions were neglected in order to simplify the kinetic model to a suitable mathematical expression to determine the reaction rate of the substrate with the hydroxyl free radical. Due to the strong affinity of hydroxyl free radicals for ferrous iron, this method is not applicable to compounds of very low solubility.

4.1.3. Competitive Kinetics Experiments

The following chlorophenols were tested in two-substrate (the chlorinated phenol and nitrobenzene) experiments: 2,4,6-trichlorophenol (246TCP), 2,3,4,6-tetrachlorophenol (2346TeCP), and pentachlorophenol (PCP). Solutions of one of these selected chlorophenols and nitrobenzene (initial concentrations about 0.01 mM) were prepared in Reagent Type I Grade water and stirred for 24 h. The pH of these solutions was adjusted to 3.5 with 0.1 M $HClO_4$. Sodium chloride was added to adjust the ionic strength to 0.05 M (accounting for the previous pH adjustment and further additions of ferrous salts). Oxygen was eliminated from the solution by bubbling it with N_2 for 30 min to avoid possible interference due to singlet oxygen. The solution was then stoppered and transferred to an anoxic chamber to avoid redissolution of atmospheric O_2. Aliquots of this solution (35 mL) were dosed into 40-mL amber glass vials and ferrous chloride was added to a final ferrous ion concentration of 0.2 mM. The resulting solutions were spiked with variable amounts of H_2O_2 (zero for the control), shaken for a few seconds and left stationary to react overnight. Each treatment was conducted in duplicate. Chemical analyses were performed the following day to minimize sample degradation.

In addition to the previous two-substrate experiments, the second-order kinetic constants for 2-chlorophenol (2CP), 2,5-dichlorophenol (25DCP), 2,4,5-trichlorophenol (245TCP), 2,3,5,6-tetrachlorophenol (TeCP), 2,4-dichlorophenol (24DCP) and 2,3,5-trichlorophenol were determined in multiple (more than two) substrate experiments. Two of these experiments were performed: one to determine the kinetic constants for 2CP, 25DCP, 245 TCP and 2356TeCP, and another with 24DCP and 2356TCP. These

experiments were performed in a similar way as the two substrate experiments, except that results of stirring initially and then leaving samples stationary to react overnight were compared to stirring overnight with a magnetic stirrer to identify potential mass transfer limitations inherent to the first protocol.

4.1.4. Substrate Analysis

The concentrations of the different analytes were determined with an HP 5890 Series II gas chromatograph with a mass spectral detector and a 50-m HP-5 crosslinked 5% PH ME silicone capillary column of 0.2 mm I.D. and 0.33 μm film thickness. The GC temperature program was: 50 °C initial temperature held for 2.0 min followed by increases of 20 °C/min to 160 °C and then at 6 °C/min to 250 °C (total run time = 22.5 min). One mL of each aqueous sample was spiked with dibromophenol as surrogate, adjusted to pH less than 1.0, extracted with 0.5 mL of chloroform, and then dosed with dibromobenzene as internal standard before injection (the final concentration of the internal standard in the extracted solution was 0.05 mM). Quantification of each analyte was performed on the basis of the respective main ion in the mass spectrum, and the extraction efficiency was evaluated by means of the surrogate. Data from samples with surrogate concentrations out of the interval of ±15% around the mean were discarded or the extracts corresponding to these samples were re-run on the GC a second time. Two different sets of standard solutions were used for the two trichlorophenol isomers due to their similar retention times and interfering quantitating ions in the spectra.

4.3. **Results**

4.1.5. Second-Order Kinetic Constants

It has been established that the attack of hydroxyl free radicals on an organic compound is an elementary step, and that the rate is first order with respect each reactant, and second-order overall (Buxton, et al., 1988). Thus, the velocity of this reaction follows the relationship $d[M]/dt = k_{OH,M}[\bullet OH][M]$, in which $k_{OH,M}$ is the second-order kinetic constant. Values of these reaction rate constants for a variety of organic chemicals, obtained by means of different methods have been tabulated (Buxton, et al., 1988); (Fartahazis and Ross, 1977). These methods are classified as either direct or indirect. Direct methods rely on the measurement of the decay of the hydroxyl free radical and/or the formation of the products. In practice, however, the decay of the hydroxyl free radical is difficult to measure directly due to its very low ultraviolet absorption. The measurement of product accumulation is also limited to a few compounds with suitable absorption spectra. For these reasons, the indirect competitive kinetics method is of more general applicability.

The competitive kinetics method developed by Walling and co-workers (Walling, 1975) (which does not follow Equation 1,.but Equation 9) was applied to determine the second order kinetic constant of pentachlorophenol. However, the low solubility of PCP and the high affinity of ferrous iron for hydroxyl free radicals resulted in inadequate (non-measurable) competition of both substrates. Because of this reason, Walling's method was not used in this work.

Logarithmic plots of the dimensionless degradation of the different substrates with respect to the dimensionless degradation of the competitive substrate were obtained

and Equation 1 was fitted to these plots. The slopes of the samples that were initially stirred for a few seconds and the samples stirred overnight were not significantly different (confidence level of 99%), as indicated by analysis of covariance (ANCOVA). This indicates that there were no potential mass transfer limitations induced by stirring the vials only initially compared to the ones that were stirred overnight. The slope of these graphs was multiplied by the second-order kinetic constant of the reference substrate, and the resulting rate constants are presented in Table 4.1. It can be observed that the higher the degree of chlorination of the phenolic ring, the lower the rate of reaction.

Table 4.1. Values for the second-order kinetic constant for phenol and chlorophenols (all are $\times 10^{09}$ $M^{-1}s^{-1}$). For experimental values obtained in this work, the regression coefficient and the number of data points are provided. For the competitive substrate, NB=nitrobenzene, RNO=p-Nitroso-N,N, Dimethyl- N,N-Dimethyl-4-amine, BzO^- = benzoate, PrOH = 2-propanol. Constants determined in the same multi-substrate competitive kinetics experiment have the same superscript ([a] or [b]).

Compound	$k_{OH,M}$ 10^{09} $M^{-1}s^{-1}$	Method used	Reference
Phenol	6.6	Direct method, product buildup kinetics	(Buxton, et al., 1988)
Phenol	14	Direct method, product buildup kinetics	(Buxton, et al., 1988)
Phenol	18	Competitive kinetics; reference: SCN^- ($k_{OH,C}$ =11)	(Buxton, et al., 1988)
Phenol	6.2	Competitive kinetics; reference: BzO^- ($k_{OH,C}$ =5.9)	(Fartahazis and Ross, 1977)
Phenol	8.6	Competitive kinetics; reference: ethanol ($k_{OH,C}$ =11)	(Fartahazis and Ross, 1977)
Phenol	9.7	Competitive kinetics; reference: PrOH ($k_{OH,C}$ =2.2)	(Fartahazis and Ross, 1977)
Phenol	11	Competitive kinetics; reference: PrOH ($k_{OH,C}$ =2.2)	(Fartahazis and Ross, 1977)

Phenol	8.5	Competitive kinetics; reference: RNO($k_{OH,C}$= 12.5)	(Fartahazis and Ross, 1977)
2CP	8.2	Competitive kinetics; reference: RNO($k_{OH,C}$= 12.5)	(Fartahazis and Ross, 1977)
2CP	12	Direct method, product buildup kinetics	(Buxton, et al., 1988)
2CP	8.2[a]	Competitive kinetics; reference: NB($k_{OH,NB}$ = 3.9), R^2=0.862, n=11	This work
3CP	7.2	Competitive kinetics; reference: RNO($k_{OH,C}$= 12.5)	(Buxton, et al., 1988)
4CP	7.6	Competitive kinetics; reference: ethanol ($k_{OH,C}$= 1.9)	(Buxton, et al., 1988)
24DCP	7.2	Competitive kinetics; reference: 2CP($k_{OH,C}$= 8.2)	(W.Z. Tang, 1992)
24DCP	7.0[b]	Competitive kinetics; reference: NB($k_{OH,NB}$ = 3.9), R^2=0.996, n=11	This work
25DCP	7.9[a]	Competitive kinetics; reference: NB($k_{OH,NB}$ = 3.9), R^2=0.876, n=11	This work
235TCP	8.5[b]	Competitive kinetics; reference: NB($k_{OH,NB}$ = 3.9), R^2=0.979, n=11	This work
245TCP	7.2[a]	Competitive kinetics; reference: NB($k_{OH,NB}$ = 3.9), R^2=0.893, n=11	This work
246TCP	5.4	Same as above R^2=0.983, n=12	This work
246TCP	6.3	Competitive kinetics; reference: 2CP($k_{OH,C}$= 8.2)	(W.Z. Tang, 1992)
2356TeCP	6.2[a]	Competitive kinetics; reference: NB($k_{OH,NB}$ = 3.9), R^2=0.965, n=9	This work
2346TeCP	4.9	Competitive kinetics; reference: NB($k_{OH,NB}$ = 3.9), R^2=0.823, n=7	This work
PCP	4.4	Same as above R^2=0.955, n=10	This work
PCP	3.5	Competitive kinetics; reference: 24DCP($k_{OH,24DCP}$=5.5) R^2=0.830, n=13	This work

4.1.6. Correlation of Rate Constants

The correlation of kinetic data for families of organic compounds has been used to corroborate common reaction mechanisms (Anbar, et al., 1966), as well as the estimation of kinetic constants of compounds for which no experimental data is available (Haag, et al., 1992). The second-order reaction rate constants determined here, together with previously reported values for phenol and chlorophenols (Table 4.1) were correlated

with the Hammett's σ constants for *para-* and *meta-* substituents (chloride), with the corrected σ+ constants for these same substituents (Brown, et al., 1958), with the number of chloride substituents in the aromatic ring, and finally with estimated diffusion coefficients (Lyman, et al., 1982).

4.1.6.1. Hammett's Equation

Hammett's Equation is a semi-empirical relationship developed for the prediction of protonation equilibrium constants for substituted aromatic compounds. This relationship is based on group contributions that are *ortho-*, *meta-* and *para-* dependent. Based on thermodynamic free energy considerations, the relationship has been extended to other types of kinetic constants, including second-order kinetic constants for hydroxyl free radical attack on substituted benzenes and benzoates (Anbar, et al., 1966) and hydroxyl free radical attack on aromatic compounds in general (Haag, et al., 1992). The form of Hammett's equation is

$$\log(k) = \log k_o + \rho\Sigma\sigma \qquad (2)$$

in which k_o is the kinetic constant for the non-substituted family compound (e.g., phenol for chlorophenols), σ is the additive contribution from each substituent group and ρ is the characteristic slope for the combination of chemical family of compounds and type of reaction.

The σ values for chlorine as a *meta-* and *para-* substituent are 0.373 and 0.227, respectively (Perrin, et al., 1981). The pseudo σ value for *ortho-* chlorine is 0.680. Pseudo σ *ortho-* values for different substituents were developed for acid-base equilibria, accounting for differences in proximity effects, field effects, steric hindrance effects and

possible hydrogen bond formation, in addition to the inductive and resonance effects for the *meta-* and *para-* substituents originally included in the σ values developed by Hammett (Perrin, et al., 1981). Therefore, the application to reactions other than solvolysis should be made with caution (Perrin, et al., 1981).

Figure 4.1 shows the correlation given by Equation 2, using Hammett's σ values and the second-order kinetic constants for the different chlorophenols. The correlation was moderate, but statistically significant (confidence level of 99%) with R^2=0.54. The statistical correction recommended for molecules with more than one substituent group of the same type (Perrin, et al., 1981) was not used since it did not improve the correlation. The value for ρ (the slope of the best-fit line in Figure 4.1.) is -0.15. Other reported values for ρ for hydroxyl free radical attack are -0.41 for *meta-* and *para-* substituted benzene and benzoates (Anbar, et al., 1966) and -0.318 for a wide range of aromatic compounds (Haag, et al., 1992). Given the successful correlation with Hammett's Equation, it can be inferred that some of the known reaction mechanisms for hydroxyl free radical attack on chlorophenols could be applicable to chlorophenols for which reaction mechanisms have not been studied.

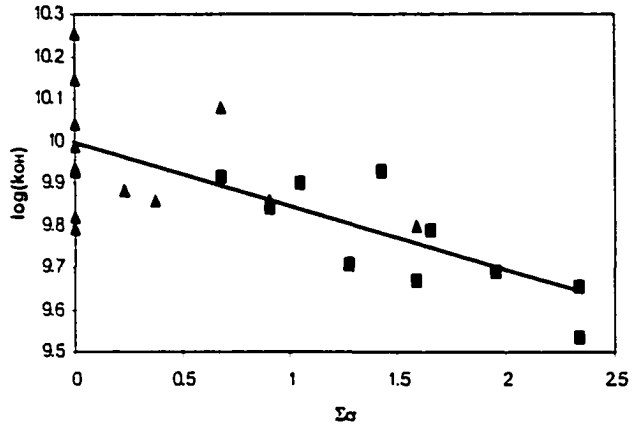

Figure 4.1. Correlation of experimental (squares) and published (triangles) values of the second-order kinetic constant for chlorophenols with Hammett's constants. The regression equation is $\log(k_{OH,M}) = 10.0 - 0.15\ \Sigma\sigma$, $R^2=0.54$.

The use of the σ+ values proposed by Brown and Okamoto (Brown, et al., 1958) has been shown to yield improved estimates from Hammett's Equation for electrophilic reactions (Walling, et al., 1963). These σ+ values for chlorine are 0.391 and 0.112 for *meta-* and *para-* substituents, respectively. It has been shown that the initial attack of hydroxyl free radical (a strong electrophile) on non-chlorinated aromatic compounds occurs due to addition of the hydroxyl free radical to the aromatic ring (Anbar, et al., 1966; Mohan, et al., 1991). For example, the radical hydroxycyclohexadienyl is initially formed after the attack of hydroxyl free radicals to benzene (Anbar, et al., 1966; Sedlak, 1991). If the aromatic ring is chlorinated, this electrophilic attack is more likely to occur at the chlorinated position, as demonstrated by the absorption energy of the hydroxyl free radical adduct with chlorinated toluenes and the sequential formation of free chloride (Mohan, et al., 1991). Analogously, the reaction of hydroxyl free radical attack with 4-chlorophenol is thought to follow a mechanism of electrophilic attack of the hydroxyl free radical, which induces dechlorination (Boncz, et al., 1997). This same reaction

mechanism has been proposed for other chlorinated phenols (2-chlorophenol, 4-chlorophenol, 2,4 dichorophenol and PCP) but no conclusive data that support this hypothesis have been generated (Trapido, et al., 1997; Barbeni, et al., 1987; Lee, et al., 1992).

Correlation with Hammett's Equation and improved fit by the use of $\sigma+$ values might support the existence of a similar electrophilic attack of the hydroxyl free radicals on the chlorinated phenols. Thus, the correlation with these $\sigma+$ values was tested. The regression equation is $\log(k_{OH,M}) = 10.0 - 0.14\Sigma\sigma+$, the correlation coefficient is $R^2=0.50$. Although this correlation is significant (confidence level of 99%) the use of these $\sigma+$ corrected values does not improve the fit of Hammett's Equation to this particular set of data, despite the fact that these $\sigma+$ values were developed specifically for electrophilic reactions.

4.1.6.2. Correlation of the kinetic data with the number of chlorine atoms on the aromatic ring

Tang (W.Z. Tang, 1992) tested the correlation between the logarithm of the second-order kinetic constant for hydroxyl free radical attack and the number of chloride substituents on the aromatic ring for 2CP, 24DCP and 246TCP. Sedlak and Anden (Sedlak, 1991) also tested a correlation of relative reaction rates with the number of non-chlorinated sites on polychlorinated biphenyls. The favorable results obtained in these previous works suggested that the chemical structure of a chlorinated aromatic (instead of its electronic properties) could be used to correlate kinetic data. The correlation with the number of chlorine atoms in the aromatic ring ($\log(k_{OH,M}) = -0.073$ **Cl** $+ 10.0$, $R^2 = 0.57$)

is statistically significant (99% confidence level) and provides an improved fit with respect to Hammett's Equation, even though it cannot account for position-dependent effects. These effects were important for polychlorinated biphenyls (Sedlak, 1991), and seem to be important for chlorophenols, judging by the rate constants for the mono-chlorophenol isomers and the two tri-chlorophenol isomers (Table 4.1).

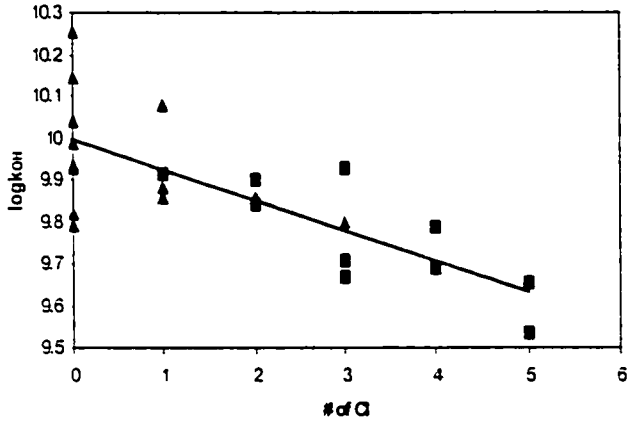

Figure 4.2. Correlation of experimental (squares) and published (triangles) values of the second-order kinetic constant for chlorophenols with the degree of chlorination. The regression equation is $\log(k_{OH,M}) = 10.0 - 0.073$ **Cl**, $R^2=0.57$.

4.1.6.3. Correlation of the kinetic data with diffusion coefficients

Since the reactions of the hydroxyl free radical with many organic substrates is thought to be diffusion limited (Buxton, et al., 1988; Mohan, et al., 1991) the correlation of the logarithm of the second-order kinetic constant with the diffusion coefficients was tested. The diffusion coefficients were estimated by means of the Hayduk and Laudie method, which itself relies on the estimated LeBas molecular volume (Lyman, et al., 1982). This estimation of the binary diffusion coefficient for a solute in aqueous solution is given by the relationship:

$$D_{B,w} = \frac{13.26E-05}{\eta^{1.14} V_B^{`}} \qquad (3)$$

in which $D_{B,w}$ is the diffusion coefficient (cm^2/s), η is the viscosity of water (1.002 cp at 20 °C) and $V_B`$ is the LeBas molar volume at the boiling point of the solute ($cm^3/mol$). The additive group contributions used to estimate $V_B`$ were 14.8 for C, 3.7 for H, 24.6 for Cl, 7.4 for O and −15 for 6C rings (Lyman, et al., 1982).

The correlation of $\log(k_{OH,M})$ and $D_{B,w}$ has an R^2 value of 0.54 and is statistically significant (99% confidence level). This R^2 value is similar to the one obtained by using Hammett's σ values. This implies that similar amount of variability among second-order kinetic constants is explained by the linear regression to diffusion coefficients compared to Hammett's σ values, despite the fact that the LeBas method to predict molar volumes cannot account for position-dependent contributions to the reactivity, an important parameter for electrophilic reactions (Mohan, et al., 1991).

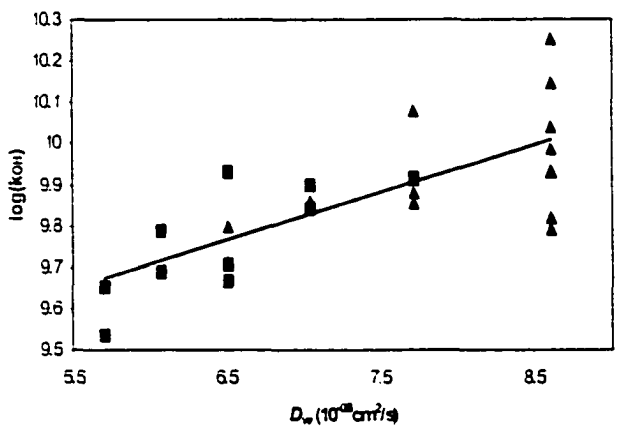

Figure 4.3. Correlation of experimental (squares) and published (triangles) values of the second-order kinetic constant for chlorophenols with diffusion coefficients, estimated by means of the Hayduk and Laudie Method and the LeBas molar volume method. The regression equation is $\log(k_{OH,M}) = 9.0 + 1.14\times10^{05} D_{B,w}$, R^2=0.54.

This finding supports the hypothesis that the reaction rates of hydroxyl free radical attack on chlorophenols are controlled by diffusion rather than controlled by reaction mechanism. Although this has been indicated before (Buxton, et al., 1988; Mohan, et al., 1991), to our knowledge this is the first report on the correlation of diffusion coefficients with kinetic data for hydroxyl free radical reactions.

4.4. Discussion

Published values of the second-order kinetic constant for phenol vary considerably. The quality of the published data for phenol has been questioned in a compilation, without providing a recommended value (Buxton, et al., 1988). This high number of values for the second-order kinetic constant for phenol (eight observations, out of a total of 24 used for all the regressions) and the high variability among them accounts partially for the lack of fit of the model, but was done for completeness.

In all four correlations tested, experimental data obtained in this work was compared with published data by means of analysis of covariance (ANCOVA). There were no significant differences between the data obtained in this work and previously reported data, for any of the four correlations tested, indicating that the variability of previously published data (obtained by different researchers by means of different methodologies) is similar to the variability of the data obtained in this laboratory. This finding also supports the idea that hydroxyl free radical is the reactive species for Fenton's reaction. Although it does not solve the long term controversy on the subject (Sutton, et al., 1989), it corroborates that the reactive species, whatever its specific hypothetical identity is - such as the peroxo ($Fe(OOH)^+$ or ferryl (FeO_2^+) radicals-, it has

indistinguishable properties (in this case rates of reaction towards the chlorophenols under study) from the hydroxyl free radical.

All four properties tested in this work (σ and $\sigma+$ values, degree of chlorination and diffusion coefficients) showed potential to correlate the kinetics of the hydroxyl free radical attack on different chlorophenols. The 95% confidence intervals for the sum of square errors for the four regressions overlapped, indicating that none of them was a significant improvement over any of the others. Furthermore, multiple linear regression using these four properties indicated high collinearity among all of them. This implies that for the family of compounds tested (chlorophenols) these properties are not independent, and a regression model including more than one of these predictors does not provide an improved fit with respect a model that considers only one of these variables as a predictor.

Due to the fact that Hammett's Equation (which considers position-dependent effects) did not provide a better regression than the regressions done with properties that did not depend on the position of the chlorine atoms on the aromatic ring (degree of chlorination and diffusion coefficients) it is questionable if these position-dependent effects on the kinetic constants are important. These effects were tested using the experimental data collected for this work. Competitive kinetics data for structural isomers (two dichlorophenols, three trichlorophenols and two tetrachlorophenols) allows five paired comparisons to test the effects of positional changes on the second-order kinetic constants for these isomers (through changes in the values of the slopes of the transformed data for Equation 1). These possible comparisons are: 24DCP vs. 25DCP; 246TCP vs. 235TCP; 246TCP vs. 245CP; 235TCP vs. 245TCP; and 2356TeCP vs.

2346TeCP. Analysis of covariance (ANCOVA) indicated that positional effects of chloride atoms on the aromatic ring on the competitive kinetics data were significant (95% confidence level) in only two (246TCP vs. 235TCP and 235TCP vs. 245TCP) of the five possible comparisons. Thus, this data set does not clarify if positional effects on the second-order kinetic constants for chlorophenols are important.

Although Hammett's Equation might account for these positional effects, this correlation provided lower regression coefficient than the correlation with the degree of chlorination, and a similar value to the obtained by means of the estimated diffusion coefficients. These two latter properties do not account for positional effects. Therefore, if these position-dependent effects were in fact important, the σ values for Hammett's Equation did not take them into account properly. This is in agreement with a previous kinetic study on the reaction between hydroxyl free radicals and polychlorinated biphenyls, which indicated important position dependent effects that Hammett's Equation could not predict adequately (Sedlak, 1991).

A significant correlation found by using the diffusion coefficients does not invalidate the concept of a similar reaction mechanism. A similar reaction mechanism might exist for the same reaction of a series of aromatic compounds (such as chlorophenols), regardless of whether the observed reaction rate is limited by the reaction mechanism or is diffusion controlled. However, if this is the case (as appears to be for chlorophenols), the use of correlations such as Hammett's Equation to generalize reaction mechanisms should be done cautiously. Thus, additional information such as intermediate accumulation might be necessary to confirm similar reaction mechanisms. In addition, the yields of these intermediates could provide insight into the nature of the

mechanism, e.g., whether it depends on electrophilic interactions or if it is determined by a non-selective, diffusion-controlled mechanism.

Equation 3 provides the means to further investigate the dependence of reaction rates on diffusion coefficients. Specifically, diffusion coefficients depend strongly in temperature, due to temperature-dependence of the viscosity of water. For example, a temperature increase from 20 to 30 °C leads to a decrease in the viscosity of water to 0.7975 cp (Lyman, et al., 1982) and to an increase of 30% in the predicted diffusion coefficient. By means of the correlation of the second-order kinetic constants found in this work $\log(k_{OH,M}) = 9.0 + 1.14\times10^{05}D_{B,w}$, and considering only diffusion effects on the reaction kinetics, this 10 °C temperature increase would result in expected increases in the second-order kinetic constant of 96%, 83%, 74%, 66%, 61%, and 56% for phenol, chlorophenol, dichlorophenol, trichlorophenol, tetrachlorophenol and pentachlorophenol, respectively. Thus, reaction rates strictly controlled by diffusion would be very sensitive to temperature effects. However, these effects would be difficult to measure by the competitive kinetics method, since the reaction rate of the competitive kinetics substrate would also depend on diffusion effects. If the second-order kinetic constant for the competitive kinetics substrate has a similar dependence on the diffusion coefficient as the tested chlorophenols, its reaction rate constant would increase by 87% in response to a 10 °C temperature increase. Since the kinetic constants of both the reference substrate and the tested chlorophenol increase to a similar extent, the measured ratios of the two constants would be within experimental error. Therefore, a direct method to determine kinetic constants would be necessary if temperature changes are used to detect diffusion-controlled kinetics.

In addition to the support that a correlation might provide for extrapolating reaction mechanisms, such a correlation also provides a useful means of predicting reaction rates for compounds for which experimental information is unavailable. In this regard, comparison of the four regressions by their mean square error indicates that all predictors were of similar quality; therefore, any of these correlations are recommended to estimate kinetic data for chlorophenols. Further improvement of all of these correlations might be achieved by multiple linear regression using a property (or properties) that is not collinear with any of the properties tested in this work.

4.5. References

1. Anbar, M., D. Meyerstein, and P. Neta. 1966. The Reactivity of Aromatic Compounds toward Hydroxyl Radicals. J. Phys. Chem. 70:2660-2062.

2. Barbeni, M., C. Minero, and E. Pelizzetti. 1987. Chemical Degradation of Chlorophenols with Fenton's Reagent. Chemosphere. 16(10-12): 2225-2237.

3. Boncz, M., H. Bruning, W. Rulkens, E. Sudholter, G. Harmsen , and J. Bijsterbosch. 1997. Kinetic and Mechanistic Aspects of the Oxidation of Chlorophenols by Ozone. Wat.Sci. Tech. 35(4):65-72.

4. Brown, H. C. and Y. Okamoto. 1958. Substituent Constants for Aromatic Substitution. J. Am. Chem. Soc. 80:4979.

5. Buxton, B. V., C. L. Greenstock, W. P. Helman, and A. B. Ross. 1988. Critical Review of Rate Constants for Reactions of Hydrated Electrons, Hydrogen Atoms and Hydroxyl Radicals in Aqueous Solution. J. Phys. Chem. Ref. Data. 17:513-886.

6. Fartahazis, P. and Ross, B. 1977. Selected Specific Rates of Reactions of Transients from Water in Aqueous Solution. Washington: NBS.

7. Glaze, W. and J. Kang. 1989a. Advanced Oxidation Process. Description of a Kinetic Model for the Oxidation of Hazardous Materials in Aqueous Media with Ozone and Hydrogen Peroxide in a Semibatch Reactor. Ind. Eng. Chem . Res. 28,1573-1580.

8. Glaze, W. and J. Kang. 1989b. Advanced Oxidation Process. Test of a Kinetic

Model for the Oxidation of Organic Compounds with Ozone and Hydrogen Peroxide in a Semibatch Reactor. Ind. Eng. Chem . Res. 28,1580-1587.

9. Haag, W. and C. D. Yao. 1992. Rate Constants for Reaction of Hydroxyl Radicals with Several Drinking Water Contaminants. Environ. Sci. Technol. 26: 1005-1013.

10. Haggblom, M. and R. Valo. 1995. eds: Young, L. and C. Cerniglia. Microbial Transformation and Degradation of Toxic Organic Chemicals. New York: Wiley-Lis; pp. 389-434.

11. Hale, D.; W. Reineke, and J. Wiegel. 1994. Biological Degradation and Bioremediation of Toxic Chemicals. Chaudry, R., ed. Portland: Dioscorides Press; pp. 74-91.

12. Hoigne, J. and H. Bader. 1976. The Role of Hydroxyl Radical Reactions in Ozonation Processes in Aqueous Solutions. Wat. Res. 10:377-386.

13. Koyama, O., Y. Kamagata, and K. Nakamura. 1994. Degradation of Chlorinated Aromatics by Fenton Oxidation and Methanogenic Digester Sludge. Wat. Res. 28 (4):895-899.

14. Lee, S. and J. Carberry. 1992. Biodegradation of PCP enhanced by chemical Oxidation Pretreatment. Wat. Environ. Res. 64(5):682-690.

15. 1982. Lyman, W.; W. Reehl, and D. Rosenblatt. Handbook of Chemical Property Estimation Methods. New York: McGraw-Hill; pp. 17-11 to 17-22.

16. McKinzi, A. and T. Dichristina. 1999. Microbially Driven Fenton Reaction for Transformation of Pentachlorophenol. Environ. Sci. Technol. 33:1886-1891.

17. Mohan, H., H. Mudaliar, D. Aravindakumar, B. Mahdav Rao, and J. Mittal. 1991. Studies of Structure-Reactivity in the Reaction of OH Radicals with Substituted Halobenzenes in Aqueous Solutions. J. Chem. Soc. Perkin Trans. 2:1387.

18. Perrin, D.; B. Dempsey , and P. Serjeant. 1981. pKa Prediction for Organic Acids and Bases. London.

19. Puhakka, J. and E. Melin. 1996. In: Crawford, R. and D. Crawford, eds. Bioremediation: Principles and Applications. Cambridge University Press; pp. 254-299.

20. Scott, J. and D. Ollis. 1995. Integration of Chemical and Biological Oxidation Processes for Water Treatment: Review and Recommendations. Env. Prog. 14:88-103.

21. Sedlak, D. and A. Andren. 1991. Oxidation of Chlorobenzene with Fenton's

Reagent. Environ. Sci. Technol. 25: 777-782.

22. Staehelin, J. and J. Hoigne. 1985. Decomposition of Ozone in Water in the Presence of Organic Solutes Acting as Promoters and Inhibitors of Radicsl Chain Reactions. Environ. Sci. Technol.. 19:1206-1213.

23. Stockinger, H., E. Heinzle, and O. Kut. 1995. Removal of Chloro and Nitro Aromatic Wastewater Pollutants by Ozonation and Biotreatment. Environ. Sci. Technol.. 29:2016-2022.

24. Sutton, H. and C. Winterbourn. 1989. On the Participation of Higher Oxidation states of Iron and Copper in Fenton Reactions. Free Radical Biol. Med. 6:53-60.

25. Trapido, M., Y. Veressinina, J. Hentunen, and A. Hirvonen. 1997. Ozonation of Chlorophenols: Kinetics, By-products and Toxicity. Environ. Technol. 18:325-332.

26. W.Z. Tang. Oxidation Kinetics and Mechanism of Chlorinated Organic Pollutants by Fenton's Reagent.: University of Delaware.; 1992.

27. Walling, C. 1975. Fenton's Reagent Revisited. Acc. Chem. Res. 8:125-131.

28. Walling, C., A. Rieger, and D. Tanner. 1963. Positive Halogen Compounds. VIII. Structure and Reactivity in N-Bromosuccinimide Brominations. J. Am. Chem. Soc. 83:3129-3136.

29. Wang, Y. 1992. Effect of Chemical Oxidation on Anaerobic Biodegradation of Model Phenolic Compounds. Wat. Environ. Res. 64:268-273.

CHAPTER V

FENTON'S OXIDATION OF PENTACHLOROPHENOL

5.1. Background

Many alternatives to biodegradation have been evaluated for the treatment of contaminants that are recalcitrant to biodegradation. Ideal technologies involve the actual destruction of the contaminant, rather than transfer of the contaminant to another phase (which requires further disposal) (Watts, et al.,). Chemical oxidation technologies have gained wide acceptance for this purpose. Among these technologies, advanced oxidation processes (AOPs), which rely on the generation of hydroxyl free radicals (•OH), have been the most effective (Venkatadri, et al., 1993). This efficiency is due to the high oxidation potential and relative lack of selectivity of the hydroxyl free radicals towards most organic compounds.

Several studies have focused on the free radical chemistry related to AOPs. These studies have reported on particular aspects of the reaction mechanism and rates of the different reactions involved in AOPs: initiation (reactions in which free radicals are produced), propagation (free radicals are transformed into other free radicals) or termination (free radicals create more stable species), as well as the factors that effect them (Staehelin, et al., 1985; Haag, et al., 1992; Glaze, et al., 1989a). However, the vast majority of the studies on AOPs and pollutants are applicability studies. These reports

typically include the dose of oxidizing agents and the extent of degradation of the parent compound. However, very few studies generate mechanistic information that allows a more general approach.

The purpose of this work was to study the mechanisms of the Fenton's degradation of water contaminated with pentachlorophenol (PCP), a wood preservative, and integrate this information into a mathematical model. The model was based on previously generated information relevant to Fenton's reaction (the combination of hydrogen peroxide and ferrous iron). Additional information about the PCP degradation due to free radicals was experimentally generated and incorporated into the model. The suitability of such a model to describe experimental kinetic data was evaluated, with and without the presence of PCP in solution as a model contaminant.

5.1.1. Fenton's reaction

Fenton's reaction is based on the generation of hydroxyl free radicals by the reaction of hydrogen peroxide with ferrous ion. Fenton's reaction and oxidation with ozone are the only AOP technologies not dependent on UV light, and are therefore not affected by media turbidity. Furthermore, Fenton's reaction is the only AOP in which the oxidants already exist in liquid solution. This leads to two important advantages over other AOPs: (1) a Fenton's process is less likely to be mass transfer limited and (2) it has no special equipment requirements (Van Kemenade, et al., 1996; Venkatadri and Peters, 1993).

Although it is widely accepted that the main reactive species of Fenton's reaction is the hydroxyl free radical, alternative reaction mechanisms involving iron in higher

oxidation states, such as Fe(IV) or its oxygen complexes (the peroxo $(Fe(OOH)^{+}$ and ferryl (FeO_2^{+}) radicals) have been postulated (Walling, 1975; McKinzi, et al., 1999). However, there is no evidence that confirms the role of any of these species in alternative reaction mechanism, and if these Fe (IV) complexes exist in homogeneous solution, their properties are indistinguishable from those of •OH (Sutton, et al., 1989). The lack of dependence of Fenton's reaction on ionic strength supports the role of an uncharged reactive species (such as the hydroxyl free radical), and provides evidence that oxygen complexes such as the ferryl ion (which would be charged if it exists at all) are not involved. Moreover, the existence of these Fe(IV)-oxygen complexes has not been independently demonstrated (Walling, 1975; Sutton, et al., 1989). Thus, the hydroxyl free radical still remains as the most accepted reactive species involved in the Fenton's system.

5.1.2. Important factors for Fenton's reaction

The most important operating parameters for oxidation of organic substrates by means of Fenton's reaction are pH and the strength of the oxidation, given by the ratios of the concentrations of oxidizing agents to organic matter in the contaminated water.

5.1.2.1. pH

The optimal pH for Fenton's reagent occurs in the range pH 3.0-4.0, although significant reactivity can be observed at pH values as high as 8 (Bigda, 1995; Venkatadri, et al., 1993; Sedlak, et al., 1991). This optimal pH is the result of the different pH-

dependent reactions involved in the Fenton's system, as well as the different reactivities of the different forms of the ionizable reactants.

As Fenton's reaction proceeds, the acid-base equilibrium is modified, due to the different acid-base properties of reaction products (including inorganic by-products and organic acids generated from oxidizable organic substrates) with respect the reactants. These changes produce an observable drop in pH due to Fenton's reaction (Bigda, 1995).

5.1.2.2. Ferrous Iron Concentration

The main initiation reaction that generates hydroxyl free radicals includes hydrogen peroxide and ferrous iron. Since the hydroxyl free radical is the most reactive species in Fenton's oxidation, the rate of oxidation of organic substrates strongly depends on the initial iron concentration (Bigda, 1995). Observed optimal H_2O_2/Fe^{+2} ratios vary from 10:1 to 5:1 (w/w) (Bigda, 1995; Tang, et al., 1997). Ferrous ion is regenerated by the reaction of the ferric ion with H_2O_2 and also by its reaction with the perhydroxyl free radical $\bullet O_2H$ (Marco, et al., 1997). Although some researchers have indicated that significant degradation of organic compounds occurs at varying initial Fe^{+2}:Fe^{+3} ratios (Chen, et al., 1997), the pH dependence of these (and other) reactions might result in different efficiencies of the regeneration of ferrous iron and the generation of hydroxyl free radicals.

5.1.2.3. Hydrogen Peroxide Concentration

Together with ferrous iron, hydrogen peroxide is the main reactive species that generates hydroxyl free radicals. Practitioners have noted that the completion of the

oxidation is dependent on the ratio of hydrogen peroxide to organic matter (Bigda, 1995). Additionally, hydrogen peroxide is one of the main factors for cost considerations of Fenton's reagent (Venkatadri, et al., 1993), since capital costs for Fenton's reaction are low compared to those of other AOPs. Thus, this ratio is one of the most important variables to optimize. The ratio of hydrogen peroxide to substrate (w/w) used ranged from 3:2 for complete degradation of chlorinated phenolic compounds (Venkatadri, et al., 1993) (Marco, et al., 1997)to 2:3 for mineralization of 87% of a PAH mixture in soil (Martens, et al., 1995). This ratio is strongly dependent on the concentration of organic compounds that coexist with the contaminant of interest in the contaminated media, since side reactions of hydroxyl free radicals (and probably other reactants) with these species are unavoidable (Gates, et al., 1995).

5.1.3. Hydroxyl Free Radical Oxidation of Lower Chlorophenols

A range of intermediates are formed during Fenton's reaction and other AOPs with phenols and chlorinated aromatic compounds because the products of initial •OH attack are themselves subject to oxidation by these free radicals. The initial attack of hydroxyl free radical on aromatic compounds induces hydroxylation. Strong evidence indicates that phenolic compounds, benzene, and naphthalene follow this mechanism: the radicals hydroxycyclohexadienyl, chloro-hydroxycyclohexadienyl and benzocyclohexadienyl are initially formed after the reaction of hydroxyl free radicals with benzene, chlorobenzene and naphthalene, respectively (Anbar, et al., 1966; Martens, et al., 1995; Sedlak, 1991; Bunce, et al., 1997). Stabilization of these organic radicals rapidly yields the corresponding quinones. Further oxidation induces ring cleavage and liberates simple

aldehydes, which are rapidly oxidized to the respective organic acids. Formic, acetic and oxalic acids have been reported as the final products of Fenton's reaction with cresol (Wang, 1992). Oxidation of 2,4-dichlorophenol resulted first in dechlorination and then in hydroxyl addition to the aromatic ring (Trapido, et al., 1997). PCP seems to follow a similar reaction mechanism (Lee, et al., 1992), although this proposed reaction mechanism has not been supported with experimental information.

5.1.4. Kinetic Model for Fenton's Reaction

5.1.4.1. Justification of a Kinetic Model for Fenton's Reaction

The hydroxyl free radical attack on many organic substrates is an elementary step, with a second-order kinetics (first order with respect each substrate). The corresponding second-order kinetic constants for many organic substrates have been also published in extensive reviews (Fartahazis and Ross, 1977; Buxton, et al., 1988). If this information is not available, it can be experimentally determined, either by direct measurement (which requires by-product buildup measurement and/or reactant decay during pulse radiolysis studies) or indirectly (by means of the competitive kinetics method). Evaluation of this kinetic constant requires the estimation of the concentrations of hydroxyl free radicals in solution in order to allow an estimate of the degradation rate of the substrate(s) of interest.

Many reactions that are important for the generation of free radicals due to Fenton's reaction (the combination of ferrous iron and hydrogen peroxide) have been published in extensive reviews (Buxton, et al., 1988; Bielski, et al., 1985; Fartahazis and Ross, 1977). These reactions allow a more rational analysis of the reaction kinetics and

reaction mechanism for Fenton's reaction. Such a kinetic model can potentially allow the estimation of the oxidation strength of Fenton's reaction under different conditions (such as the concentration of hydrogen peroxide and iron salts) by providing an estimate of the concentrations of the hydroxyl free radical, the main reactive species of these systems. This information, together with the reaction rate of the reaction between hydroxyl free radicals and organic substrates in solution, yields a more rigorous approach to modeling the kinetics of Fenton's degradation of many organic substances of environmental relevance.

Such a mechanistic model can account for the scavenging effects due to chemicals common to water (such as phosphates, carbonates) that are reactive towards free radicals, and for which reaction mechanisms and kinetics have been proposed, provided that the concentrations of such scavengers are known.

This type of analysis has been successfully applied to other AOPs, such as ozonation (Stockinger, 1995) and the combination of ozone and hydrogen peroxide (Glaze, et al., 1989a; Glaze, et al., 1989b) and sets a common basis to analyze and compare different AOPs.

5.1.4.2. Historical Development of Kinetic Information about Fenton's Reaction

Walling and Weil (Walling, et al., 1974) proposed a reaction scheme to model the oxidation of ferrous iron and hydrogen peroxide in aqueous solution at acidic pH. This mechanism consisted of some of the equations presented in Table 5.1. (Equations t1, t2, p1 and t1 - t3). In this table, the kinetic constant subscripts and equation numbering includes a letter to indicate the type of reaction (-i for initiation, p for propagation or t for

termination-). Due to the lack of some reaction rates at the time, these researchers did not consider all of the actual reaction rates, but used ratios of some of these rates. The particular valus of these constants used by Walling and Weil were: $k_{i1} = 2x10^{-03}$ (at pH=1.7), $k_{t2} = 76$, $k_{t2} = 3x10^{08}$, $k_{t2}/k_{p1} = 6.67$ and $k_{t3}/k_{t1} = 0.024$ (at pH=1.7). Inverse dependence of k_{i1} and k_{t3} on $[H^+]$ was also considered.

This model was validated by Walling and Weil by comparing time-dependent model predictions with experimental degradation of hydrogen peroxide under different conditions (pH, ferrous iron and hydrogen peroxide dose). However, the model was not validated by comparing model-predicted with experimental data for the oxidation of ferrous iron.

Some of the reactions shown in Table 5.1 were used also by Walling and co-workers to determine actual reaction rates of the hydroxyl free radical attack of hydroxyl free radicals on different organic compounds (alkanes, alcohols, and aromatic compounds) (Walling, 1975). This method included reactions i2, t1, and chain reactions of various organic free radicals generated from different reactive sites on the substrate (reactions 1a to 1c). These organic free radicals formed stable compounds by dimerization, reduction of ferric iron, or oxidation of ferrous iron (reactions 2a to 2c). Application of the pseudo-steady state approximation for free radicals yielded a linearized expression that allowed the estimation of the relative rate of reaction of the organic substrate with respect to ferrous iron. Such an expression was only valid at pH<2, and for initial reaction rates (which implied low degradation of the organic substrate).

$$OH\bullet + R_iH \xrightarrow{k_{1i}} H_2O + R_i\bullet \qquad (1a)$$

$$OH\bullet + R_jH \xrightarrow{k_{1j}} H_2O + R_j\bullet \qquad (1b)$$

$$OH\bullet + R_kH \xrightarrow{k_{1k}} H_2O + R_k\bullet \qquad (1c)$$

$$Fe^{+3} + R_i\bullet \xrightarrow{k_3} Fe^{+2} + intermediates \qquad (2a)$$

$$2R_k\bullet \xrightarrow{k_5} dimer \qquad (2b)$$

$$Fe^{+2} + R_k\bullet + H^+ \xrightarrow{k_6} Fe^{+3} + R_kH \qquad (2c)$$

Application of this simplified reaction mechanism to more general situations (e.g. high degradation rates, or pH values higher than 2) was not possible, since many secondary reactions that take place after the initial reaction were neglected in order to simplify the kinetic model to determine the reaction rate of the substrate with the hydroxyl free radical.

More recently, there have been formulations of more complete reaction schemes, made possible due to the availability of specific values of the kinetic constants for some of the reactions for which no values were available earlier. Some of these values have been reported in extensive compilations (Bielski, et al., 1985; Buxton, et al., 1988; Fartahazis and Ross, 1977; Rush, et al., 1985). Additionally, some additional reactions (and their rates) have been identified in these same reports. This information can be integrated into a mathematical model of more general application. For example, the values of reaction rate constants k_{p1} and k_{t2} have been reported, and there is no longer a need to assume ratios of these reactions as Walling did when first proposed a mechanistic model. One such model was used to validate the specific interactions of quinones and

dihydroxy-cyclohexadienyl radicals produced from the Fenton's treatment of phenol with ferric and ferrous ions in Fenton's systems at pH 2.8 (Chen, et al., 1997).

5.1.4.3. Development of a kinetic model for Fenton's reaction

A mathematical model was developed in this study to explain the degradation of PCP due to Fenton's oxidation at a pH 3.5 (within the reported optimal range) and a fixed amount of ferrous iron ($2.0x10^{-04}$ mol/L). For this purpose, relevant reported reactions and their rates were obtained from previous compilations (Buxton, et al., 1988; Bielski, et al., 1985; Fartahazis and Ross, 1977). After the model was developed, it was validated by comparison with the time-course concentrations of hydrogen peroxide and ferrous iron ($2.0x10^{-04}$ mol/L) in batch experiments, in the absence of free radical scavengers. Once validated, the model was applied to simulate the time-course concentrations of hydrogen peroxide, ferrous iron and PCP, as well as the equilibrium concentrations of PCP subject to different hydrogen peroxide doses and a constant dose of ferrous iron in batch reactors.

The pH dependence of some of the reactions in Table 5.1 has been explained by acid-catalyzed mechanisms. For example, the reduction of ferric iron by hydrogen peroxide (Equation i1) follows the mechanism:

$$H_2O_2 + Fe^{3+} \xleftarrow{Ki1a} H^+ + FeOOH^{2+} \qquad \text{(i1a)}$$

$$FeOOH^{2+} \xrightarrow{ki1b} Fe^{+2} + \bullet O_2H \qquad (i1b)$$

which implies that $k_{i1} = k_{i1b} K_{i1a}/[H^+]$. The $FeOOH_2^+$ complex has been postulated to explain the observation of a dark colored complex with maximum absorption at λ= 430 nm (Evans, et al., 1948).

Given the values $k_{i1b} = 1.1x10^{-02}$ s^{-1} and $K_{i1a}=3.65x10^{-03}$ (Evans, et al., 1948), the resulting value for k_{i1} is $4x10^{-05}$/ $[H^+].s$). This is in agreement with the $k_{i1} = 2x10^{-03}$ L/Mol.s value at pH 1.7 assumed by Walling and Weil (1974). The values for this constant of 0.01 and 0.02 L/Mol.s used by other researchers would be in agreement with this expression at pH of 2.4 and 2.7, respectively (Chen, et al., 1997; Walling, et al., 1973).

This dependence of the k_{i1} on pH is linear (in accordance with the proposed acid-catalyzed mechanism) from pH 1.0 to 2.8, at which the value of the kinetic constant (estimated by optical methods) shows lower pH dependence, up a pH of 3.0. No mechanism has been proposed to explain this behavior at pH>3.0. Although no values for this constant have been reported at higher pH conditions, the value at pH = 2.8 might be the most representative value at slightly higher pH than 3.0.

Additional features of the model developed in this work were reactions of organic substrates with hydroxyl free radicals (such as PCP and intermediates). The reaction rate constants for PCP with hydroxyl free radicals was generated previously (see Section 4.1.5). The scavenging effects of the PCP by-products were estimated by considering the observed PCP degradation rates. The approach followed in this work to account for these effects as a lumping parameter has been successfully applied to estimate scavenging effects of different media treated with different AOPs: photo-Fenton's reactions (Zepp, et al., 1979), ultraviolet light radiation studies in natural waters (Haag, et al., 1985) and soil slurries (Huling, et al., 1998). Mineralization reactions (production of carbon dioxide due to chemical oxidation of organic compounds with hydroxyl free radicals) at the tested conditions were neglected, in accordance with experimental results. Reactions of the

perhydroxyl and superoxide free radicals with organic substrates have been neglected, due to the much lower reactivity of these radicals towards organic molecules (Bielski, et al., 1985). The resulting kinetic model for Fenton's reaction is shown in Figure 5.1.

Some secondary side reactions, such as the reaction between two free radicals (termination) are shown in Table 5.2. These termination reactions are first order with respect to each radical. Since free radical concentrations are very low, reaction rates for these reactions can be neglected, despite the fact that their second-order reaction rate constants are high (Stockinger, 1995).

Other reactions that involve ionizable species (presented in Table 5.3) for which concentrations at low pH approach zero also can be neglected. For example, the perhydroxyl ion (the ionized form of hydrogen peroxide) can be neglected at pH values lower than 9.9, due to the high pK_a of hydrogen peroxide (pK_a=11.9) (Buxton, et al., 1988).

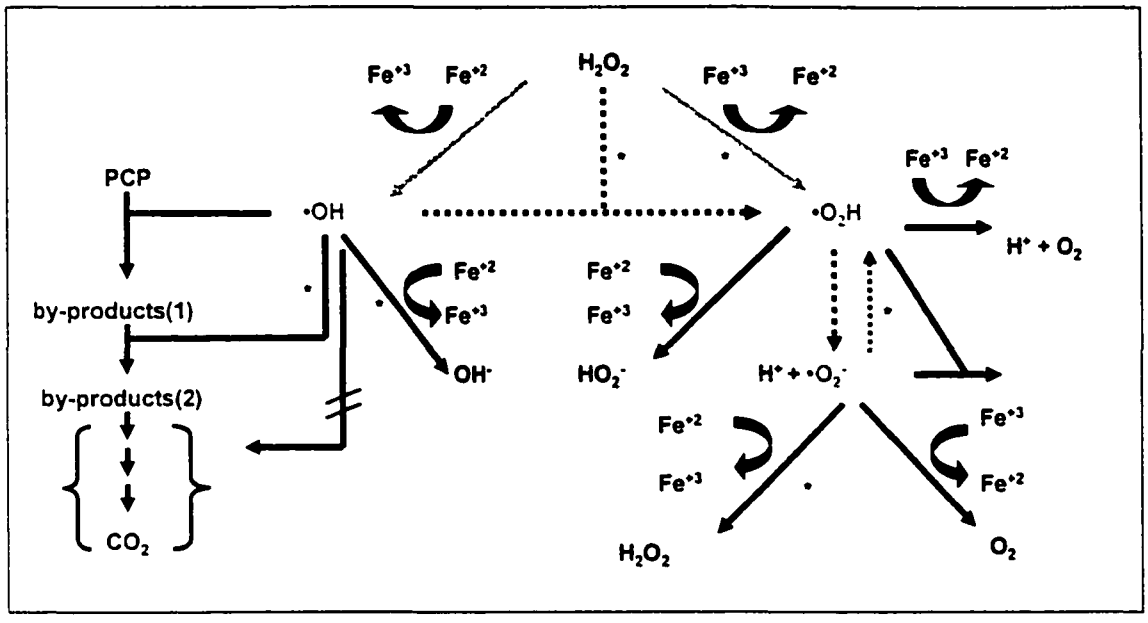

Figure 5.1. Schematic diagram of the kinetic model for Fenton's system. Initiation reactions are indicated with gray arrows, propagation reactions are indicated with dotted arrows and termination reactions are indicated with solid black lines. The reported reaction rate constants for reactions with an * consist of ranges instead of single values.

5.1.4.4. Model Limitations

Although an effort was made to include most of the available reactions reported to date in order to generate a mathematical model of general application, the application of the model presented in this work at other conditions should be cautions. Due to the strong pH dependence of some of the reactions involved in the Fenton's system, application at different pH should be validated first.

The model presented in this work accounts for the reactions of the free chemical species. However, it has been demonstrated that some complexes might play important roles in the Fenton's system. For example, chloride and sulfate ions can complex ferric ion (Nadtochenko, et al., 1998; Rush, et al., 1985), ferric ion can become a hydrate complex (Nadtochenko, et al., 1998); some organic compounds (such as oxalate and

fulvic acids) can complex ferrous iron and modify its reaction rates at different conditions (Kosaka, et al., 1998; Voelker, et al., 1996; Lindsey, et al., 2000). Such reactions were not included in the model, although they might be important under specific conditions (such as high concentrations of the complexing compounds).

Other reactions that were not included in the kinetic model included possible interactions of the organic matter (specifically PCP degradation by-products) with some other species present in the system. For example, some organic free radicals might oxidize or reduce ferrous or ferric ions (as in Equations 2a and 2c in Section 5.1.4.2). It has been demonstrated that quinones, which are phenol by-products of Fenton's treatment, exert such effects to an important extent (Chen, et al., 1997).

Table 5.1. Reactions and rates for a kinetic model for Fenton's reaction. The subscripts i, p and t are for initiation, propagation, and termination reactions, respectively.

Reaction	Reaction #	Kinetic Constant (L/mol .s)	Reference	Value used in this work (L/mol.s)
$H_2O_2 + Fe^{3+} \xrightarrow{k_{i1}} Fe^{+2} + \bullet O_2H + H^+$	i1	$k_{i1} = 4x10^{-05}/[H^+]$ at the range1.0<pH<2.8. Constant from 2.8<pH<3.2 k_{i1} =0.01-0.02	(Evans, et al., 1948) (Chen, et al., 1997)	k_{i1}=0.02 *
$H_2O_2 + Fe^{2+} \xrightarrow{k_{i2}} Fe^{+3} + OH^- + \bullet OH$	i2	k_{i2} = 76	(Walling, 1975)	k_{i2} = 76
$H_2O_2 + OH\bullet \xrightarrow{k_{p1}} H_2O + \bullet O_2H$	p1	$k_{p1} = 2.7x10^{07}$ ($1.2x10^{07}$ – $3.8x10^{07}$) $k_{p1} = 1.2x10^{07}$ (pH=3.0)	(Buxton, et al., 1988) (Fartahazis and Ross, 1977)	k_{p1} = $3.8x10^{07}$ *
$\bullet O_2H \xleftarrow{Ka} \bullet O_2^- + H^+$	$K_a = k_{p2}/k_{p3}$ p2(forward) p3(backward)	$K_a = 1.58x10^{-05}$ $k_{p2} = K_a k_{p3}$ $k_{p3} = 5.0x10^{10}$ (pH=4) $k_{p3} = 7.2x10^{10}$ (pH = 2) $k_{p3} = 4.8x10^{10}$	(Buxton, et al., 1988) (Chen, et al., 1997) (Bielski, et al., 1985)	k_{p3} = $5.0x10^{10}$ *
$OH\bullet + Fe^{+2} \xrightarrow{k_{t1}} Fe^{+3} + OH^-$	t1	k_{t1}=$3.0x10^{08}$ k_{t1}=$3.8x10^{08}$ k_{t1}=$4.3x10^{08}$	(Walling, 1975) (Walling, et al., 1974) (Chen, et al., 1997)	k_{t1}=$3.0x10^{08}$ *
$\bullet O_2H + Fe^{+3} \xrightarrow{kt2} Fe^{+2} + H^+ + O_2$	t2	k_{t2}=$1.0x10^{04}$	(Bielski, et al., 1985) (Fartahazis and Ross, 1977)	k_{t2}=$1.0x10^{04}$

$\bullet O_2H + Fe^{+2} \xrightarrow{k_{t3}} Fe^{+3} + HO_2^-$	t3	$k_{t3} = 1.2x10^{06}$	(Bielski, et al., 1985) (Chen, et al., 1997)	$k_{t3}=1.2\ x10^{06}$
$Fe^{+3} + \bullet O_2^- \xrightarrow{kt4} Fe^{+2} + O_2$	t4	$k_{t4}=1.5x10^{08}$	(Rush, et al., 1985)	$k_{t4}=1.5\ x10^{08}$
$Fe^{+2} + \bullet O_2^- \xrightarrow{kt5} Fe^{+3} + H_2O_2$	t5	$k_{t5}=1.0x10^{07}$ $k_{t5}=3.1x10^{07}$	(Rush, et al., 1985) Huling, et al 1988	$k_{t5}=1.0x10^{07}$ *
$\bullet O_2H + \bullet O_2^- \xrightarrow{kt6} O_2 + H_2O_2$	t6	$k_{t6}=9.7x10^{07}$	(Bielski, et al., 1985)	$k_{t6}=9.7x10^{07}$
$PCP + \bullet OH \xrightarrow{k_{tPCP}} Products(1)$	tPCP	$k_{tPCP}=4.5x10^{09}$ No other reported values	This work	k_{tPCP} $=4.4x10^{09}$
$Products(1) + \bullet OH \xrightarrow{k_{tscav}} Products(2)$	tscav	N/A	This work	k_{tscav}/k_{tPCP} $=0.205$

Table 5.2. Reactions and rates for reported reactions that are negligible under low oxidation regimes. The subscripts i, p and t are for initiation, propagation, and termination reactions, respectively.

Reaction	Reaction #	Kinetic Constant (L/Mol.s)	Reference
$\bullet OH + \bullet O_2^- \xrightarrow{kt7} OH^- + O_2$	t7	$k_{t7}=8.0\times10^{09}$	(Buxton, et al., 1988)
$\bullet OH + \bullet O_2H \xrightarrow{kt8} O_2 + H_2O_2$	t8	$k_{t8}=6.0\times10^{09}$	(Buxton, et al., 1988)
$2\bullet OH \xrightarrow{kt9} H_2O_2$	t9	$k_{t9}=5.3\times10^{09}$	(Walling, 1975)
$2\bullet O_2H \xrightarrow{kt10} O_2 + H_2O_2$	t10	$k_{t10}=1.1\times10^{10}$	(Buxton, et al., 1988)

Table 5.3. Reactions and rates for reported reactions that are negligible under acidic pH. The subscripts i, p and t are for initiation, propagation, and termination reactions, respectively.

Reaction	Reaction #	Kinetic Constant (L/mol.s)	Reference
$O_2H^- + \bullet O_2^- \xrightarrow{k_{t11}} H_2O_2 + O_2$	t11	k_{t11}=2 (pH 8.9 to 12.7)	(Bielski, et al., 1985)
$\bullet OH + O_2H^- \xrightarrow{k_{p4}} \bullet O_2H + OH^-$	P4	$k_{p4}=7.5\times10^{09}$	(Buxton, et al., 1988)
$\bullet OH + OH^- \xrightarrow{k_{p5}} \bullet O^- + H_2O$	P5	$k_{p5}=1.2\times10^{10}$	(Buxton, et al., 1988)

5.2. Experimental Section

5.2.1. Chemicals

Pentachlorophenol (99%) was purchased from Sigma, as was the surrogate (dibromophenol, 95%) and internal standard (dibromobenzene, 98%) used for extraction and analysis. $FeSO_4 \cdot 7H_2O$ (99%+) was purchased from Baxter.

Hydrogen peroxide (non-stabilized, 31.4%), sodium chloride (99.9%) and sulfuric acid (conc.) were all purchased from Fisher. pH adjustment was achieved by addition of 0.1 N sulfuric acid.

Pesticide-grade solvents used for the analysis of PCP and PCP-organic by-products (chloroform and ethyl acetate) were purchased from Fisher.

Organic acid standards previously reported as by-products of phenol and chlorophenol under different AOP treatments were compared to the observed ionizable by products concentrated by SPE and analyzed by means of HPLC. These organic acid standards were: maleic (Aldrich, 99%), muconic (Aldrich, 99%), glyoxylic (Aldrich, 50% solution in water), formic (Sigma, reagent grade), fumaric (Sigma, reagent grade), succinic (Sigma, reagent grade), and oxalic (Sigma, reagent grade).

5.2.2. Analytical Methods

5.2.2.1. Organic Substrates

The concentration of pentachlorophenol (PCP) was determined with an HP 5890 Series II gas chromatograph with a mass spectral detector and a 50-m HP-5 crosslinked 5% PH ME silicone capillary column of 0.2 mm I.D. and 0.33 μm film thickness. The

GC temperature program was: 50 °C initial temperature held for 2.0 min followed by increases of 20 °C/min to 160 °C and then at 6 °C/min to 250 °C (total run time = 22.5 min). One mL of each aqueous sample was spiked with 0.2 mM dibromophenol (as surrogate) in acetone solution, adjusted to pH less than 1.0, extracted with 0.5 mL of chloroform, and then dosed with dibromobenzene as internal standard before injection (the final concentration of the internal standard in the extracted solution was 0.05 mM).

Acidification and dose of the surrogate solution was done immediately after sampling. Quenching of the PCP degradation after sampling was achieved by acidification of the sample and addition of an excess of acetone dosed from the surrogate solution. The effectiveness of this quenching procedure was verified by the quantitative recovery of the surrogate, typically 90% or higher. Quantification of PCP was performed on the basis of the respective main ion from the mass spectrum of each compound (266 for PCP and 252 for the surrogate) normalized with respect the main ion of the internal standard (236). The extraction efficiency was evaluated by means of the surrogate. Data from samples with surrogate concentrations out of the interval of ±15% around the mean were analyzed a second time.

5.2.2.2. Oxidizing Reagents

5.2.2.2.1. Hydrogen Peroxide

Concentration of the stock hydrogen peroxide solution was determined before use with standard 0.3 N potassium permanganate to confirm its lack of degradation during storage. Aliquots were diluted to 250 mL with water for analysis and acidified with 10.0 mL concentrated sulfuric acid before titration.

Lower concentrations of hydrogen peroxide (< 10 ppm) were analyzed by means of the titanium sulfate method (APHA, et al., 1980). The detection limit of this method is 0.3 mg/L. One mL samples were added to 100 μL of 6.7 g/L $TiSO_4 \cdot 8H_2O$ in 17% sulfuric acid aqueous solution. The color of the yellow peroxo-complex was allowed to develop for about 5 min., and then absorbance was read at 405 nm and compared to calibration standards (obtained by dilution of a potassium permanganate-titrated hydrogen peroxide solution). Hydrogen peroxide analysis was done immediately after sampling (adding the sample to a 1.5 mL cuvet containing the titanium reactant) to avoid the need for quenching with sulfites, since an excess of sulfites was shown to interfere with this assay. Lack of interference of ferrous and ferric iron (at the concentrations used in this work) with this analysis was tested and confirmed. A more sensitive method using 2,9 dimethyl, 1,10-phenanthroline (Kosaka, et al., 1998) could not be used due to interference of ferrous iron.

5.2.2.2.2. Ferrous Iron

Ferrous iron was measured by the 1,10 phenanthroline method. One mL samples were treated with 200 μL of ammonium acetate buffer solution (pH 3.2, 250 g/L in water), and 150 μL of 1,10 phenanthroline solution (1.0 g/L in water). Absorbance was measured at 508 nm and compared to ferrous iron calibrations standards with a concentration range from 0 to 10 ppm (APHA, et al., 1980). Ferrous iron calibration standards were prepared from stock iron solution at 100 ppm (containing 0.7022 g $Fe(NH_4)_2(SO_4)_2 \cdot 6H2O$ dissolved into 29% H_2SO_4 in water and then the volume adjusted to 1.0L). The following reactants were added to the 1.0 mL calibration standard

solutions: 100 μL of hydroxylamine solution (10 g $NH_2OH \cdot HCl$ in 100 mL ddH2O), 100 μL of sodium acetate buffer (100 g $NaC_2H_3O_2 \cdot 3H_2O$ in 400 mL glacial acetic acid) and 150 μL of 1,10 phenanthroline solution (1.0 g/L in water). Ferrous iron analysis was done immediately after sampling (by adding the sample to a 1.5 mL cuvet containing the rest of the reactants) to avoid the need for quenching with sulfites since an excess of these was shown to interfere with this assay. Lack of interference of hydrogen peroxide with this assay at concentrations lower than 1 mM was tested. The detection limit of this assay is close to $5.0x10^{-07}$ mol/L (approximately 0.3 ppm).

5.2.2.3. Chemical Oxidation By-products

5.2.2.3.1. Chloride Analysis

Chloride ion was measured by means of the mercuric thiocyanate method. One mL of sample was added to 80 μL of mercuric thiocyanate solution (Hach No. 22121) and 40 μL of ferric ion solution (Hach No. 22122-42). Color was allowed to develop, absorbance was read at 455 nm and compared to calibration standards (from 0 to 10 ppm). Quenching with sulfites was not done, since interference of an excess of sulfites with this analysis was observed. Instead, samples were processed immediately after sampling, adding the sample to a 1.5 mL cuvet containing all the rest of the reactants. Lack of interference of residual hydrogen peroxide on this analysis due was confirmed by spiking prepared samples with hydrogen peroxide (up to 0.01%=$3x10^{-03}$ mol/L) without change in absorbance of the solution.

5.2.2.3.2. Organic PCP By-products

5.1.2.3.2.1. Concentration by Solid Phase Extraction

Ionizable by-products were concentrated by means of 100 mg ion-exchange Supelclean C-SAX solid phase extraction (SPE) tubes (Supelco). The tubes were conditioned with 2 mL of 1M NaCl, and washed with 10 mL of deionized water. The neutralized sample was drawn through the tube at 1 mL/min by means of a peristaltic pump, and then washed with 2mL of deionized water. Finally, the concentrated ionizable compounds were eluted with 500 μL of HCl 0.1 M in water before HPLC analysis.

5.1.2.3.2.2. High Pressure Liquid Chromatography

Ionizable by-products were analyzed with a Waters HPLC, using a Bio-rad Aminex HPX-87H column (Bio-Rad 125-0140) and a UV detector at 210 nm after concentration with SPE. The mobile phase was sulfuric acid 0.008 N, prepared in Nanopure water with a conductivity of 18 mΩ and degassed by boiling for 20 min under vacuum. A flow rate of 0.6 mL/min was used at a temperature of 35 °C.

5.1.2.3.2.3. Derivatization

A derivatization procedure developed to analyze organic acids in urine (H. Liebich , et al., 1999) was applied to the SPE-concentrated samples for identification purposes, combined with gas chromatography combined with mass spectrometry. This method is suitable for derivatization of organic acids in aqueous solution, using trimethyl oxonium tetrafluoroborate (TMO, obtained from Aldrich) (H. Liebich , et al., 1999).

The derivatization with trimethyl oxonium tetrafluoroborate (TMO) consists of:

a) Add approximately 20 mg of Na_2CO_3 to 2.0 mL of sample, to alkalize.

b) Add approximately 30 mg of TMO in five portions, during 4 minutes. Wait one minute and neutralize with approximately 15 mg $NaHCO_3$.

c) Repeat previous step two more times (three times total).

d) Repeat step b) one more time, omitting neutralization. Instead, alkalize to pH 8 with approximately 20 mg Na_2CO_3.

e) Repeat step b) one more time, but neutralize with 20 mg $NaHCO_3$ (instead of 15 mg).

f) Stopper vial and incubate for 2 min at 100 °C.

g) Cool to room temperature.

h) Extract with 0.5 mL of chloroform before GC analysis.

Derivatized samples were run with the same GC/MS equipment used for the analysis of chlorophenols. The derivatization method was validated with formate, oxalate, maleate, succinate and muconate standards in water at a concentration of 10 ppm each. The GC temperature program was optimized for separation of the derivatized organic acid standards presented in Table 5.4. as follows: 30 °C initial temperature held for 2.0 min followed by increases of 10 °C/min to 260 °C (total run time = 25 min). The mass spectrometer was initially on, then turned off from 5.5 to 7.5 min. The derivatized (methylated) organic acids were identified by their mass spectra, with their respective retention time indicated in Table 5.4. Derivatization of the PCP ionizable by-products observed by SPE-HPLC (see Sections 5.1.2.3.2.1 and 5.1.2.3.2.2) was not successful.

Table 5.4. GC/MS analysis of derivatized organic acid standards.

Analyte	Retention time (min)
Methyl Formate	From 3 to 4.2 min (before solvent front)
Dimethyl Oxalate	7.52
Dimethyl Maleate	12.55
Dimethyl Succinate	12.65
Dimethyl Muconate	16.95

5.1.2.3.2.4. Liquid-Liquid Extraction

PCP reaction by-products were analyzed by means of extraction with ethyl acetate after acidification with phosphoric acid. 50 μL of concentrated phosphoric acid and 2.0 mL of ethyl acetate were added to 2.0 mL of sample. The mixture was shaken for 20 min. and the organic phase was then concentrated to 100 μL under a gentle N_2 stream. Dibromobenzene was used as internal standard before analysis: a concentrated dibromobenzene solution in acetone was added, to achieve a final concentration of 0.025 mM. The concentrated extracts were analyzed with the same GC/MS method used to analyze PCP, except that a modified temperature profile was used to achieve better separation of the different observed peaks: 50 °C initial temperature held for 2.0 min followed by increases of 20 °C/min to 150 °C and then at 3 °C/min to 250 °C (total run time = 37 min).

5.2.3. Total Organic Carbon

Purgeable total organic carbon (TOC) was analyzed with a Dohrmann DC-80 TOC Analyzer after acidifying the sample with phosphoric acid (2 drops per 25 mL) and purging with oxygen for 7 min to eliminate interferences from CO_2. One mL of sample was injected into the analyzer. Calibration for this analysis was done using a potassium phthalate solution equivalent to 10.0 ppm of TOC (this solution was prepared by diluting a 2000 ppm standard solution, which contained 0.425g/L of reagent-grade potassium hydrogen phthalate). This assay is based on oxidation of the organic carbon in the sample by means of oxidation with potassium persulfate (2% solution) in the presence of ultraviolet light, generating stoichiometric amounts of CO_2, which is detected with a non-dispersive infra-red (NDIR) detector. The integrated area of the NDIR signal is directly related to the carbon concentration in the sample.

5.3. Experiments

5.3.1. Batch Experiments

Shake flask (batch) experiments were carried out to characterize the Fenton's oxidation of PCP. The pH of the PCP-saturated solution was adjusted to 3.5, which is within the reported optimal range of 3.0 to 4.0 for Fenton's reaction (Bigda, 1995; Venkatadri, et al., 1993; Zepp, et al., 1979). Aliquots were dosed into vials, dosed with a concentrated solution of ferrous iron (to reach a concentration of $2x10^{-04}$ mol/L) and then variable amounts of H_2O_2 (from 0 to 10 molecules of H_2O_2 per molecule of PCP). The dose of Fe^{+2} ($2x10^{-04}$ mol/L) was selected from reported optimal H_2O_2/Fe^{+2} ratios, which vary from 10:1 to 5:1 (w/w) (Bigda, 1995; Tang, et al., 1997).

Batch experiments were performed by dosing 36 mL of pH adjusted (pH =3.5) PCP solution in 40 mL amber glass vials (baked for 4 hours at 440 °C) with teflon-lined caps. Vials were dosed with small aliquots of ferrous (or ferric) sulfate solution to reach a concentration of iron ions of $2x10^{-04}$ mol/L and small aliquots of hydrogen peroxide (sequentially), prepared from standarized stock. These solutions were freshly prepared, and their volumes were less than 1% of the total volume of the PCP solution. The vials were vigorously shaken after the dose of the reactants.

Reaction time was measured from the dose of hydrogen peroxide. One mL samples were immediately analyzed for ferrous iron, hydrogen peroxide and chloride (for samples obtained from PCP solutions only). Samples for PCP analysis were acidified, and spiked with surrogate at the sampling time. Finally, samples were extracted at the end of the experiment for analysis.

Two types of shake flask experiments were performed. For the first type of experiment, vials were dosed with reactants (ferrous iron to reach a concentration of $2.0x10^{-04}$ mol/L and hydrogen peroxide from zero, for controls, up to $8.5x10^{-04}$ mol/L) and left shaking overnight until they reached equilibrium. Additionally, controls with H_2O_2 but no iron were done, since it has been reported that hydrogen peroxide can itself degrade some organic compounds (Venkatadri, et al., 1993).

The second type of experiment involved monitoring the time-dependent concentration of reactants for short intervals (starting after hydrogen peroxide dose) until steady state was reached (identified by null changes in reactant concentrations).

For both types of experiments, the initial concentration of reactants was estimated by means of controls for which no hydrogen peroxide was dosed (for PCP and ferrous

iron analysis) or no iron was dosed (for hydrogen peroxide analysis). Typical experimental conditions for both time-dependent and equilibrium experiments are included in Table 5.5.

Table 5.5. Typical experimental conditions used in this work for the Fenton's degradation of PCP.

Variable	Value
pH	3.5
Ferrous iron concentration	2.0×10^{-04} mol/L
Hydrogen peroxide concentration	$0.0\text{-}8.5 \times 10^{-04}$ mol/L
Reaction time	From 0 until equilibrium was reached, or 12 h to insure equilibrium
Temperature	Ambient (25 °C)

5.3.2. Model Solution

The reaction mechanism presented in Table 5.1. was used to generate a mathematical model to predict the time evolution concentrations of H_2O_2 and Fe^{+2} in batch reactors. The model was solved by applying the pseudo-steady state assumption to the differential mass balances of the free radicals. This assumption states that since the concentrations of these species are very small, changes in their concentrations with time are very small (and can be neglected). Thus, the mass balances (for free radicals only) become algebraic equations instead of differential equations. The resulting system of differential and algebraic equations was numerically solved with a fourth-order Runge-

Kutta method, implemented with the software EES (Engineering Equation Solver). The step size was varied in order to control the relative error, resulting in relative residuals lower than $1x10^{-10}$; the EES solution was also verified with the software SIMUSOLV, using the more robust Adams-Moulton method, a predictor-corrector linear multistep method, with identical results.

Since the reported values for the reaction rates of some of the equations in Table 5.1. (k_{i1}, k_{p1}, k_{p3}, k_{t1}, and k_{t5}) consists of ranges instead of single values, specific values were selected. These values were selected to provided the best fit to one set of data, obtained by measuring the time course concentrations of hydrogen peroxide and ferrous iron of duplicate batch experiments at initial concentrations of hydrogen peroxide and ferrous iron concentration of $7.0x10^{-04}$ mol/L and $2.0x10^{-04}$ mol/L, respectively. This parameter estimation was done by means of the software SIMUSOLV. After the optimal kinetic parameters were selected, there were used to simulate the rest of the data presented in this work.

5.4. Results

5.4.1. Reaction of Hydrogen Peroxide and Iron in the Absence of Organic Substrates

Experiments in which the time-dependent concentration of hydrogen peroxide and ferrous iron were measured for short intervals (starting after hydrogen peroxide dose) until steady state was reached (identified by null changes in reactant concentrations) were used to validate the model. In order to validate the model suitability in the absence of additional free radical scavengers, some of these experiments were performed in pure water solutions of hydrogen peroxide and ferrous iron alone. Model solutions and

experimental data for the time courses of hydrogen peroxide and ferrous iron concentrations at different hydrogen peroxide doses are presented in Figure 5.2 to 5.5. The data in Figure 5.2 were used to find the values of model parameters that yielded the best model fit to parameters previously described by ranges instead of single values (k_{i1}, k_{p1}, k_{p3}, k_{t1}, and k_{t5}). These values are indicated with * in Table 5.1. Figures 5.3 to 5.5 show model predictions (together with the experimental data).

Sensitivity analysis of the model on the reactions in Table 5.2 indicated that accounting for these reactions does not have any effect on the model solution, and thus only reactions shown in Table 5.1. were included into the model. This is in accordance with some of the assumptions taken to develop an earlier kinetic model for ozonation (Stockinger, 1995).

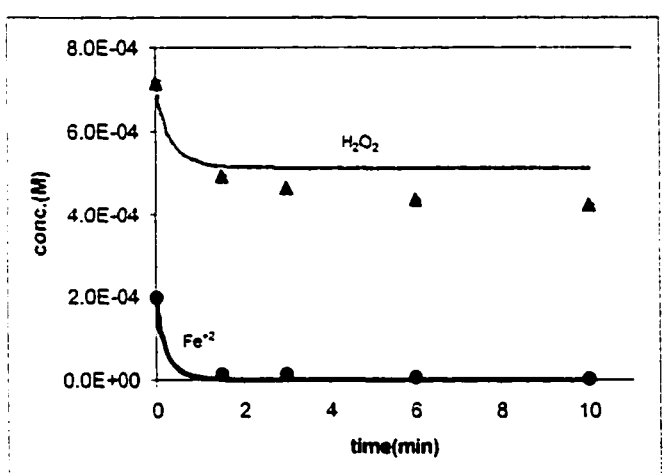

Figure 5.2. Degradation of hydrogen peroxide (▲) and ferrous iron (●) at high hydrogen peroxide dose ($[H_2O_2]_o = 7.0 \times 10^{-04}$ mol/L) and initial ferrous iron concentration of $[Fe^{+2}]_o = 2.0 \times 10^{-04}$ mol/L. This set of data was used to find the values of the kinetic constants that provided the best model fit (indicated with an * in Table 5.1). Selected values of these kinetic constants were within reported ranges. The gray line is the model-predicted hydrogen peroxide concentration and the black line is the model-predicted ferrous iron concentration. Error bars (partially obscured by the symbols) represent the standard deviation of measurements from duplicate vials.

Lowering the initial hydrogen peroxide concentration to $0.8x10^{-04}$ and $0.5x10^{-04}$ mol/L (while keeping the initial ferrous iron dose at $2.0x10^{-04}$ mol/L) caused hydrogen peroxide concentrations to fall below the detection limit at the first sampling point (see Figure 5.3 and Figure 5.4, respectively). The oxidation of ferrous iron achieved with these low doses of hydrogen peroxide was only partial (as opposed to what was observed at the hydrogen peroxide dose of $7.0x10^{-04}$ mol/L). In these situations, the model-predicted ferrous iron concentrations are in good agreement with the experimental data.

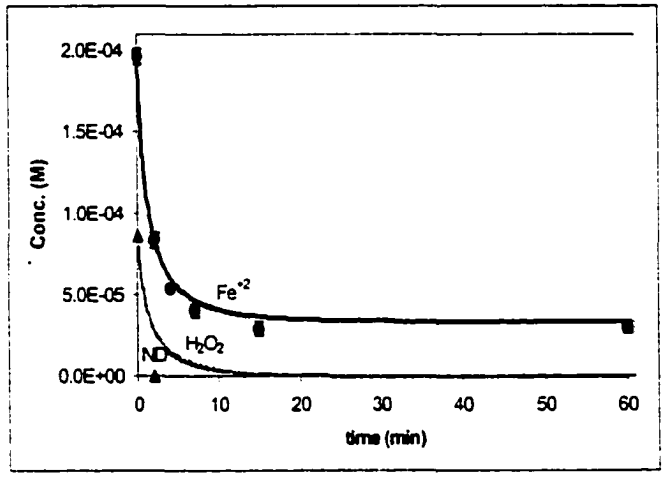

Figure 5.3. Degradation of hydrogen peroxide (▲) and ferrous iron (●) at low hydrogen peroxide dose ($[H_2O_2]_o = 0.8x10^{-04}$ mol/L) and initial ferrous iron concentration of $[Fe^{+2}]_o = 2.0x10^{-04}$ mol/L. The concentration of hydrogen peroxide at the first sampling point was below the detection limit. The gray line is the model-predicted hydrogen peroxide concentration and the black line is the model-predicted ferrous iron concentration. Error bars represent the standard deviation of measurements from duplicate vials.

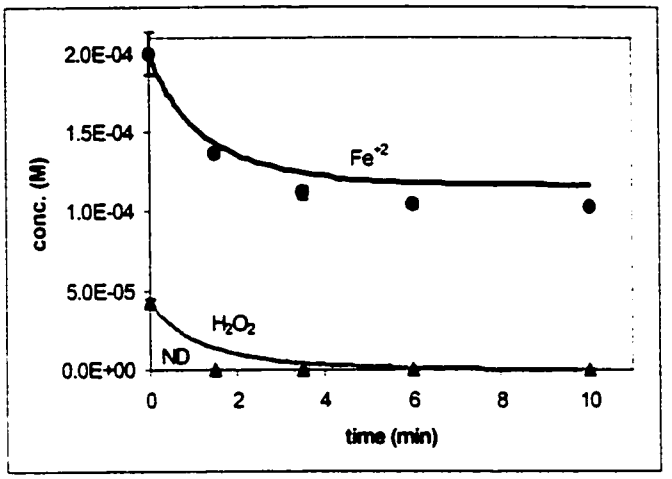

Figure 5.4. Degradation of hydrogen peroxide (▲) and ferrous iron (●) at low hydrogen peroxide dose ($[H_2O_2]_o$ =0.5 x 10^{-04} mol/L) and initial ferrous iron concentration of $[Fe^{+2}]_o$=2.0x10^{-04} mol/L. The concentration of hydrogen peroxide at the first sampling point was below the detection limit. The gray line is the model-predicted hydrogen peroxide concentration and the black line is the model-predicted ferrous iron concentration. Error bars represent the standard deviation of measurements from duplicate vials.

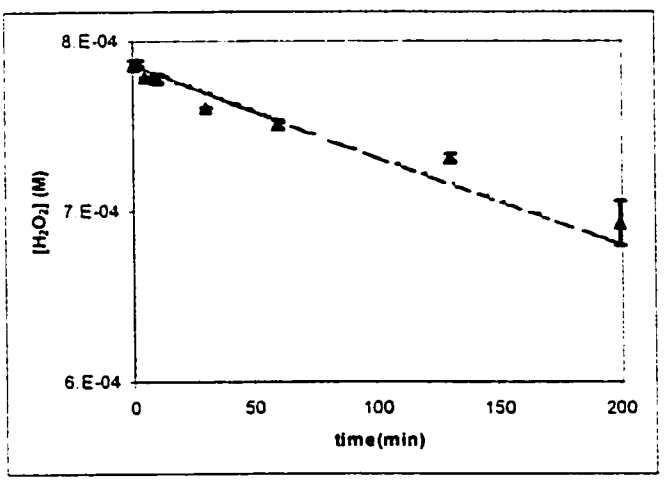

Figure 5.5. Degradation of hydrogen peroxide (▲) at high hydrogen peroxide dose ($[H_2O_2]_o$ =7.8x10^{-04} mol/L), initial ferrous iron concentration of $[Fe^{+2}]_o$=0.0x10^{-04} mol/L, and initial ferric iron concentration of $[Fe^{+3}]_o$=2.0x10^{-04} mol/L. The gray line is the model-predicted hydrogen peroxide concentration. Error bars represent the standard deviation of measurements from duplicate vials.

The concentration of hydrogen peroxide (at the relatively high initial concentration of $7.8x10^{-04}$ mol/L) as a function of time in the presence of ferric iron at a concentration of $2.0x10^{-04}$ is presented in Figure 5.5. The hydrogen peroxide concentration fell to about 87% of the initial dose after 200 min. Model-predicted hydrogen peroxide concentrations were in remarkably good agreement with these data.

5.4.2. Time-dependent Degradation of PCP by Fenton's Reagent

Once the model was validated in the absence of hydroxyl free radical scavengers, and single values of the kinetic constants in Table 5.1. for which ranges of values were available had been found, the suitability of the model to predict time-course degradation of PCP, hydrogen peroxide and ferrous iron in PCP solutions was compared to the time-dependent concentration of these reactants.

5.4.2.1. Effect of Hydrogen Peroxide Concentration in the Presence of Ferrous Iron

The degradation of PCP and the corresponding hydrogen peroxide and ferrous iron concentrations as a result of low hydrogen peroxide dose ($1.2x10^{-04}$ mol/L) are presented in Figure 5.6. It is observed that at these conditions 65% of the PCP was degraded in the first two minutes after the hydrogen peroxide was dosed. Hydrogen peroxide fell below the detection limit after the first sampling point, indicating that the degradation of PCP was limited by the dose of hydrogen peroxide. This set of data was used to estimate the hydroxyl free radical scavenging effects due to the PCP intermediates. The value of $k_{tscav}/ k_{tPCP} = 0.205$ provided the best model fit to the experimental data. This value is expressed on a basis of per carbon molecule

(considering that one PCP molecule generates 6 molecules of carbon as by-products), and assumes no mineralization of the carbon. This assumption was supported by the results from the batch experiments done to completion (see Section 5.4.3.1.). The values for the kinetic constants for which ranges of values were found in literature (as opposed to single values) were estimated in the previous section by fitting data for experiments with pure hydrogen peroxide and ferrous iron solutions (see Section 5.4.1.).

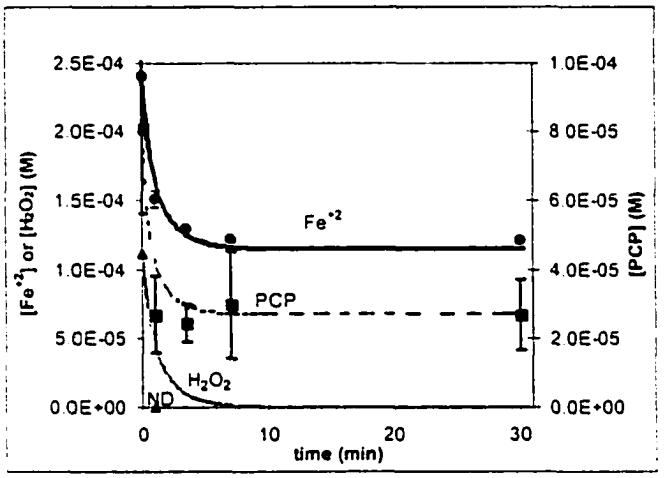

Figure 5.6. Experimental H_2O_2 (▲) and Fe^{+2} (●) concentrations and model solution at low hydrogen peroxide dose ($1.2x10^{-04}$ mol/L) and initial ferrous iron concentration of $[Fe^{+2}]_o=2.0x10^{-04}$ mol/L. This set of data was used to determine the scavenging effects of the PCP by-products. The concentration of hydrogen peroxide at the first sampling point was below the detection limit. ■ represent PCP concentrations and the dotted line is the model-fitted PCP concentration. Error bars represent standard deviation of measurements from duplicate vials.

The effect of increasing the hydrogen peroxide dose to $8.4x10^{-04}$ mol/L is shown in Figure 5.7. It can be observed that the PCP concentration was reduced below 95% within the first minute after hydrogen peroxide was dosed into the vials. The production of free chloride mirrors the degradation of PCP, although complete dechlorination was

not observed. The observed dechlorination is approximately 65% of the dechlorination that would be observed if every molecule of PCP would yield 5 molecules of chloride. Given the difference between fractional PCP degradation and Cl^- yield, it would be expected that at least some of the PCP by-products would be partially chlorinated, although at a considerably lower extent than the degree of chlorination of PCP (which has a chlorine to carbon ratio of 5:6).

Hydrogen peroxide degradation under these conditions was only partial, while the ferrous iron oxidation approached completion during the first minute after dose of hydrogen peroxide.

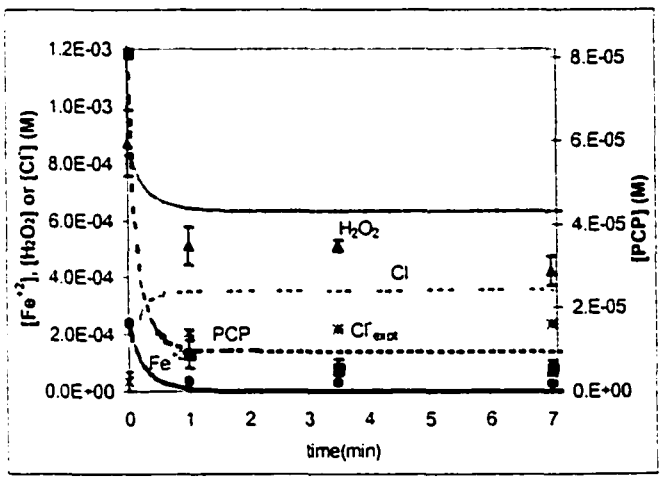

Figure 5.7. Experimental H_2O_2 (▲) and Fe^{+2} (●) time evolution and model solution at high hydrogen peroxide dose ($8.4x10^{-04}$ mol/L) and initial ferrous iron concentration of $[Fe^{+2}]_o=2.0x10^{-04}$ mol/L. The concentration of hydrogen peroxide at the first sampling point was below the detection limit. ■ represent PCP concentrations and the dotted line is the model-predicted PCP concentration. * represent experimental Cl^- concentrations and the dotted line is the model-predicted Cl^- concentration. Error bars represent standard deviation of measurements from duplicate vials.

5.4.2.2. Effect of Hydrogen Peroxide in the Presence of Ferric Iron

The time-dependent concentration of hydrogen peroxide and PCP in the presence of ferric iron (at an initial concentration $2.0x10^{-04}$ mol/L), without the dose of any ferrous iron is presented in Figure 5.8. The degradation of PCP was not significant even two hours after dosing the hydrogen peroxide. Hydrogen peroxide was degraded, although to a very low extent. Model predictions are in good agreement with the experimental data.

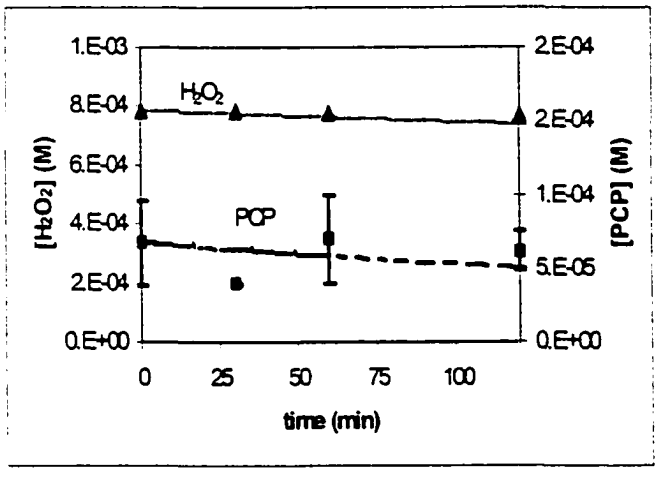

Figure 5.8. Experimental H_2O_2 (▲) and PCP (■) concentrations and model solutions at high hydrogen peroxide dose ($7.9x10^{-04}$ mol/L), initial $[Fe^{+2}]$=0.0 and $[Fe^{+3}]$=$2.0x10^{-04}$ mol/L. Error bars represent standard deviation of measurements from duplicate vials.

5.4.3. Batch Experiments: Reaction to Completion

Once the model suitability to predict the time-course Fenton's degradation of PCP was determined, the suitability of the model to predict experimental PCP degradations over longer time (at which equilibrium concentrations were reached) was tested at initial ferrous iron concentration of $2.0x10^{-04}$ mol/L and variable hydrogen peroxide doses.

5.4.3.1. Degradation of PCP, dechlorination and mineralization

The degradation of PCP and the corresponding production of free chloride as a function of oxidation achieved by different hydrogen peroxide doses are presented in Figure 5.9. Additionally, the stoichiometric (theoretical) production of chloride as a result of PCP degradation (considering that 5 molecules of Cl^- can be produced from one molecule of PCP) is also shown. It is observed that the extent of PCP degradation are higher at lower H_2O_2 doses; however, when the H_2O_2 dose increases, the degradation extent of PCP decreases. This is due to the effect of the PCP by-products, which scavenge free radicals and reduce the degradation rate of the parent compound (PCP). These effects were noticeable even at hydrogen peroxide doses in which time course experiments showed that all the hydrogen peroxide was consumed and an excess of ferrous iron remained in solution (see Figure 5.6.).

pH and purgeable total organic carbon (TOC) were also measured along this experiment (Figure 5.10 and Figure 5.11, respectively). The PCP solution was adjusted to pH 3.4 at the beginning of the experiment. After the reaction a pH reduction of about 0.15 pH units was observed. This change could have been caused by more acidic organic intermediates resulting from the degradation of PCP. Additionally, effects on the acid-base equilibrium due to reactions in which inorganic compounds that can be weak acids (such as hydrogen peroxide, or the perhydroxyl ion) can be expected.

The concentration of TOC during this experiment is presented in Figure 5.11. It is observed that even at the highest hydrogen peroxide dose there is no reduction of TOC. This indicates that mineralization (conversion of the organic carbon to CO_2) does not

occur at all in this range of hydrogen peroxide doses, despite the almost complete degradation of PCP. In contrast, previous reports indicate that strong AOP oxidation of many organic substrates leads to CO_2 production (Stockinger, et al., 1995; Scott, et al., 1995; Heinzle, et al., 1992; W.Z. Tang, 1992).

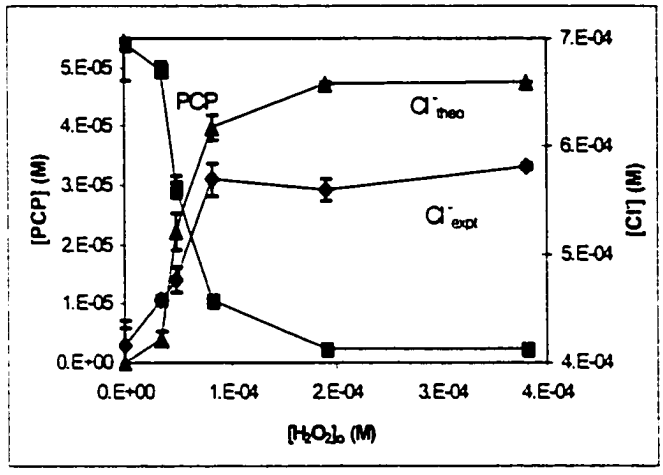

Figure 5.9. PCP (■) and Cl^- (◆) concentrations achieved at different H_2O_2 initial doses and initial ferrous iron concentration of $[Fe^{+2}]_o=2.0x10^{-04}$ mol/L and reaction time of 12 h. Initial PCP concentration was $5.5x10^{-05}$ mol/L. Theoretical Cl^- concentrations (▲) were estimated by considering that degradation of one molecule of PCP yields five molecules of chloride. Error bars represent standard deviation of measurements from duplicate vials.

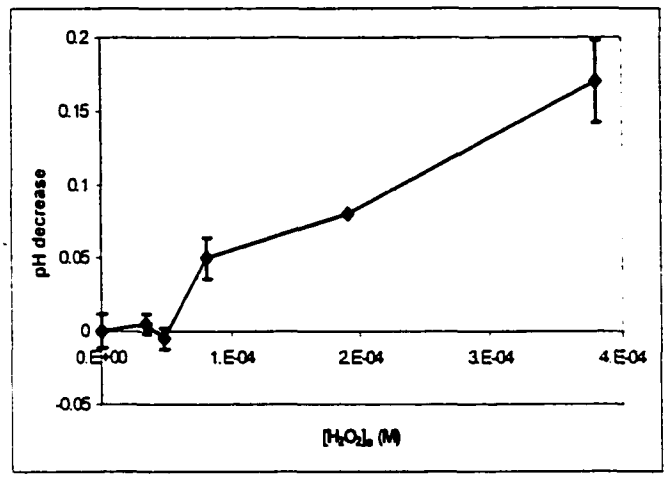

Figure 5.10. Changes in pH achieved due to different H_2O_2 initial doses in PCP solutions and initial ferrous iron concentration of $[Fe^{+2}]_o=2.0x10^{-04}$ mol/L, after a reaction time of 12h. Initial PCP concentration was $5.5x10^{-05}$ mol/L. The initial pH of the solution was adjusted to 3.4. Error bars represent standard deviation of measurements from duplicate vials.

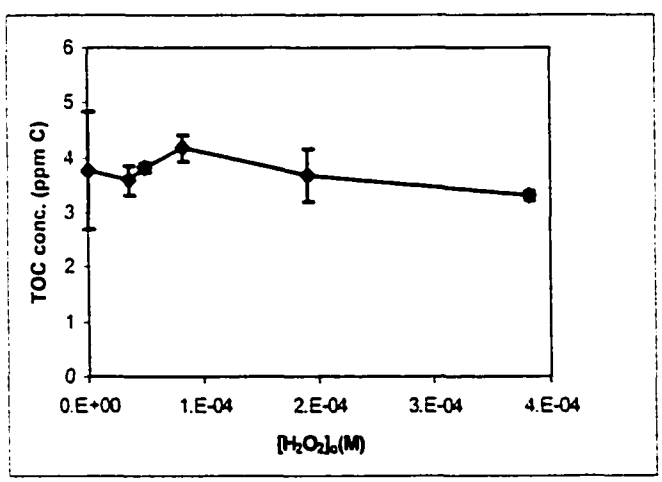

Figure 5.11. Total organic carbon (TOC) concentrations (◆) achieved at different H_2O_2 initial doses of the PCP solution and initial ferrous iron concentration of $[Fe^{+2}]_o=2.0x10^{-04}$ mol/L after a reaction time of 12h. Initial PCP concentration was $5.5x10^{-05}$ mol/L. Error bars represent standard deviation of measurements from duplicate vials.

The PCP degradation data from Figure 5.9 and the steady-state model-predicted PCP extents of degradation are shown together in Figure 5.12. There is good accordance of both experimental and model-predicted PCP concentrations. Thus, the value of $k_{tscav}/k_{tPCP} = 0.205$, previously determined during a time-evolution experiment, also provides a good estimate of the scavenging effects of the PCP intermediates for experiments conducted to completion. Although it can be expected that the nature of these intermediates (and therefore their scavenging effects) might depend on the extent of the PCP (and intermediates) oxidation, neglecting such effects still provided adequate predictions of the PCP degradation.

Model-predicted PCP degradation and experimental data (a different set from the one shown in Figure 5.9, obtained at the same conditions) are shown in Figure 5.13. Good agreement of this data and model predictions is also observed. To investigate the importance of hydroxyl free radical scavenging by by-products, the model prediction with $k_{tscav} = 0.0$ is also shown. Whereas still a good model prediction is obtained for low hydrogen peroxide doses (which achieve up to 40% degradation of PCP), not accounting for scavenging effects causes the model to over-predict PCP degradations at higher hydrogen peroxide doses.

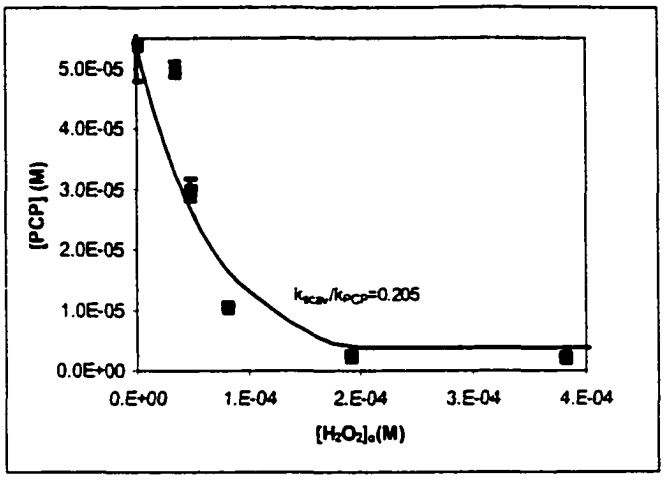

Figure 5.12. Experimental (■) and model-predicted (solid line) PCP concentrations after the Fenton's reaction proceeded to completion at various hydrogen peroxide doses and initial ferrous iron concentration of $[Fe^{+2}]_o=2.0x10^{-04}$ mol/L. Error bars represent standard deviation of measurements from duplicate vials.

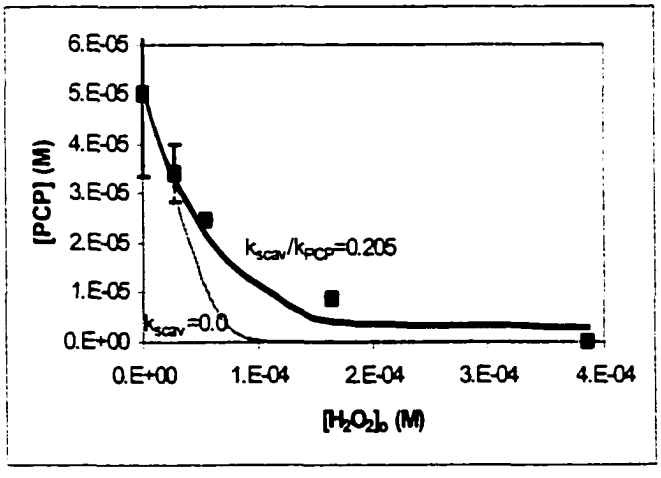

Figure 5.13. Experimental (■) and model-predicted (solid line) PCP concentrations after the Fenton's reaction proceeded to completion at various hydrogen peroxide doses and initial ferrous iron concentration of $[Fe^{+2}]_o=2.0x10^{-04}$ mol/L. Model-predicted PCP degradations without accounting for scavenging effects of PCP by-products are represented with a gray line. Error bars represent standard deviation of measurements from duplicate vials.

PCP concentrations after 12 h of dosing variable hydrogen peroxide concentrations in the absence of iron salts are shown in Figure 5.14. It is observed that even at the highest hydrogen peroxide dose of $4.0x10^{-04}$mol/L, there is no degradation of PCP. Even at the highest hydrogen peroxide dose, chloride concentrations remained non-detectable, confirming also the lack of degradation of PCP. Thus, under the tested conditions, hydrogen peroxide by itself does not achieve any degradation of PCP.

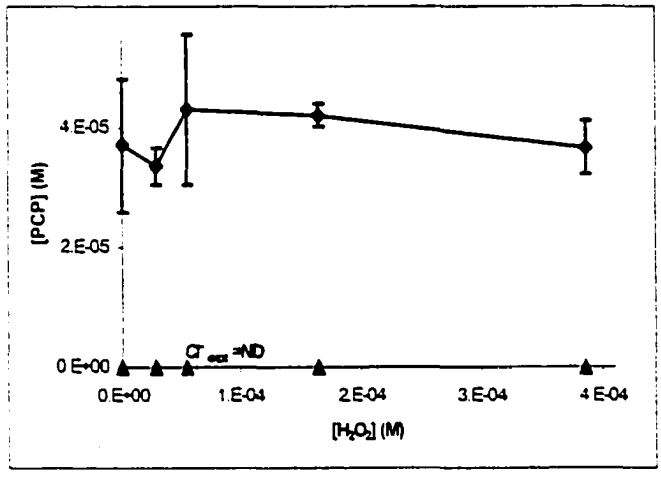

Figure 5.14. Degradation of PCP (◆) achieved at different H_2O_2 initial doses in PCP solutions with no iron salts, after a reaction time of 12h. Chloride concentrations (▲) were non-detectable in all cases. Error bars represent standard deviation of measurements from duplicate vials.

5.4.3.2. Production of Organic Intermediates

5.4.3.2.1. Ionizable Intermediates

Ionizable PCP by-products were concentrated by SPE by a factor of 50.0 (Section 5.1.2.3.2.1.). The concentrated solution containing the ionizable compounds was

analyzed using an HPLC method optimized for organic acids; the column effluent was passed through a UV detector at λ=210 nm (section 5.1.2.3.2.2.). Different by-products were observed on the chromatogram. The retention time of these by-products is shown in Table 5.6. Comparison of these retention times with those of standards of organic acids previously reported as by-products of phenol and lower chlorophenols (shown in Table 5.7) indicates that none of these reported by-products of phenol and lower chlorophenols were present. Thus, identification of the observed by-products by comparison with the standards was not possible.

Table 5.6. Retention time of the observed PCP by-products by SPE/HPLC.

Observed by-product (peak number)	Retention time (min)
S1	7.01
S2	7.96
S3	9.50
S4	10.74
S5	19.70

Table 5.7. Previously reported by-product of phenol and chlorophenols and their retention times using the HPLC method described in the text.

Standard	Retention time (min)	References
Catechol	6.50	(Alnaizy, 1999; Gould, et al., 1976)
Oxalic Acid	6.85	(Alnaizy, 1999; Gould, et al., 1976; Wang, 1992)
Maleic Acid	8.77	(Alnaizy, 1999; Gould, et al., 1976)
Glyoxilic Acid	9.84	(Alnaizy, 1999; Gould, et al., 1976; Wang, 1992)
Formic Acid	14.24	(Alnaizy, 1999; Wang, 1992)
Fumaric Acid	16.52	(Alnaizy, 1999; Gould, et al., 1976)
Muconic Acid	31.05	(Alnaizy, 1999; Gould, et al., 1976)

Derivatization of these PCP ionizable by-products by means of a method based on the methylating agent TMO, originally developed to analyze organic acids in urine was not successful. Although these by-products were most likely ionizable (due to their concentration by ion exchange) it is possible that none of them was an organic acid.

Since these by-products could not be identified, it was impossible to build a calibration curve to determine their concentrations. However, the integrated areas of the different peaks of the chromatograms still provide semi-quantitative information. These areas are shown in Figure 5.15 and Figure 5.16. The first one of these figures shows the data for the two by-products that had highest integrated areas (on the order of $1x10^{06}$) and the second plot shows the data for the other three by-products; which had smaller

integrated areas (on the order of $1x10^{05}$). None of these by-products were detected in the controls that were not dosed with hydrogen peroxide. All of them, except the by-product S1 (which eluted at 7.01 min) were also non-detectable at the highest hydrogen peroxide dose.

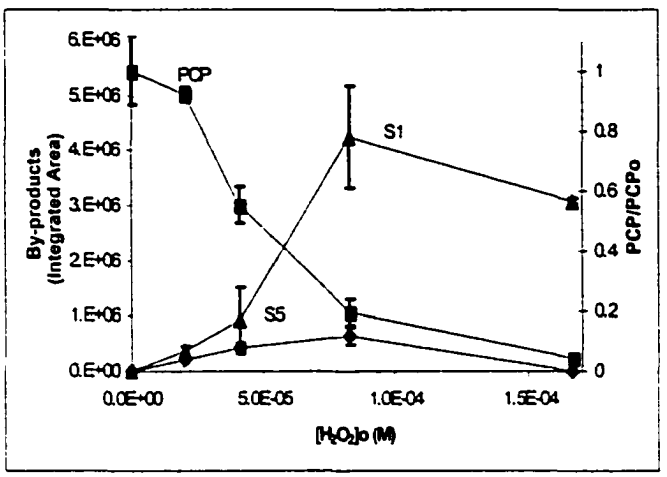

Figure 5.15. Integrated areas of the two observed PCP by-products (concentrated by SPE-HPLC) with largest areas (◆and ▲) and PCP dimensionless concentrations (■) after Fenton's treatment. Both by-products were non-detectable when no hydrogen peroxide was dosed. By-product S5 was not detectable at the highest hydrogen peroxide dose. Error bars represent standard deviation of measurements from duplicate vials.

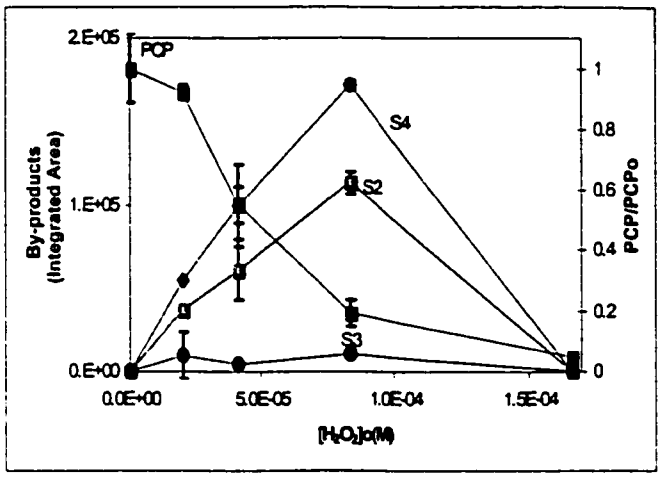

Figure 5.16. Integrated areas of the three observed PCP by-products (concentrated by SPE-HPLC) with smallest areas and PCP dimensionless concentrations (■) after Fenton's treatment. All of the by-products were non-detectable when no hydrogen peroxide was dosed, and also at the highest hydrogen peroxide dose. Error bars represent standard deviation of measurements from duplicate vials.

5.4.3.2.2. Liquid-liquid extractable intermediates

PCP intermediates were not detected by the chloroform extraction used for the analysis of PCP (see Section 5.2.2.1.), even when the method was modified to include a concentration step to achieve a concentration factor of 50. Thus, an extraction with ethyl acetate was used (see Section 5.1.2.3.2.4), combined with a concentration step to achieve a concentration factor of 20.

Two PCP intermediates were observed with this method. The GC/MS method used for PCP analysis (see Section 5.2.2.1) was modified to achieve better separation of the observed by-product and PCP (see Section 5.1.2.3.2.4). One of them, which eluted after PCP was tentatively identified by comparison of its mass spectrum with the mass spectral database (National Bureau of Standards, NBS75) as tetrachlorohydroquinone (TCHQ). At this modified conditions the observed by-product eluted at 25.9 min.

Injection of TCHQ standards confirmed the identity of this PCP oxidation by-product (both by comparison of the mass spectrum and the retention time). The quality of the matches of these mass spectra was 96% for the observed by-product and the spectrum of TCHQ in the database, and 99% for the observed by-product and the injected TCHQ standard.

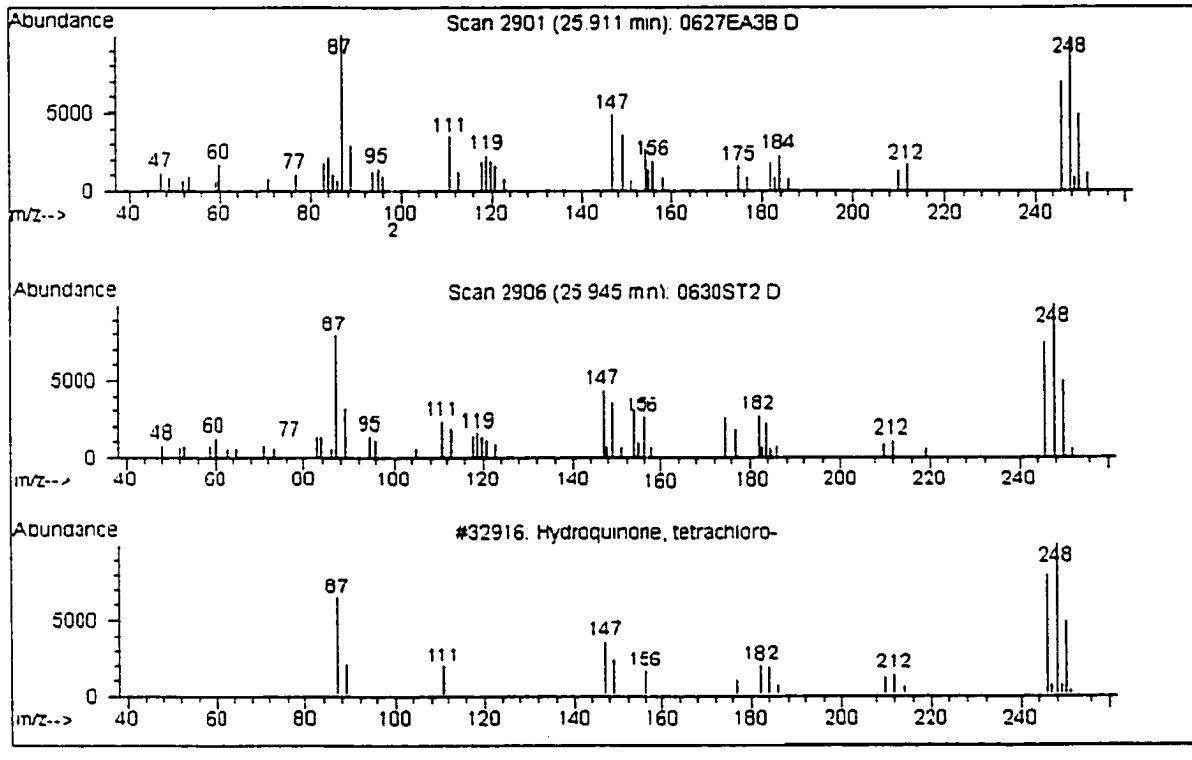

Figure 5.17. From top to bottom: a) Mass spectrum of the observed by-product that eluted at 25.95 min (after PCP). b) Mass spectrum of the injected tetrachlorohydroquinone standard (which eluted at the same retention time as the observed PCP by-product). c) Mass spectrum from the NBS75 database for tetrachlorohydroquinone. The quality of the matches was 96% for a)-c) and 99% for a)-b).

The second PCP by-product (designated as S6) eluted at 8.5 min under the modified method that achieved adequate separation of TCHQ and PCP. The closest

match of the mass spectrum of this by-product (shown in Figure 5.18.a) with any of the compounds in the database was 43% with 1,4-dichloro 1,3-butadiene (shown in Figure 5.18.b). However, the mass spectrum of the observed by-product includes two main ions with molecular weight of 166 and 96 that do not belong to 1,4-dichloro 1,3-butadiene. The GC/MS method was modified to test if separation of the observed peak into two peaks occurred, which might indicate that the peak was formed by two co-eluting compounds. The modified temperature profile was 50 °C initial temperature held for 2.0 min followed by increases of 5 °C/min to 150 °C and then at 3 °C/min to 250 °C (total run time = 57 min). The by-product eluted at a later time (21.91 min), but still as a single peak (the start and end time of the peaks of the different extracted ions included in the mass spectrum also matched closely). Thus, identification of this by-product was not possible.

The larger molecular weight of ion 166 in the mass spectrum of this unidentified by-product S6, indicates a molecule larger than 1,4-dichloro 1,3-butadiene. The isotope ratios of the ions 96 and 166 indicate that the molecule is dichlorinated (Smith and Busch, 1999). It is likely that this unknown compound has a similar basic structure to 1,4-dichloro 1,3-butadiene (two conjugated double bonds with at least four carbons, dichlorinated).

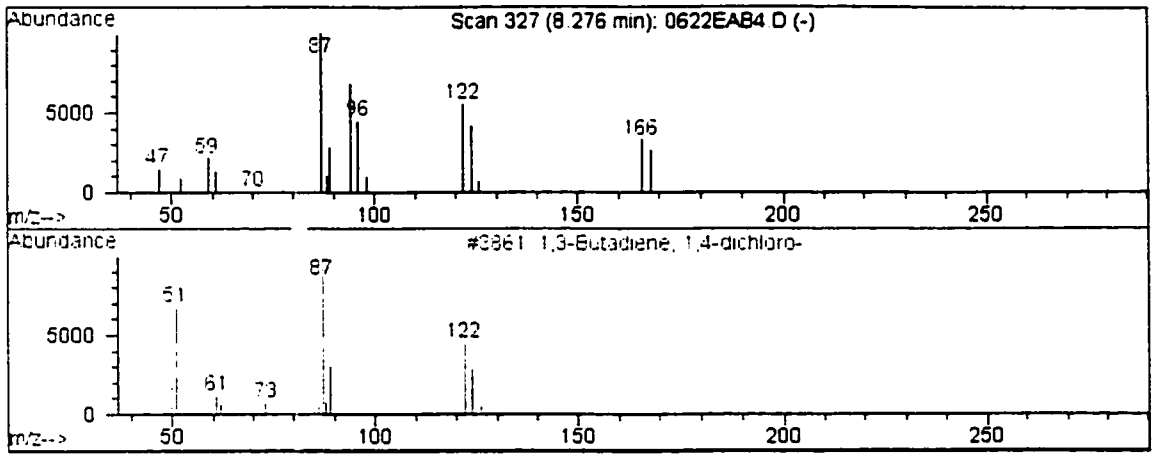

Figure 5.18. From top to bottom: a) Mass spectrum of an unidentified PCP by-product (S6). b) Mass spectrum of 1,4-dichloro 1,3-butadiene, the closest match from the mass spectrum database (the quality of the match was 43%).

Identification of tetrachlorohydroquinone (TCHQ) as a by-product allowed construction of a calibration curve. The production of TCHQ as a result of PCP degradation due to Fenton's reagent is shown in Figure 5.19. Production of TCHQ increased with the degradation of PCP, although the highest concentration of hydrogen peroxide achieved a non-detectable concentration of this PCP by-product. The experimental molecular yield of TCHQ produced per molecule of PCP degraded was maximum (4.5%) at the lowest non-zero hydrogen peroxide dose tested (see Figure 5.20). This indicates that TCHQ, a product of the PCP degradation due to hydroxyl free radicals, is itself reactive with hydroxyl free radicals.

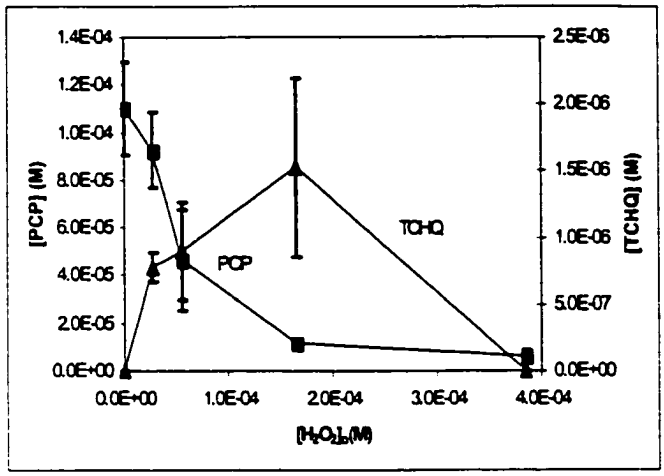

Figure 5.19. Tetrachlorohydroquinone (TCHQ) (▲) and PCP (■) concentrations observed as a result of variable dose of hydrogen peroxide. Error bars represent standard deviation of measurements from duplicate vials.

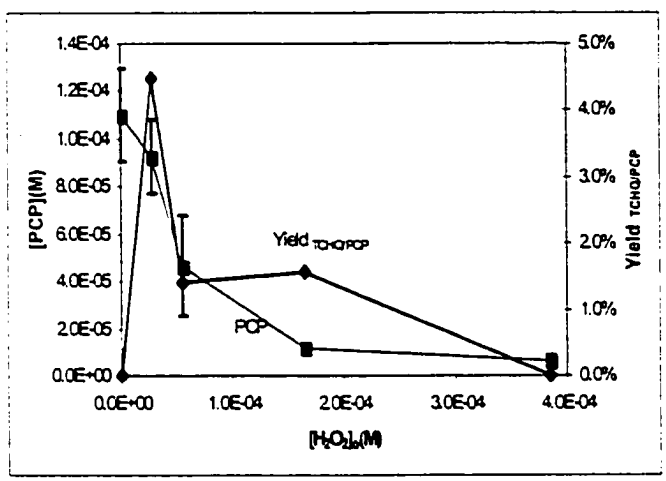

Figure 5.20. Observed yield of tetrachlorohydroquinone (TCHQ) due to PCP degradation (■) by Fenton's reagent. Error bars represent standard deviation of measurements from duplicate vials.

Due to the lack of identification of the observed by-product S6, it was not possible to prepare a standard curve for quantification. However, the ratio of the area of the extracted ion 87 (the main ion of this unknown PCP by-product) to the area of the

main ion of the internal standard (236, for dibromobenzene) provides semi-quantitative results. Figure 5.21 shows that the concentration of this by-product increased with the degradation of PCP. In contrast to TCHQ, the concentration of S6 did not decrease at the highest dose of hydrogen peroxide.

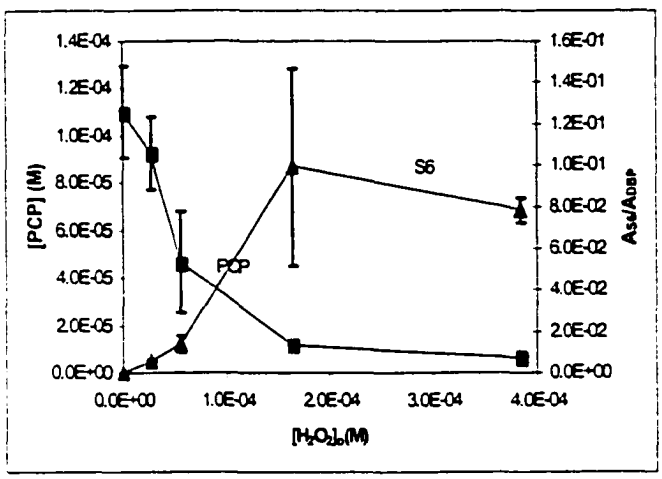

Figure 5.21. Ratio of the integrated area of the unidentified PCP by-product (S6) with respect the area of the internal standard (dibromobenzene) due to PCP degradation (■) by Fenton's reagent. Integrated areas were from the main ions (87 for S6 and 236 for the internal standard). Error bars represent standard deviation of measurements from duplicate vials.

5.4.3.3. Effect of Biomass and Supplementary Nutrients

The combination of AOP degradation of contaminants with biodegradation has been the subject of many studies (Scott, et al., 1995). Moreover, with the objective of achieving chemical oxidation of the parent compound and allowing the biodegradation of these intermediates as soon as they are produced, different recycle configurations have been proposed and tested for the continuous combined AOP and biodegradation treatment of different wastes (Heinzle, et al., 1992; Stockinger, et al., 1995; Stern, et al.,

1997). Performing more than one chemical oxidation-biodegradation sequence has also been studied in batch mode (Karrer, et al., 1997).

In any of these cases, a biodegradation stage prior to chemical oxidation would result in the presence of biomass (generated during the biodegradation stage) in the waste to be treated, unless the biomass is filtered (which would generate additional operating costs). Residual nutrient medium (a requirement for microbial growth) also might be present in the stream to be treated during a second (or further) cycle of chemical oxidation. Biomass is a complex mixture of oxidizable molecules and some of its components might scavenge hydroxyl free radicals, thus reducing the efficiency of the chemical oxidation (Buxton, et al., 1988). Microbial nutrients also include some compounds (e.g., phosphates) that are reactive towards hydroxyl free radicals (Buxton, et al., 1988). For this reason, the effects of biomass and nutrients (at stoichiometric concentrations with respect the solubility of PCP) on the Fenton's oxidation of PCP were tested.

Figure 5.22 shows the PCP and chloride concentrations after 12 h of reaction time during shake flask experiments in which PCP aliquots at pH 3.5 were subject to initial ferrous concentration of 2.0×10^{-04} mol/L and variable hydrogen peroxide doses. Before dosing hydrogen peroxide, the aliquots were dosed with concentrated medium containing *Pseudomona putida* F1 as model biomass. The concentration of biomass in the medium was determined by the optical density of the solution at 600 nm, using a pH 7.0 buffer blank and an optical density-dry weight calibration curve (the calibration curve was A_{600} = 0.9995 * mg dry weight /mL). The biomass concentration in the PCP medium was chosen to be stoichiometric to the carbon in a PCP-saturated solution, considering a

biomass "molecular formula" of $CH_{1.67}N_{0.2}O_{0.27}$ (Shuler and Kargi, 1992) and the use of 75% of the carbon originally contained in the PCP-saturated solution for biomass growth. A comparison of the PCP degradation in the presence and absence of biomass is shown in Figure 5.23. At the biomass concentration tested, no significant effects due to the biomass on the degradation of PCP were observed.

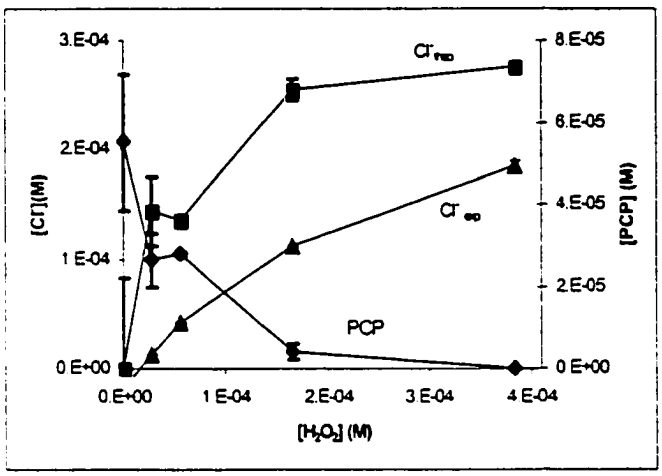

Figure 5.22. PCP (◆) and Cl^- (▲) concentrations in the presence of biomass at 12 h reaction time. Initial ferrous iron concentration was $2.0x10^{-04}$, and initial PCP concentration was $5.5x10^{-05}$ mol/L. Theoretical Cl^- (■) concentrations were obtained considering the maximum yield of 5 Cl^- per molecule of PCP degraded. Error bars represent standard deviation of measurements from duplicate vials.

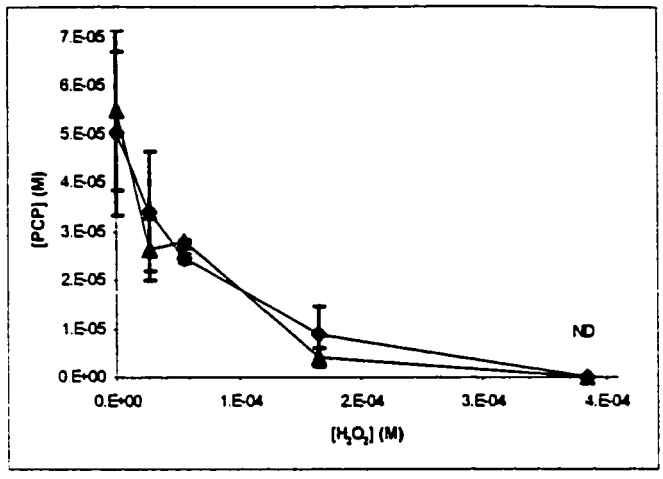

Figure 5.23. Comparison of PCP degradation by Fenton's reagent in the presence of biomass (at stoichiometric concentration, considering that 75% of the carbon in PCP-saturated media is transformed into biomass), represented by ▲, and in the absence of biomass (◆). Reaction time was12 h. Initial ferrous iron concentration was $2.0x10^{-04}$, and initial PCP concentration was $5.5x10^{-05}$ mol/L. Error bars represent standard deviation of measurements from duplicate vials.

Figure 5.24 shows the PCP and chloride concentrations after 12 h of reaction time during shake flask experiments in which PCP aliquots at pH 3.5 were subject to initial ferrous concentration of $2.0x10^{-04}$ mol/L and variable hydrogen peroxide doses. Before hydrogen peroxide was added, the aliquots were dosed with concentrated PAS supplementary medium (Bedard, et al., 1986). The size of this dose was determined according to the nutrient requirements of biomass grown on 75% of the carbon contained in a saturated PCP solution (14 ppm or $5.5x10^{-05}$ mol/L). Specifically, the nutrient was balanced to the carbon on a theoretical ratio of 0.2:1 (Shuler and Kargi, 1992). Comparison of the PCP degradation in the presence of microbial nutrients to the degradation of PCP without any nutrients present in the medium is shown in Figure 5.25. At the concentration of microbial nutrients tested, no significant effects due to these nutrients on the degradation of PCP were observed.

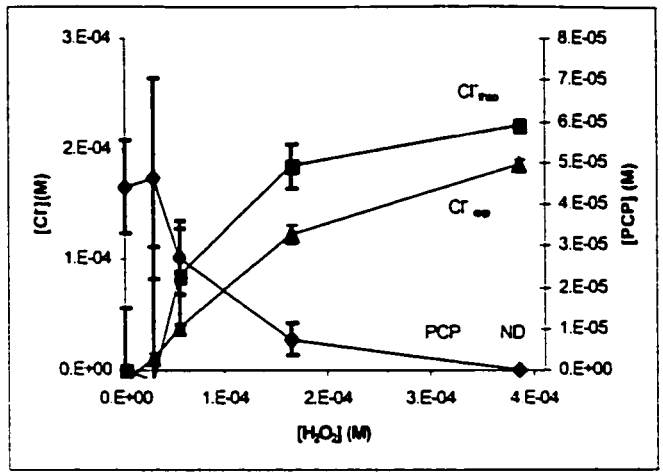

Figure 5.24. PCP (◆) and Cl^- (▲) concentrations in the presence of microbial nutrients. Theoretical Cl^- (■) concentrations were obtained considering the maximum yield of 5 Cl^- per molecule of PCP degraded. Reaction time was12 h. Initial ferrous iron concentration was $2.0x10^{-04}$, and initial PCP concentration was $5.5x10^{-05}$ mol/L. Error bars represent standard deviation of measurements from duplicate vials.

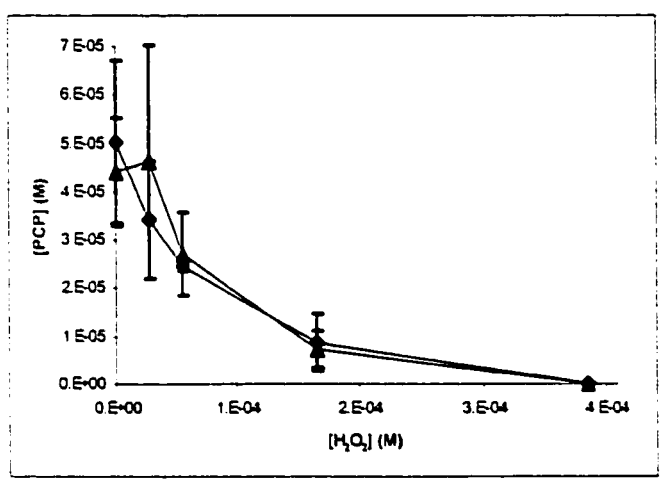

Figure 5.25. Comparison of PCP degradation by Fenton's reagent in the presence of microbial nutrients, represented by ▲, and in the absence of biomass (◆).Reaction time was12 h. Initial ferrous iron concentration was $2.0x10^{-04}$, and initial PCP concentration was $5.5x10^{-05}$ mol/L. Error bars represent standard deviation of measurements from duplicate vials.

5.4.3.4. Effect of Chloride Ion

Chloride ions are reactive with hydroxyl free radicals, with a reported second-order kinetic constant between $9.0x10^{07}$ and $6.0x10^{08}$ (Buxton, et al., 1988). The reaction generates the chloride free radical (Equation 3). This radical is a very reactive species that can chlorinate organic compounds. Chloride ions can exert other effects by forming complexes with ferric ions, and these can significantly reduce the effectiveness on Fenton's systems (Kiwi, et al., 2000)

$$\bullet OH + Cl^- \xrightarrow{k=9e07\ to\ 6e08} OH^- + \bullet Cl \qquad (3)$$

Because chloride is itself a product of PCP degradation due to Fenton's reagent (see Sections 5.4.2 and 5.4.3.1), this reaction between chloride and hydroxyl free radicals was of concern. A 12 h batch experiment was performed to test these effects at conditions similar to those of previous experiments. Chloride was dosed at an initial concentration of $3.3x10^{-04}$ mol/L (chosen based on the maximum theoretical yield of chloride from a PCP-saturated solution). The effects of this high initial dose of chloride vs. no initial dose of chloride are shown in Figure 5.26. No effects on the degradation of PCP were observed. Although comparable increases in the chloride concentrations were observed at high hydrogen peroxide doses between samples with different initial chloride concentrations, there were some appreciable effects at the lowest hydrogen peroxide dose. At this low hydrogen peroxide dose, dechlorination was inhibited in the presence of high initial chloride concentrations, despite the fact that PCP degradation proceeded to the same extent that in the absence of initial chloride. It is possible that the lower hydroxyl free radical concentrations achieved due to this low oxidation treatment were

used to generate chloride free radicals, which in turn might have chlorinated the organic substrates available. This would result in the concentration of free chloride in solution remaining constant. This effect was only observed at the lowest hydrogen peroxide dose.

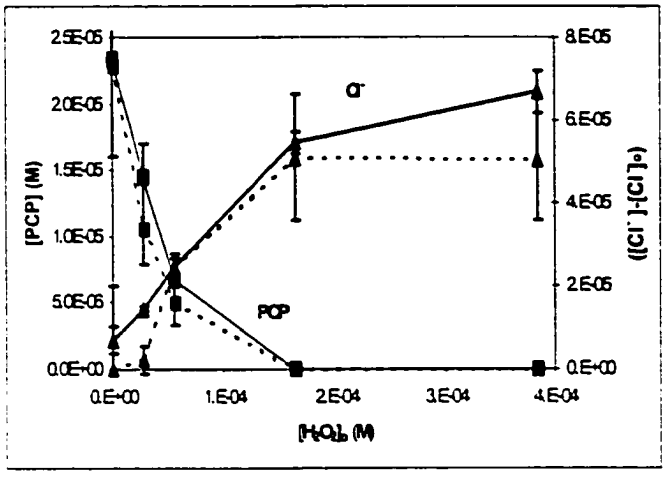

Figure 5.26. PCP degradation (■) and Cl^- production(▲) in the presence of variable concentration of chloride. Reaction time was12 h. Initial ferrous iron concentration was $2.0x10^{-04}$, and initial PCP concentration was $5.5x10^{-05}$ mol/L. Solid lines represent the PCP degradation and chloride production at low initial chloride concentration, while dotted lines represent the PCP and chloride production in the presence of high initial chloride concentration ($3.0x10^{-04}$ mol/L).

5.5. Discussion

For the system in which iron ions reacted with hydrogen peroxide in the absence of any other compounds that might react with hydroxyl free radicals, it was observed that the oxidation of ferrous iron depended on the hydrogen peroxide dose. At high hydrogen peroxide doses (up to $7.0x10^{-04}$ mol/L), all of the ferrous iron was oxidized. Partial oxidation of ferrous iron was observed at the lower hydrogen peroxide doses ($0.8x10^{-04}$ and $0.5x10^{-04}$ mol/L). The kinetic model proposed in this work provided adequate

predictions for most of these data, obtained under varied conditions. The model under-predicted the degradation of hydrogen peroxide at high hydrogen peroxide dose and initial ferrous ion concentration of $2.0x10^{-04}$ mol/L, although the initial observed reaction rates, were adequately predicted. This is probably due to the uncertainty related to the rate constant for the reaction between ferric ion and hydrogen peroxide (k_{i1}) at pH values higher than 2.8. The value of k_{i1} (within the reported range) that provided the best fit is consistent with the highest reported value (which corresponds to the acid-catalyzed mechanism at pH 2.8 to 3.0). It is possible that the actual value at pH 3.5 is lower than the value shown in Table 1. Another possibility is that the model does not account for other important reactions in the system. The adequate model-predicted degradation of hydrogen peroxide at high doses in the presence of ferric iron instead of ferrous iron (at a concentration of $2.0x10^{-04}$ mol/L) does not confirm the need for a higher value for the constant k_{i1}, and thus supports the possibility that the model lacks one or more side reactions.

Very high initial reaction rates were observed, and the reactions achieved completion in the first few minutes. An exception was the reaction between hydrogen peroxide (at a high dose) and ferric iron, which continued after three hours.

Inclusion of the reaction of PCP with hydroxyl free radicals (equation tPCP) and the scavenging reaction of PCP by-products (reaction tscav) provided adequate predictions for the transient and long-term PCP degradation. Whereas scavenging effects of PCP by-products on the degradation of PCP were not very important at the low oxidation treatments tested in this work (up to $0.5x10^{-04}$ mol/L, as indicated by Figure 5.13), these effects were very important at higher hydrogen peroxide tested. This is due

to the fact that the scavenging effects depend on two parameters: the characteristic scavenging kinetic constant k_{tscav}, as well as the concentration of PCP by-products (hydroxyl free radical scavengers). A constant value of k_{tscav} was able to adequately predict the degradation of PCP at a wide range of hydrogen peroxide initial concentrations, even though it seems reasonable that the properties of the PCP-by products, including their reactivity towards hydroxyl free radicals, might depend on the oxidation strength. On the other hand, the concentration of the PCP-by products (which are not mineralized to carbon dioxide, as indicated by the observed lack of mineralization of PCP even at the highest hydrogen peroxide dose tested) effectively create a weighting factor for the scavenging effects: scavenging effects are null when the PCP degradation is null, and become stronger when PCP degradation is higher.

Production of chloride (from dechlorination) was concomitant with the degradation of PCP. This observation was consistent for experiments in which data were measured during the first minutes after the reaction was initiated, and also for experiments in which the reaction was allowed to proceed to completion. However, the observed dechlorination never reached the theoretical maximum yield of 5 moles of chloride per mole of PCP degraded.

It is possible that the chloride-to-PCP yield might also depend on the strength of the oxidation: although only one chloride is necessary to transform PCP into a dechlorinated intermediate, further dechlorination of this intermediate proceeded as fast as the degradation of PCP, having the effect of an observed yield of chloride to PCP close to 60% of the theoretical maximum of 5 (see Figure 5.9). This indicates that the

degradation of PCP, the first step of this dechlorination chain reaction, might be the rate-limiting step.

Analysis of by-products by SPE/HPLC indicated that at least some of these by-products are ionizable, although they are different than previously reported by-products of AOP-degraded phenol and chlorophenols. The high degree of chlorination of PCP, (which has an effect on the electronegativity of the aromatic ring) might effect the reaction pathway and the chemical structure of the by-products. Most of these observed by-products were themselves degraded at the highest hydrogen peroxide concentrations tested. The degradation of these by-products without any decrease of TOC in solution indicates a more complex mixture of PCP by-products, few of which were observed by the different analytical techniques used in this work.

Analysis of PCP by-products by GC/MS combined with liquid-liquid extraction provided the identification of tetrachlorohydroquinone as a PCP by-product. This by-product is consistent with the higher reactivity of the para-position of aromatic compounds for hydroxyl free radical attack, which has been previously reported. For example, Fenton's treatment of chlorobenzene produced higher concentrations of para-chlorophenol than the meta- and ortho- by-products, while the ortho- and para- by-products of the hydroxyl free radical attack on 2-, 3- and 4-chlorophenols were predominant over the meta-by-product (Sedlak, 1991). Studies on the ozonation of 2,4,5- and 2,4,6-trichlorophenol yielded the same intermediate as the one produced from the 2,5- and 2,6-dichlorophenol, indicating that the chlorine group in the para-position of the trichlorophenols was substituted with a hydroxyl group, while the hydroxyl free radical attack of the dichlorophenols yielded hydroxylation at the para-position (Utsumi, et al.,

1998). The absorption of the different adducts formed during pulse radiolysis studies of several substituted halobenzenes indicated that the para-position for hydroxyl free radical attack was favored over the ortho- and meta- positions in most cases (Mohan, et al., 1991).

Based on the identification of tetrachlorohydroquinone as a by-product, a proposed reaction mechanism is shown in Figure 5.27. The formula in brackets represents an activation complex that would yield the observed TCHQ and chloride. This is in accordance with the substitution reaction mechanism proposed by Metilitsa to explain the dechlorination of para-chlorophenol to yield hydroquinone (Potter, et al., 1993).

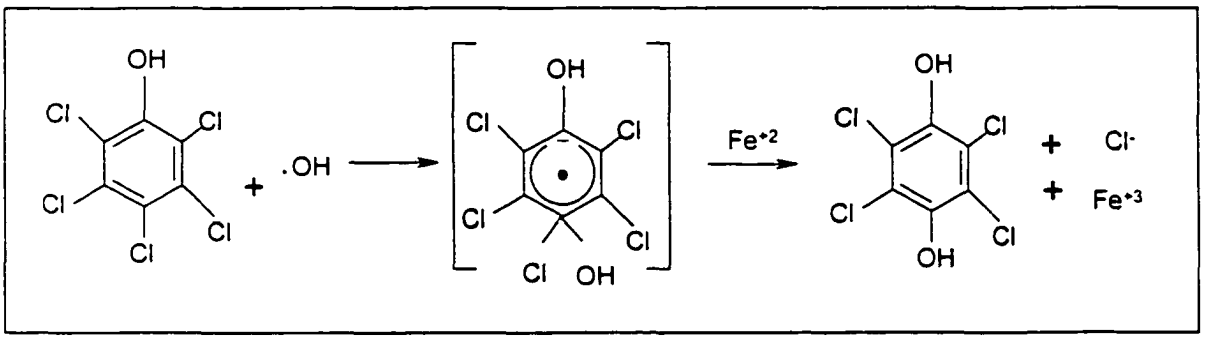

Figure 5.27. Proposed reaction mechanism of hydroxyl free radical attack on PCP at the para- position, in agreement with the observed by-product tetrachlorohydroquinone.

The highest yield of TCHQ at the lowest PCP degradation (4.5%) was reduced first to 1.5% and then to 0% at higher hydrogen peroxide treatments. This means that TCHQ is itself reactive towards hydroxyl free radicals, and supports the hypothesis that the degradation of PCP might be the rate-limiting step in the chain of reactions that yields the observed yield of chloride of 3 molecules of chloride per molecule of PCP degraded.

The proposed degradation pathway of PCP to produce the first degradation product implies that ferrous ion is oxidized (required to provide the additional electron to stabilize the activation complex). Despite the fact that the kinetic model does not account for this effect (and similar effects exerted by reaction mechanisms in which the unidentified PCP by-products might be involved), the model-predicted concentrations of ferrous iron and hydrogen peroxide (shown in Figure 5.7) are of about the same quality as the model fit under similar conditions but in the absence of the organic substrate PCP and its by-products (shown in Figure 5.2). Thus, the effect of this reaction on the model-predicted ferrous iron concentration might be negligible, probably due to the very low concentrations of organic substrates (limited by the solubility of PCP, $5.5x10^{-05}$ mol/L), compared to the higher ferrous and hydrogen peroxide concentrations used for the Fenton's treatment.

Neither biomass or microbial nutrients had any significant effects on the Fenton's degradation of PCP. This result supports the idea that a chemical oxidation stage after a biodegradation stage, either in batch or continuous (recycle) mode, might not be detrimental for the degradation of PCP at the conditions tested in this work.

The presence of chloride (at an initial concentration of $3.3x10^{-04}$ mol/L) during the degradation of PCP had effects on the production of chloride only at the lowest hydrogen peroxide concentration tested ($0.3x10^{-04}$ mol/L), compared with the PCP solution that was not initially dosed with chloride. A previous report on the Fenton and photo-Fenton's degradation of the dye Orange II (sodium 4-(2-hydroxy-1-naphthylazo)benzenesulfonate) found that a chloride concentration of $1.0x10^{-02}$ mol/L had inhibitory effects on the rate of degradation of the dye (at an initial concentration of

$1.0x10^{-04}$ mol/L), and that the by-products of the dye degradation in the presence of chloride were chlorinated (Kiwi, et al., 2000), probably due to the addition of the formed chloride free radicals to the organic substrates. In this work, it is possible that chloride free radicals were formed and chlorinated the available organic substrates at a comparable rate that the actual dechlorination due to hydroxyl free radical observed in the absence of chloride. If these effects were due to the explained mechanism (instead of being due to experimental error), they were negligible at higher hydrogen peroxide doses.

5.6. References

1. Alnaizy, R. Mechanism and Kinetic Study for the Hydroxyl Free Radical Mediated Photoxidation of Organic Contaminated Aqueous Solutions. Fort Worth: Texas A&M University; 1999.

2. Anbar, M., D. Meyerstein, and P. Neta. 1966. The Reactivity of Aromatic Compounds toward Hydroxyl Radicals. J. Phys. Chem. 70:2660-2062.

3. APHA, AWWA, and WPCF. Standard Methods for the Examination of Water and Wastewater. 15th ed. Washington; 1980.

4. Bedard, D., R. Unterman, L. Bopp, M. Brenna, M . Haberl , and C. Johnson. 1986. Rapid Assay for Screening and Characterizing Microorganisms for the Ability to Degrade Polychlorinated Biphenyls. Appl. Environ. Microbiol. 51(4):761-768.

5. Bielski, B. H. J., D.E. Cabelli, R.L. Arudi, and A. Ross. 1985. Reactivity of HO_2/O_2- Radicals in Aqueous Solution. J. Phys. Chem. Ref. Data.

6. Bigda, R. 1995. Consider Fenton's Chemistry for Wastewater Treatment. Chemical Engineering Progress. 62-66.

7. Bunce, N., L. Liu, J. Zhu, and D. Lane. 1997. Reaction of Naphthalene and Its Derivatives with Hydroxyl Radicals in the Gas Phase. Environ. Sci. Tech. 31:2252-2259.

8. Buxton, B. V., C. L. Greenstock, W. P. Helman, and A. B. Ross. 1988. Critical Review of Rate Constants for Reactions of Hydrated Electrons, Hydrogen Atoms and Hydroxyl Radicals in Aqueous Solution. J. Phys. Chem. Ref. Data. 17:513-886.

9. Chen, R. and J. Pignatello. 1997. Role of Quinone Intermediates as Electron

Shuttles in Fenton and Photoassisted Fenton Oxidation of Aromatic Compounds. Envrion. Sci. Technol. 31:2399-2406.

10. Evans, M. G., P. George, and N. Uri. 1948. The [Fe(OH)]+2 and [Fe(O2H)]+2 Complexes. 230-239.

11. Fartahazis, P. and Ross, B. 1977. Selected Specific Rates of Reactions of Transients from Water in Aqueous Solution. Washington: NBS.

12. Gates, D. and R. Siegrist. 1995. In-Situ Chemical Oxidation of Trichloroethylene Using Hydrogen Peroxide. J. Environ. Eng. (9):639-644.

13. Glaze, W. and J. Kang. 1989a. Advanced Oxidation Process. Description of a Kinetic Model for the Oxidation of Hazardous Materials in Aqueous Media with Ozone and Hydrogen Peroxide in a Semibatch Reactor. Ind. Eng. Chem . Res. 28,1573-1580.

14. Glaze, W. and J. Kang. 1989b. Advanced Oxidation Process. Test of a Kinetic Model for the Oxidation of Organic Compounds with Ozone and Hydrogen Peroxide in a Semibatch Reactor. Ind. Eng. Chem . Res. 28,1580-1587.

15. Gould, J. and W. Weber. 1976. Oxidation of Phenols by Ozone. Journal WPCF. 48(1):47-60.

16. H. Liebich and E. Gesele. 1999. Profiling of organic acids by capillary gas chromatography-mass spectrometry after direct methylation in urine using trimethyloxonium tetrafluoroborate. J. of Chromatography A . 843:237-245.

17. Haag, W. and C. D. Yao. 1992. Rate Constants for Reaction of Hydroxyl Radicals with Several Drinking Water Contaminants. Environ. Sci. Technol. 26: 1005-1013.

18. Haag, W. and J. Hoigne. 1985. Photo-sensitized Oxidation in Natural Water Via .OH Radicals. Chemosphere. 14(11/12):1659-1671.

19. Heinzle, E., F. Geiger, M. Fahmy, and O. Kut. 1992. Integrated Ozonation-Biotreatment of Pulp-Bleaching Effluents Containing Chlorinated Phenolics. Biotech. Prog. 8:67-77.

20. Huling, S., R. Arnold, R. Sierka, and M. Miller. 1998. Measurement of Hydroxyl Radical Activity in a Soil Slurry Using the Spin Trap alpha-(4-pyridyl-1-oxide)-N-tert-butylnitrone. Environ. Sci. Technol. 32:3436-3441.

21. Karrer, N. J., G. Ryhiner, and E. Heinzle. 1997. Applicability Test for Combined Biological-Chemical Treatment of Wastewaters Containing Biorefractory Compounds. Wat. Res. 31(5):1013-1020.

22. Kiwi, J., A. Lopez, and V. Nadtochenko. 2000. Mechanism and Kinetics of the OH-

Radical Intervention during Fenton Oxidation in the Presence of a Significant Amount of Radical Scavenger (Cl-). Environ. Sci. Technol. 34:2162-2168.

23. Kosaka, K., H. Yamada, S. Matsui, S. Echigo, and K. Shishida. 1998. Comparison among the Methods for Hydrogen Peroxide Measurements to Evaluate Advanced Oxidation Processes: Appliation of a Spectrophotometric Method Using Copper(II) Ion and 2,9-Dimethyl-1,10-phenanthroline. Environ. Sci. Technol. 32:3821-3824.

24. Lee, S. and J. Carberry. 1992. Biodegradation of PCP enhanced by chemical Oxidation Pretreatment. Wat. Environ. Res. 64(5):682-690.

25. Lindsey, M. and M. Tarr. 2000. Inhibition of Hydroxyl Radical Reaction with Aromatics by Dissolved Natural Organic Matter. Environ. Sci. Technol. 34:444-449.

26. Marco, A., S. Esplugas, and G. Saum. 1997. How and Why combine Chemical and Biological Processes for Wastewater Treatment. Wat. Sci. Tech. 35(4):321-327.

27. Martens, D. and W. Frankenberger. 1995. Enhanced Degradation of Polycyclic Aromatic Hydrocarbons in Soil Treated with an Advanced Oxidative Process-Fenton's Reagent. J. Soil Contam. 4(2):1-16.

28. McKinzi, A. and T. Dichristina. 1999. Microbially Driven Fenton Reaction for Transformation of Pentachlorophenol. Environ. Sci. Technol. 33:1886-1891.

29. Mohan, H., H. Mudaliar, D. Aravindakumar, B. Mahdav Rao, and J. Mittal. 1991. Studies of Structure-Reactivity in the Reaction of OH Radicals with Substituted Halobenzenes in Aqueous Solutions. J. Chem. Soc. Perkin Trans. 2:1387.

30. Nadtochenko, V. and J. Kiwi. 1998. Primary Photochemical Reactions in the Photo-Fenton System with Ferric Chloride. 1. A Case Study of Xylidine Oxidaiton as a Model Compound. Environ. Sci. Technol. 32:3273-3281.

31. Potter, J. and J. Roth. 1993. Oxidation of Chlorinated Phenols Using Fenton's Reagent. Haz. Waste Haz. Mat. 10(2):151-17.

32. Rush, J. and B. Bielski. 1985. Pulse Radiolytic Studies of the Reactions of HO2/O2- with Fe(II)/Fe(III) Ions. The Reactivity of HO2/O2- with Ferric Ions and Its Implications on the Occurrence oof the Haber-Weiss Reaction. J. Phys. Chem. 5062-5066.

33. Scott, J. and D. Ollis. 1995. Integration of Chemical and Biological Oxidation Processes for Water Treatment: Review and Recommendations. Env. Prog. 14:88-103.

34. Sedlak, D. and A. Andren. 1991. Oxidation of Chlorobenzene with Fenton's Reagent. Environ. Sci. Technol. 25: 777-782.

35. Sedlak, D. and A. Andren. 1991. Aqueous Phase Oxidation of Polychorinated Biphenyls by Hydroxyl Radicals. Environ. Sci. Technol. 25:1419-1427.

36. Shuler, M. and Kargi. 1992. Principles of Biochemical Engineering.

37. Smith, M. and K. Busch. 1999. Undertanding Mass Spectra. New York: John Wiley.

38. Staehelin, J. and J. Hoigne. 1985. Decomposition of Ozone in Water in the Presence of Organic Solutes Acting as Promoters and Inhibitors of Radicsl Chain Reactions. Environ. Sci. Technol.. 19:1206-1213.

39. Stern, M., E. Heinzle, O. Kut , and K. Hungerbuhler. 1997. Removal of Substituted Pyridines by Combined Ozonation/Fluidized Bed Biofilm Treatment. 35. 4:329-335.

40. Stockinger, H. Removal of Biorefractory Pollutants in Wastewater by Combined Ozonation-Biotreatment. Zurich: Swiss Federal Institute of Technology; 1995.

41. Stockinger, H., E. Heinzle, and O. Kut. 1995. Removal of Chloro and Nitro Aromatic Wastewater Pollutants by Ozonation and Biotreatment. Environ. Sci. Technol.. 29:2016-2022.

42. Sutton, H. and C. Winterbourn. 1989. On the Participation of Higher Oxidation states of Iron and Copper in Fenton Reactions. Free Radical Biol. Med. 6:53-60.

43. Tang, W. Z. and C. Huang. 1997. Stoichiometry of Fenton's Reagent in the Oxidation of Chlorinated Aliphatic Organic Pollutants. Env. Technol. 18:13-23.

44. Trapido, M., Y. Veressinina, J. Hentunen, and A. Hirvonen. 1997. Ozonation of Chlorophenols: Kinetics, By-products and Toxicity. Environ. Technol. 18:325-332.

45. Utsumi, H., S. Han, and K. Ichikawa. 1998. Enhancement of Hydroxyl Radical Generation by Phenols and Their Reaction Intermediates During Ozonation. Wat. Sci. Tech. 38(6):147-154.

46. Venkatadri, R. and R. Peters. 1993. Chemical Oxidation Technologies: Ultraviolet Light/Hydrogen Peroxide, Fenton's Reagent, and Titanium Dioxide-Assisted Photocatalysis. Haz. Waste Haz. Mat. 10:107-149.

47. Voelker, B. and B. Sulzberger. 1996. Effects of Fulvic Acid on Fe(II) Oxidation by Hydrogen Peroxide. Environ. Sci. Technol. 30(4):1106-1114.

48. W.Z. Tang. Oxidation Kinetics and Mechanism of Chlorinated Organic Pollutants by Fenton's Reagent.: University of Delaware.; 1992.

49. Walling, C. 1975. Fenton's Reagent Revisited. Acc. Chem. Res. 8:125-131.

50. Walling, C. and A. Goosen. 1973. Mechanism of the Ferric Ion Catalyzed Decomposition of Hydrogn Peroxide. Effect of Organic Substrates. J. Ame. Chem. Soc. 95(9):2987-2991.

51. Walling, C. and T. Weil. 1974. The Ferric Iron Catalyzed Decomposition of Hydrogen Peroxide in Perchloric Acid Solution. Int. J. of Chem. Kinetics. VI:507-516.

52. Wang, Y. 1992. Effect of Chemical Oxidation on Anaerobic Biodegradation of Model Phenolic Compounds. Wat. Environ. Res. 64:268-273.

53. Watts, R. M. Udell and R. Monsen. Use of Iron Minerals in Optimizing the Peroxide Treatment of Contaminated Soils. Wat. Environ. Res. 65(7):839-844.

54. Zepp, R. and P. Schlotzhauer. 1979. Photoreactivity of Selected Aromatic Hydrocarbons in Water. In: P.W. Jones and P. Leber, eds. Polynuclear Aromatic Hydrocarbons. Ann Arbor: Ann Arbor Science Publishers; pp. 141-156.

CHAPTER VI

CONTINUOUS COMBINED FENTON'S OXIDATION AND BIODEGRADATION FOR THE TREATMENT OF PENTACHLOROPHENOL-CONTAMINATED WATER

6.1. Introduction

Pentachlorophenol is a common water contaminant, released into the environment as a result of wood treating and pulp and paper bleaching operations and leaching into groundwater from contaminated soil. Due to the nature of these sources, PCP is often present in mixtures with other contaminants, constituting the most recalcitrant fraction of such mixtures (Graves and T. Joyce, 1994; Leuenberger, et al., 1985).

PCP biodegradation has been reported under both aerobic and anaerobic conditions (Hale, et al., 1994). Aerobic degradation of PCP requires pentachlorophenol monooxygenase, which catalyzes the transformation of PCP to 2,3,5,6-tetrachlorohydroquinone. Further degradation can be achieved by a chain of reactions that requires several specific enzymes (Hale, et al., 1994; Zeng, 2000). This process is often slow (requiring sometimes a treatment time of up to several weeks) and achieves only partial degradation of PCP (Puhakka, et al., 1996). Improvement of the PCP biodegradation has been achieved by means of highly specialized cultures (Puhakka, et al., 1996). Isolation of these highly specialized cultures is achieved under controlled

conditions, which are often very different to the prevailing conditions at contaminated sites or bioreactors, and this results in very slow biodegradation rates and low stability to disturbances in the environment (Scott, et al., 1995).

Anaerobic degradation of PCP (to lower chlorinated tetra-, tri-, di- and mono-chlorinated phenol mixtures) is also feasible, but often requires treatment times up to several months (Hale, et al., 1994).

Given these reports of limited success of bioremediation for the treatment of PCP and other recalcitrant compounds, there has been increased interest in alternative treatment technologies that ideally achieve destruction of the contaminant, rather than mere transfer to another phase. Advanced oxidation processes (AOPs) rely on the generation of hydroxyl free radicals, a highly reactive chemical species. (Venkatadri, et al., 1993). These technologies can achieve complete mineralization (stoichimetric generation of carbon dioxide) of different recalcitrant compounds (Stockinger, et al., 1995; Scott, et al., 1995; Heinzle, et al., 1992; Tang, et al., 1997). However, mineralization of contaminants by means of AOPs often requires long treatment time and strong doses of the oxidizing reagents. Often, less reactive intermediates are generated that inhibit the degradation of the parent compound.

Once the recalcitrant compounds have been transformed by means of the chemical treatment, their properties, including biodegradability, are also modified. Often the intermediates have reduced recalcitrance with respect to the parent compound. Since biological processes are known to be 5 to 20 times less expensive than chemical processes (Marco, et al., 1997), addition of a biodegradation stage can improve the economy of the overall process.

Combinations of chemical oxidation and biological processes have potential applications to different wastes, including recalcitrant compounds (Scott, et al., 1995). Many examples of this combined treatment exist (see Sections 2.2.1.1. and 2.2.1.2.). However, most of these reports are applicability studies, generating empirical or semi-empirical information. For this reason, it is generally believed that integration of processes must be experimentally evaluated on a case-by-case basis (Vogelpohl, et al., 1996). In contrast, the objective of this work is to use a mechanistic approach that emphasizes rate laws for parent compounds and intermediates in both the chemical and biological processes, and thus allows extrapolation of results to other wastes.

The purpose of this work is to provide a mechanistic study of the combined Fenton's oxidation (an AOP that generates hydroxyl free radicals based on the combination of hydrogen peroxide and ferrous iron) and biodegradation of water contaminated with PCP. Experiments were conducted in a continuous stirred tank reactor (CSTR) in which Fenton's degradation of PCP occurred; the effluent from this reactor was continuously treated on a second stirred tank, combined with a packed bed bioreactor in which the PCP intermediates were biodegraded.

A mathematical model was developed for the combined system. This combined model included mass balances for both continuous reactors. A previously developed kinetic model for Fenton's reaction (see Section 5.1.4.) was applied to the continuous system studied in this chapter. Additionally, Monod-type microbial degradation kinetics were obtained from the experimental results of the biodegradation of the PCP intermediates.

The suitability of such a combined mathematical model to describe experimental data was evaluated. The effect of hydrogen peroxide dose, residence time in the bioreactor and recycle of the bioreactor effluent back to the chemical reactor on the combined system performance were studied. The mathematical model also provided a mechanistic basis to understand the observed effects and to recommend reactor operating strategies to optimize the performance of the combined system, based on the PCP degradation and mineralization achieved due to fixed doses of hydrogen peroxide to the system.

6.2. Experimental

6.2.1. Chemicals

Pentachlorophenol was purchased from Sigma, as was nitrobenzene (used for competitive kinetics experiments) and the surrogate and internal standards used for extraction and analysis. The purity of these chemicals was 98% or higher (except for dibromophenol, which was 95% pure). $FeSO_4 \cdot 7H_2O$ (99%+) was purchased from Baker.

Hydrogen peroxide (non-stabilized, 31.4%), sodium chloride (99.9%) and perchloric acid (conc.) were all purchased from Fisher. pH adjustment was achieved by either diluted sodium hydroxide, sulfuric acid or perchloric acid. Sulfuric acid was used for pH adjustment during continuous operation of the Fenton's-biodegradation system and batch experiments of Fenton's oxidation of PCP. Sodium hydroxide was used to adjust the pH of the continuous system, and to prepare PCP-saturated solutions.

Pesticide-grade solvents used for organic analysis (chloroform and ethyl acetate) were purchased from Fisher.

6.2.2. Continuous System

A bench scale continuous combined system was used to study the combination of Fenton's degradation of PCP and the biodegradation of the Fenton's-treated waste. The system consisted of two continuously stirred tank reactors (CSTRs) in series (2.0 L Bioflo C-30 reactors, from New Brunswick Scientific) (see Figure 6.1.) with glass stirring vessels. The volume of each of these reactors (250 mL for the chemical reactor and 750 mL for the bioreactor) was controlled by means of an exit tubing line attached to a peristaltic pump and set at a the desired height. In the first reactor Fenton's treatment of the PCP contaminated was achieved at pH 3.5, which is the reported optimum for Fenton's treatment (Glaze, et al., 1989; Bigda, 1995). pH control for this reactor was achieved by means of a Markson pH/ORP controller 630 equipped with an Ingold combination pH electrode. The solution used for pH control was NaOH 0.5 N. Ferrous iron and hydrogen peroxide were dosed at the levels at which batch experiments were run (see Sections 5.4.2 and 5.4.3.): ferrous iron at $2.0x10^{-04}$ mol/L and hydrogen peroxide at concentrations below $5.0x10^{-04}$mol/L). These conditions were selected according to the PCP solubility: the hydrogen peroxide dose was from 0 to 10 molecules of H_2O_2 per molecule of PCP, and the dose of Fe^{+2} ($2x10^{-04}$ mol/L) was selected from reported optimal H_2O_2/Fe^{+2} ratios, which vary from 10:1 to 5:1 (w/w) (Bigda, 1995; Tang, et al., 1997). The chemical reactor was protected from light to avoid direct production of hydroxyl free radicals due to photocatalyzed degradation of hydrogen peroxide.

The effluent from the Fenton's reactor was fed to a bioreactor, in which the low pH exit stream from the Fenton's reactor was neutralized with NaOH 0.2N solution. pH

control was achieved by means of an Omega pH/ORP controller PHCN-36 630 equipped with an Ingold combination pH electrode. The solution used for pH control was NaOH 0.2 N. Supplementary nutrients (phosphates, trace minerals and nitrogen) were fed to this reactor (Section 6.2.3.4).

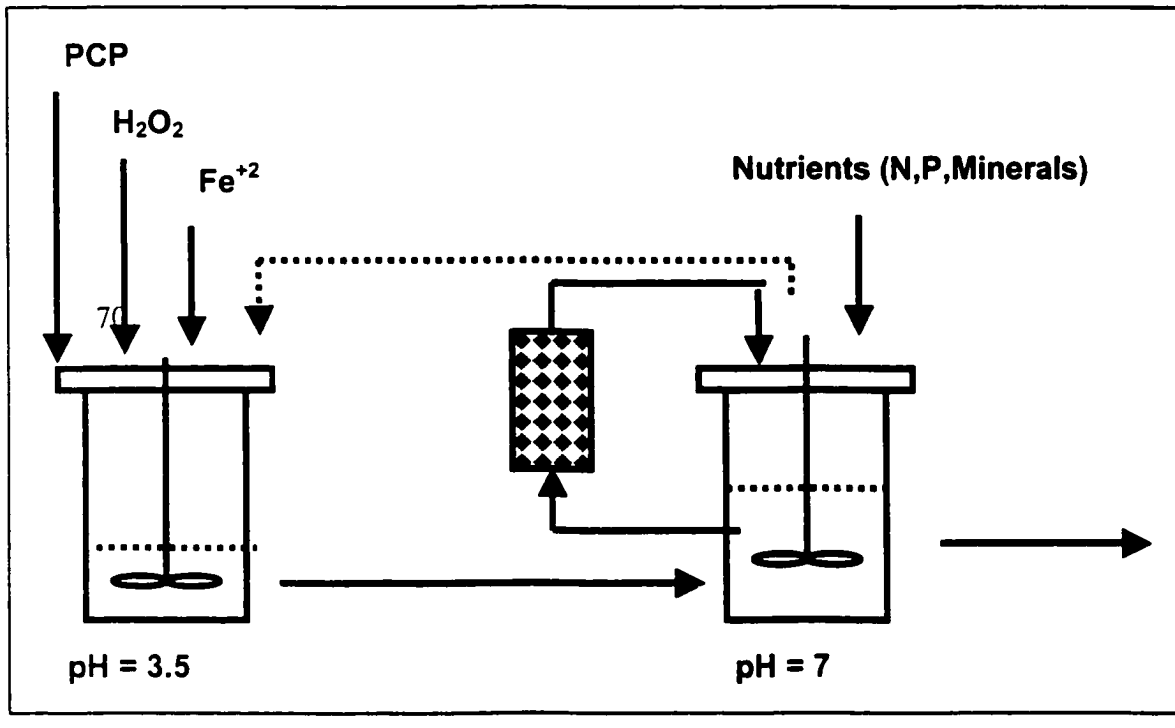

Figure 6.1. Continuous combined system for Fenton's oxidation and biodegradation of PCP contaminated water.

Since the concentration of carbon in the feed stream was limited by the low solubility of PCP (14 ppm, or $5.5x10^{-05}$ mol/L), there was the concern that a microbial culture of suspended cells might not grow at high enough rates. Thus, a packed bed column (glass, 3.8 cm OD, 14.5 cm long) was provided, to which the contents of the main bioreactor stirring vessel were recirculated. The packing material consisted of 38.8

g of Celite biocatalyst carrier R-635 (Manville), washed previously with DI water until the washing water had a neutral pH. The mean weight of the beads was estimated as 0.148 g/pellet, from a sample of 19 pellets, so the packed column contained an estimated 240 pellets. The bioreactor was initially inoculated with 3.0 mL of activated sludge from the aerobic basin of the Fort Collins wastewater treatment plant. Flow through this packed column was upward. A stainless steel sieve at the top end kept the Celite pellets from leaving the packed column. High recirculation flow rates to the packed bed ensured a well-mixed bioreactor. The ratio of recirculation to the packed bed was 20 times higher than the feed to the stirred tank.

Additional benefits of this packed bed bioreactor configuration with respect to a suspended cells bioreactor are improved resistance of the biofilm to inhibitory chemicals from the chemical reactor (such as hydrogen peroxide) and reduced growth rates. A potential disadvantage of biofilms with respect to suspended cells are mass transfer limitations from the surrounding medium to the cells inside the biofilm.

The tubing of this system consisted of Norprene (Masterflex 6404-Cole Parmer, compatible with peristaltic pump heads), which is recommended for applications requiring high chemical, heat, ozone and UV light resistance, or PTFE (covered with a dark tube to avoid light) when possible.

Sorption experiments conducted for 24 h in which PCP solution was shaken on a vial in the presence of Celite and Norprene tubing indicated that PCP did not sorb or degrade significantly in the presence of these materials.

6.2.3. Chemicals

6.2.3.1. PCP solution

The PCP solution was prepared with deionized and dechlorinated water. Chlorine residual concentrations were of concern to both the Fenton's oxidation stage and to the biodegradation stage since chlorine rapidly degrades H_2O_2, and it is also a microbial inhibitor.

Dechlorination of the water used to prepare the PCP solution was achieved by bubbling compressed air through the deionized water for at least 24 h and then autoclaved (121 °C for 20 min) and allowed to cool to room temperature. Then, 0.8 mL of 0.1 M NaOH were added to facilitate the dissolution of PCP. Finally, PCP was weighed to achieve the reported solubility at neutral pH (14 ppm) and added to the previously prepared water. The final pH of solutions prepared in this way was close to 10.0. PCP dissolution under these conditions was achieved in less than 48 h. If the pH adjustment was omitted, PCP would take about one week to dissolve. In some cases, without pH adjustment, PCP dissolution was not complete. The flow rate of this solution to the combined chemical oxidation and biodegradation system was 3.5 L/day. The actual dose of this solution was verified by volume measurements on a volumetric scale in the 26L glass carboys used to prepare and hold the solution.

6.2.3.2. Hydrogen Peroxide

Hydrogen peroxide solutions were prepared with Reagent Type I Grade water (Nanopure Barnstead water with a conductivity of 18 mΩ) by dissolving concentrated (31.5%) hydrogen peroxide to achieve a final concentration of 0.3 and 0.6 g/L ($8.8x10^{-03}$

and $1.8x10^{-02}$ mol/L, respectively). After preparation, this reactant was protected from light by covering the glass container with aluminum foil. The flow rate of this reactant to the system was kept at low levels, to avoid dilution effects of the main PCP feed. The actual dosage to the system was measured by weighing the flask holding the solution. This solution was fed to the chemical reactor at a flow rate of 85 mL/day, which represented about 2.5% of the total flow rate to the combined system. Accounting for dilution rate, the $8.8x10^{-03}$ and $1.8 x10^{-02}$ mol/L solutions yielded doses of $2.2x10^{-04}$ mol/L and $4.4x10^{-04}$ to the chemical reactor, respectively.

6.2.3.3. Ferrous Iron

The solution used to dose ferrous iron to the continuous system was prepared with Reagent Type I Grade water (Nanopure Barnstead water with a conductivity of 18 mΩ). Ferrous iron salts (2.3 g of $FeSO_4 \cdot 7H_2O$, Baker) were dissolved in about 700 mL of water. Concentrated H_2SO_4 (6.4 mL) was added to avoid spontaneous oxidation of ferrous iron before the solution reached the Fenton's reactor and the volume was adjusted to 1.0 L. A solution prepared in this way is $8.3x10^{-03}$ mol/L. After preparation, this reactant was protected from light using aluminum foil. Flow rate of this reactant to the system was kept at low levels, to avoid dilution effects of the main PCP feed. Actual dosage of this reactant to the system was measured by weighing the holding flask. This solution was fed to the chemical reactor at a flow rate of 85 mL/day, which represents about 2.5% of the total flow rate to the combined system. This dilution rate yields an actual dose of $2.0x10^{-04}$ mol/L to the chemical reactor.

6.2.3.4. Supplementary Nutrient Medium

The supplementary nutrient medium was based on the composition of a mineral salts based agar (PAS), used for plating tests. This medium was modified in order to eliminate chloride that could interfere with the chloride ion analysis (according to Table 6.1).

The effect of recycling the effluent from the biodegradation stage back to the Fenton's reactor was tested in this project. Thus, residual nutrients in this recycle stream were expected. For this reason, nitrogen in the supplementary nutrient medium was in the form of nitrates instead of the ammonium chloride originally included in the medium. The reported reactivity of nitrate toward hydroxyl free radical is about two orders of magnitude smaller than the one of ammonia, and about five orders of magnitude smaller than the one of nitrite (Buxton, et al., 1988; Fartahazis and Ross, 1977).

Since the process of assimilatory nitrate reduction (which allows the utilization of nitrates as the nitrogen source and involves intracellular enzymatic reduction of nitrates to nitrite and then to ammonia) is widespread among bacteria (Prescott, et al., 1999), the bioavailability of this substitute nitrogen source was considered not to be an issue.

Nitrogen supplementation was stoichiometric to the carbon concentration in the PCP feed, considering an optimal nitrogen to carbon molar ratio of 0.2:1 (Shuler and Kargi, 1992). The ratio of phosphates and trace nutrients to nitrogen was the same as the ones in the PAS medium (see Section 6.2.4.5.3). This stoichiometric dose of nutrients was achieved by diluting 424 μL of PAS 100x salts solution and 3.26 mL of PAS concentrate to 1.0 L of nutrient medium, which was then fed to the bioreactor at a flow

rate of 85 mL/day. This flow rate represents approximately 2.5% of the total flow rate to the combined system.

Table 6.1. Composition of the two solutions used to make chloride-free PAS supplementary nutrients.

PAS Concentrate (added to 500 mL water)	**PAS 100x Salts** (added to 500 mL water)
$NaNO_3$ 22.1g	$CaSO_4 \cdot 2H_2O$ 0.18g
KH_2PHO_4 10.97g	$FeSO_4 \cdot 7H_2O$ 0.5g
K_2HPO_4 28.39 g	$MnSO_4 \cdot H_2O$ 2.5g
	$MgSO_4$ 9.75g
	H_2SO_4 2 drops

6.2.4. Analytical Methods

6.2.4.1. Organic Substrates

The concentration of PCP was determined with an HP 5890 Series II gas chromatograph with a mass spectral detector and a 50-m HP-5 crosslinked 5% PH ME silicone capillary column of 0.2 mm I.D. and 0.33 μm film thickness. The GC temperature program was: 50 °C initial temperature held for 2.0 min followed by increases of 20 °C/min to 160 °C and then at 6 °C/min to 250 °C (total run time = 22.5 min). One mL of each aqueous sample was spiked with dibromophenol as surrogate in acetone solution, adjusted to pH less than 1.0, extracted with 0.5 mL of chloroform, and then dosed with dibromobenzene as internal standard before injection (the final

concentration of the internal standard in the extracted solution was 0.05 mM). Acidification and dosage of the surrogate solution was done immediately after sampling. Quenching of the PCP degradation was achieved by acidification of the sample and an excess of acetone dosed from the surrogate solution. The effectiveness of this quenching procedure was verified by the quantitative recovery of the surrogate. Quantification of each analyte was performed on the basis of the respective main ion in the mass spectrum (e.g., 266 for PCP, 252 for the surrogate and 236 for the internal standard) normalized with respect the internal standard. The extraction efficiency was evaluated by means of the surrogate, which typically was higher than 90%. Data from samples with surrogate concentrations out of the interval of ±15% around the mean were analyzed a second time.

6.2.4.2. Oxidizing Reagents

6.2.4.2.1. Hydrogen Peroxide

Concentration of the stock hydrogen peroxide solution was determined before use with standard 0.3 N potassium permanganate to confirm its stability during storage. The end point was identified by a slight pink color due to an excess of potasssium permanganate. Hydrogen peroxide solutions were diluted to 250.0 mL with water for analysis to a final concentration between 0.1 and 0.5%. Aliquots (25.0 mL) of this dilute solution were diluted with about 250 mL in an Erlenmeyer flask, then acidified with 10.0 mL concentrated sulfuric acid before titration.

Lower concentrations of hydrogen peroxide (< 30 ppm) were analyzed by means of the titanium sulfate method (APHA, et al., 1980). The detection limit of this method is about 1.0 mg/L ($3x10^{-05}$ mol/L). One mL samples were added to 100 μL of 6.7 g/L

$TiSO_4 \cdot 8H_2O$ in 17% sulfuric acid aqueous solution. The color of the yellow peroxo-complex was allowed to develop before the absorbance was read at 405 nm and compared to calibration standards (a dilution of a potassium permanganate-titrated hydrogen peroxide solution). Hydrogen peroxide analysis was done immediately after sampling (by adding the sample to a 1.5 mL cuvet containing the titanium reactant) to avoid the need for quenching with sulfites since an excess of these was shown to interfere with this assay. Lack of interference of ferrous and ferric iron (at the concentrations used in this work) with this analysis was tested. A more sensitive 2,9 dimethyl, 1,10-phenanthroline method (Kosaka, et al., 1998) could not be used due to interference of ferrous iron.

6.2.4.2.2. Ferrous Iron

Ferrous iron was measured by the 1,10 phenanthroline method. One mL samples were treated with 200 μL of ammonium acetate buffer solution (pH 3.2, 250 g/L in water), and 150 μL of 1,10 phenanthroline solution (1.0 g/L in water). Absorbance was measured at 508 nm and compared to ferrous iron calibrations standards with a concentration range from 0 to 10 ppm (APHA, et al., 1980). Ferrous iron calibration standards were prepared from stock iron solution at 100 ppm (containing 0.7022 g $Fe(NH_4)_2(SO_4)_2 \cdot 6H2O$ dissolved into 29% H_2SO_4 in water and then the volume adjusted to 1.0L). The following reactants were added to the 1.0 mL calibration standard solutions: 100 μL of hydroxylamine solution (10 g $NH_2OH \cdot HCl$ in 100 mL ddH2O), 100 μL of sodium acetate buffer (100 g $NaC_2H_3O_2 \cdot 3H_2O$ in 400 mL glacial acetic acid) and 150 μL of 1,10 phenanthroline solution (1.0 g/L in water). Ferrous iron analysis was

done immediately after sampling (by adding the sample to a 1.5 mL cuvet containing the rest of the reactants) to avoid the need for quenching with sulfites since an excess of these was shown to interfere with this assay. Lack of interference of hydrogen peroxide with this assay at concentrations lower than 1 mM was tested. The detection limit of this assay is close to $5.0x10^{-07}$ mol/L (approximately 0.3 ppm).

6.2.4.3. Chemical Oxidation By-products

6.2.4.3.1. Chloride Analysis

Chloride ion was measured by means of the mercuric thiocyianate method. One mL of sample was added to 80 μL of mercuric thiocyanate solution (Hach # 22121) and 40 μL of ferric ion solution (Hach # 22122-42). The color was allowed to develop, absorbance was read at 455 nm and compared to calibration standards (from 0 to 10 ppm). Chloride analysis was done immediately after sampling (by adding the sample to a 1.5 mL cuvet containing the rest of the reactants) to avoid the need for quenching with sulfites since an excess of these was shown to interfere with this assay. Lack of interference of residual hydrogen peroxide on this analysis was confirmed by spiking treated samples with hydrogen peroxide (up to 1%) without change in absorbance after the color had been formed. Quenching achieved by this procedure was probably due to the excess of methanol in which the ferric iron solution was prepared.

6.2.4.3.2. Organic PCP By-products

PCP reaction by-products were analyzed by means of extraction with ethyl acetate after acidification with phosphoric acid. Two mL of sample were acidified with 50 μL of

concentrated phosphoric acid and then 2.0 mL of ethyl acetate were added. The mixture was shaken for 20 min and the organic phase was then concentrated to 100 μL under a gentle N_2 stream. Dibromobenzene was used as internal standard before analysis: a concentrated dibromobenzene solution in acetone was added to achieve a final concentration of 0.025 mM. These solutions were analyzed using the same GC/MS method used to analyze PCP (see Section 6.2.4.1), except that a modified temperature profile was used to achieve better separation of the different observed peaks: 50 °C initial temperature held for 2.0 min followed by increases of 20 °C/min to 150 °C and then at 3 °C/min to 250 °C (total run time = 37 min).

6.2.4.4. Total Organic Carbon

Purgeable total organic carbon (TOC) was analyzed with a Dohrmann DC-80 TOC Analyzer, after acidifying the sample with phosphoric acid (2 drops per 25 mL) and purging with oxygen for 7 min to eliminate interferences from CO_2. One mL of sample was injected into the analyzer. Calibration for this analysis was done using a potassium phthalate solution equivalent to 10.0 ppm of TOC (this solution was prepared by diluting a 2000 ppm standard solution, which contained 0.425 g/L of reagent-grade potassium hydrogen phthalate). This assay is based on oxidation of the organic carbon in the sample by means of oxidation with potassium persulfate (2% solution) in the presence of ultraviolet light, generating stoichiometric amounts of CO_2, which is detected with a non-dispersive infra-red (NDIR) detector. The integrated area of the NDIR signal is directly related to the carbon concentrated in the sample.

Samples that contained biomass were first centrifuged at 13,200xg using concentrated sulfuric acid- washed teflon bottles. The supernatant was used for TOC analysis, after being transferred to an acid-washed glass vial. The precipitate from centrifugation was used for protein analysis (see Section 6.2.4.5.1).

The mean TOC concentration of the saturated PCP feed prepared as described in Section 6.2.4.4 was 4.7 mg/L (±0.43), which corresponds with the theoretical TOC concentration of saturated PCP solution (14 mg/L of PCP, equivalent to 4.0 mg/L of TOC). Three samples of deionized water used to prepare the PCP feed yield a reading of 0.208 (±0.07 mg/L).

6.2.4.5. Biomass Analysis

Two quantitative assays were used to measure biomass indirectly: protein and DNA. Additionally, plating tests were used to determine the ability of the biomass to grow on two different carbon sources: PCP and TSB media (non-selective).

6.2.4.5.1. Protein

Biomass was estimated indirectly by means of a protein assay since iron oxide and hydroxide precipitates could interfere with direct dry mass determination or the measurement of optical density (600 nm) that is commonly used to estimate biomass concentration. Samples were collected and frozen until analysis. Samples were centrifuged in 250 mL Teflon bottles for 25 min. at 13200xg. The biomass pellet was washed (resuspended) with potassium phosphate pH 7 buffer (0.04 M KH_2PO_4 and 0.061 M K_2HPO_4) and centrifuged again. The resuspension-centrifugation cycle was repeated

twice, and the biomass was concentrated to a final volume of 3.0-10.0 mL. The biomass concentrate was lysed with a sonicator (Ultrasonic Processor XL, Heath Systems) for 20 min (in 50% on-off mode during 4-s cycles) and analyzed for protein using the micro-BCA assay (Pierce Catalog No. 23235ZZ). An aliquot of 500 μL of freshly prepared BCA reactant were added to 500 μL of the cell lysate and incubated at 60 °C for 1 h. The absorbance was read at 562 nm and compared to bovine serum albumine standards. Protein concentrations were estimated by means of the dilution factor achieved during the biomass concentration stage.

6.2.4.5.2. DNA

Large size DNA was extracted from effluent from the bioreactor, after gently shaking the packed column. The sample was centrifuged and transferred to a 40-mL polycarbonate centrifuge tube. An aliquot of 75 mg of lysozyme and 7.5 mL 200 mM phosphate buffer (pH 8.0) were added to the tube. The tube was then vortexed for 30 s and heated for 90 min at 37 °C. After heating, 450 μL of 20% sodium dodecyl-sulfate (SDS) were added to the tube and the tube was vortexed for 30 s. The centifuge tubes were frozen at –80 °C for 30 min to begin a freeze-thaw lysis cycle. After 30 min, the tube was placed in a 65 °C water bath for 20 min to thaw. The freeze-thaw cycle was repeated twice more and then the tube centrifuged at 10,000xg for 15 min. The supernatant (containing the cell lysate) was separated and saved. This last step was repeated again, after resuspending the pellet and heating the suspension for 10 min at 65 °C. The supernatant from this step was combined with the one obtained from the previous step. An aliquot of 15 mL of Tris-buffered liquid phenol (pH 8.0) were added to

each of the tubes with the supernatant to remove contaminating compounds and protect the DNA from nucleases. The tube was centrifuged at 10 °C and 5500xg for 5 min. The upper aqueous phase was recovered again into another 40 mL centrifuge tube. Potassium acetate (2.8 mL, 8M) was added to the tube, and the tube placed in an ice bath for 10 min. Then the tube was centrifuged again for 15 min at 10000xg. The supernatant was recovered again into a 40 mL tube containing 30 mL of 95% ethanol. The suspension was kept at –20 °C overnight to precipitate the DNA. Then the tube was centrifuged for 25 min at 10000xg. The supernatant was discarded and the pellet dried for 8-16 h at room temperature over a tared weigh boat, before final gravimetric determination of the DNA.

6.2.4.5.3. Microbial Plating

The ability of the biomass present in the packed bed to degrade PCP was tested by means of plating tests on an agar medium that contained PCP as the only carbon source at a concentration of 0.5 mg/L. This low concentration of PCP was chosen to avoid potential inhibitory effects. This medium was made by mixing 7.5 g of Bacto-Agar with 38.5 mL PAS concentrate (which includes phosphates and nitrogen) and 5 mL of PAS 100x salts solution (which includes trace minerals required for microbial growth), and then diluted to 500 mL (Bedard, et al., 1986). The composition of the solutions used to make this medium is given in Table 6.2. Plates were poured after autoclaving the medium.

The ability of the biomass present in the packed bed to grow on a readily available carbon source was tested by plating on Tripticase Soy Broth (TSB), which is a

non-selective medium. This TSB medium was at a 1:4 dilution (¼ strength) to simulate an oligotrophic (low nutrient) environment, representative of the Fenton's-treated PCP wastewater.

Table 6.2. Composition of the two solutions used to make PAS Medium.

PAS Concentrate (added to 500 mL water)	**PAS 100x Salts** (added to 500 mL water)
NH_4Cl 13.8 g	$CaCl_2 \cdot 2H_2O$ 0.15g
KH_2PHO_4 10.97g	$FeSO_4 \cdot 7H_2O$ 0.5g
K_2HPO_4 28.39 g	$MnSO_4 \cdot H_2O$ 2.5g
	$MgSO_4$ 9.75g
	H_2SO_4 2 drops

6.2.5. pH

pH was measured using an Orion Research digital ionalyzer/501, previously calibrated with phosphate buffer solutions at pH 7.0 and 4.0.

6.2.6. Dissolved Oxygen

Dissolved oxygen was measured with a Cole Parmer 01971-00 analyzer, equipped with a 16 mm steam-sterilizable polarography oxygen electrode (Phoenix Electrode Co.). The electrode was calibrated at 0% oxygen saturation with N_2-purged water for 20 min,

and at 100% with water bubbled with air for 20 min. Measurements were temperature-compensated.

6.3. Experiments

The continuous system was fed with a saturated PCP solution (14 mg/L, or $5.5x10^{-05}$ mol/L), ferrous iron at a concentration of $2.0x10^{-04}$ mol/L and two doses of hydrogen peroxide 1.5 $x10^{-04}$ mol/L and $2.6x10^{-04}$ mol/L. The residence time in the chemical reactor was 1.5 h. The effect of two residence times of 5.5 and 11 h in the bioreactor on the biodegradation rate were tested in this study, at the two above mentioned hydrogen peroxide concentrations.

In addition to the basic reactor configuration of sequential chemical and biodegradation treatment, the effect of recycling part of the bioreactor effluent back to the chemical reactor was tested, at the low residence time of 5.5 h in the bioreactor, and two doses of hydrogen peroxide. Two recycle rates (0.2 and 0.4) were used for this purpose. This recycle rate (α) is defined as the ratio of the flow rate of the bioreactor effluent that is send back to the chemical reactor (represented by a dotted line in Figure 6.1.) with respect the total inlet flow to the system.

After a new operating condition was established, 48 h were allowed to pass to achieve steady before sampling. This period of 48 h represents 32 residence times for the chemical reactor and 8.7 residence times for the bioreactor (operating at a residence time of 5.5 h). A set of samples at a hydrogen peroxide dose of $2.2x10^{-04}$ mol/L was also taken at 36 hours. The 36-h samples from the chemical reactor were analyzed for PCP and the ones from the bioreactor were analyzed for TOC, yielding similar results than the

samples taken at 48 h, supporting the idea that 48 h was enough time for the system to achieve steady state. Typical operating conditions for the combined system are included in Table 6.3.

Table 6.3. Typical operating conditions for the treatment of PCP contaminated water in the combined chemical oxidation and biodegradation system.

Chemical reactor	
Variable	**Value**
pH	3.5
Ferrous iron concentration	$2.0x10^{-04}$ mol/L
Hydrogen peroxide concentration	0.0,$1.5x10^{-04}$, or $2.6x10^{-04}$ mol/L
Residence time	1.5 h
Temperature	Ambient (25 °C)
Bioreactor	
Variable	**Value**
pH	7.0
Nutrient dose (trace minerals, phosphorous and nitrogen)	Stoichiometric to the carbon in the PCP-saturated solution
Residence time	5.5 h
Temperature	Ambient (25 °C)

6.4. Mathematical Model for the Combined Reactor

The combined chemical oxidation and biodegradation system consisted of two reactors in series. In the first reactor, the pH was adjusted to 3.5, within the reported optimum for Fenton's reaction (between 3 and 4). The pH of the outlet stream of this reactor was neutralized in the bioreactor. Since the optimal conditions for Fenton's oxidation are very different from the optimal conditions for biodegradation, and these conditions were adjusted in this study, it can be assumed that only reactions relevant to a Fenton's system occurred in the first reactor, while only biodegradation occurred in the second reactor. In other words, the rate of the relevant reactions to Fenton's oxidation that could occur at the bioreactor and the rate of biodegradation that could occur at the chemical reactor are both negligible.

A kinetic model previously developed for Fenton's reaction (applied to batch reactors in Section 5.4) was used to write the mass balances for a continuous stirred tank reactor (CSTR), the experimental configuration of this work. Additionally, kinetic information about the observed biodegradation of PCP by-products was incorporated into a biodegradation kinetic model. Finally, the two models were integrated. This combined mathematical model also included a recycle configuration.

6.4.1. Fenton's Reaction Model

The sequence of reactions and kinetics that control the reaction rates of the different chemical species (PCP, ferric iron, ferrous iron, hydrogen peroxide, hydroxyl free radicals, perhydroxyl free radicals and superoxide free radicals) under a Fenton's

system has been explained in detail in Section 5.1.4. In that section, it was found that the chemical oxidation degraded PCP (a saturated aqueous solution) and generated intermediates (measured in the form of TOC) that acted as free radical scavengers.

The mass balance for a chemical species i undergoing a series of reactions in a CSTR is:

$$S_{i,ChRx} = S_{i,FChRx} + rate_{i,Ch}\,\tau_{ChRx}$$

in which S is the molar concentration, the subscripts $_{ChRx}$ and $_{FChRx}$ indicate the chemical reactor and feed stream to this reactor, $rate_{Si}$ is the rate of reaction of the chemical species i (mol/L s), and τ_{ChRx} indicates the residence time (s) in the chemical reactor. As in the batch reactor kinetic model, the PCP-free TOC fraction was estimated as the difference of PCP in the feed and the PCP in the chemical reactor, multiplied by 6, the number of carbon atoms contained on a PCP molecule.

6.4.2. Bioreactor model

An assumption used to model the bioreactor was that due to the neutral pH in this reactor, chemical oxidation due to Fenton's reactions did not occur; i.e., only biodegradation reactions occurred. Although the packed bed bioreactor (which contained the majority of the biomass present in the system) is not directly exposed to the mixing action of the impeller, the high recirculation rate from the mixing vessel to the packed bed ensured a well mixed system. In this reactor, the PCP-free fraction of the Fenton's-treated PCP contaminated water is biodegraded. Biodegradation kinetics were based on a Monod-type kinetic model, using the PCP-free TOC as substrate.

The mass balance for a substrate that is utilized as carbon source by biomass in a well mixed continuous bioreactor (or chemostat) is:

$$S_{i,BioRx} = S_{i,FBioRx} + rate_{i,Bio}\,\tau_{BioRx}$$

in which S is the molar concentration, the subscripts $_{BioRx}$ and $_{FBioRx}$ indicate bioreactor and feed stream to this reactor, $rate_{i,Bio}$ is the rate of reaction of the chemical species i (mol/L s), and τ_{BioRx} indicates the residence time (in time units) in the chemical reactor. The rate of substrate bioregradation, $rate_{i,Bio}$, depends on the total concentration of biomass contained in the bioreactor (X_T), and the yield of biomass to substrate i ($Y_{X/Si}$), and usually follows Monod microbial kinetics:

$$rate_{i,Bio} = -\mu_i \frac{X_T}{Y_{X/Si}} = -\frac{\mu_{i,max} S_i}{k_i + S_i} \frac{X_T}{Y_{X/Si}}$$

For a reactor in which the stream is recirculated at high rates to a packed bed column, in which most of the biomass is contained in the column, X_T can be assumed constant.

6.4.3. Integrated Chemical Reaction and Biodegradation Model

The models for Fenton's reaction and biodegradation were integrated into a combined model, in which the effluent from the chemical oxidation reactor is the feed to the bioreactor.

Under a recirculation regime ($\alpha > 0$), the combined model requires estimates of all the concentrations of the Fenton's reactive species (such as ferrous and ferric iron,

hydrogen peroxide and the organic compounds) in the bioreactor. The following assumptions were taken in this regard:

a) Free radical concentrations in the bioreactor were negligible, due to the neutral pH and long residence time in the bioreactor (hours, compared with the half life of a few seconds of these highly reactive species).

b) The already low ferrous iron concentrations in the effluent from the chemical reactor (due to oxidation by hydrogen peroxide) get further reduced, due to the neutral pH and exposure to light and oxygen in the bioreactor. Under these circumstances, it can be assumed that all the iron is in its oxidized form (ferric) and it precipitates as ferric hydroxide. Given sufficient time, it was assumed that the ferric iron concentration in solution reaches equilibrium (from 10^{-09} to 10^{-10} mol/L) with this precipitate (Snoeyink, 1980).

c) Chemicals incorporated into the bioreactor stream (excess of nutrients) did not have any effect on the degradation of PCP by Fenton's reaction. Additionally, biomass present in the effluent stream from the bioreactor did not have any scavenging effect on the Fenton's degradation of PCP. The lack of reactivity of these excess microbial nutrients and biomass (at stoichiometric concentrations with respect to a PCP saturated solution) were demonstrated in previous batch experiments (see Section 5.4.3.3.).

With a recirculating stream from the bioreactor to the chemical reactor, the mass balance for the chemical reactor becomes:

$$S_{i,ChRx} = \frac{S_{i,Feed} + rate_{i,Ch}\,\tau_{ChRx} + \alpha S_{i,BioRx}}{1+\alpha}$$

and the mass balance for the bioreactor becomes:

$$S_{i,BioRx} = S_{i,ChRx} + \frac{rate_{i,Bio}\,\tau_{BioRx}}{1+\alpha}$$

In both of these expressions, α is the ratio of recycle flow rate from the bioreactor to the chemical reactor to the total (inlet or outlet) flow rate to the system.

6.5. Results

6.5.1. Experimental Results

6.5.1.1. Hydrogen Peroxide Losses due to Side Reactions

Control experiments were conducted in which hydrogen peroxide and PCP but no ferrous iron were dosed into the continuous Fenton's reactor. For this purpose, hydrogen peroxide was dosed at concentrations of 1.78×10^{-04} and 4.06×10^{-04} mol/L (given the concentration of this reactant in the hydrogen peroxide feed and the flow rates of the hydrogen peroxide, ferrous iron and PCP solutions to the system) into the system. The acidified nanopure water was substituted for the ferrous iron solution for this purpose. Significant losses of hydrogen peroxide occurred without the addition of any ferrous iron salts. At the lower hydrogen peroxide dose (1.78×10^{-04} mol/L), the measured hydrogen peroxide concentration in samples taken from the chemical reactor were 29.1% lower than the dose. The measured hydrogen peroxide concentration in the feed flask was constant for extended time (up to a week, which was the time to deplete this reactant and prepare fresh feed), and was in agreement with the theoretical concentration, considering the dilution used and the concentration of the stock hydrogen peroxide solution. At the higher hydrogen peroxide dose (4.06×10^{-04} mol/L) the measured hydrogen peroxide

concentration in samples taken from the chemical reactor were 29.9% lower than the dose. The measured hydrogen peroxide concentration in the feed flask was again in good agreement with the theoretical concentration.

These controls indicate that about 30% of the hydrogen peroxide dosed to the system was lost in reactions that did not involve ferrous iron in solution. These losses most likely occurred at the stainless steel surfaces, such as the reactor impeller and baffles (which were covered with iron precipitates, due to the long term operation of the system), since surface impurities in stainless steel have been reported to be reactive towards hydrogen peroxide (Solvay Interox, 1910).

Fenton's-type reactions have been reported with iron minerals (probably involving heterogeneous mechanisms) (Watts, et al., 1997). Therefore, there was concern that these hydrogen peroxide losses were degrading PCP. However, PCP analysis at the highest hydrogen peroxide dose indicated that no significant degradation of PCP occurred due to these reactions.

Decomposition of hydrogen peroxide due to homogeneous catalysts involves oxidation and reduction reactions (which do not produce free radicals) with the net result of decomposition of hydrogen peroxide (Schumb, et al., 1955):

$$H_2O_2 + \textit{reduced catalyst} \longrightarrow H_2O + \textit{oxidized catalyst}$$

$$H_2O_2 + \textit{oxidized catalyst} \longrightarrow O_2 + \textit{reduced catalyst}$$

It has been proposed that heterogeneous surfaces of metal hydroxides might follow a similar reaction pathway. Significant hydrogen peroxide losses have been observed in the presence of lead, silver, cobalt, iron, chromiun and other metal hydroxides. The observed maximum hydrogen peroxide decomposition rate at pH 3.5 in

the presence of colloidal ferric hydroxide coincides with the large surface area of the precipitates observed at this pH (Schumb, et al., 1955).

Due to the proportional (30%) observed losses of hydrogen peroxide, all the subsequent hydrogen peroxide concentrations tested in this work were corrected, to provide a more realistic estimate of the actual hydrogen peroxide available for Fenton's mechanisms. These corrected concentrations, based on the concentration of the hydrogen peroxide in the feed, the dilution achieved by the flow rates of all the solutions dosed into the system, and finally adjusted for the hydrogen peroxide loses (30% of the actual dose) in the chemical reactor are referred hereafter as the effective hydrogen peroxide doses.

6.5.1.2. Biomass Characterization

The system was dosed with ferrous iron at a concentration of $2.0x10^{-04}$ mol/L and an effective hydrogen peroxide of $2.6x10^{-04}$ mol/L, operating at a retention time of 1.5 h in the chemical reactor and 5.5 h in the bioreactor, without any recycle stream among the two reactors. The combined system was allowed to operate for several months at these reactant doses to ensure the development of a stable microbial community. Under these conditions, the PCP degradation achieved in the chemical reactor was 65% (with respect the PCP concentration in the feed) and the TOC degradation achieved in the bioreactor was 13%. To determine the biomass production rate, 1.05 L of bioreactor effluent were centrifuged, and the biomass suspension obtained was concentrated to 10.0 mL and analyzed for DNA, yielding a concentration in the original bioreactor effluent of 14.3 μg/L (assuming a genome size of $5x10^{06}$ base pairs). A 235 mL portion of this same bioreactor effluent were concentrated to 10.0 mL and analyzed for protein, yielding a

concentration of 0.41 mg/L (c.v.=11%). This effluent was also found to contain $1.3x10^{05}$ CFU, indicated by plating tests in TSB ¼ strength media (after 48 h of incubation).

The biomass in the packed column was analyzed for its ability to grow on PCP as a carbon source by plating on PCP medium. No colonies were observed even after a week of incubation, indicating that the microbial population present in the bioreactor could not use PCP as the only carbon source (although it could readily grown in the non-selective in TSB ¼ strength media).

Two samples of five pellets each were taken from the packed bed and analyzed for dry and organic matter (by drying them at 35 °C to constant weight and then incinerating and weighing). This analysis indicated that the organic content of the pellets was 0.41% (± 0.13%), and that the mean pellet weight was 0.164 g (in accordance with the previous measurement explained in Section 6.2.2.). Thus, considering the total mass of pellets in the column, an estimate of the biomass content of the column is 160 mg.

Three pellets from the column were crushed, sonicated and analyzed for protein. After the protein analysis was completed, the pellets were incinerated, to estimate the organic-free dry weight. The mean protein content per pellet was 0.3% (±0.096%) of protein/g of pellet. Then, the approximate protein content of the biomass (organic matter) present in the column was 69%, which is in accordance with the reported range from 40% to 70% (Shuler and Kargi, 1992).

The estimates of biomass and protein in the column and the protein analysis in the effluent from the bioreactor indicate that most of the biomass present in the bioreactor was located in the packed bed. Thus, most of the microbial activity occurred at the packed column.

6.5.1.3. Effect of Hydrogen Peroxide Dose

The degradation of PCP (with respect the PCP concentration in the feed stream) achieved in the chemical reactor (operating at a residence time of 1.5 h without any recycle stream from the bioreactor) under a constant dose of ferrous iron of $2.0x10^{-04}$ mol/L at different doses of hydrogen peroxide is shown in Figure 6.2. Two sets of control experiments (with duplicate samples) showed that there was no degradation of PCP due to ferrous iron in the absence of hydrogen peroxide. A control experiment (with duplicate samples) without any ferrous iron and a high hydrogen peroxide dose showed that no PCP degradation occurred under these circumstances, despite the fact that hydrogen peroxide losses occurred due to side reactions.

The degradation of PCP in the chemical reactor released free chloride. The production of chloride was in agreement with the degradation of PCP, as is shown in Figure 6.3. The ratio of the observed over the theoretical chloride concentration was 84% (± 9%).

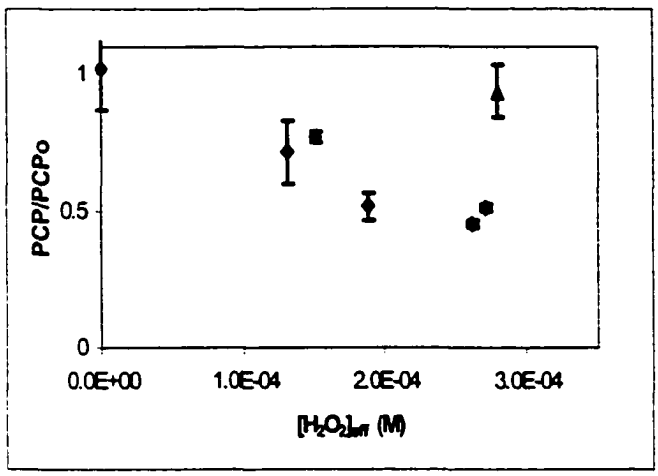

Figure 6.2. Pentachlorophenol concentrations achieved at different effective hydrogen peroxide doses in the continuous chemical reactor. The ferrous iron dose was $2.0x10^{-04}$. Error bars represent the standard deviation of repeated samples. ◆ represent dimensionless concentration of PCP in the chemical reactor, with respect the feed. ▲ is the result of a control experiment with a high dose of hydrogen peroxide and no ferrous iron.

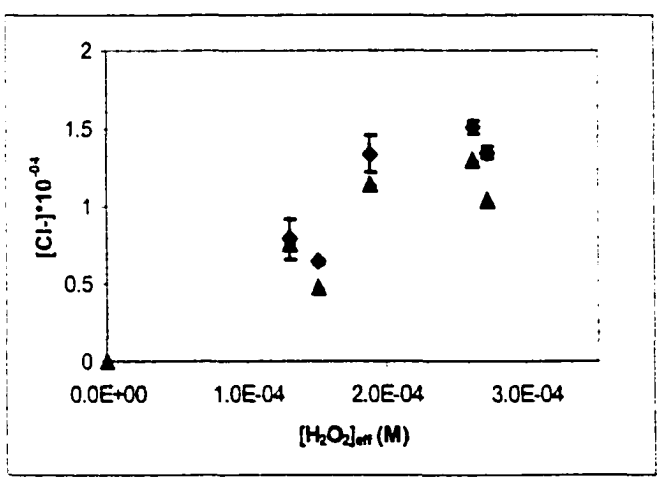

Figure 6.3. Release of free chloride achieved at different effective hydrogen peroxide doses in the continuous chemical reactor due to PCP degradation. Ferrous iron dose was $2.0x10^{-04}$. Error bars represent the standard deviation of repeated samples. ◆ represent theoretical chloride releases due to the observed PCP degradation. ▲ represent the measured chloride releases.

The dimensionless concentration of PCP, TOC in the feed, chemical reactor and bioreactor are presented in Figure 6.4. The average TOC concentration in the saturated PCP feed was 4.7 mg/L (±0.43), which is slightly higher than the theoretical TOC concentration of saturated PCP solution (4.0 ppm). Three samples of deionized water (dechlorinated and autoclaved) used to prepare the PCP feed yielded a reading of 0.208 (±0.07) mg/L, ensuring that this process was not introducing extraneous carbon into the water. In addition, the chloride (at the same three points along the system) and protein in the effluent from the bioreactor are presented in Figure 6.5.

Without any hydrogen peroxide dosed to the system, there were no PCP losses at the chemical reactor or the bioreactor. Correspondingly, without hydrogen peroxide dose to the chemical reactor, no TOC degradation occurred at any point in the system, and the chloride production was below detection limit. There was a lack of TOC biodegradation when there was no chemical oxidation of PCP. The non-zero protein concentration in the effluent of the bioreactor can be explained in terms of cell wash-out from the packed bed reactor.

Degradation of PCP and production of free chloride in the chemical reactor depended strongly on the hydrogen peroxide dose to the system. However, no additional PCP degradation and chloride production occurred at the bioreactor, indicating that PCP was not used as a carbon source in that stage of the process, and that the microbial population in the column did not achieve significant additional substrate dechlorination.

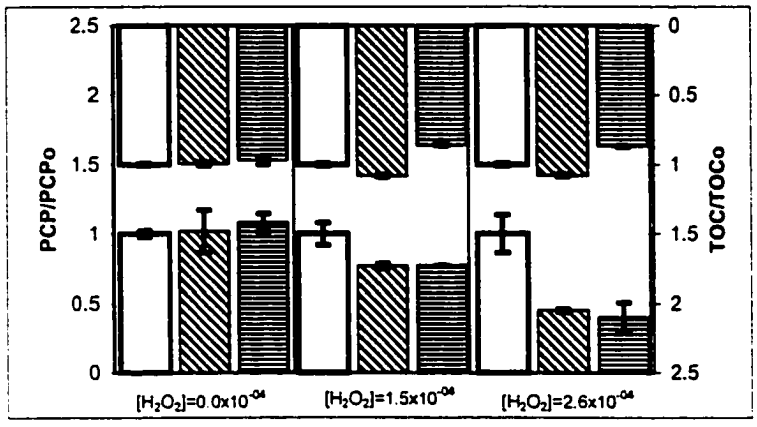

Figure 6.4. Dimensionless concentrations of PCP (bottom) and TOC (top) at different hydrogen peroxide doses. White bars represent feed concentrations, bars with diagonals represent concentrations at the chemical reactor and bars with horizontal lines represent concentrations at the bioreactor. Residence time in the chemical reactor was 1.5 h and 5.5 h in the bioreactor. Error bars represent the standard deviation of duplicate samples.

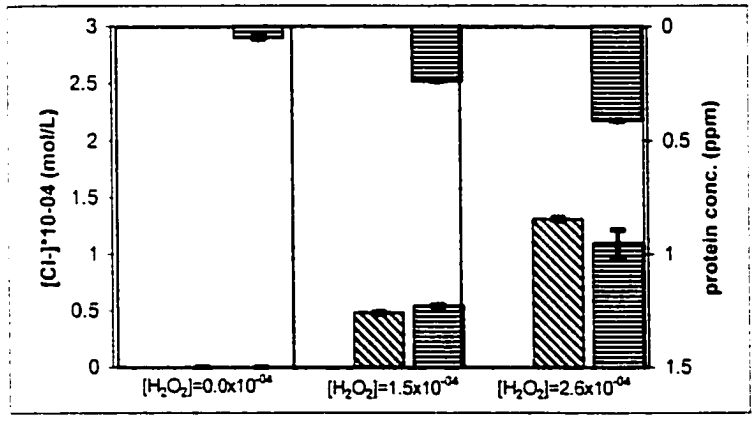

Figure 6.5. Concentrations of chloride (bottom) and protein (top) at different hydrogen peroxide doses. White bars represent feed concentrations, bars with diagonals represent concentrations at the chemical reactor and bars with horizontal lines represent concentrations at the bioreactor. Residence time in the chemical reactor was 1.5 h and 5.5 h in the bioreactor. Error bars represent the standard deviation of duplicate samples.

Two PCP by-products of Fenton's oxidation previously observed in batch reactions by means of liquid-liquid extraction with ethyl acetate and gas chromatography-

mass spectrometry (see Section 5.4.3.2.2 and Section 6.2.4.3.2.) were also observed as intermediates of Fenton's oxidation in the continuous system (see Figure 6.6). These intermediates are tetrachlorohydroquinone and an unidentified by-product with main ion 87.

The yields of tetrachlorohydroquinone produced due to PCP Fenton's oxidation in the continuous system at the two different hydrogen peroxide doses ($1.5x10^{-04}$ mol/L and $2.6x10^{-04}$ mol/L,) were 3.04% (±1.1%) and 2.97% (±0.4%), respectively. These observed yields in the continuos chemical reactor are consistent to the observed yields in batch experiments (which ranged up to 4.5%). It was observed that at the two hydrogen peroxide doses and retention time of 5.5 h in the bioreactor, tetrachlorohydroquinone was biodegraded to non-detectable levels.

The unidentified intermediate with main ion 87, previously detected during batch experiments was also detected in the continuous Fenton's reactor. Due to the lack of identification of this by-product, it quantification was not possible. However, the ratio of the area of the extracted ion 87 (the main ion of this unknown PCP by-product) to the area of the main ion of the internal standard (236, for dibromobenzene) provided semi-quantitative results. The observed yields of this by product in the continuous chemical reactor were similar to the yields found in previous batch experiments (see Section 5.4.3.2.2.), in which the ratio of the integrated area of the main ion of this unknown analyte with respect the area of the main ion of the dibromobenzene internal standard ranged up to $9 x10^{-02}$. Figure 6.6 indicates that this Fenton's reaction intermediate was only partially biodegraded at the tested conditions.

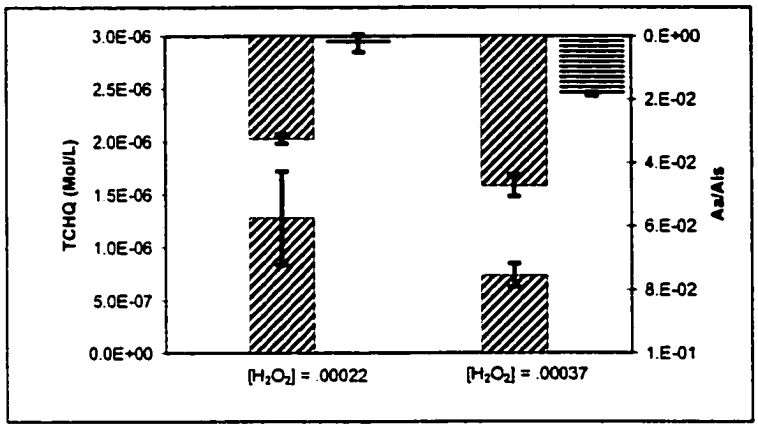

Figure 6.6. Concentration of two previously observed PCP intermediates in the combined system. Tetrachloroydroquinone (TCHQ) concentrations (bottom) and an unidentified intermediate response factors (top) at different hydrogen peroxide doses. White bars represent feed concentrations, bars with diagonals represent concentrations at the chemical reactor and bars with horizontal lines represent concentrations at the bioreactor. Residence time in the chemical reactor was 1.5 h and 5.5 h in the bioreactor. Error bars represent the standard deviation of duplicate samples.

Dissolved oxygen was measured in at these three hydrogen peroxide doses in samples taken from the bioreactor. In all cases the concentration was higher than 7.0 ppm, close to the 6.9 ppm value of air-saturated aqueous solutions. Without hydrogen peroxide dose, this can be explained due to the lack of microbial activity, due to the absence of biodegradable substrates. At higher hydrogen peroxide doses, there was microbial growth due to TOC degradation, but generation of oxygen during the previous Fenton's treatment and the low organic carbon concentration in the stream precluded any oxygen limitations.

6.5.1.4. Effect of Increased Residence Time in Bioreactor

Since only a relatively small fraction of the PCP-free TOC fraction of the Fenton's treated PCP waste was biodegraded, there was the issue that the residence time in the bioreactor was limiting the extents of biodegradation. Therefore, the residence time in the bioreactor was doubled from 5.5 to 11 h. As in the previous case, the residence time in the chemical reactor was 1.5 h and the effective hydrogen peroxide doses to the system were 0, $1.5x10^{-04}$, and $2.6x10^{-04}$. The results from this set of experiments are shown in Figure 6.8 and Figure 6.8. The concentrations of PCP and chloride in the chemical reactor were consistent with the observations shown in Figure 6.4 and Figure 6.5, indicating the reproducibility of the behavior of the chemical reactor. Two-way analysis of variance indicated that the extent of TOC biodegradation and production of protein observed at 11 h were not significantly higher (95% confidence level) than at the lower residence time of 5.5 h.

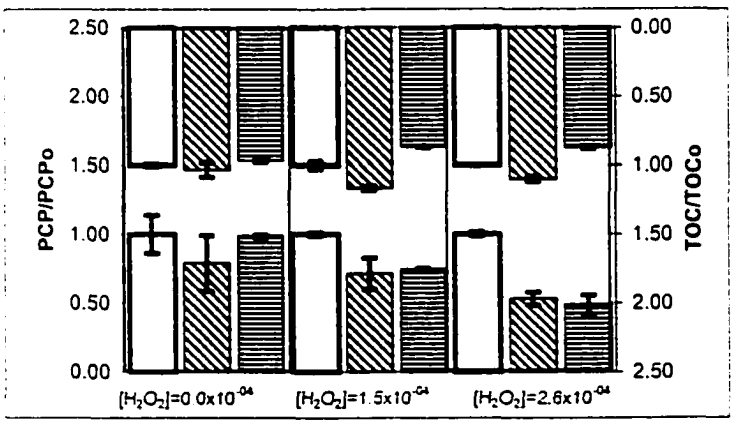

Figure 6.7. Dimensionless concentrations of PCP (bottom) and TOC (top) at different hydrogen peroxide doses. White bars represent feed concentrations, bars with diagonals represent concentrations at the chemical reactor and bars with horizontal lines represent concentrations at the bioreactor. Residence time in the chemical reactor was 1.5 h and 11 h in the bioreactor. Error bars represent the standard deviation of duplicate samples.

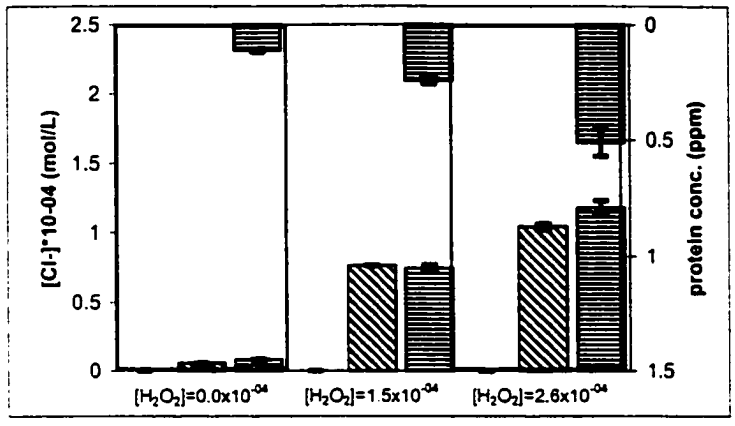

Figure 6.8. Concentrations of chloride (bottom) and protein (top) at different hydrogen peroxide doses. White bars represent feed concentrations, bars with diagonals represent concentrations at the chemical reactor and bars with horizontal lines represent concentrations at the bioreactor. Residence time in the chemical reactor was 1.5 h and 11 h in the bioreactor. Error bars represent the standard deviation of duplicate samples.

6.5.1.5. Effect of Recycle

The effect of recycling the effluent from the bioreactor back to the chemical reactor for further treatment was tested at a residence time of 1.5 h in the chemical reactor and 5.5 h in the bioreactor. For this, 20 and 40% of the total flow rate to the system were recycled from the bioreactor back to the chemical reactor (α=0.2 and α=0.4). These experiments were run at both low ($1.5x10^{-04}$ mol/L) and high ($2.6x10^{-04}$ mol/L) hydrogen peroxide concentrations.

The results from these experiments at low hydrogen peroxide dose are shown in Figures 6.9 and 6.10. Results from the experiments carried out at high hydrogen peroxide dose are shown in Figures 6.11 and 6.12.

Two-way analysis of variance, using hydrogen peroxide dose (at two concentrations), position along the system (at the three levels of feed, chemical reactor or

bioreactor) and recycle rate (three levels) as the factors and the dimensionless PCP concentration (with respect the feed) as the response variable indicated that recycling did not have any significant effect (confidence level = 95%) on the effluent PCP concentrations at either recycle level (20% or 40%), compared with no recycle. Chloride concentrations followed the same pattern.

Analysis of variance for the dimensionless TOC concentrations (with respect the feed) as a response variable indicated that three-way interaction between the factors hydrogen peroxide dose, position along the system (feed, chemical reactor or bioreactor) and recycle rate (at the levels of 0, 0.2 and 0.4) existed. Therefore, the analysis was done separately at low and high hydrogen peroxide doses. At the low hydrogen peroxide dose, there were no significant effects of the different degrees of recycle on the TOC degradation that occurred at the biodegradation stage. In contrast, at the high hydrogen peroxide dose, significant effects of the different degrees of recycle on the TOC degradation that occurred at the biodegradation stage existed. The low recycle ratio of 0.2 had the effect of increasing the TOC reduction that occurred at the biodegradation stage. Further increase of the recycle ratio to 0.4 showed a similar effect, with respect the zero recycle rate (although no different from the α=0.2 level).

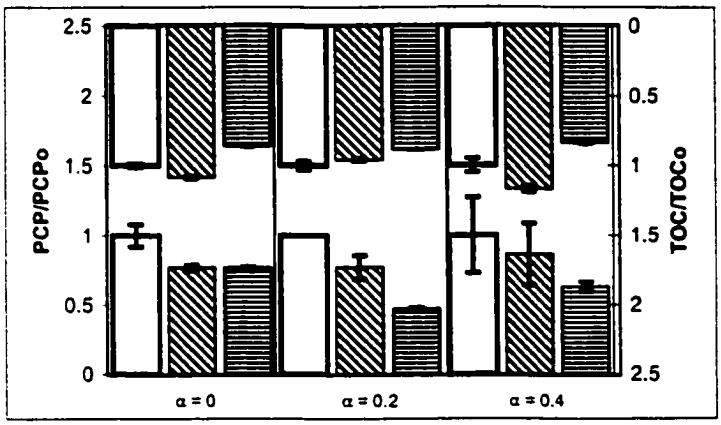

Figure 6.9. Dimensionless concentrations of PCP (bottom) and TOC (top) at three different recycle ratios and hydrogen peroxide effective dose of $1.5x10^{-04}$ mol/L. White bars represent feed concentrations, bars with diagonals represent concentrations at the chemical reactor and bars with horizontal lines represent concentrations at the bioreactor. Residence time in the chemical reactor was 1.5 h and 5.5 h in the bioreactor. Error bars represent the standard deviation of duplicate samples.

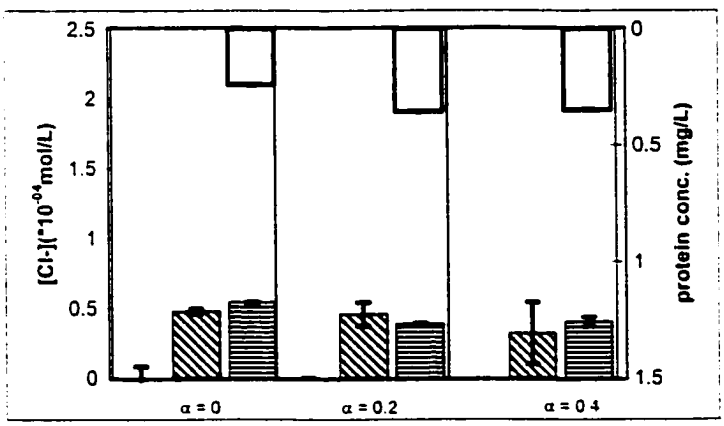

Figure 6.10. Concentrations of chloride (bottom) and protein (top) at three different recycle ratios and hydrogen peroxide effective dose of $2.6x10^{-04}$ mol/L. White bars represent feed concentrations, bars with diagonals represent concentrations at the chemical reactor and bars with horizontal lines represent concentrations at the bioreactor. Residence time in the chemical reactor was 1.5 h and 5.5 h in the bioreactor. Error bars represent the standard deviation of duplicate samples.

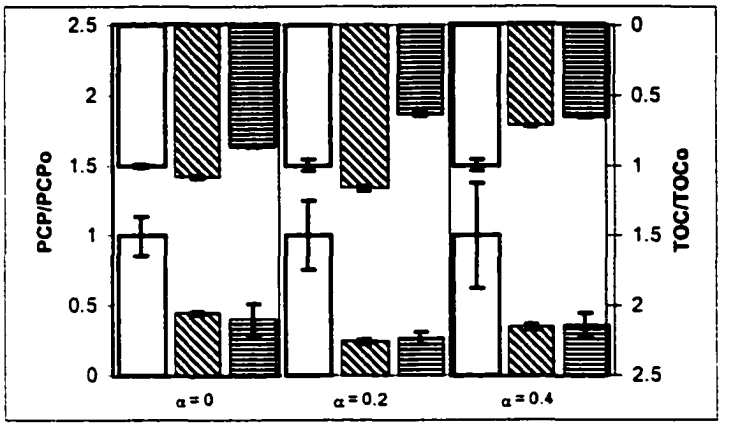

Figure 6.11. Dimensionless concentrations of PCP (bottom) and TOC (top) at three different recycle ratios and hydrogen peroxide effective dose of 2.6×10^{-04} mol/L. White bars represent feed concentrations, bars with diagonals represent concentrations at the chemical reactor and bars with horizontal lines represent concentrations at the bioreactor. Residence time in the chemical reactor was 1.5 h and 5.5 h in the bioreactor. Error bars represent the standard deviation of duplicate samples.

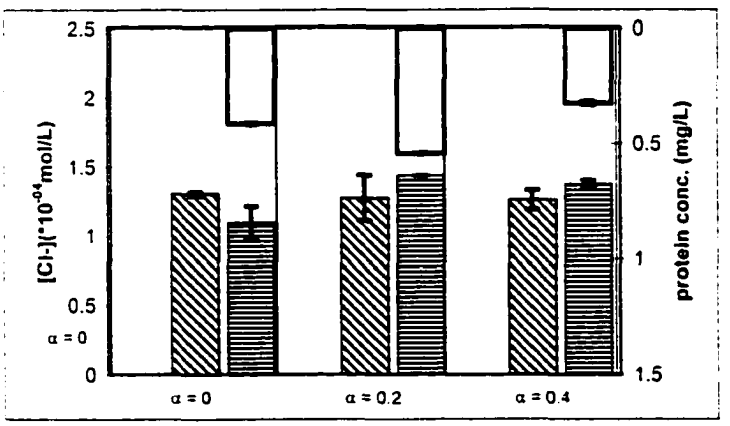

Figure 6.12. Concentrations of chloride (bottom) and protein (top) at three different recycle ratios and hydrogen peroxide effective dose of 1.5×10^{-04} mol/L. White bars represent feed concentrations, bars with diagonals represent concentrations at the chemical reactor and bars with horizontal lines represent concentrations at the bioreactor. Residence time in the chemical reactor was 1.5 h and 5.5 h in the bioreactor. Error bars represent the standard deviation of duplicate samples.

6.5.2. Model Results

6.5.2.1. Fenton's Oxidation Model

Solution of the model for Fenton's oxidation in the CSTR (residence time = 1.5 h) is shown in Figure 6.13, together with results from a control experiment in which the reactor was dosed with hydrogen peroxide and no ferrous iron. The lowest value of the model-predicted dimensionless concentration of PCP with respect the feed is 25% (i.e., 75% degradation). However, the lowest PCP concentrations actually achieved in the system were close to 45%.

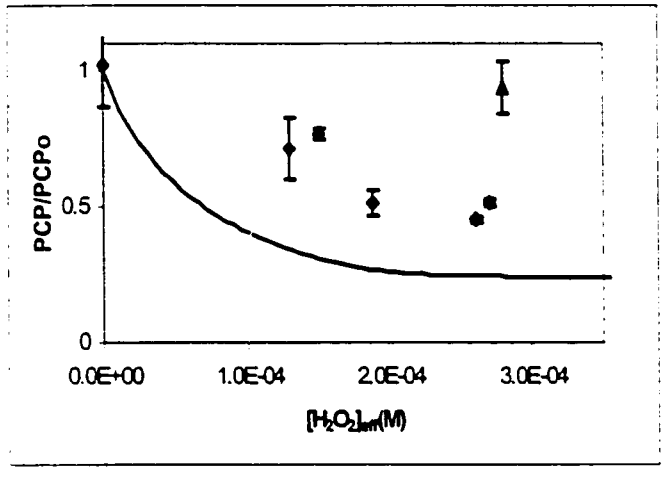

Figure 6.13. Pentachlorophenol concentrations achieved at different effective hydrogen peroxide doses in the continuous chemical reactor. Ferrous iron dose was 2.0×10^{-04}. Error bars represent the standard deviation of repeated samples. ■ represent dimensionless concentration of PCP in the chemical reactor, with respect the feed. ▲ is the result of a control experiment with a high dose of hydrogen peroxide and no ferrous iron.

6.5.2.2. Biodegradation Kinetics Model

The biodegradation data presented in Figures 6.3., 6.4., and 6.6 to 6.11. were used to estimate the Monod biodegradation kinetics of the PCP-free TOC. The yield

coefficient was estimated to be 5.2 (± 2.2) g/L of protein produced per mol/L of TOC consumed based on the measured concentrations of protein in the effluent from the bioreactor.

For this purpose, degradation rates were estimated as the difference in PCP-free TOC in samples taken from the chemical reactor and samples taken from the bioreactor. These steady-state substrate concentrations in the bioreactor (based on the PCP-free TOC fraction that was consumed in the bioreactor) were obtained. A commonly used technique to obtain Monod biodegradation kinetic parameters is to do a regression of the inverse degradation rate vs. the inverse substrate concentration (Shuler and Kargi, 1992). The linear least-squares regression applied to the inverse substrate concentration (as the independent variable) and inverse degradation rates (as the dependent variable) resulted in the equation: $y = 0.13x + 5324$, $R^2 = 0.5369$. The two points obtained at a residence time in the bioreactor of 11 h were not included in this regression since they did not obey the linear behavior of the curve (probably due to the high residence time in the bioreactor). Using this regression equation, values of $k_s = 2.5x10^{-04}$ mol/L TOC and $\mu_{max} = 3.1x1^{-03}$ h^{-1} were obtained.

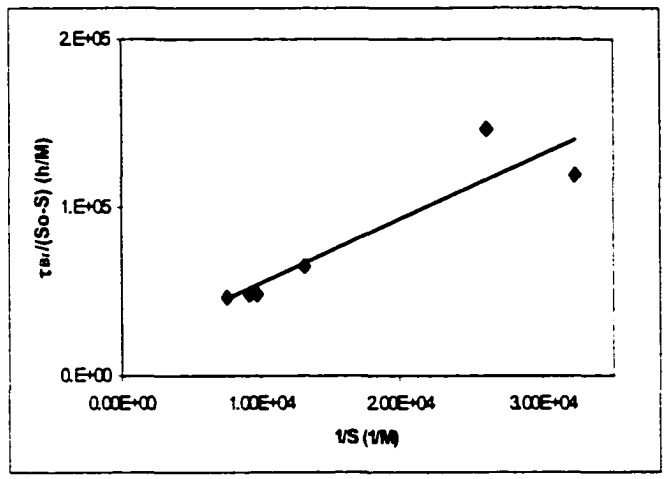

Figure 6.14. Linearized biodegradation rates of the PCP-free TOC fraction of the Fenton's-treated PCP waste.

6.6. Discussion

The continuous model for Fenton's oxidation of PCP (at a ferrous iron dose of $2.0x10^{-04}$ mol/L) predicts a lack of sensitivity of the PCP degradation to hydrogen peroxide doses beyond a hydrogen peroxide dose of $2.0x10^{-04}$ mol/L, reaching a PCP degradation of 75%. The highest experimental degradation of PCP measured in this work in the combined system was about 55%.

Due to variability in pump performance, slight variations from the target flow rates were experienced. Since the actual flow rates of the different inlet streams to the system were measured, correction of the target doses was possible. This analysis indicated that the mean ferrous iron dose was $1.95 (\pm 0.2)x10^{-05}$ mol/L. Since ferrous iron is one of the main chemical species that produces hydroxyl free radicals, variations in this reactant dose are potentially responsible for the observed variability among the PCP degradation, and possibly also to the lack of model fit. Figure 6.15 shows model solutions accounting for variations of $\pm 0.2 x10^{-04}$ mol/L around the target value of $2.0x10^{-04}$ mol/L. It can be observed that the model is not highly sensitive to this

parameter. Thus, variability of PCP degradation cannot be explained exclusively based on the variability of ferrous iron doses. The model over-prediction of PCP degradation cannot be justified by the variability of the ferrous iron dose either. Figure 6.15 also shows the model-predicted PCP degradation in a batch reactor. It can be observed that the model predicts that scavenging effects due to PCP-by products on the degradation of PCP are more important in a CSTR than in a batch reactor. This is in agreement with the data included in this work.

The lack of agreement between experimental and model-predicted dimensionless PCP degradation is probably based on side reactions of free radicals at reactive surfaces in the system. These surfaces were also reactive towards hydrogen peroxide, but as shown by the control experiment in which the PCP feed was dosed to the system together with a high dose of hydrogen peroxide in the absence of ferrous iron, these hydrogen peroxide scavenging reactions did not result in significant degradation of PCP. Detailed evaluation of the nature of the interactions of active surfaces with Fenton's reactive species (such as free radicals) was beyond the scope of this work

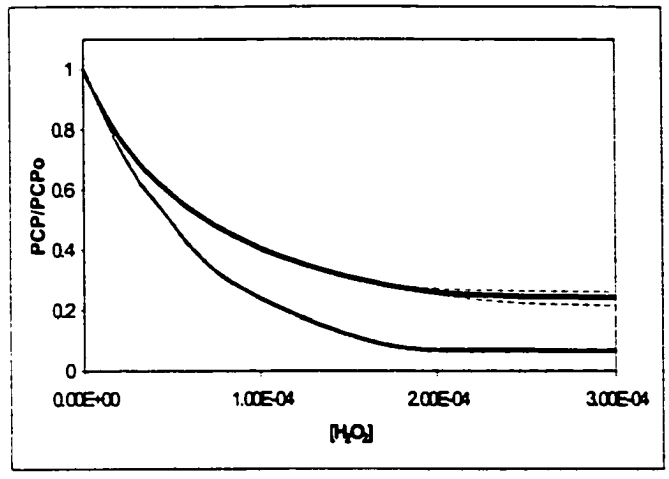

Figure 6.15. Model-predicted dimensionless degradation of PCP at a ferrous iron dose of $2.0x10^{-04}$ mol/L (black line) and variable hydrogen peroxide dose. Dotted lines represent model solutions at ferrous iron doses around one experimental standard deviation around $2.0x10^{-04}$ mol/L. The gray line represents the model solution for a batch reactor.

Experiments in which biodegradation of the continuously Fenton's-treated PCP waste occurred indicated that microbial growth (based on protein measurements) was supported by a fraction of the PCP-free TOC as a carbon source. On the other hand, the lack of biodegradation of PCP at all the tested conditions and the plating tests on PCP media indicate that it is not an adequate carbon source for the microbial population under study. Lack of dechlorination in the bioreactor was also observed, indicating that non-dechlorination biodegradation reactions occurred, and confirming the unsuitability of PCP as a carbon source for microbial use. This observation might also indicate a preference for the non-chlorinated intermediates over the chlorinated ones as a carbon source.

The highest TOC concentration of the waste, assuming a PCP-saturated solution is $3.3x10^{-04}$ mol/L TOC. However, since partial degradation of PCP occurred in the Fenton's system, the PCP-free TOC fraction was at most 55% of this value. Experiments showed that at a residence time of 5.5 h in the bioreactor, the maximum TOC reductions

were about 14%, and that further increases of the retention time in the bioreactor did not significantly increase this TOC degradation. Protein analysis confirmed this finding. These low biodegradation rates observed might had been caused by different reasons:

a) A zero-order microbial degradation kinetics. The Monod microbial kinetics expression can explain this behavior at high substrate concentrations (at which the value of the half saturation constant is negligible). However, given the value of $k_s = 2.5 \times 10^{-04}$ mol/L and the maximum theoretical TOC concentration of the waste of 3.3×10^{-04} mol/L TOC, this explanation is questionable.

b) Another possible explanation of the observation that a longer residence time in the bioreactor did not achieve larger degradation extents might be indicative that the observed biodegradation rates are limited by the maximum capacity of the packed column to hold biomass.

c) Microbial degradation kinetics of the complex mixture formed by the Fenton's treated PCP is not adequately described by a simple model. The different compounds in this mixture might have different biodegradabilities. Analysis of the observed intermediates (tetrachlorohydroquinone and an unidentified compound), which indicated that tetrachlorohydroquinone was biodegraded to non detectable levels in the bioreactor, while the unidentified compound was only partially biodegraded confirms this. Interactions (such as competitive inhibition) among the different compounds in this mixture might be important. Given the observed lack of dechlorination, and toxicity of highly chlorinated compounds (such as PCP), this might be a feasible explanation of the

observed lack of sensitivity to extended residence time and low PCP-free TOC biodegradation.

Assuming that the protein content of the biomass present in the system effluent is the same as the one of the biomass present in the column, an estimate of biomass dry weight/mol/L TOC consumed is 7.5 g/mol TOC. Considering a theoretical biomass formula of $CH_2N_{0.25}O_{0.5}$ (Shuler and Kargi, 1992) and the following theoretical reaction, some stoichiometric considerations can be made.

$$C + aO_2 + bNH_3 \rightarrow CH_{0.2}N_{0.25}O_{0.5} + dH_2O + eCO_2$$

Considering that all the carbon present in the substrate can be potentially transformed into biomass, the maximum yield would be 25.5 g biomass dry weight/mol TOC. The observed yield is only 30% of this theoretical maximum yield. The difference (70%) of the reduction of TOC in the bioreactor might be due to mineralization to CO_2. This estimate provides only a rough measurement of the extent of mineralization that occurs in the bioreactor, and by no means should be considered equivalent to measurements of CO_2 production of the system. A more accurate estimate of the biomass yields could be done based on thermodynamic considerations. However, these would require knowledge about the nature of the substrates (other than their concentration, based on TOC), specifically the degree of oxidation (Roels, 1983). An estimate of this degree of oxidation could be obtained by means of the chemical oxygen demand (COD) analysis.

Recycle of the bioreactor effluent back to the chemical reactor had small significant effects only at the high hydrogen peroxide dose, at both recycle rates tested in this work (20% and 40%). These effects were only significant for the TOC production and were confirmed by the protein analysis.

The mathematical model for the combined system was used to provide a mechanistic understanding of the system behavior. For this purpose, the model-predicted TOC and PCP concentrations under different recycle ratios (0., 0.4, and 2.0) were studied under two different scenarios:

a) Constant hydrogen peroxide and ferrous iron doses of $3.0x10^{-04}$ mol/L and $2.0x10^{-04}$ mol/L, respectively. Additionally, the residence time in the bioreactor was varied, while keeping the residence time in the chemical reactor constant at 1.5 h.

b) A constant residence time in each reactor (equal to the experimental residence time of the continuous system): 1.5 h in the chemical reactor and 5.5 h in the bioreactor. Additionally, the hydrogen peroxide dose was varied, while keeping the ferrous iron dose constant at $2.0x10^{-04}$ mol/L.

It should be noted that this model represents a great simplification of the combined system, for both the chemical oxidation process and the biodegradation process. It has already been noted that the chemical oxidation model over-predicts the degradation of PCP. The limitations of the biodegradation model have already been noted in previous paragraphs. However, despite these limitations, a mechanistic model might provide further insight in the study of the process.

Model-predicted PCP and TOC dimensionless concentrations at recycle ratios of 0.4 and 2.0 and variable residence time under the first scenario are shown in Figure 6.16. At zero recycle rate, the model-predicted degradation of PCP achieved by the combined system is limited by the degradation of PCP achieved in the chemical reactor. This is because Fenton's reaction is the only mechanism to degrade PCP in the combined system. A recycle rate of 0.4 and 2.0 achieved only small increases in the degradation of PCP in the chemical reactor. This is in agreement with the observed lack of sensitivity of PCP degradation in the experimental combined system at recycle rates of 0.2 and 0.4.

In contrast, the model-predicted degradation of TOC under a constant hydrogen peroxide dose and variable residence time, indicates that there is a significant increase in the efficiency of the TOC reduction achieved by the combined system due to the recycle of the bioreactor effluent back to the chemical reactor.

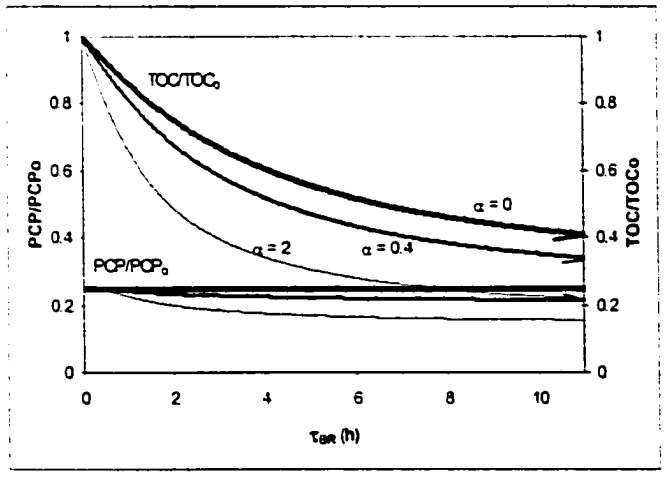

Figure 6.16. Model-predicted dimensionless degradation of PCP and TOC at variable residence time in the bioreactor. The residence time in the continuous reactor was constant at 1.5 h. Hydrogen peroxide and ferrous iron doses were $3.0x10^{-04}$ mol/L and $2.0x10^{-04}$ mol/L, respectively. Thicker lines represent model solutions at lower recycle rates.

Model-predicted PCP and TOC dimensionless concentrations at a variable hydrogen peroxide dose, a constant ferrous iron dose of $2.0x10^{-04}$ mol/L, recycle ratios of 0.4 and 2.0, and constant residence time in each reactor (1.5 h in the chemical reactor and 5.5 h in the bioreactor) are shown in Figure 6.17 and Figure 6.18, respectively. At the three tested recycle rates (0. 0.4, and 2), the PCP degradation was not sensitive to additional hydrogen peroxide doses above $2.0x10^{-04}$ mol/L. Recycle rates of 0.4 and 2.0 achieve small increases on the degradation of PCP in the combined system. The observed lack of sensitivity of PCP degradation achieved by the experimental combined system at recycle rates of 0.2 and 0.4. can be explained in terms of the sensitivity of the PCP and chloride analysis to detect these changes.

The model-predicted degradation of TOC under a variable hydrogen peroxide dose and constant residence time, shown in Figure 6.18, indicate a similar behavior than the PCP degradations, except that increases in the degradation of TOC achieved by the combined system were larger.

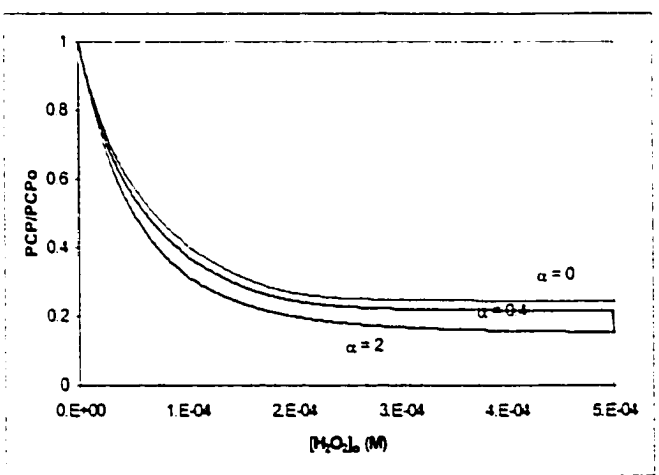

Figure 6.17. Model-predicted dimensionless degradation of PCP in the combined system at variable hydrogen peroxide dose. Residence time in the chemical reactor was 1.5 h, and 5.5 h in the bioreactor. Ferrous iron dose was $2.0x10^{-04}$ mol/L.

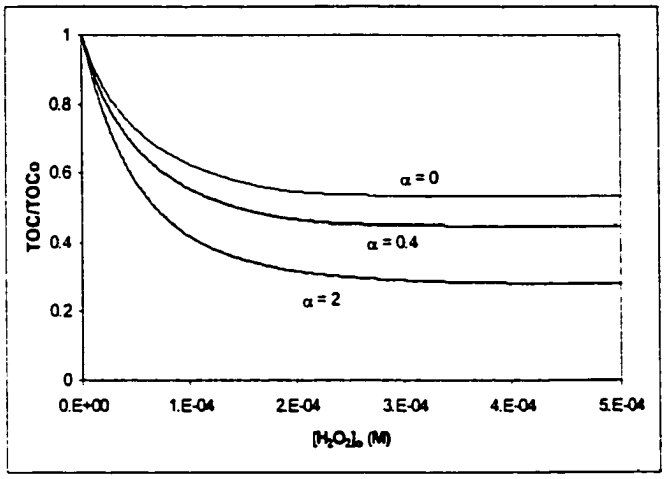

Figure 6.18. Model-predicted dimensionless degradation of TOC in the combined system at variable hydrogen peroxide dose. Residence time in the chemical reactor was 1.5 h, and 5.5 h in the bioreactor. Ferrous iron dose was 2.0×10^{-04} mol/L.

Under the assumptions included in the model, the increased sensitivity of the model-predicted TOC degradation with respect to the model-predicted PCP degradation at the same recycle rates depend can be explained in terms of the biodegradation kinetic constants and the scavenging effects of the PCP-by products on the chemical oxidation of PCP. The two limiting cases for the Monod-type kinetics are zero and first order kinetics, which occur under conditions of high and small substrate concentrations with respect to k_s, respectively. At zero-order biodegradation kinetics (implying high substrate concentrations), any operating condition (such as hydrogen peroxide concentration) that increases the PCP degradation achieved in the chemical reactor would have a null effect on the TOC degradation, according to the lack of model sensitivity to the concentration of bioavailable substrates. However, at first-order biodegradation kinetics (which based on the Monod model occur at small substrate concentrations), any operating condition that increases the PCP degradation would have a significant effect on the TOC

degradation (proportional to the concentration of bioavailable substrate). Thus, differences in sensitivity of PCP with respect to TOC under different recycle rates depend on the magnitude of this first order constant (or the ratio between μ_{max} and k_s, considering a Monod kinetic model).

6.7. References

1. APHA, AWWA, and WPCF. Standard Methods for the Examination of Water and Wastewater. 15th ed. Washington; 1980.

2. Bedard, D., R. Unterman, L. Bopp, M. Brenna, M . Haberl , and C. Johnson. 1986. Rapid Assay for Screening and Characterizing Microorganisms for the Ability to Degrade Polychlorinated Biphenyls. Appl. Environ. Microbiol. 51(4):761-768.

3. Bigda, R. 1995. Consider Fenton's Chemistry for Wastewater Treatment. Chemical Engineering Progress. 62-66.

4. Buxton, B. V., C. L. Greenstock, W. P. Helman, and A. B. Ross. 1988. Critical Review of Rate Constants for Reactions of Hydrated Electrons, Hydrogen Atoms and Hydroxyl Radicals in Aqueous Solution. J. Phys. Chem. Ref. Data. 17:513-886.

5. Fartahazis, P. and Ross, B. 1977. Selected Specific Rates of Reactions of Transients from Water in Aqueous Solution. Washington: NBS.

6. Glaze, W. and J. Kang. 1989. Advanced Oxidation Process. Test of a Kinetic Model for the Oxidation of Organic Compounds with Ozone and Hydrogen Peroxide in a Semibatch Reactor. Ind. Eng. Chem . Res. 28,1580-1587.

7. Graves, J. W. and T. Joyce. 1994. A critical review of the ability of biological treatment systems to remove chlorinated organics discharged by the paper industry. Wat. S.A. 20(2):155-159.

8. Hale, D.; W. Reineke, and J. Wiegel. 1994. Biological Degradation and Bioremediation of Toxic Chemicals. Chaudry, R., ed. Portland: Dioscorides Press; pp. 74-91.

9. Heinzle, E., F. Geiger, M. Fahmy, and O. Kut. 1992. Integrated Ozonation-Biotreatment of Pulp-Bleaching Effluents Containing Chlorinated Phenolics. Biotech. Prog. 8:67-77.

10. Kosaka, K., H. Yamada, S. Matsui, S. Echigo, and K. Shishida. 1998. Comparison among the Methods for Hydrogen Peroxide Measurements to Evaluate Advanced Oxidation Processes: Appliation of a Spectrophotometric Method Using Copper(II) Ion

and 2,9-Dimethyl-1,10-phenanthroline. Environ. Sci. Technol. 32:3821-3824.

11. Leuenberger, C., W. Giger, R. Coney, J.W. Graydon , and E. Molnar-bica. 1985. Peristent Chemicals in Pulp Mill Effuents. Wat. Res. 19(7):885-894.

12. Marco, A., S. Esplugas, and G. Saum. 1997. How and Why combine Chemical and Biological Processes for Wastewater Treatment. Wat. Sci. Tech. 35(4):321-327.

13. Prescott, L.; J. Harley , and D. Klein. 1999. Microbiology. Boston: McGraw-Hill.

14. Puhakka, J. and E. Melin. 1996. In: Crawford, R. and D. Crawford, eds. Bioremediation: Principles and Applications. Cambridge University Press; pp. 254-299.

15. Roels, J. A. 1983. Energetics and Kinetics in Biotechnology.

16. Schumb, W.; C. Satterfield, and R. Wentworth. 1955. Hydrogen Peroxide. New York: Reinhold Publishing.

17. Scott, J. and D. Ollis. 1995. Integration of Chemical and Biological Oxidation Processes for Water Treatment: Review and Recommendations. Env. Prog. 14:88-103.

18. Shuler, M. and Kargi. 1992. Principles of Biochemical Engineering.

19. Snoeyink, V. and D. Jenkins. 1980. Water Chemistry. New York: John Wiley and Sons.

20. Solvay Interox, Inc., publisher. 1910 Oct; Accessed 2000. Available at: http://www.solvay-interox.com/resource.htm#RES_H2O2.

21. Stockinger, H., E. Heinzle, and O. Kut. 1995. Removal of Chloro and Nitro Aromatic Wastewater Pollutants by Ozonation and Biotreatment. Environ. Sci. Technol.. 29:2016-2022.

22. Tang, W. Z. and C. Huang. 1997. Stoichiometry of Fenton's Reagent in the Oxidation of Chlorinated Aliphatic Organic Pollutants. Env. Technol. 18:13-23.

23. Venkatadri, R. and R. Peters. 1993. Chemical Oxidation Technologies: Ultraviolet Light/Hydrogen Peroxide, Fenton's Reagent, and Titanium Dioxide-Assisted Photocatalysis. Haz. Waste Haz. Mat. 10:107-149.

24. Vogelpohl, A. and S. Geissen. 1996. Conference Review: International Conference of Oxidation Technologies for Water and Wastewater Treatment.

25. Watts, R., A. Jones, P.Cheng, and A. Kelly. 1997. Mineral-catalyzed Fenton-like Oxidation of Sorbed Chlorobenzenes. Wat. Env. Res. 69(3):269-275.

26. Zeng, Y, Page Author. Pentachlorophenol Family Pathway Map [Web Page]. 2000 Aug 24; Accessed 2000 Oct 9. Available at: http://www.labmed.umn.edu/umbbd/pcp/pcp_map.html.

CHAPTER VII

CONCLUSIONS AND RECOMMENDATIONS

7.1. Introduction

This research investigated the combined Fenton's oxidation and biodegradation of pentachlorophenol (PCP)-contaminated water as a model recalcitrant compound. A mechanistic approach to understanding and describing the continuous sequential treatment was pursued, with the ultimate goal of developing a mathematical model of the combined system as an alternative to the case-by-case experimental approach. The following steps were followed in order to accomplish this goal:

a) The kinetics of the Fenton's degradation of PCP were studied by the competitive kinetics method, in order to obtain a kinetic constant that characterizes this reaction. In combination with an estimate of the concentrations of hydroxyl free radical, this kinetic constant allows the estimation of the degradation rate of the contaminant under study.

b) The stoichiometry of the Fenton's degradation of PCP was also studied. Although limited characterization of the chemical mixture of PCP-treated waste was only partially successful, enough information was obtained to account for the scavenging effects of the PCP intermediates.

c) The kinetic and stoichiometric information generated in part b) was incorporated into a more comprehensive Fenton's model for batch reactors. This model allowed the estimation of the hydroxyl free radical concentration by including relevant reactions and rates for the reactive chemical species generated by the combination of hydrogen peroxide and ferrous iron at acidic pH.

d) The Fenton's reaction kinetic model was incorporated into mass balances for a continuos Fenton's reactor. Biodegradation kinetics were obtained from the continuous bioreactor performance. This information was incorporated into the combined Fenton's oxidation and biodegradation system to explain the behavior of the combined system, and to develop reactor design and optimization guidelines.

Conclusions from these separate parts of this research have already been discussed in previous chapters. In the following section, conclusions about this work as a whole will be discussed.

7.2. Project Conclusions

- Fenton's oxidation of PCP in batch experiments allowed the characterization of the system under study: development and validation of analytical methods for intermediates, and a kinetic model for PCP degradation. These reactions led to extensive but not complete dechlorination. However, limited success was achieved in identifying specific organic intermediates (for example, the first dechlorination by-

product tetrachlorohydroquinone was identified, but it accounted for less than 5% of the carbon balance). The use of the total organic carbon assay allowed a lumped approach for the study of these intermediates and their hydroxyl free radical scavenging effects on the degradation of PCP.

- Fenton's degradation of PCP in continuous experiments was studied based on the knowledge obtained from batch experiments. This approach facilitated the study of the latter system, despite the limited amount of data and the more difficult characterization inherent to continuous reactors. The production of chloride and some of the observed intermediates during these continuous experiments was consistent with the previous data collected during batch experiments. However, the extent of these reactions for the continuous system was substantially shorter than in batch reactors. This observation allowed identification of important effects that were present in the continuous reactor that were not observed during batch experiments. Specifically, reactive surfaces (stainless steel and glass surfaces covered with iron precipitates) were responsible for important hydrogen peroxide losses that did not involve hydroxyl free radical generation.
- The complex composition of the Fenton's-treated PCP mixture and the lumped approach to study the chemical oxidation and biodegradation kinetics of this mixture were in some respects an oversimplification. Whereas this lumped approach allowed adequate predictions for the Fenton's degradation of PCP in batch reactors and identification of additional important factors present during the continuous Fenton's reactor operation (discussed in the previous paragraph), it still lacks potentially important effects in the biodegradation system. In particular, the different fractions of

the Fenton's treated PCP waste have different biodegradability, and other fractions might even have inhibitory effects on the biodegradation of this waste.

- Despite these limitations of the combined chemical oxidation and biodegradation model, it provided insight into some of the observed combined system behavior (such as the effect of extended residence time in the bioreactor and recycle reactor configurations). These effects were strongly dependent on the specific values of the Monod-type biodegradation kinetic constants, their ability to describe the biodegradability of the actual waste, and the scavenging effects of the PCP-by products on the chemical oxidation of PCP. Thus, the approach followed in this work contributes to a better understanding of combined chemical oxidation and biodegradation for the treatment of recalcitrant wastes.
- The combined model provided information that confirmed the two project hypotheses (which were also supported by experimental data): a combined chemical oxidation and biodegradation process allows higher mineralization than a single stage process, and the degree of mineralization might be improved by a reactor configuration in which more than a single chemical oxidation and biodegradation cycles are performed. The first project hypothesis is supported by the lack of mineralization observed in the chemical reactor and the inability of the biomass present in the bioreactor to degrade untreated PCP. Thus, whereas a single chemical oxidation process might be able to degrade PCP and dechlorinate the waste, mineralization did not occur at the tested hydrogen peroxide doses. In contrast, without biomass that can use the parent compound as a carbon source, a single biodegradation process cannot mineralize this waste, unless it is chemically pre-treated to generate biodegradable

intermediates. Thus, only a combined system could achieve mineralization of the waste. Although higher hydrogen peroxide doses presumably might achieve mineralization due to chemical oxidation, the efficiency of such a process (defined in this work as the ratio of mineralization to hydrogen peroxide use) would be very low. The second project hypothesis is supported by the scavenging effects of the PCP-by products on the Fenton's degradation of PCP. Recycling was shown to be a means of biodegrading the PCP-by products faster than without recycle, which reduced the scavenging effects in the Fenton's reactor and enhanced the Fenton's degradation of PCP. Since the bioavailability of carbon sources depended on this extent of degradation of the parent compound, recycling also improved the performance of the bioreactor. Thus, a more integrated combined system by means of recycling has potential to improve the combined process performance.

- The mechanistic approach followed in this work was applied to water contaminated with PCP as a model recalcitrant waste. In addition, it has been documented that combined chemical oxidation and biodegradation processes might be beneficial for the treatment of other wastes: inhibitory compounds, mixed biodegradable and recalcitrant compounds, and biodegradable compounds that generate dead-end intermediates (Scott and Ollis, 1995). Applications of combined chemical oxidation and biodegradation systems to other types of waste might require different considerations (such as reactor configurations and operating strategies), but nothing precludes a similar approach to these problems to the followed in this work. Completion of similar mechanistic studies is the only alternative that will allow the application of previously generated knowledge to different situations as an alternative

to the case-by-case empirical approach traditionally applied in the study of this combination of technologies.

7.3. Recommendations for Future Work

This study evaluated the Fenton's oxidation of pure PCP solutions in water. Many additional factors exist in practical applications that potentially have effects on the performance of the Fenton's system. Some examples of these potential effects are:

- Iron-complexing effects of different ions (including sulfate, chloride, and oxalate) have been demonstrated (Rush and Bielski, 1985; Kiwi, et al., 2000).
- The existence of a theoretical optimal ratio of hydrogen peroxide to ferrous iron (since hydrogen peroxide is the main reactant that produces hydroxyl free radicals, but is itself a hydroxyl free radical scavenger) has been demonstrated (Tang and Huang, 1997).
- The existence of a theoretical optimal pH for Fenton's reaction has been explained in terms of the pH-dependence of many of the relevant reactions on this system.

The mathematical model developed in this work might provide a quantitative tool to evaluate such effects. It should be noted that despite the apparent complexity of the Fenton's kinetic model proposed in this work, the basic idea is the relatively simple mass balance approach. Thus, considering that the kinetics of the process are known, the complexity of this approach to different types of reactors is purely operational. Moreover, this approach provides a much better basis to understand different situations than does a case-by-case analysis.

This work was focused on a two-stage chemical oxidation and biodegradation process. The use of a two-stage process was guided by the decision to operate at the reported optimal acidic conditions (pH 3 to 4) for Fenton's treatment, which would be incompatible with the pH required for optimal biodegradation. In addition, a two-stage reactor would separate the microbial community used in the biodegradation stage from the aggressive conditions occurring during Fenton's reaction. However, a more detailed review of the available literature indicates that significant Fenton's reaction rates have been observed at pH closer to neutrality, and also that biofilms can have a high resistance to chemicals with inhibitory properties (such as hydrogen peroxide). Thus, it might be feasible to find operating conditions in which both chemical oxidation and biodegradation occur in the same reactor. It is therefore recommended to evaluate the PCP degradation rates under more neutral conditions. A two-stage, single-reactor process might be feasible, depending on the extent of these rates.

Many questions still remain about the continuous combined system under study. The nature of the interactions between the reactive surfaces of the continuous Fenton's reactor with hydrogen peroxide was previously discussed (and explained in terms of cycles of oxidation and reduction reactions in which hydrogen peroxide generates oxygen and water). These interactions should be studied further in order to provide an improved predictive ability of the mathematical model applied to this system.

According to the biodegradation model, the biodegradation kinetic parameters are very important in determining the suitability of different reactor operating strategies (such as recycling). Thus, it is recommended further exploration of these microbial degradation kinetics. Given that a small set of data was used to determine the Monod-

type kinetic parameters, and that these data was obtained at a single (long) residence time, the accuracy of these parameters is questionable. For this reason, it is recommended that the microbial kinetics be determined using the more traditional use of a continuous stirred tank reactor (chemostat): provide a feed of constant composition, vary the residence time, and measure the resulting steady-state substrate concentration. Feeds in which the PCP has been chemically degraded to different extents (probably under batch conditions to ensure their homogeneous chemical composition) might prove useful to determine whether the Monod-type parameters are constant of depend on the extent of oxidation. Once this is known, complex interactions among the different compounds included in the Fenton's-treated PCP waste can either be ruled out or a more detailed approach (which requires a better characterization of the chemical mixture under study) will be necessary.

A substantial effort was made in this work to characterize the by-products of the Fenton's-PCP reaction, with limited results. Without adequate analytical techniques, probably combined with compatible concentration methods, this quest is a time consuming and long pathway of uncertain results. For this reason, it is recommended to follow instead a lumped parameter approach. In this work, measurement of TOC proved very useful. Other readily available lumped assays that might provide insights into the properties of the chemical mixture and their effects on the combined system performance are: chemical oxygen demand (COD, which in combination with TOC allows the calculation of the average oxidation state of the mixture), adsorbable organic halide (AOX), and biochemical oxygen demand (BOD).

Additionally, it is suggested to evaluate the inhibitory effects of PCP and its Fenton's-treated mixture on the TCO (BOD) biodegradation kinetics. One approach for this task would be supplying a well-defined, readily available carbon source, combined with different ratios of PCP and its intermediates, in order to evaluate the quantitative effects of these substances on the consumption of the readily available carbon source.

7.4. References

1. Kiwi, J., A. Lopez, and V. Nadtochenko. 2000. Mechanism and Kinetics of the $OH^{\cdot}$ Radical Intervention during Fenton Oxidation in the Presence of a Significant Amount of Radical Scavenger (Cl^{-}). Environ. Sci. Technol. 34:2162-2168.

2. Rush, J. and B. Bielski. 1985. Pulse Radiolytic Studies of the Reactions of HO_2/O_2^{-} with Fe(II)/Fe(III) Ions. The Reactivity of HO2/O2^{-} with Ferric Ions and Its Implications on the Occurrence of the Haber-Weiss Reaction. J. Phys. Chem. 5062-5066.

3. Scott, J. and D. Ollis. 1995. Integration of Chemical and Biological Oxidation Processes for Water Treatment: Review and Recommendations. Env. Prog. 14:88-103.

4. Tang, W. Z. and C. Huang. 1997. Stoichiometry of Fenton's Reagent in the Oxidation of Chlorinated Aliphatic Organic Pollutants. Env. Technol. 18:13-23.

APPENDIX 1

Gas Chromatography-Mass Spectrometry Method for Pentachlorophenol

GAS CHROMATOGRAPH PARAMETERS

A) Injection

Volume 1.0 microliters

B) HP5890 Oven Parameters

Zone Temperatures:	State	Setpoint
Inlet A:	Off	250 °C
Inlet B:	On	250 °C
Detector A:	Off	50 °C
Detector B:	On	280 °C
Auxiliary:	Off	50 °C

Oven Parameters:

Oven Equib Time:	0.00 minutes
Oven Max:	325 °C
Oven State:	On
Cryo State:	Off
Cryo Blast:	Off
Ambient:	25 °C

Oven Program:

Initial Temperature:	50 °C
Initial Time:	2.00 minutes

Level	Rate (°C/minute)	Final Temperature (°C)	Final Time (minutes)
1	20.0	160	0.00
2(A)	6.0	250	0.00
3(B)	0.0	50	0.00
Next Run Time:		22.50 minutes	

C) HP5890 Inlet Pressure Parameters

Inlet B:

Constant Flow:	Off
Constant Flow Pressure:	0.0 psi
Constant Flow Temperature:	50 °C
Initial Pressure:	45.0 psi
Initial Time:	0.25 minutes

Level	Rate (psi/minute)	Final Pressure (psi)	Final Time (minutes)
1	98.93	25.0	0.00
2(A)	0.00	0.0	0.00
3(B)	0.00	0.0	0.00

Total Program Time: 0.45 minutes

Column Length:	50.00 m
Column Diameter:	0.200 mm
Gas:	He
Vacuum Compensation:	On

MS ACQUISITION PARAMETERS

A) General Information

Tune File:	atune.u
Acquistion Mode:	Scan

B) MS Information

Solvent Delay:	7.00 min
EM Absolute:	True

C) Scan Parameters

Low Mass:	50
High Mass:	350
Threshold:	500
Sample #:	2

APPENDIX 2

TYPICAL CALIBRATION CURVE FOR PCP AND THE SURROGATE (DIBROMOPHENOL) FOR GC-MS ANALYSIS

Calibration curves were normalized with respect to the concentrations (represented by C) and areas (represented by A) of the internal standard (dibromobenzene, or DBP) on each sample. The concentration of the internal standard in these solutions was 0.157 mg/mL (and the concentrations of both analytes are also in mg/mL units). Figure A.1 shows the calibration curve for PCP, and Figure A.2 shows the calibration curve for the surrogate dibromophenol (DBP).

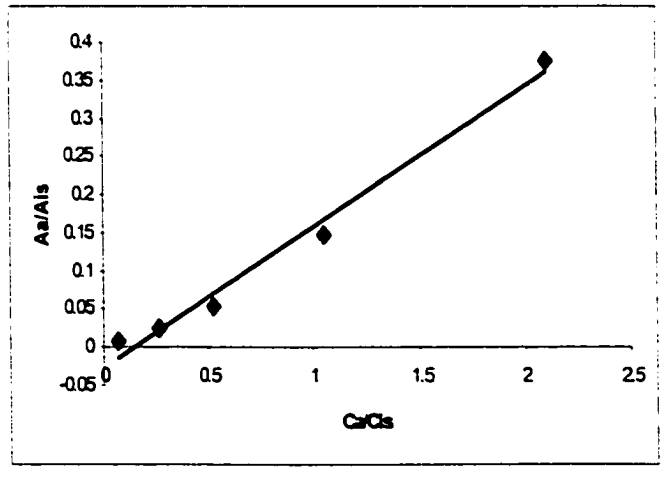

Figure A.1. The calibration curve equation is: Area $_{PCP}$/ A $_{is}$ = 0.1849 C_{PCP}/C_{is} - 0.0263. R^2 = 0.9848.

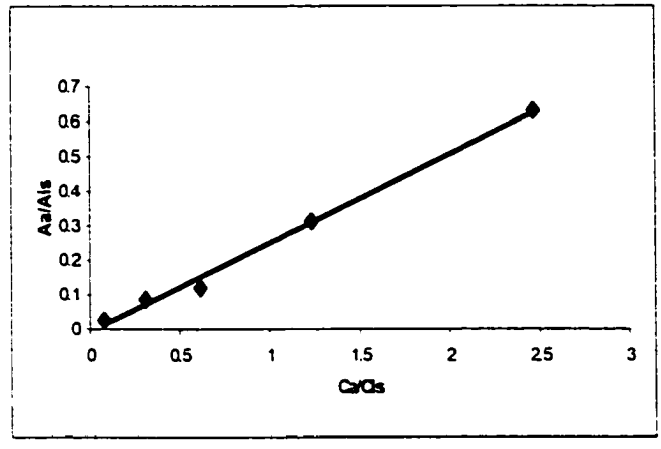

Figure A.2. The calibration curve equation is: Area $_{DBP}$/ A $_{IS}$ = 0.2563 C_{DBP}/C_{IS} - 0.006. R^2 = 0.9944.

APPENDIX 3

TYPICAL CALIBRATION CURVE FOR FERROUS IRON ANALYSIS

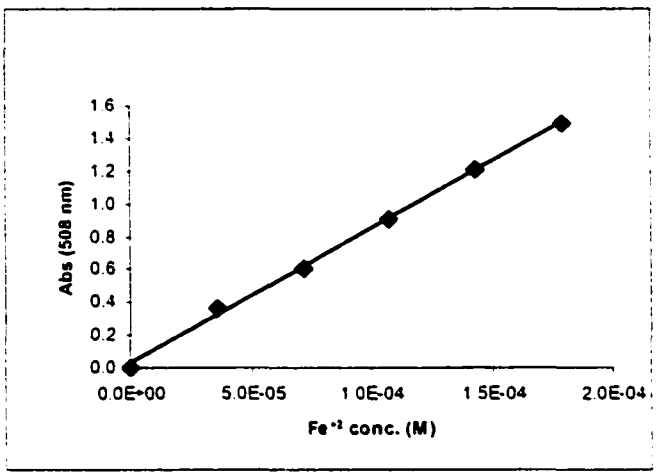

Figure A.3. Calibration curve for ferrous iron using the 1,10-phenanthroline method. The calibration curve is $Abs_{508} = 8197.3\ [Fe^{+2}] + 0.0282$. $R^2 = 0.998$.

APPENDIX 4

TYPICAL CALIBRATION CURVE FOR CHLORIDE ANALYSIS

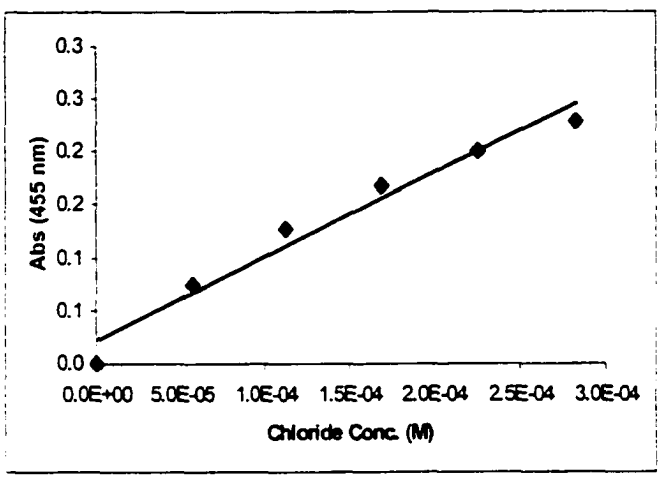

Figure A.4. Calibration curve for chloride ion using the mercuric thyocianate method. The calibration curve is $Abs_{455} = 790.69\ [Cl^-] + 0.0219$. $R^2 = 0.966$.

APPENDIX 5

TYPICAL CALIBRATION CURVE FOR HYDROGEN PEROXIDE ANALYSIS

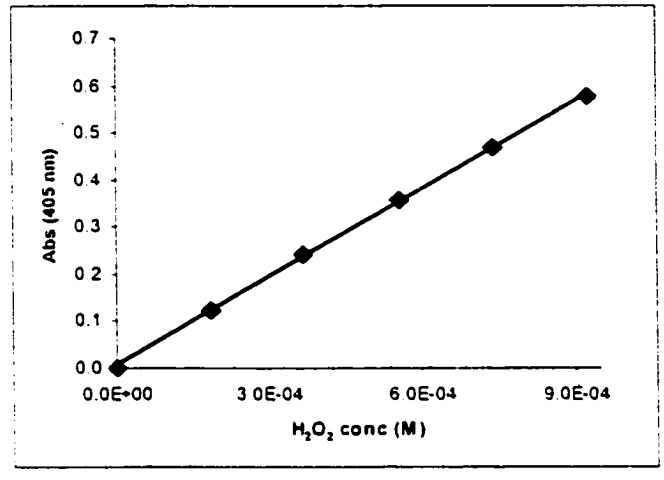

Figure A.5. Calibration curve for hydrogen peroxide using the titanium sulfate method. The calibration curve is $Abs_{405} = 622.86 [H_2O_2] + 0.0067$. $R^2 = 0.9994$.

APPENDIX 6

TYPICAL CALIBRATION CURVE FOR PROTEIN ANALYSIS

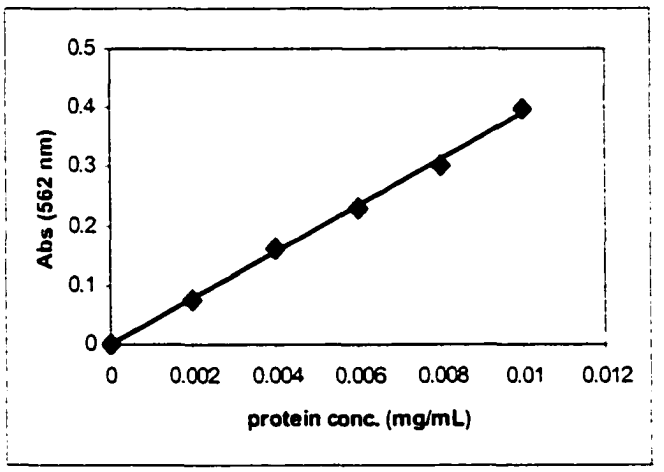

Figure A.6. Calibration curve for protein using the micro BCA method and bovine serum albumine standards. The calibration curve is $Abs_{562} = 38.97$ [mg/mL protein] - 0.0009. $R^2 = 0.998$.